UNIVERSITAT POLITÈCNICA DE CATALUNYA

ASSESSING DEBRIS-FLOW HAZARD FOCUSING ON STATISTICAL MORPHO-FLUVIAL SUSCEPTIBILITY MODELS AND MAGNITUDE-FREQUENCY RELATIONSHIPS

APPLICATION TO THE CENTRAL-EASTERN PYRENEES

Author:

Guillaume G. CHEVALIER

Supervisors:

Dr. Allen BATEMAN PINZÓN

Dr. Marcel HÜRLIMANN ZIEGLER

April 2013

À mon Grand-Père

Parce que les grains de sable se comptent

Resum

Els casos de fluxos de detritus han rebut poca atenció als Pirineus, probablement a causa del petit risc que presenta bona part d'aquesta serralada. No obstant això, l'esdeveniment de Biescas, que va tenir lloc en el mes d'agost de 1996 i que va causar 87 morts (Alcoverro *et al.* 1999), demostra l'existència de zones d'alt risc a la regió i justifica la valoració de la perillositat dels fluxos de detritus presentada en aquesta tesi.

Es van seleccionar cinc fluxos de detritus que es varen succeir el 2008; es van analitzar les localitzacions i es van realitzar descripcions específiques, considerant criteris geològics i morfològics. Els resultats es van comparar amb dades de tot el món, presentant algunes conclusions sobre la valoració de la perillositat. Aquesta anàlisi preliminar de diversos fluxos de detritus de rellevància al Pirineu Occidental constitueix el context de la tesi.

Disposar d'un inventari de casos, és de vital importància per a l'avaluació de la perillositat dels fluxos de detritus. Amb aquest objectiu, es van utilitzar criteris de reconeixement dissenyats per poder ser aplicats a fotografies aèries. D'aquesta manera, es van identificar 691 recorreguts que presenten una activitat passada de fluxos de detritus.

Sobre la base de l'inventari realitzat, i utilitzant un sistema d'informació geogràfica, aquesta tesi presenta una valoració de la perillositat dels fluxos de detritus basada en paràmetres fluvials-morfològics de les conques de primer i de segon ordre.

Les capçaleres de conques muntanyenques són un objecte freqüent dels estudis geomorfològics. Sovint estudiat a escala local, el context en el qual les capçaleres de conques es desenvolupen ha estat poc estudiat al Pirineu centro-oriental. Aquesta tesi presenta una sèrie de paràmetres obtinguts per a les conques de capçalera dels Pirineus centro-orientals, consistents en 3005 conques de primer ordre i 655 conques de segon ordre. Adquirides a partir d'un model digital d'elevacions, aquestes conques han estat digitalitzades, identificades i avaluades pel que fa a cada paràmetre. Els rangs d'aquests paràmetres obtinguts en aquest treball coincideixen amb els presentats en estudis previs. Per primera vegada, els valors aporten detalls sobre les conques de capçalera del Pirineu centro-oriental.

S'han aplicat tècniques de mineria de dades als paràmetres morfomètrics per implementar i avaluar tres models diferents d'avaluació de la perillositat, dels quals el primer és una regressió logística. Els altres dos són arbres de classificació, que constitueixen dos models de susceptibilitat relativament nous referent als fluxos de detritus. Els resultats obtinguts del conjunt de dades d'entrenament mostren que el comportament dels models optimitzats coincideix amb rangs d'estudis previs, encara que cau prop del seu límit inferior (entorn del 70%). Quan els models s'apliquen al conjunt de dades de prova, la regressió logística ofereix la millor predicció, ja que els resultats dels conjunts d'entrenament i de prova són molt similars en termes de comportament. Els arbres són millors en l'extracció de lleis des d'un conjunt d'entrenament, però la validació a través d'un conjunt de prova obté pitjors resultats per a la predicció a escala regional.

La determinació de la magnitud d'un esdeveniment històric es pot realitzar analitzant els seus dipòsits. No obstant això, no és una tasca trivial en els casos d'acumulació de dipòsits de diversos fluxos de detritus consecutius, especialment si només es realitza una anàlisi geomorfològica convencional. Els dipòsits dels esdeveniments poden ser cartografiats i, posteriorment, els arbres malmesos pel flux poden ser analitzats per datar els esdeveniments. Utilitzant aquesta metodologia, es va elaborar una relació magnitud-freqüència dels fluxos de detritus per a la conca torrencial del Rebaixader (Pirineu central) i es va comparar amb un estudi existent del barranc de Tordó (Pirineu oriental) A més, es va elaborar un inventari del Parc Nacional d'Aigüestortes i Estany de Sant Maurici, al Pirineu central, i es va comparar la seva relació magnitud-freqüència a escala regional amb la de Rebaixader. Ambdues corbes presenten un fort efecte "rollover" entorn dels 2000 m^2, i esdeveniments de major magnitud es poden representar per una llei potencial d'exponent entre -1.5 i -1.9.

Aquesta tesi és un primer pas cap a l'avaluació de la perillositat dels fluxos de detritus als Pirineu centro-oriental. Encara que s'aporta molta informació, queda encara més treball per fer, cara a entendre completament la importància dels fluxos de detritus en l'evolució del paisatge.

Resumen

La ocurrencia de flujos de detritos ha recibido poca atención en los Pirineos, probablemente debido al pequeño riesgo mostrado por la mayor parte de esta cordillera. No obstante, el acontecimiento de Biescas, que tuvo lugar en el mes de agosto de 1996 y causó 87 muertos (Alcoverro *et al.* 1999) demuestra la existencia de sitios de alto riesgo en la región y justifica la valoración de la peligrosidad de los flujos de detritos presentada en esta tesis.

Se seleccionaron cinco flujos de detritos que ocurrieron en 2008; se analizaron las localizaciones y se realizaron descripciones específicas, considerando criterios geológicos y morfológicos. Los resultados se compararon con datos de todo el mundo, presentando algunas conclusiones sobre la valoración de la peligrosidad. Este análisis preliminar de varios flujos de detritos de relevancia en el Pirineo Occidental constituye el contexto de la tesis.

Poseer un inventario de ocurrencias pasadas es de crucial importancia para la evaluación de la peligrosidad de los flujos de detritos. Con este objetivo, se utilizaron criterios de reconocimiento diseñados para poder ser aplicados a fotografías aéreas. De esta manera, se identificaron 691 recorridos que presentan una actividad pasada de flujos de detritos.

En base al inventario realizado, y utilizando un sistema de información geográfica, se presenta en esta tesis una valoración de la peligrosidad de los flujos de detritos basada en parámetros fluviomorfológicos de las cuencas de primer y segundo orden.

Las cabeceras de cuencas montañosas son un objeto frecuente de los estudios geomorfológicos. A menudo estudiado a escala local, el contexto en el cual las cabeceras de cuencas se desarrollan ha sido poco estudiado en los Pirineos centro-orientales. Esta tesis presenta una serie de parámetros obtenidos para las cuencas de cabecera de los Pirineos centro-orientales, consistentes en 3005 cuencas de primer orden y 655 cuencas de segundo orden. Adquiridas a partir de un modelo digital de elevaciones, estas cuencas han sido digitalizadas, identificadas y evaluadas con respecto a cada parámetro. Los rangos de estos parámetros obtenidos en este trabajo coinciden con los presentados en estudios previos. Por primera vez, los valores aportan detalles sobre las cuencas de cabecera de los Pirineos centro-orientales.

Se han aplicado técnicas de minería de datos a los parámetros morfométricos para implementar y evaluar tres modelos diferentes de evaluación de la peligrosidad, de los cuales el primero es una regresión logística. Los otros dos son árboles de clasificación, que son modelos de susceptibilidad relativamente novedosos en lo referente a los flujos de detritos. Los resultados obtenidos del conjunto de datos de entrenamiento muestran que el comportamiento de los modelos optimizados coincide con rangos de estudios previos, aunque cae cerca de su límite inferior (en torno al 70%). Cuando los modelos se aplican al conjunto de datos de prueba, la regresión logística ofrece la mejor predicción, ya que los resultados de los conjuntos de entrenamiento y de prueba son muy similares en términos de comportamiento. Los árboles son mejores en la extracción de leyes desde un conjunto de entrenamiento, pero la validación a través de un conjunto de prueba resulta en peores resultados para la predicción a escala regional.

La determinación de la magnitud de un evento histórico se puede realizar analizando sus depósitos. Sin embargo, no es una tarea trivial en los casos de acumulación de depósitos de varios flujos de detritos consecutivos, especialmente si sólo se realiza un análisis geomorfológico convencional. Los depósitos de los eventos pueden ser cartografiados y, posteriormente, los árboles dañados por el flujo pueden ser analizados para datar los eventos. Utilizando esta metodología, se elaboro una relación magnitud-frecuencia de los flujos de detritos para la cuenca torrencial de El Rebaixader (Pirineo central) y se comparó con un estudio existente del barranco de Tordó (Pirineo oriental) Además, se elaboró un inventario del Parque Nacional de Aigüestortes i Estany de Sant Maurici, en los Pirineos centrales, y se comparó su relación magnitud-frecuencia a escala regional con la de Rebaixader. Ambas curvas presentan un fuerte efecto “rollover” en torno a los 2000 m^2, y eventos de mayor magnitud se pueden representar por una ley potencial de exponente entre -1.5 y -1.9.

Esta tesis es un primer paso hacia la evaluación de la peligrosidad de los flujos de detritos en los Pirineos centro-orientales. Aunque se aporta mucha información, queda aún más trabajo por hacer de cara a entender completamente la importancia de los flujos de detritos en la evolución del paisaje.

Abstract

Occurrence of debris flows has received little attention in the Pyrenees, probably due to the small risk faced by most of the debris-flow prone sites in this mountain range. Nevertheless, the event of Biescas, which occurred in august 1996 and causing 87 casualties (Alcoverro *et al.* 1999), demonstrates the existence of high-risk spots in the region and justifies the elaboration of the debris-flow hazard assessment presented in this thesis.

Five debris flows, which occurred in 2008, are selected; and site-specific descriptions and analysis, regarding geology and morphology, were performed. The results are compared with worldwide data and some conclusions on hazard assessment are presented. The preliminary analysis of some major Eastern Pyrenean debris flows represents the background for this thesis.

The necessity of possessing an inventory of past occurrences is of crucial importance when assessing debris-flow hazard. Criteria of reconnaissance were thought to be visible from aerial viewing. 691 tracks through which debris flows are thought to have travelled have been revealed.

Based on debris-flow inventories and using a geographical information system, the debris-flow hazard assessment presented in this thesis takes into account fluvio-morphologic parameters, gathered for every 1st-order catchment as well as every 2nd-order catchment.

Mountainous headwaters are a common subject in geomorphological studies. Often investigated at local scale, the geomorphological context in which headwaters evolve has been poorly reported in the Central-Eastern Pyrenees or worldwide. A series of parameters obtained for Central-Eastern Pyrenean headwaters catchments consisting of 3005 1st- and 655 2nd-order catchments are presented. Acquired from a digital elevation model, these catchments have been digitalised, identified and attributed a value for each parameter. Previously reported parameters' ranges agree with those presented in this study. For the

first time, the ranges of values give details about the Central-Eastern Pyrenees headwater catchments.

Data mining techniques are used on the morphometric parameters, to calculate and test three different models. The first model is a logistic regression. The other two are classification trees, which are rather novel susceptibility models associated with debris flows. Results related to the training dataset show that the optimized model's performance lies within existing reported range although closer to the lowest end (near 70%). When the models are applied to the test set, the logistic regression seems to offer the best prediction, as training and test set results are very similar in terms of performance. Trees are better at extracting laws from a training set, but validation through a test set gives poorer results for a prediction at regional scale.

The determination of the magnitude of a historic event can be done by distinguishing its deposits. However this is not a trivial task in debris fans that accumulate deposits, corresponding to consecutive debris flows, especially if only a conventional geomorphological analysis is carried out. The event deposits can be mapped and, subsequently, trees damaged by the flows sampled for dating events. A magnitude-frequency relationship was prepared for El Rebaixader site, at local scale, and is compared to that of the Tordó creek. Moreover, a debris-flow inventory was created in the "Aigüestortes i Estany de Sant Maurici" National Park in the Central Pyrenees, Spain, and this regional magnitude-frequency relationship is compared to that of Rebaixader. Both curves include a strong rollover effect at about 2000 m^2, and events larger than this magnitude can be represented by a power law, with an exponent between −1.5 and −1.9.

This thesis is a first step toward the assessment of debris-flow hazard in the Central-Eastern Pyrenees. Although a lot of information is provided, more work is still to be done, in order to fully capture debris-flow importance in landscape evolution.

Acknowledgements

First and foremost, I would like to thank my supervisors Allen Bateman and Marcel Hürlimann for trusting me with this thesis. With great faith and ambition, they succeeded in pulling me over the fluvial side of the debris-flow Force. Together, they have offered me guidance, good advices, encouragement and support over the years. *Gracias!*

A special thank you is addressed to Modesto Portilla Gamboa, from National University of Colombia in Bogotá, for picturing debris flows in my mind and in the field. Field investigations are not the same when no one fills my bags with stones! *Gracias Modesto.*

Muchísimas gracias a Dr. Vicente Cesar de Medina Iglesias. His expertise in data mining and computer languages, and his communicative *joie de vivre* are an incredible stimulator. The countless hours helping me with the models and the maps were priceless. *Un abrazo a la familia!*

The GITS Office: Andres Diaz, Albert Herrero Casas, Anna Mujal, and especially Francesco Bregoli, who accompanied me in the field and in many discussions circling around debris flows, landslides and other landslide tsunamis. That was a chance to spend three years of my time in such an admirable company. The GITS office will always be my Spanish family. Thank you!

Talking about family, I am, and will always be in debt of Marti Roca and his family. I could never have dreamt of a better flatmate. Thank you for guiding my first steps in Barcelona, and accompanying me till my last. Thank you!

I would also like to thank Claudia Abancó I Martínez de Arenzana. For the field work, for the office work, for the coffees, for the discussions, for the patience, for the Past and for the Future, for Andorra, for Rebaixader and Ensija, for everything and for everywhere. Moltes graciés!

I want to thank the *tesinandos* who shared my vision of the work: Robert Roy Gallart, Marc Llorens and Rebeca Aizpiri Garcia. Thank you and congratulations on your diploma.

I am grateful to Anaïs Ramos, Alan Ritchie, Anna Ripolles Lorente and Lee “Kiwi” Barlow, who played a major role in making the manuscript decipherable by all. An immense thank you!

I cannot write the acknowledgements without referring to José Moya. I would like to address here my most sincere thank you for sharing with me his field experience in dendrochronological techniques.

When I will think of Barcelona, I will see many faces passing in front of my eyes, remembering parties and good times, between the university’s walls, on its roof or down town. Among them: Francesco “Dude” Bregoli, Anaïs “Dudette” Ramos, Francisco “Paco” Nuñez, Gonzalo “Gonzo” Olivares, Andres “Gallina” Diaz, Vicente “SugarDaddy 2.0” Medina, Anna “La Mujal” Mujal, Albert “Ironman” Herrero and Sergí Capape, Carles Ferrer i Boix, Olga Mavrouli, Benoit Garitte, Mauricio Tapias Camacho (with who sharing an office was definitely great fun!), Christian Scheidl, Fabio Ciervo and all the others I forget. Thank you all!

I would like to show my gratitude to Tim Davies. I owe him my interest in avalanching, sliding, rolling, falling, bouncing and flowing rocks and debris. It all started with a *Montheith’s Black*. Thank you!

A special thank you is addressed to my family, for their unquestionable support, acceptance of my choices and unconditional love. Marion, Gautier, Maman: *je vous aime, et ces quelques pages sont aussi pour vous.*

This thesis was funded by the 3-year European project IMPRINTS, and field trip was supported by the 3-year Spanish national projects of the Spanish Ministry of Education: DEBRISCATCH and DEBRISTART. I also acknowledge the Spanish national project DEBRIS FLOW (CGL 2009-13039) from the same ministry.

Finally, my most profound respect and deepest gratitude go to the healthcare teams of *Hospital del Mar* (Barcelona) and *Centre Oscar Lambret* (Lille).

TABLE OF CONTENT

LIST OF FIGURES

LIST OF TABLES

INTRODUCTION

Objectives and motivations

Mountainous environments are a genuine place of high erosion that, coupled together with tectonic uplift, controls the exhumation rate of ranges. Erosional processes evoke mass movements that comprise of a vast range of phenomena (Fig. I.1). Differences in mechanisms of trigger, propagation and deposition, in material's textures and contents or in locations of occurrences allowed distinction between the different processes and editing classifications to recognize them.

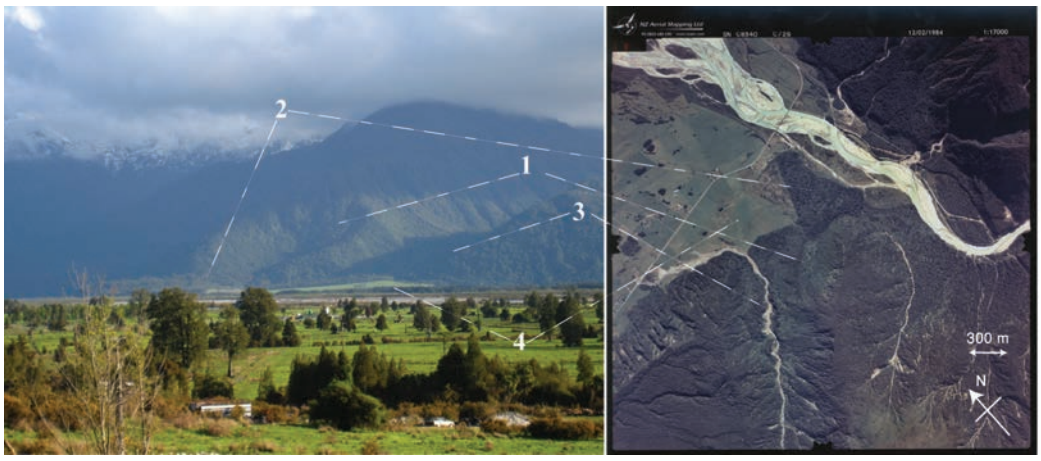

Figure I.1: Example of two different processes in situ. 1) Rock avalanche scarp, 2) rock avalanche deposit, 3) debris-flow prone gully and 4) debris-flow fan (Hari Hari, West coast, New Zealand – see Chevalier *et al.* 2009).

Debris flows are a mixture of water and solid material (debris), and possibly organic matter (vegetation like tree's trunks), travelling downslope and generally observed at high elevation and a high slope but not only. They have been witnessed in many different geological and climatological contexts and frequently strike communities settled in potentially dangerous regions (Fig. I.2).

Figure I.2: Damages witnessed on the 15/06/09 at the Andorran Border Customs house after a debris flow hit on 1/08/08 (see Portilla *et al.* 2010).

The hazard posed by this threat often implies the erection/elaboration of protection measures for people and infrastructures (Fig. I.3). The purpose of protecting the Society led the Authorities to draw attention to natural hazards to better understand them in order to increase safety by diminishing zones at risk. Assessing the risk is generally a multi-step procedure, which implies inter alia the assessment of the hazard.

Hazard assessment is not a trivial task. It implies the full knowledge of the phenomena to consider as hazards, and can generally be shortened by the dominant idea: Past occurrences serve to predict future activity. This thesis shows what can be learnt from past debris flows in the Central-Eastern Pyrenees, and aims at increasing the safety of the community living within the reach of debris flows, without even knowing a risk exists.

Figure I.3: Protection measures seen at Erill-la-Vall (Pyrenees): gabion check dam (left) and net ^

Framework

Three scientific projects have moulded the framework of the work presented. Their guidelines have contributed to provide this thesis with a particular vision and crucial considerations.

For the EC FP7 EU-project IMPRINTS (contract ENV-2008-1-226555) the general idea was to develop the work over a large area, seeking an international application. This project does not only focus on debris flows, but also includes flash floods in the investigation. The work presented in this thesis has ramifications to one of the three methodologies developed in IMPRINTS: a probabilistic rule-based forecasting system.

From the beginning, it was clear that the work had to be carried out over large areas. However, debris flows are a local phenomenon. The national project DEBRISCATCH (contract CGL2008- 00299/BTE) was a project dealing with debris-flow, monitoring and analyses over a small area. For this reason the participation to the DEBRISCATCH project was a fruitful way of getting familiar with debris-flow from local aspects, encouraging field studies, crucial for the work intended in this thesis. The elaboration of a database for debris-flow

events, further presented in this thesis as inventory, is a goal sought by this project.

To a lesser extent, this thesis also has implications in the DEBRISTART project, which is a complementation of DEBRISCATCH. The study of local debris flows at catchment scale is currently further refined and developed. The results presented here for the magnitude-frequency relationship are the first steps towards an evaluation of the effects of a likely future climate change.

The combination of these frameworks, ideally setting the bases of a hazard assessment of debris flows, was applied to the Central-Eastern Pyrenees. Both aspects, hazard assessment and study area, are introduced in the following paragraphs.

Risk and hazard assessment – a brief review of concepts

In the study of the potential risks faced by population and infrastructures at risk, like found on accumulation fans in mountainous environments, the first task is to identify and assess the hazard (Jakob & Hungr 2005, Glade 2005). In other words questions like what type of processes occurs, what is at risk and what is the probability of occurrence, have to be answered.

Hazard is commonly defined as a condition with the potential for causing an undesirable consequence. In Gentile *et al.* (2008), hazard is defined as a potentially damaging physical event, phenomenon or human activity, related to the probability of event occurrence and generally assessed in terms of frequency - intensity. Definitions of hazard can differ among the authors, but its assessment has to be based on event inventories, field investigations and computer modelling (Jakob & Hungr 2005).

In Jakob (2005a) the author provides the reader with information and concepts for (debris-flow) hazard assessment. The analysis of debris-flow hazard is a six - step procedure. First, debris flow hazard has to be recognised. Then their

probability is estimated, as well as their magnitude and intensity. Afterwards comes the production of (debris-flow) frequency - magnitude relationships, followed by the estimation design of (debris-flow) magnitude and intensity. A presentation of (debris-flow) hazards map and a report on debris flow hazard analysis are the last steps.

In Fuchs *et al.* (2008) the hazard analysis comprises the analysis of terrain and environment, the definition of scenarios/design events, and modelling and simulations. Rickenmann *et al.* (1995) proposed to analyse the hazard following a two - step method. 1) The probability of occurrence of a (debris-flow) event in the studied torrent is determined. In other words, the recurrence interval and the frequency of the event have to be known. 2) The principal (debris-flow) parameters needed for the hazard assessment, such as event magnitude, runout length and depositional areas have to be quantitatively estimated.

Following Guzzetti *et al.* (2005) and their probabilistic assessment of a landslide hazard, the definition of landslide hazard has to incorporate the concepts of location, time and size. Beside, the evaluation of the susceptibility, which accounts for the spatial occurrence, requires the identification and the quantitative assessment of the factors leading to the initiation, propagation and deposition (of debris flows) (Carrara *et al.* 2008).

Study area – The Central-Eastern Pyrenees

The Pyrenees spreads over 430 kilometres (km) onshore following an East-West axis (Fig. I.4a) and delimits the boundary between France and Spain, with the Principality of Andorra lying within it.

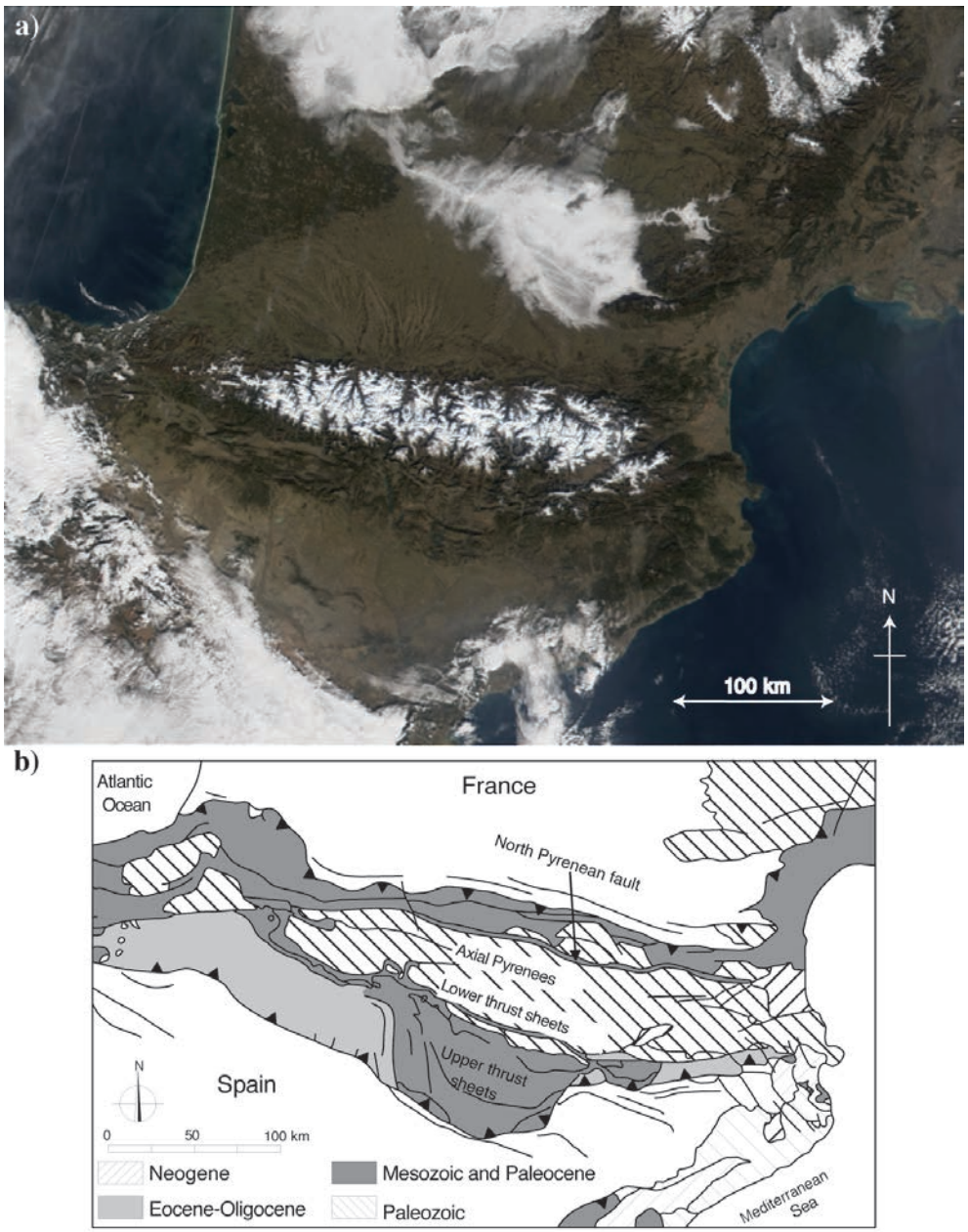

Figure I.4: a) The Pyrenees viewed from satellite, from 2002 (Credit: Jacques Descloitres, MODIS Land Rapid Response Team, NASA/GSFC - http://visibleearth.nasa.gov/view.php?id=57593) and b) Pyrenean geological context (After ECORS team 1988).

The Central-Eastern Pyrenees is the focus of this study. Its stratigraphy runs from Ordovician to Devonian, including Tardy-Hercynian intrusions (Fig. I.4b). The material making up the Pyrenees started to uplift some 40 million years ago (Muñoz 1992; Teixell 1998; ICC 2003). A dense and complex fault network also characterizes Pyrenean stratigraphy. There is however little tectonic activity,

and exhumation rates are low (Fitzgerald *et al.* 1999; Lynn 2005). Figure I.5 shows a look at the USGS seismic monitor website (IRIS, USGS) which confirms the historical trends in the region.

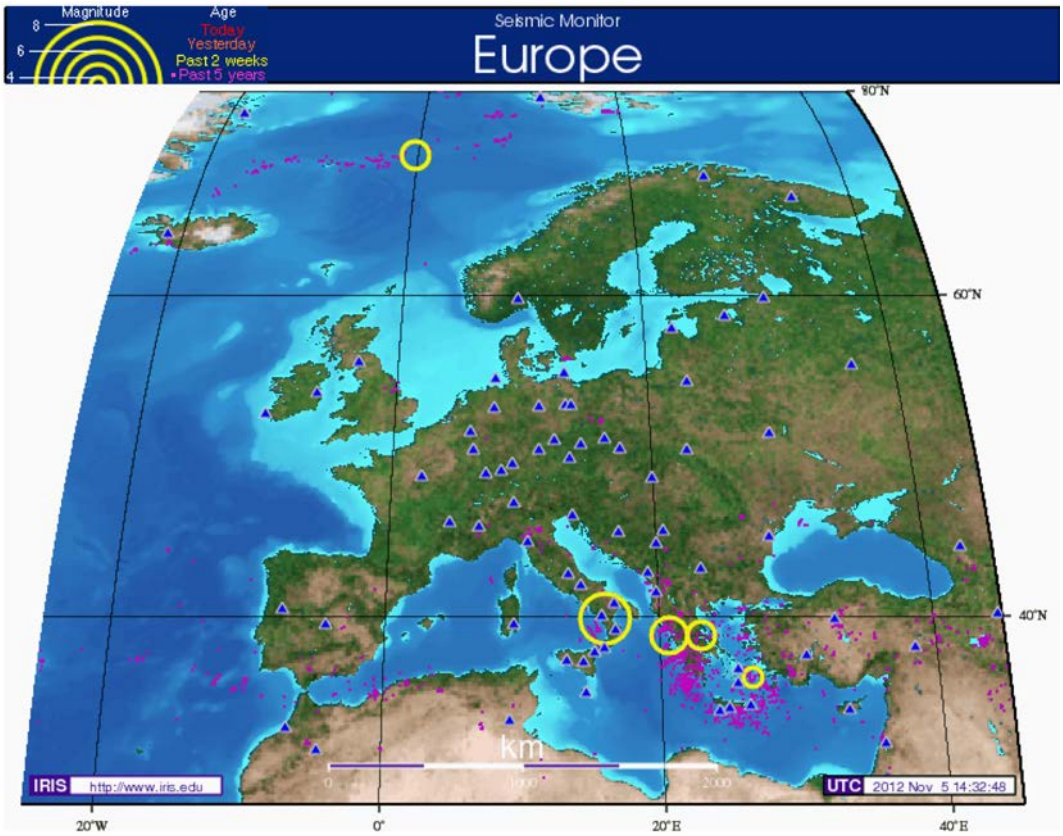

Figure I.5: Tectonic activity on the 5th of November 2012, going back to 5 years ago. Blue triangles are recording stations (http://www.iris.edu/seismon/ - 1/12/2012).

Pyrenean relief starts at sea level near eastern and western extremities, and reaches over 3400 metres above sea level (m asl). Past glaciations have generated U-shaped valleys and cirques in the landscape. These are signs of the erosion's power and extent of regional glaciers. Deglaciation forced the destabilisation of steep slopes during the last glacial cycle. Landslide activity is their current remnant and induces a discontinuous sequence of deposition, emphasized by colluviums lying over bedrock or tills (Fig. I.6). Those outcrops

are common in the Axial Pyrenees, which is, together with the pre-Pyrenees, comprehensively described by the ECORS Pyrenean Team (1988).

Dryness and convective storms characterise summers. During the rest of the year, humidity culminates in autumn with the highest precipitation periods. These extreme seasonal variations are the result of a latitudinal situation within a temperate zone (Cuadrat & Pita 1997; Martín & Olcina 2001). Yearly precipitation, ranging from 850 millimetres (mm) to 1200 mm, is influenced by a high relief combined with prevailing winds from the west and the proximity of the Mediterranean Sea. Concerning winds, a recent study showed that winds coming from the North West proved to be the most damaging in Catalonia (Peña *et al.* 2011).

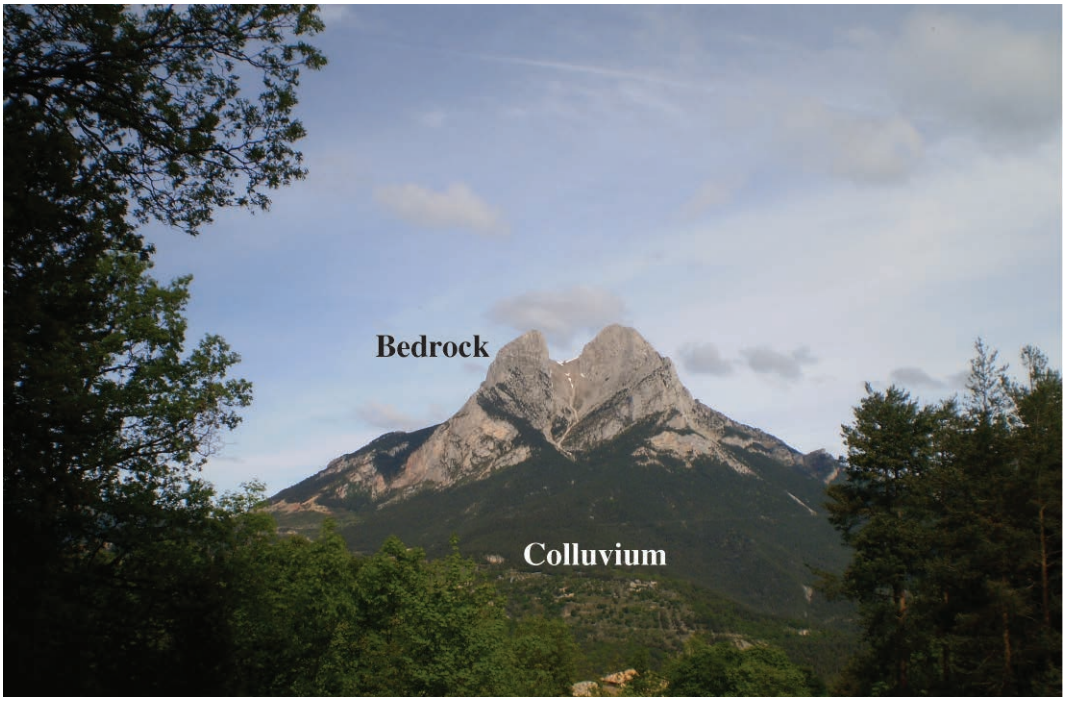

Figure I.6: Massif de la Pedraforca (in 2010), bedrock and colluvium.

Outline

This thesis summaries a three-year investigation of debris flows and their hazard assessment during which data from close to 4000 catchments have been gathered and treated; complemented by a detailed inventory of debris-flow prone catchments in four zones of the study area described. The progress made during this project provides new insights into statistical susceptibility models and the application of data mining techniques to a regional debris-flow hazard assessment.

Chapter 1 - The different themes tackled in this thesis are introduced in context of the current state-of-the-art. This first chapter explains the main themes of this thesis. It first describes debris flows and their associated hazard. Then the fundamentals of hazard assessments in regard to this thesis are presented. Follows the description of the idea behind susceptibility models. Finally dendrochronology and aerial pictures studies are proved useful in the study of debris flows.

Chapter 2 - Case studies of local debris flows spreading over the Central-Eastern Pyrenees are firstly examined. Then the steps leading to the creation of an inventory of past debris flows are detailed. The chapter accounts for the reconnaissance of debris-flow hazard.

Chapter 3 – Analysis of headwaters' morphometry is explored. The unit at which the study is carried out is detailed before the methodology used to gather the information provided. Then the results are shown and discussed.

Chapter 4 - The susceptibility analysis starts with the selection of the datasets, which is complemented by a statistical characterization of these datasets. The end part of this chapter focuses on models, from their elaboration to their evaluation, predicting the likely location of debris-flow activity.

Chapter 5 - Besides the modelling of debris-flow occurrences, the relationship between magnitude and frequency is to be known and documented. This chapter presents this relationship considering two Pyrenean case studies: El Rebaixader and Aigüestortes National Park. Study areas, methodologies and results can be found relative to each case.

A general conclusion is provided at the end of the thesis, taking into account each chapter, together with the future research outlooks that emerge from the current work. Moreover, after the conclusions, the last pages report the appendixes the author wanted to add in order to give the reader a supplement of information.

CHAPTER 1 STATE-OF-THE-ART

1.1. Introduction

The state-of-the-art is divided into 4 parts: what (erosional processes), where (reconnaissance), how (statistics) and how much, how often (frequency).

WHAT? Before entering the core of this thesis the concept of hazard assessment is tackled. Geological hazards, involving landscape's evolution are numerous. Erosion of mountainous ranges has multiple facets. From truly gigantic rock avalanches to microscopic silts' collisions, the scale of the erosional phenomena is extremely wide. Among them, debris flows form a family recognized to have enough power to sculpt the landscape. The first part of this chapter accounts for a description of this particular hazard.

WHERE? In this thesis, the landscape of the Central-eastern Pyrenees has been digitalized in a geographical information system (GIS). Headwaters' catchments have been computed and extracted. Thus enabling morphometric studies however, such morphometric studies are scarcely tackled. Forming the backbone of this thesis, it was necessary to understand the background before using it through the susceptibility analysis. For this reason, the second part focuses on past morphometric studies, and the common standards in the concepts.

HOW? Studying the susceptibility of the landscape toward geological hazards can be done following diverse methodologies, and different techniques. Before starting, one must be aware of the methods available and the techniques reproducible. Behind each method/technique hides a model, in this case a susceptibility model. The third part concentrates on susceptibility models found in the literature.

HOW MUCH, HOW OFTEN? Each environment has its own response to climatic stress, and its own rhythm. Various parts of the world have already supported studies that investigated the temporal occurrences of geological hazards, where frequency and magnitude are closely connected. This last chapter accounts for the link existing between frequency and magnitude, using data gathered from fieldwork at local scale or aerial pictures at regional scale.

1.2. Debris-flow hazard

1.2.1. Hazard

Hazard is commonly understood as a potential damaging physical event, phenomenon or human activity (ISDR 1999). It is a probability, relating frequency, intensity and location. Debris-flow hazard, to be fully considered, must, over a given pre-defined area, have a known frequency (events per year/decade/century), a known intensity (generally referred to as magnitude, based on volume) and a known location (prediction of the trigger's emplacement). In a hazard assessment, frequency and magnitude are generally tackled together, in what is called a frequency-magnitude (F-M) analysis whereas the study of the location is called the susceptibility analysis (or spatial occurrences' analysis in Guzzetti *et al.* 2005). The analysis of the susceptibility of the landscape toward any hazard, as well as F-M analysis, necessarily encompasses event inventories, field investigations and computer modelling (Jakob 2005b; Fuchs *et al.* 2008). As Guzzetti *et al.* (1999) emphasized, future activity is to occur following the same conditions that triggered it in the past so analyses of the landscape to report locations of past events form the backbone of

debris-flow and landslide susceptibility assessments (e.g. Guzzetti *et al.* 2005). In the literature, previous occurrences have been tackled following different themes. For instance, Godt & Coe (2007) studied alpine debris flows triggered in 1999 by a thunderstorm in the central Front Range (Colorado, USA) and link rainfall, topography and alpine soils. In Deb & El-Kadi (2009), the authors assessed the susceptibility of shallow landslides on Oahu (Hawaii, USA) through the use of the SINMAP model, which integrates a mechanistic infinite-slope stability model and a hydrological model. In the same area (Oahu, Hawaii, USA), Ellen *et al.* (1993) used topography to map debris-flow hazard. In Cannon *et al.* (2001), the authors relate wildfire and debris-flow initiation process in Colorado (USA). Berti & Simoni (2005) simulated the generation of channel runoff for the initiation of debris flows through a simple hydrological model, which proved capable of providing a physical basis for the understanding of debris-flow triggering threshold. In Brayshaw & Hassan (2009), debris-flow initiation and amount of material in gullies are linked. These are some of the possible themes likely to be tackled while studying debris flows and on which this thesis has abundantly got its inspiration.

1.2.2. Debris flows

Debris-flow hazard poses a substantial threat in mountainous environments (Hungr *et al.* 1984; Iverson 1997). Damages, consequences of debris-flow events are numerous and spread worldwide (in Coussot & Meunier (1996): *"from Scotland to China"*). To name but one example from the literature, in Hungr *et al.* (1984), occurrence of debris flows through the Canadian Rockies is reported to be reasonably frequent, or at least not infrequent. The European Alps (Italy, France, Switzerland, Austria) have suffered (and still suffer) countless debris-flow events. Issued from this thesis is the example of the Custom House of Andorra, which suffered a debris-flow event in 2008, fortunately at night and therefore, few casualties. Before starting this thesis, personal experiences also led the author to encounter an historic debris-flow prone site on the West coast of the South island of New Zealand, eventually promoting the idea that the

phenomenon is truly widespread in mountainous environments of all geological and geomorphological settings.

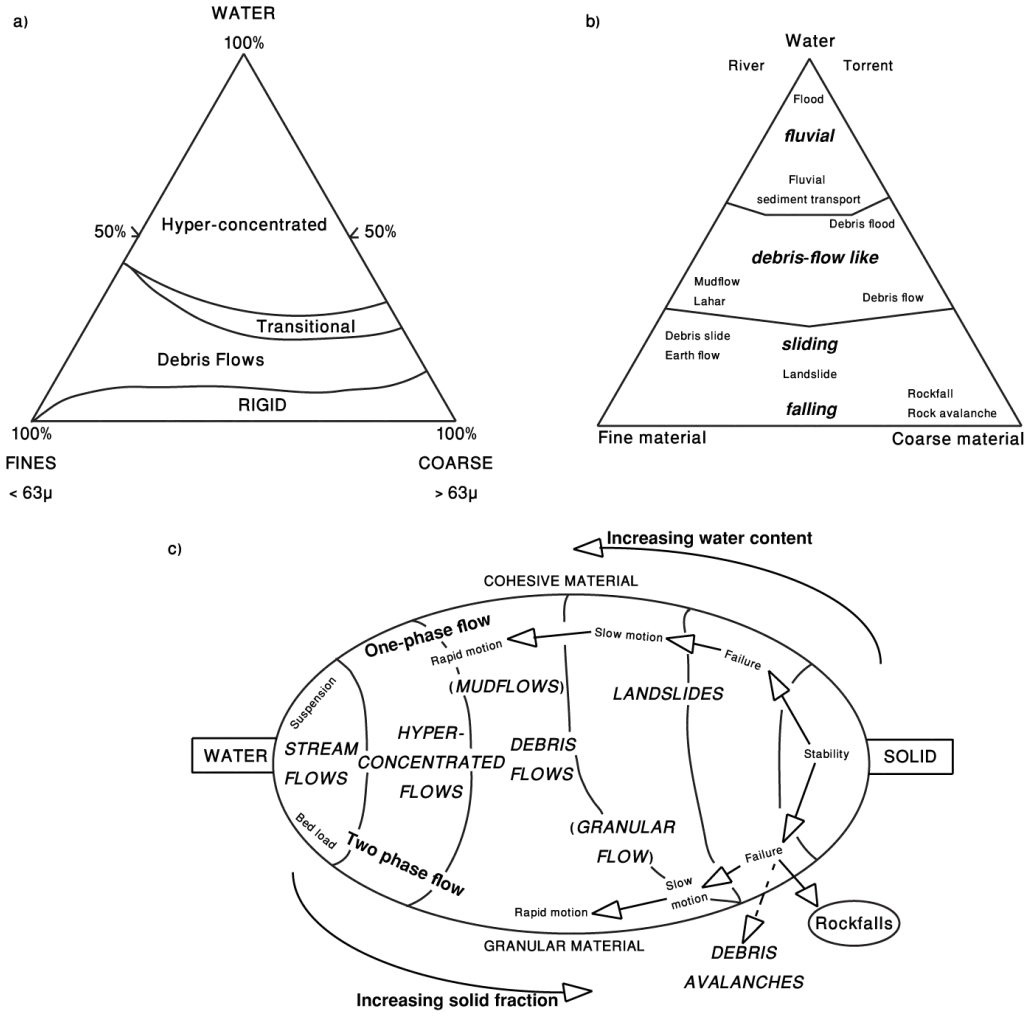

Figure 1.1: a) Three-phase diagram of Bullock Creek and Tarndale Slip debris flow materials. Textural zones are partly based on Pierson & Scott's (1985) terminology (Phillips & Davies 1991); b) Phase diagram of torrential mass movements, modified after Phillips & Davies (1991) (Scheidl 2009); c) Classification of mass movements on steep slopes as a function of solid fraction and material type (Coussot & Meunier 1996).

Figure 1.1 shows 3 diagrams: 2 phase diagrams (Fig. 1.1a & b) and a classification of mass movements on steep slopes (Fig. 1.1c). Figure 1.1a is a three-phase diagram that was edited after the study of the material of 2 debris flows. Domains of existence of hyper-concentrated flows and debris flows can be

found together with a transitional zone and rigid texture's zone. Figure 1.1b shows a similar diagram (as Fig. 1.1a) but concern torrential mass movements. Regarding debris flow, it appears that the domain of existence is found at higher quantity of water. The 2 debris flows from Figure. 1.1a proved less watery than the general vision of debris-flow events. Moreover, in Figure 1.1b, one can see that different processes have similar properties and domain of existence as debris flows. They are called debris-flow like processes and encompass debris flows, mudflows, lahars and debris floods. Figure 1.1c shows a classification of mass movements on steep slopes as a function of a solid fraction and material type. All these diagrams pledge for a continuity between torrential mass movements and show that care is needed when dealing with debris flows (the process is not to be confounded with the debris-flow like processes' family).

Figure 1.2: Debris-flow torrent in Hari Hari, West coast, New Zealand.

Debris flows develop when water and material in adequate proportion travel downhill (Bovis & Jakob 1999). From the different diagrams making up Figure 1.1, one can understand why no finer estimations than in adequate proportion are possible. Phenomena mixing water and sediments (either coarse or fine) are continuous (no clear limits exist), thus it is not scarce that an initial landslide develops in debris flow in the first stages of the event and end up provoking a flood, when sufficient water has been involved.

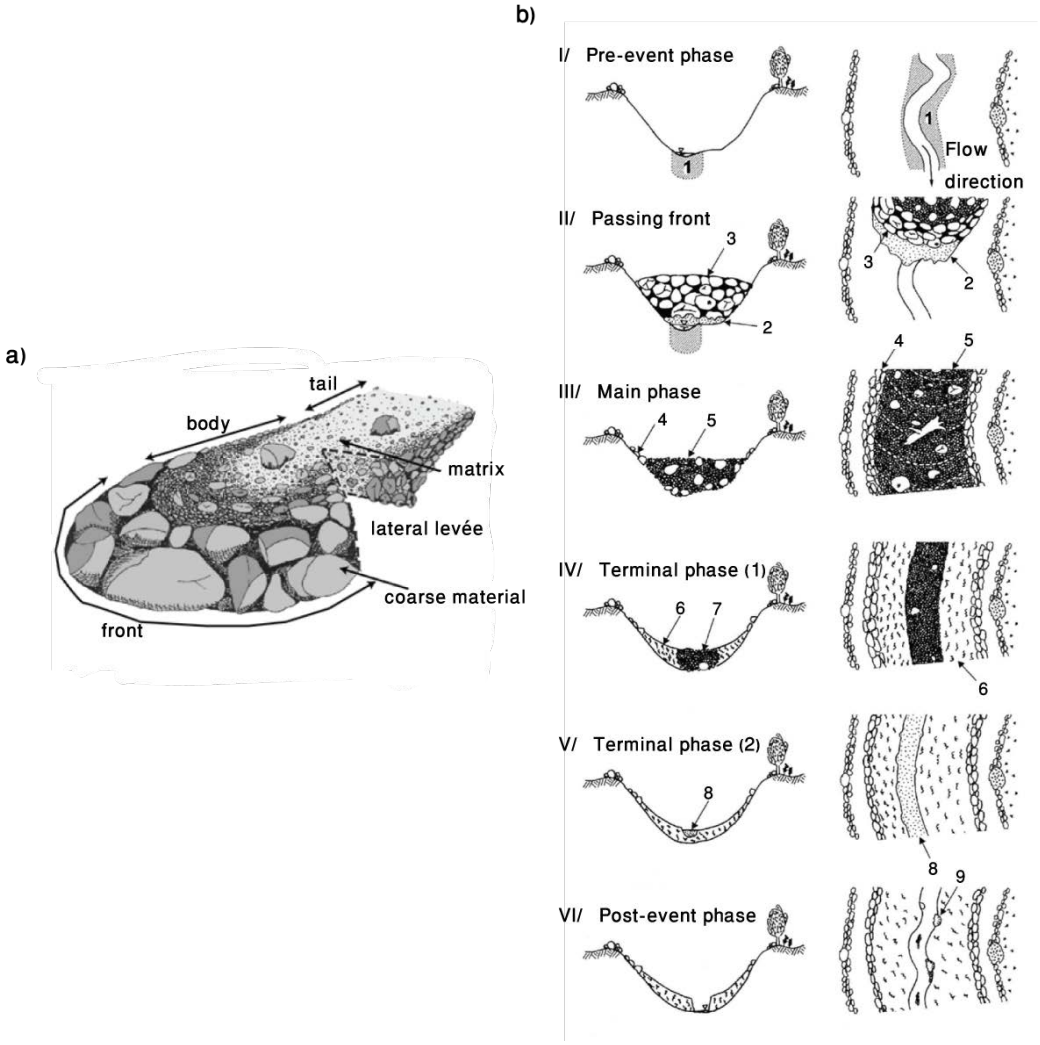

Figure 1.3: a) Functional entities of a debris flow, after Bardou (2002) (in Remaître 2006); b) Different phases of a debris flow, after Bardou (2002) (in Remaître 2006).

Solid and fluid forces must act in concert to produce them, unlike avalanches and floods, which respectively involve grain forces and fluid forces in their physics (Iverson 1997). However, debris flows display features of its own, which help differentiate them from other phenomena. Generally debris flows are made of poorly sorted, water-saturated sediment, with grain size ranging from clay to boulders (Fig. 1.2). Debris flows invariably move as pulses or even surges; steady, uniform flow is seldom, if ever it occurs. When multiple surges occur in individual debris flows, each exhibits a conspicuous head and tail (Fig. 1.3a). Sketching the phenomenon is not part of this work, nor is the description of the successive phases while propagating through the torrent (Fig. 1.3b), but such reproduction can be found in Davies (1986), Hungr *et al.* (2001) or Bardou (2002) and the whole process is extensively explained in Remaître (2006).

Figure 1.4: Lateral levees in Rebaixader torrent, pointed at by blue arrows; the black arrow shows the flow direction.

Volumes involved are spanning a large range of values, from some tens to many millions cubic meters. Solid fraction ranges from 50 to 90% in general, and velocity from 0.5 to 20 m/s being reported (possibly reaching 30 m/s for the bouldery front – Costa 1984; Rickenmann 1999). Debris flows are reported here to take the form of rapid surges flowing over long distances in stream channels. The presence of lateral levees in streams is due to a fluid flow depth decrease from the front to the tail of the surge (Fig. 1.3). The theme of the lateral levees is further studied in Felix & Thomas (2004), where formation and propagation in pyroclastic deposits have been studied. The levees result from the combination between lateral static zones on each border of the flow and the drainage of the central part of the flow after the supply stops. A link between deposit morphology and parameters of the dynamics of the flow exist and parameters like thickness of the channel, or height of the levees, or width of the deposit, can be related to flux, or velocity, or height of the flow. It leads to the possibility to study flow dynamics from only measurements of the deposit.

Debris-flow occurrence and recurrence leave traces in the landscape (Coussot & Meunier 1996) that are generally found at high elevation and high slope (Rickenmann 1997), likely to follow and stay confined in established channels (Hungr *et al.* 2001) (Fig. 1.4 & 1.5).

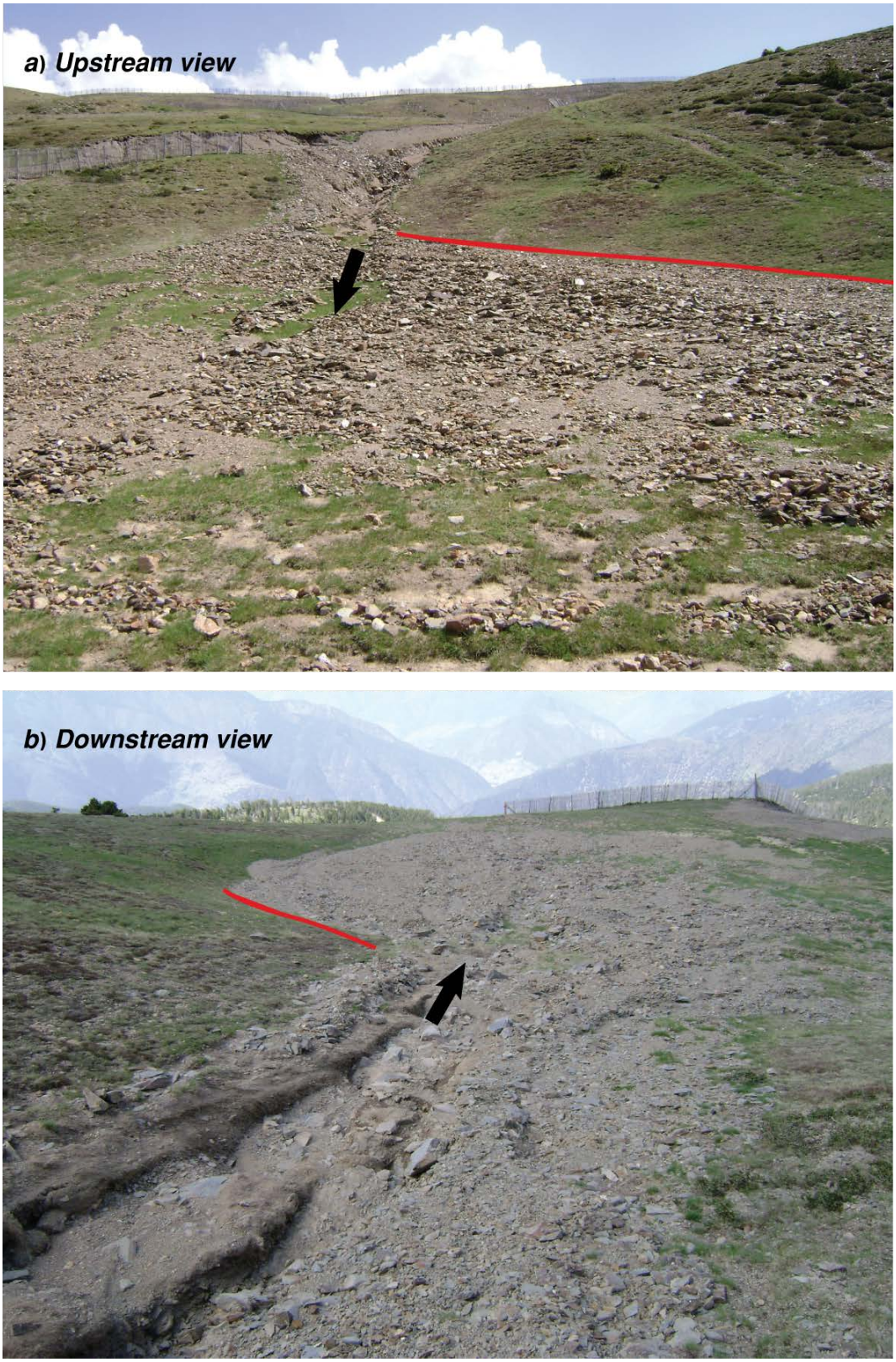

Figure 1.5: Small-scale debris flow, example found in Port-Aîné (2009); a) upstream view; b) downstream view.

1.2.3. Classification

The term debris flow is first mentioned in Varnes (1954), and further refined in 1978, where a classification of mass movements is proposed. It is based on two terms: the first describes the material and the second the type of movement. In Davies (1986) debris flows are treated as "*a macroviscous flow of large stones in a slurry of fine solids in water*", if characteristics such as boulder transport, deep bed erosion and intermittent jamming (causing surges) are to be explained. Still from the same author, debris flows are due to the conjunction of small-scale bank slides or collapses, bed erosion and solid transport. In Pierson & Costa (1987), the different kinds of flow are classified and the definition of debris flows, following this classification, is found in Table 1.1.

Table 1.1: Debris-flow characteristics as in Pierson & Costa (1987).

Fluid type	non-Newtonian
Interstitial fluid	water + fines
Flow category	slurry flow
Flow behaviour	plastic

In Hutchinson (1988) debris flows are part of the debris movements of flow-like form, which also includes mudslides and other flow slides. They are characterized by, very to extremely rapid flows of wet debris. When involving weathered rock debris, hillslope debris flows and channelized debris flows can be distinguished (Fig. 1.6). In Cruden & Varnes (1996), the classification elaborated in Varnes (1978) is further refined in introducing a multi-dimensional taxonomic framework and two classes emerge now for debris flows, instead of the only class of 1978: Open debris flows, creating their own path and a sinuous channel, are opposed to channelized (debris) flows, following existing channels and often occurring during torrential runoff. It unsurprisingly corresponds to the two classes Hutchinson highlighted in 1988. In Coussot &

Meunier (1996), solid fraction and material type are the parameters on which a distinction of flow and mass movements in mountain areas are elaborated. Based on the difference in the initiation, Coussot & Meunier (1996) also recognized two main classes: debris flows issued from a landslide and debris flows issued from the surficial erosion of the stream basin. They closely relate to the two classes previously envisaged.

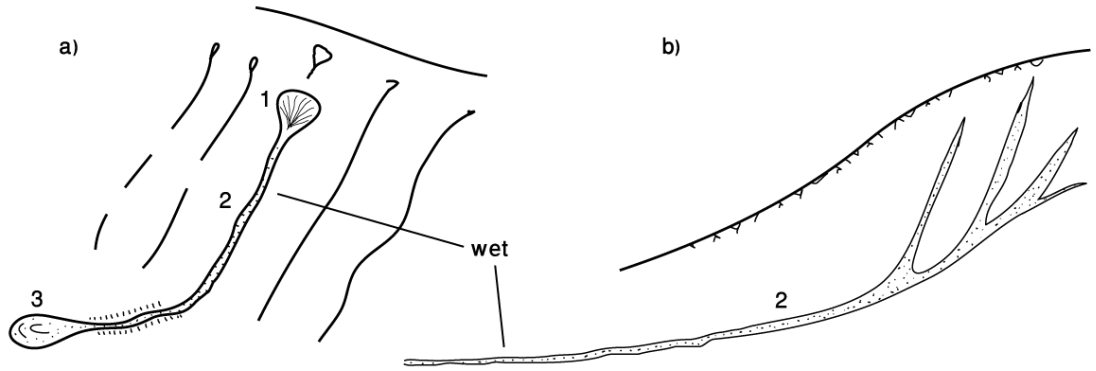

Figure 1.6: Main types of debris flows from Hutchinson (1988). a) Hillslope debris flow and b) channelized debris flows (after Hutchinson (1988)). 1) Initiation zone, 2) transit zone and 3) depositional zone.

Criteria other than material and type have also been used to distinguish between mass movements. Jakob (2005a) argues that a classification that incorporates size characteristics could be used in regional studies. The variables proposed in this study include; debris flows volume, peak discharge and area inundated, and a description of potential consequences to estimate the magnitude. The classification applies to volcanic and bouldery debris flows. It defines 10 classes, ranging, for instance in volume, from less than 10^2 m^3 to over 10^9. Potential consequences, for class 1, are very localized, known to have killed forestry workers in small gullies and damaged small buildings. For class 10, the potential consequences include vast and complete destruction over hundreds of km^2. This type of classification, rather straightforward is nonetheless regarded as very

hazardous when extrapolated to interregional studies (Coussot & Meunier 1996).

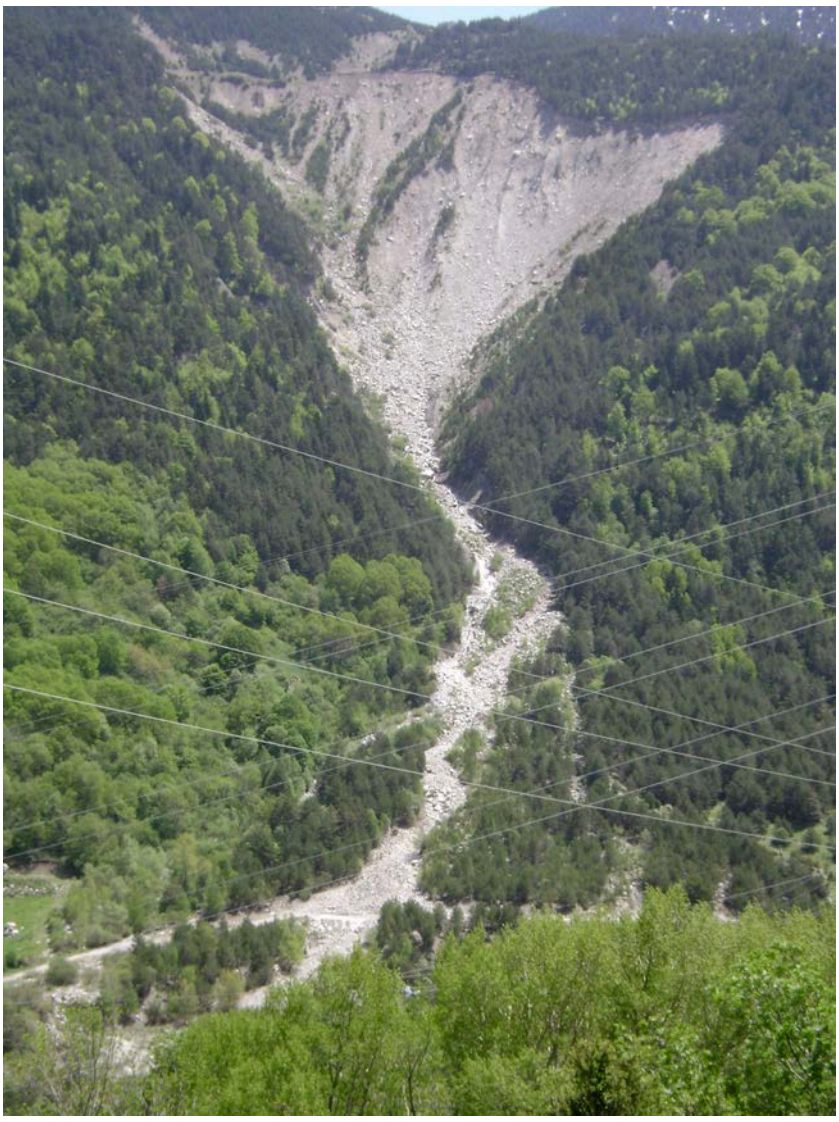

Figure 1.7: Typical debris-flow catchment (Rebaixader torrent, Eastern Pyrenees, Spain): Initiation zone, channel and fan.

Eventually, the definition of debris flows considered in this thesis follows that of Hungr *et al.* (2001). Ultimately it is a classification widely used in the literature. The definition proposed is short, clear and detailed, and answers what is a debris flow and how to recognize them on the field. From the beginning, it states that

the terminology is inconsistent and definitions of landslide's type ambiguous, thus "common types of flow-like mass movements have become entrenched in the language of engineering geology". In a nutshell, for debris flows, the material involved is debris (remains of geological activities) possibly accompanied by organic matter (for instance remnants of trees or shrubs), saturated with water. Debris flows propagate through established channels (Fig. 1.7). Established channels are to be understood as exhibiting the presence of a defined channel over a large part of the path, and an established deposition landform (fan). Debris flow is a recurrent phenomenon within its path, while debris avalanche is not. The content of water is increasing as the flow travels down, relative to in-situ source material. Velocities are reported to be extremely rapid. Thus, quoting from the original, "debris flow is a very to extremely rapid flow of saturated non-plastic debris in a steep channel (Plasticity Index superior to 5% in sand and finer fractions)" (Hungr *et al.* 2001). A recent update of this definition of debris flow can be found in Hungr *et al.* (2012).

1.3. Debris-flow analysis by morpho-fluvial approaches

Debris flows are recurrent within their path. As opposed to debris avalanches, debris flows create, follow and dig established channels. Thus, in a debris-flow prone landscape, development and propagation of the phenomena induce the presence of channels or streams. Catchments are a geographical notion designating the ensemble of a basin draining superficial water toward a main stream (Fig. 1.8). They include superficial water as well as subterraneous water.

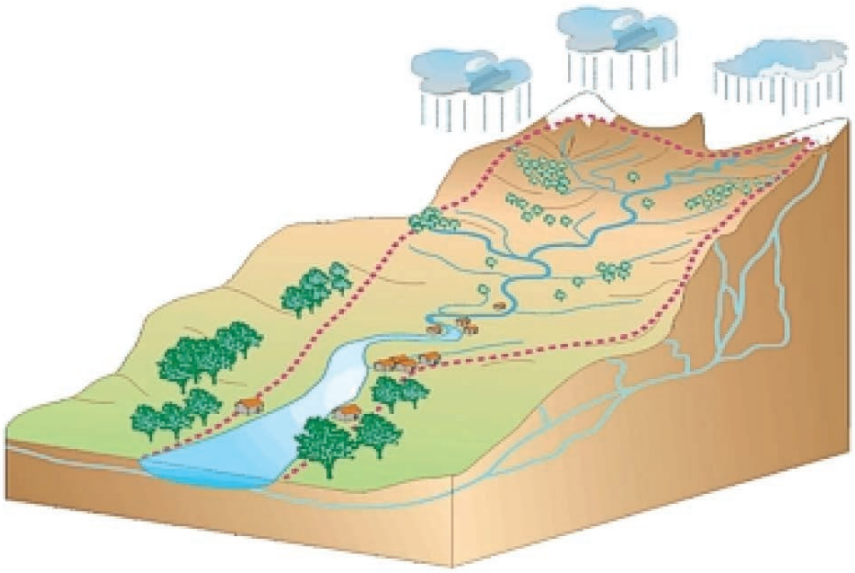

Figure 1.8: Sketch representing what is understood as a catchment, contained within the red dots (EPIDOR 2006).

One catchment includes one main stream and many tributaries. As soon as a stream is created, a catchment can be related. Every drop that falls in the catchment ultimately feeds stream's water, following gravity forces and terrain irregularities. It is thus reasonable to suggest that the study of debris-flow landscape can be related to the study of channels, and thus catchments. Fortunately, study of catchments and geomorphology have been linked. Numerous researchers worldwide focus on the subject and many ways of apprehending their association have been described. In Strahler (1957), the author studied quantitative watershed geomorphology. Melton (1965) studied the significance of alluvial deposits on morphologic and paleoclimatic points of view. White *el al.* (1996) studied the sediment transport rates in a small high mountain catchment. Lin & Ogushi (2006) used analysis of digital elevation model (DEM) to characterize longitudinal and transverse profiles of steep mountainous watersheds. Recently Perucca & Angilieri (2011) evaluated flash-flood hazard and hydrological aspects of a torrential regime basin through a morphometric characterization.

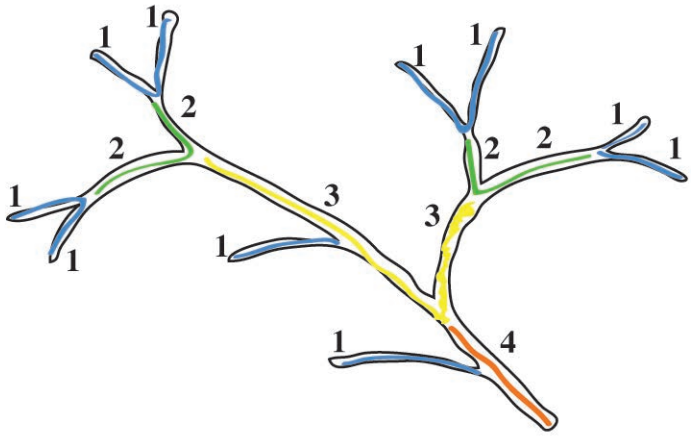

Figure 1.9: Notion of stream orders as defined by Strahler (1952).

Streams have historically been characterized in terms of order (Fig. 1.9). Two systems exist: the one from Strahler (1952; 1957) and the one from Horton (1945). It consists of defining the size of the stream based on the hierarchy of tributaries. A drainage system originates with a stream of order 1. When two streams of order 1 meet, the continuing stream become a stream of order 2. Two 2nd-order streams, when they meet, give birth to a 3rd-order stream. When a stream of order 1 meets a stream of order 2, the continuing stream doesn't change its order (same logic applies for a 2nd-order stream meeting a 3rd-order stream). Originally applied to stream, the use of orders can be extended to catchments. For instance, a stream of order 3 is to be related to a catchment of order 3: The stream of order X is found within the corresponding catchment of order X.

Geographical information systems are a common tool in landscape evolution's studies as it allows the digitalization of the landscape and the management of large quantity of information. Features in the landscape can thus be studied focusing on different themes such as tectonic (Jordan *et al.* 2005; Font *et al.* 2010), glacial geomorphology (Napieralski *et al.* 2007), debris-flow fans morphometry (Staley *et al.* 2005; Welsh & Davies 2010) to name but a few.

Investigations on catchments and streams have already benefitted from such tool's use (Lopez-Vicente *et al.* 2009). However few tackle Central-Eastern Pyrenees' landscape.

Extracting numerical parameters through GIS techniques is frequent in catchments studies (Obi Reddy *et al.* 2004; Ng 2006; Ames *et al* 2009; Kar *et al.* 2009). The list of gatherable parameters is endless and the interest in a given parameter may differ depending on the site and the goals of the study. Combinations are numerous but certain past studies can help restrain the choice. For instance, for debris-flow hazard analysis on a fan, the Melton ratio of a catchment, together with the mean slope of the fan, reveals itself of importance (Kostaschuk *et al.* 1986). The choice of the Melton ratio may be of interest when studying debris-flows occurrences in catchments.

The south facing half of the Pyrenees has often been the playground of researchers studying fluvial activity and requiring morphometric data (Cammeraat 2002; Bathurst *et al.* 2007; Lana-Renault & Regües 2009). Among them is White *et al.* (1996) who investigated sediment transport rates in a small high-mountain catchment in the Central Pyrenees. The purpose of the studies cited above and focusing on Pyrenean landscapes, varies from one study to the other, when the unit/zone of study is frequently scaled to fit a (few) catchment(s) (Seeger *et al.* 2004; Garcia-Ruiz *et al*. 2005; Ng 2006; Kiel *et al.* 2010). It is facilitated by the easy manipulation of GIS information for such a geographical extent or the time required for the calculations to be performed. Generally the smaller the scale, the more details are caught, and it often appears in the grid size of the DEM used.

In the case presented in this thesis, the choice was between DEM's grids of 30m or 5m. As a regional scale, the use of 30m's grids fitted fine. Information would have been quickly gathered. However, the thesis needed a certain degree of precision that only the 5m DEM could give. The effect of its use was first noticed on the time required to gather the information - if quickly applies to the time of calculation over 30m grids, thus very long suits 5m grids'. That could contribute

to the scarcity of small-scaled studies in the literature. From the studies of Cammeraat (2002) and Dragut *et al.* (2011), it appears that complications may emerge from the complexity of scales in morphometric studies involving a large study area.

However, such studies do exist. Bhagwat *et al.* (2011) has investigated spatial variations through the characterization of 5th-order catchments. Strager *et al.* (2010) used a GIS interface to support decision-making, thanks to the watersheds' characterization, by analysing their hydrology. Erkeling *et al.* (2010) looked at the morphometry of dendritic valleys on Mars. Closer to us, Spain and the Pyrenees have never been studied at a regional scale, nor characterized the way that has been done in this work.

Generally, four landslide zoning maps' scales are considered, depending on the indicative range of scales and the typical area of zoning (Fell *et al.* 2008): detailed, large, medium and small. Catchment's scale is often referred to as detailed, and Guzzetti *et al.* (2006) reports that statistics are best suited to large areas/small scale landslides susceptibility's studies.

Without making a history of fluvial studies, it appears that the mid-fifties (50's) mark a turn in describing and modelling fluvial systems (Horton 1945; Strahler 1952; Schumm 1956; Chorley 1966). Still in today's study drainage basins are often considered as a fundamental geomorphic unit (Coehlo-Netto *et al.* 2006). Occurrences of debris flows are by definition concomitant to the presence of this fundamental geomorphic unit. Debris-flow hazard assessment is unsurprisingly abundantly tackled at a very detailed scale, that of a catchment (Okunishi & Suwa 2001; Bacchini & Zannoni 2003; Melelli & Taramelli 2004; Catani *et al.* 2005). It is however not limited to this scale and Liu *et al.* (2002) is an example of a regional study. This thesis is another example.

1.4. Susceptibility models

In many cases, susceptibility is performed, based on field inventory mapping or heuristic classification of the terrain. However, it can benefit from computer modelling (e.g. Jakob 2005b). Analyses of the landscape to report locations of past events are numerous and form the backbone of debris-flows and landslides susceptibility assessments. Moreover, many different approaches have been envisaged for landslides (Guzzetti *et al.* 2006) including the linkage between geomorphology and debris flows (Glade 2005).

Debris-flow susceptibility models imply the use of meaningful parameters gathered from past events and appropriate to describe the phenomenon (e.g. Iverson 1997), and aim at predicting the location of future activity. Morphometric indicators have already proved to greatly contribute to landslides studies, thanks to their easy determination Models have been developed following this trend for debris-flow hazard (Coe *et al.* 2004; Chen & Yu 2011).

Models performance is an issue emerging with the increasing numbers of models found in the literature. Estimation of models quality, comparisons between models and evaluation of their performance have been the focus of recent studies for debris-flow and landslide susceptibility (Guzzetti *et al.* 2006; Carrara *et al.* 2008; Frattini *et al.* 2010). In Guzzetti *et al.* (2006), a discriminant analysis of 46 thematic variables using the presence of shallow landslides, obtained from a multi-temporal inventory map as the dependent variable for statistical analysis, classified 77% of the mapping units correctly. It led to the study of the model's reliability (role of variables) and sensitivity (changes in the input data). Eventually two other, more recent, inventory maps were confronted to the model, which was found capable of predicting the newly triggered landslides. In Carrara *et al.* (2008), statistical and physically based debris-flow susceptibility models have been compared in terms of performance, which was evaluated from the percentages of terrain units that each model correctly classifies, the number of debris flows falling within the area classified as unstable by each model, and through the metric of receiver operating characteristic (ROC) curves (see

chapter 4 for details). In Frattini *et al.* (2010), the models investigated in Carrara *et al.* (2008) serve as a base to a series of techniques for evaluating the performance of susceptibility models. It shows that simple statistics can be problematic, and that ROC curves can be used to efficiently visualize and compare the performance of models.

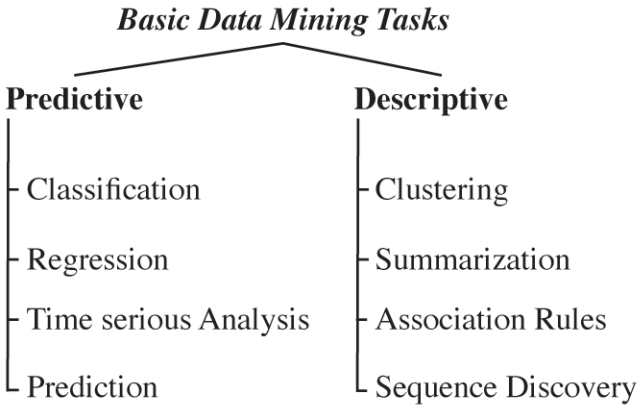

Figure 1.10: List of the basic data mining tasks, inspired from BigDataNerd (2011).

When compared to complex statistical models (Chung & Fabbri 2003; Remondo *et al.* 2003), simple, heuristic methodologies and analyses of landslides susceptibility seem to give a similar level of performance (Guinau *et al.* 2005), which however doesn't imply a similar spatial distribution observed in the resulting maps (Sterlacchini *et al.* 2011).

In this thesis, predictive data mining techniques were applied. Data mining is defined as the process of discovering patterns in data (Witten *et al.* 2011), which consists in analysing data from different perspectives and summarising it into useful information. Two main tasks are generally recognised: prediction and description (Fig. 1.10). These techniques have the advantage to permit the treatment of a large quantity of data and classification trees simplify vision given to results (Wan *et al.* 2008; Wan & Lei 2009). Trees are not common in literature,

as opposed to matrices (Fawcett 2006; Frattini *et al.* 2010). Supporting modelling results and assessing robustness of the models are facilitated by these techniques, because success and prediction rate curves are easily gathered (e.g. Santacana *et al.* 2003). Care and attention are nonetheless necessary when interpreting these results (Blahut *et al.* 2010).

Pyrenean shallow landslides susceptibility studies already benefitted from past studies (Baeza & Corominas 2001; Baeza *et al.* 2010). Most of these studies consider a regional scale and use a statistical approach. They have guided the work presented in this thesis.

1.5. Magnitude-frequency analysis of debris flows: Dendrochronology and aerial pictures studies

Dating landslides can be achieved following different techniques. The most common way is to use radiocarbon dating, which is based on the chemical abundance of ^{13}C over ^{14}C, on organic latter in or on the deposit. Other compounds can also be used (for instance ^{11}Be). Often expensive, these methods demand an access to radiochronology laboratories. They have the advantage of giving an absolute age but proved difficult with the calibration, particularly with ^{14}C in young deposits. However, alternative methods exist such as dating the living vegetation: trees and lichens. Again, the results are an absolute age, but the uncertainty on the age given is likely to be greater (compared to radiochronology). Beside absolute ages, relative age can also be sought by comparing the deposit to the surrounding surfaces. In this case the result is an order of deposition, based on stratigraphic and structural relationships encountered in the field. In this thesis, absolute ages have been used for determining frequency and magnitude of past events, although relative dating techniques were also considered in assessing the magnitude.

Debris flows leave traces in the landscape and vegetation: landslide scars, incised channels, depositional areas (possibly overlapping each other), lateral levees, bent or wounded trees. Thanks to dendrogeochronological techniques, it is

possible to date the traces left on trees, and their cohorts, growing on the fan (Fig. 1.11). Dendrogeochronology is the application and interpretation of tree ring analysis to the study of geomorphic processes (Alestalo 1971). Past studies have shown the adequacy of such techniques when debris flows are involved (Stoffel *et al.* 2006; Stoffel & Bollschweiler 2008; Bollschweiler *et al.* 2008; Corominas & Moya 2010). However, trees do not hold all the information. The study of aerial pictures of different ages can also highlight activity not visible in the field, or confirm activity inferred from field studies. It mostly helps with depositional areas (or fans) thanks to the difference in ground's reflection of sunlight. The comparative study of aerial pictures is a common tool in geomorphological studies (e.g. Chevalier *et al.* 2009).

Figure 1.11: Coring of trees in progress, (Hari Hari, New Zealand, 2007). Credit: L. Barlow.

From these two techniques, it is possible to work out the years of activity and the extent of the activity. In other words, what is dealt with is frequency and size (or magnitude) of a process. The relationship between the magnitude and the frequency of an active erosional process is fundamental information. It is often referred to as M-F relationships. Landslide hazard and risk assessments rely on its accuracy. Thus, for a comprehensible debris-flow assessment, data on magnitude and frequency distribution are crucial (Jakob & Hungr 2005). There are different types of M-F relationships, but the most common represents magnitude versus cumulative frequency, MCF (e.g. Guzzetti *et al.* 2005; Hungr *et al.* 2008). The general form of this MCF relationship is equivalent to a power law and can be given by:

$$F_{cum} = aM^{-b} \quad (1.1)$$

where F_{cum} is the cumulative frequency, M the magnitude, a and b are two constants.

Curves representing M-F relationships can be easily created. At local scale it can be done thanks to dating techniques such as dendrogeochronology (e.g. Corominas & Moya 2010). At regional scale, Malamud *et al*. (2004) counsel the use of landslide inventories.

While many research studies have been published on general landslides types, especially on rockfalls (e.g. Hungr *et al.* 1999; Brardinoni & Church 2004; Malamud *et al.* 2004; Guzzetti *et al.* 2005), less effort has been carried out to increase knowledge on debris-flow M-F relationships at regional scale (Guthrie & Evans 2004; Hungr *et al.* 2008). In addition, there are various studies applying dendrochronology at catchment scale to obtain a local debris-flow M–F curve (Bollschweiler *et al.* 2007; Corominas & Moya 2010; Jakob & Friele 2010).

1.6. Conclusive reminder

This first chapter accounts for the state-of-the-art relative to the work tackled in this thesis.

Debris flows are a common and widespread erosional process in mountainous environments. Made from a mixture of water and debris, a debris flow exhibits specific physical properties that enable the debris flow to be recognized from other geological hazards. Moreover, debris-flow term also refers to as the physical characteristics from a flow of water and debris. Debris-flow behaviour is not reserved to debris flows. Hyper-concentrated flows or lahars may have the same physical properties as debris flows. However, they cannot be called debris flows because of crucial differences in the processes, like the quantitative ratio water/debris of the flow or the context of flow's occurrence (where/when/how) or the quantity of clay in the flow. This thesis focuses on debris flows only.

The aim of this thesis is to apprehend debris flows in such a way that it allowed the study of a rather large area. Most of debris-flow studies are worked out at local scale (or small area). It permits to study the debris flow itself in its environment of occurrence, often a catchment. Thus the debris flow is tackled in reference to a catchment. In the case of this thesis, this vision was unrealistic, given the size of the study area. Debris flows are tackled here through catchments in reference to a landscape. In that case large areas are not a problem. Moreover, studying debris-flow spatial occurrences through catchments made possible to characterize the landscape thanks to morphometry. Extracting topographical and morphological data is not new and reveals itself of interest when debris flows are to be tackled at a small scale. This thesis focuses on headwaters' catchments.

Once the phenomenon and the unit at which it will be studied have been defined, one must envisage the methods/techniques offered to compose the best salad with the ingredients at hand. The benefits of statistics have been shown when debris-flow susceptibility is analysed. In this thesis the study of fluvio-morphological parameters relative to headwaters' catchments is associated to data mining techniques. Originally used when big quantities of data are to be studied, data mining has been chosen because it offers different statistical approaches. Moreover, although the whole process associated to data mining is rather complicated, the output is fairly easy to visualize and process. This study applied data mining techniques to work out the susceptibility.

After determining the likely spatial occurrences of debris flows, the next step of the thesis is to assess the frequency of occurrence. Two ways can be considered: at local scale or at regional scale. The techniques used differ depending on the scale. In this study, both scales are inspected. Dendrochronological data from field studies and aerial pictures' comparisons revealed two interesting ways to determine when past debris flows occurred, especially when no information is obtainable from an already existing, detailed inventory. This approach takes into consideration frequency, but also magnitude. This thesis investigates magnitude-frequency relationships for debris flows in headwaters catchments.

The axes of research related to this thesis have been introduced in this chapter. The following chapters of this thesis will show how these considerations are gathered and mixed in order to come up with a hazard assessment.

CHAPTER 2 RECONNAISSANCE OF DEBRIS-FLOW HAZARD

2.1. Introduction

In the Central-Eastern Pyrenees, shallow landslides and debris flows are not as widely reported as in other mountainous catchments. However, they represent a non-negligible hazard that should be assessed. Until now, most of the local descriptions or analyses focused on shallow landslides and have been carried out at regional scale, applying geographical information system (GIS) techniques (e.g. Baeza & Corominas 2001; Santacana *et al.* 2003), involving inventory data (Gallart & Clotet 1988) or elaborating models (Bathurst *et al.* 2006). Additionally, most of these studies focus on failures triggered during one particular event: the catastrophic 1982 rainstorm. Recent years' scarce investigations of local debris flows led to a lack of information as well as research on debris-flow initiation, behaviour and hazard in the Eastern Pyrenees. Only in the Principality of Andorra has this analysis been carried out on debris-flow hazards for urban planning's purposes (Hürlimann *et al.* 2006).

During the summer of 2008, several mass movements occurred and caused important damages to infrastructures and economic losses in the Central-eastern Pyrenees. The first part of this chapter is a study of 5 of these 2008 debris flows, which helped in elaborating a series of criteria in which an inventory has been

based. This inventory is presented in the second part of the chapter. A multi-temporal inventory was sought to better render the susceptibility further detailed. 1) Pre-existing databases were filtered (because not only debris flows were tackled) and debris flows retained and 2) the rest of the debris flows makes up the forthcoming inventory that follows criteria of recognition that cannot allow to precisely date the trigger.

The goal of this chapter is to present recent local debris-flow activity, as well as to present the way the database necessary to assess the susceptibility of the landscape toward debris flows was prepared, taking into account past events and observable features in the landscape.

2.2. Analysis of 2008 debris flows

2.2.1. Events description

This section accounts for an interdisciplinary description of 5 debris flows (Fig. 2.1).

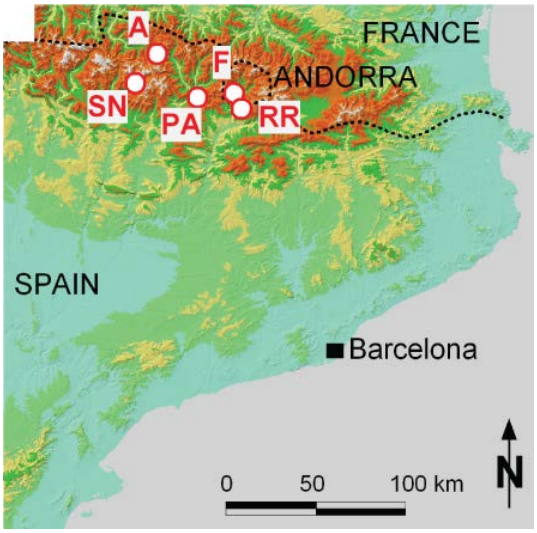

Figure 2.1: Location of the 5 debris flows. A: Andreuet; F: Fontanals del Pui; PA: Portaîné; RR: Riu Runer; SN: Sant Nicolau.

Geology, morphology, hydrology, elements at risk, damages and process description are reported, for each event. It focuses first on in-channel debris flows; then landslide triggered debris flows are tackled. Data used in these parts are presented in Table 2.1, which were gathered through the study of aerial pictures and topographic maps, as well as archives like newspapers or administrative reports or field observations.

Table 2.1: Geomorphological parameters, assessed by field observations (volumes), topographic maps, aerial pictures and archives.

	Riu Runer	*Fontanals del Pui*	*Portaîné*	*Andreuet*	*Sant Nicolau*
Volume (m3)	14000	1500	26000	1000	1800
Catchment area (km² - from apex)	8.2	0.2	5.5	0.029	0.26
Orientation	W	ESE	N	S	S
*Maximum/minimum elevation (m asl) **	2150/ 885	1240/ 950	2400/ 975	1975/ 1550	1985/ 1480
Mean slope angle of fan (degree)	11	13	9	10	10
Mean slope angle of channel (degree)	13	37	16	32	35
Runout, L (m)	5175	710	4400	890	995
Vertical drop, H (m)	1154	290	1155	425	505
H/L (-)	0.22	0.41	0.26	0.48	0.51
Melton ratio	0.45	0.67	0.61	2.91	0.98

- For Riu Runer and Portaîné, maximum elevations correspond to the catchments maximum elevation. For the others, maximum elevations refer to the landslide crown zone. The minimum elevation is always referred to as the elevation of the fan's apex.

2.2.1.1. In-channel generated debris flows

Two of the debris flows have not initiated from a landslide. Following Coussot & Meunier (1996), they are referred to as in-channel generated debris flows. Basically, the material is issued from the streambed (and possibly bank collapses).

2.2.1.1.1. Riu Runer

The Riu Runer catchment is located at the border of Spain and the Principality of Andorra, and drains a total area of 8.2 km^2 (Fig. 2.2a). The bedrock in this area dates from Silurian and consists of slate (ICC 2003). Colluvium and fluvial glacial deposits make up the majority of the catchment.

This catchment is a place of pasture (upper part) and forest (lower/middle part) with little signs of human activity (Fig. 2.3 and 2.4). The profile of the torrent's slope can be found in Fig. 2.5. Along its channel, only a few past lateral contributions of material (shallow landslides and/or banks destabilization) were observed.

On the evening of the 1st of August 2008, the Andorran Border Customs house was severely hit by a debris flow triggered by a short and intense thunderstorm. This debris flow seemed to be the result of the progressive incorporation of bed material within the channel, due to a high discharge, since no traces of landslides are visible in the initiation area. The torrent in the upper reach (down to 2000 m asl; see Fig. 2.5) shows signs of moderate fluvial erosion (V-shaped channel erosion) and some deposition (small areas of accumulation of loose material). Below 2000 m asl the slope's steepness increases and the torrent shows a greater degree of activity and silent witnesses (Aulitzky 1980 in Hungr et al. 2001): lateral levees, scouring activity (likely to reach the bedrock in numerous sections), deposition areas developed as lobes, and wounds on trees because of impacts of material. As the flow travels down, the solid material content increases due to scouring, shallow lateral slides and the incorporation of trees. In

the channel, at the fan apex, there is a small number of one-to-two metre boulders in a sandy/gravelly matrix. There is a small portion of fine material.

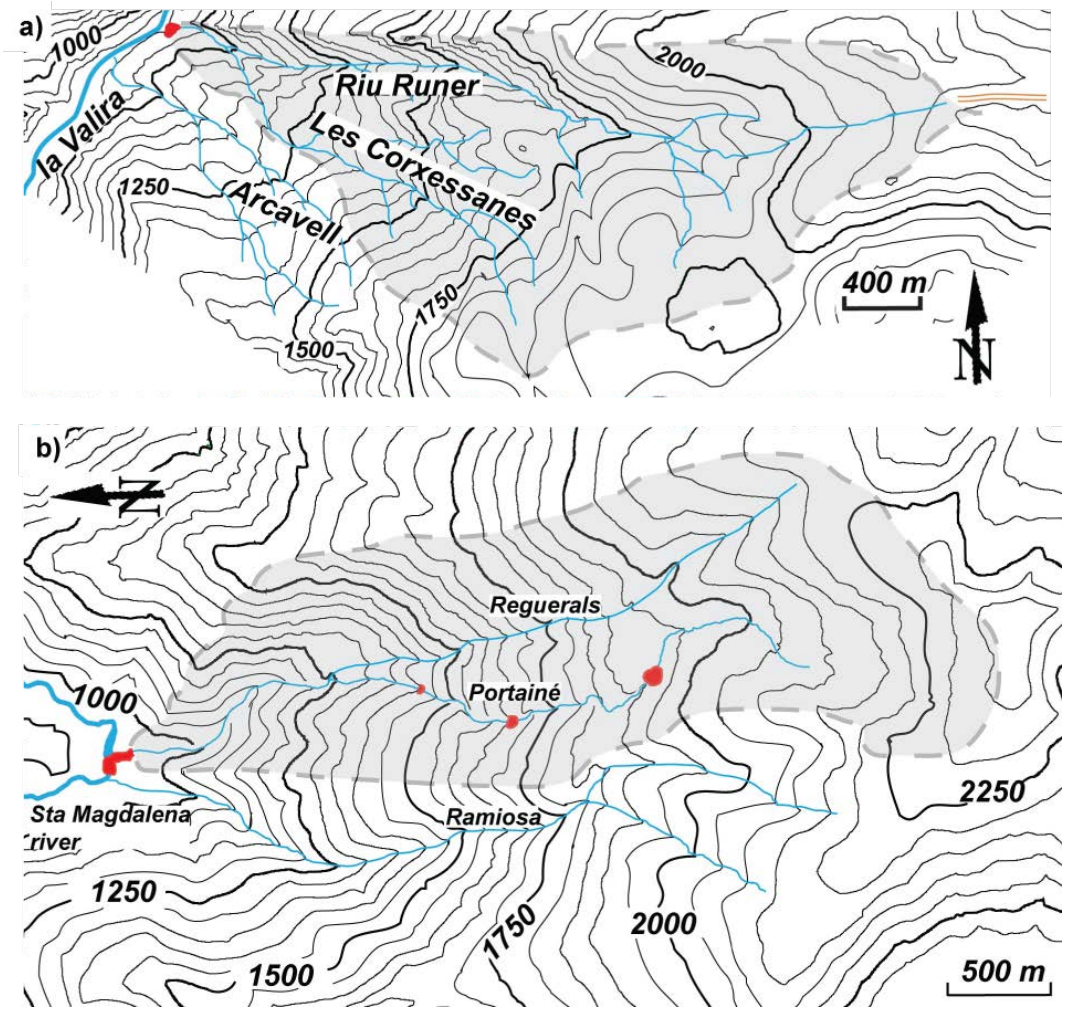

Figure 2.2: Catchment maps of Riu Runer (a) and Portaîné (b). The river courses are drawn wider than the torrents and both in light blue, in red depositional areas, and in grey the catchment surface. Contour intervals are every 50 meters.

The deposit area starts just a couple of hundred metres upstream of the Andorran Border Customs house at the fan apex (900 m asl). Eventually the torrent's channel could not drain the flows discharge; a culvert was obstructed, blocking the flow and forcing both material and trees to deposit. The consequence of this accumulation of material partly buried buildings and cars

close to the customs house. The water supply in proximity to this event was also disturbed; two aqueducts present in the channel were destroyed. Fortunately there were no casualties reported, due to its occurrence at night.

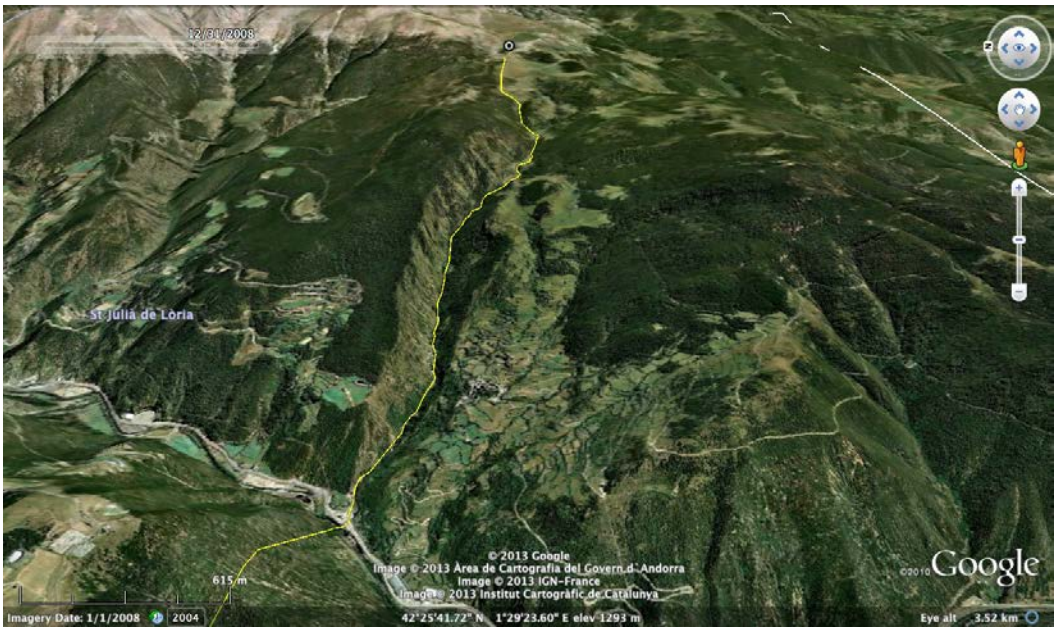

Figure 2.3: Perspective of Riu Runer's landscape viewed in Google™Earth

Figure 2.4: Riu Runer. On the right: the torrent as in the upper reaches of the catchment. On the left: inside the torrent as close to the fan.

An estimate of the scoured material quantity, as well as contributions along the debris flow path, was carried out and cross-checked with the total volume of

material deposited at the fan, which was estimated on the field. Finally, the total volume of the debris flow was assumed to be 14 000 m^3 (Table 2.1).

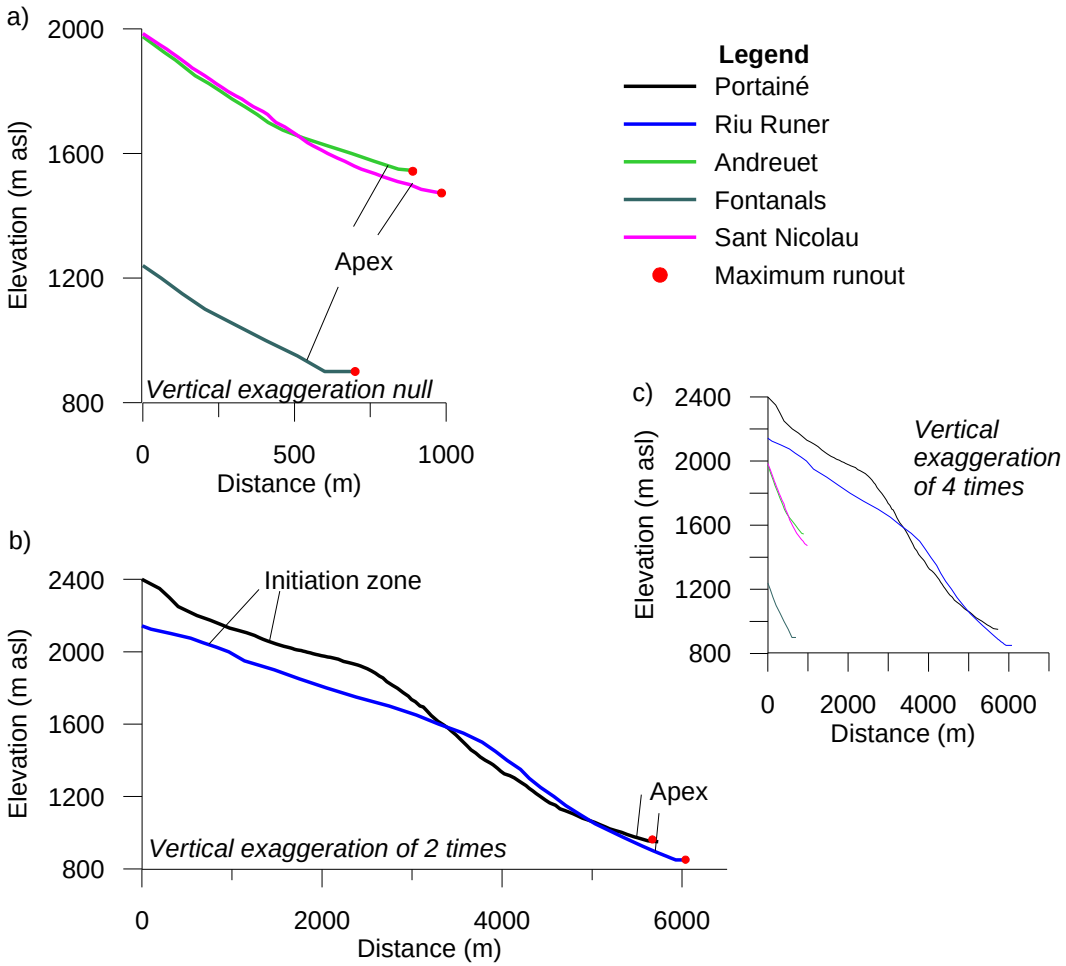

Figure 2.5: Topographic profiles of a) the landslide triggered debris flows (profiles start at the landslide's headscar), b) the in-channel generated debris flows and c) both sorts of debris flows.

2.2.1.1.2. Portaîné

In the Portaîné ski resort area, bedrock is the oldest outcropping in the Pyrenees, Cambrian to Ordovician in age (ICC 2003), and consisting of sedimentary units

made of pelite, sandstone and greywacke. To some extent colluviums and fluvio-glacial deposits overtop them.

Figure 2.6: Perspective of Port-Ainé's landscape viewed in Google™Earth.

The catchment consists of two main torrents, the Portaîné torrent in the West and the Reguerals torrent in the East (Fig. 2.2b). The morphology of the basin can be divided into two parts: a smooth higher part, where the presence of rills can be observed; and a steep lower part, where incised channels were formed (Fig. 2.5 for profile, Fig. 2.6 and 2.7 for field correspondence). In the steep section, the flanks of the torrents are unstable and lateral failures due to erosion of the slope's toe are recurrent, although small (about several tens of cubic metres).

Figure 2.7: Portaîné. On the left: inside the torrent as close to the fan, near the electric plant. On the right: the torrent as in the upper reaches of the catchment.

On the evening of the 12th of September 2008, a rainstorm hit the area and triggered one of the largest debris flows that took place in the Eastern Pyrenees. No clear initiation failure could be observed, thus promoting the idea that the flow probably started by minor erosion along rills in the higher parts. It probably transformed into a mature debris flow in the subsequent steep section of the torrent, where scouring rates of up to ~10 m^3/m led the bedrock to outcrop in some portions and the amount of material transported to considerably increase. Several secondary failures of adjacent slopes were also observed, which enlarged the total volume of the debris flow. Although the access road to the ski resort crosses the torrent in three distinct points and even though material deposition occurred at those points, as well as excessive failure of the road foundation, the main volume of the debris flow was deposited at the fan. The presence on the fan, thus on the debris-flow path, of an electric plant should be noted, including a dam and a retention lake, only marginally hit by the debris flow.

The total solid volume of the debris flow was estimated by assessing the volume of material built up on the fan and also a volume estimate of scoured material along the flow trajectory was carried out. Finally, a total volume of about 26 000 m^3 was assumed (Table 2.1). A detailed granulometric analysis of the debris-flow material was not possible, but two-to-three metre boulders in large proportion

are visible in a gravel matrix, with a small fine fraction that could be observed in the lowest part of the flow trajectory.

The Portaîné's debris flow seems to have been affected by the presence of the previously cited structures related to human activity in the catchment. But the opposite is also true: 1) the ski resort faced profound reshaping of the surface, 2) roads were severely damaged, and 3) an important volume of material superficially covered the electric plant facilities.

2.2.1.2. Landslide triggered debris flows

Another class of debris flows originates from one or numerous landslides in the upper reaches of a catchment. As opposed to the former class, they are called landslide triggered debris flows (Coussot & Meunier 1996).

2.2.1.2.1. Fontanals del Pui

Fontanals del Pui torrent is located in Andorra. The lithology of the site consists of Silurian slate and Quaternary slope debris, similar to the ones in Riu Runer catchment. However, a difference should be pointed out since no glacial features are exhibited. The vegetation on this slope is almost absent, only patches of shrubs colonise the scree.

The rainfall that triggered the Riu Runer's debris-flow event, due its trajectory, had also consequences in the surrounding areas. Approximately 5 km northward this rainfall induced the Fontanals del Pui event.

Figure 2.8: Perspective of Fontanals del Pui's landscape viewed in Google™Earth.

This debris flow was triggered by a small failure of the scree, in the middle of the catchment. The transit path downstream of this initiation point shows an alternation of erosion and no scouring (accumulation). Together with the presence of trees bent and partially covered by fine material, it pledges for the occurrence of the flow. As the flow crossed the road at the down part of the flow path, a first deposition area developed. There was another area of deposition further downstream, where the same road was crossed again. The artificial channel downstream at this point was mostly filled with sediments. The particle size mobilised by the debris flow was smaller than in Riu Runer, including mainly gravels and boulders no bigger than 50–70 cm across. Given the small magnitude of the debris flow (~1500 m^3), the urbanised area developed on the fan did not suffer important damages (Fig. 2.8 and 2.9).

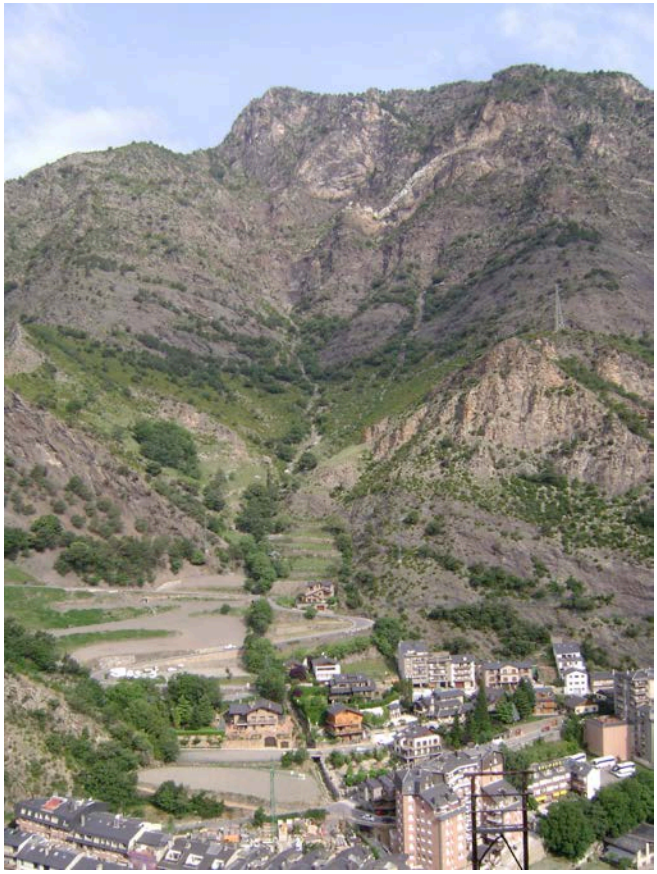

Figure 2.9: Fontanals del Pui, front view.

2.2.1.2.2. Andreuet torrent

In Andreuet's catchment, only metamorphic rocks made of slate and phyllite outcrop. They are covered by colluvium material of metamorphic origin in the lower part. Clay and gravel make up the colluvium material's grain size. The upper part of the catchment displays bushes and grass, while the lower part consists in trees and shrubs.

At night, between the 25th and 26th of June 2008, a rainstorm induced a shallow landslide in the upper part of the catchment that developed into a debris flow. This flow began its erosional process when it reached the colluvium at mid-length and deposited as soon as it hit the road, present at the slope's toe. Within

the torrent, lateral levees were observed and related to the last event (Fig. 2.10 and 2.11).

Figure 2.10: Perspective of Andreuet's landscape viewed in Google™Earth.

Figure 2.11: Inside the torrent of Andreuet.

2.2.1.2.3. Sant Nicolau

Sant Nicolau torrent is located close to the national park of Aigüestortes in the Axial Pyrenees (Fig. 2.12). Granitic rocks constitute the lithology outcropping in the catchment and are covered by colluvium material in the lower part of the catchment. Colluvium thickness is of a couple of metres in the fan area and increases to a few metres as it reaches contact with the bedrock. Regarding the grain size of the colluvium, metre-sized boulders supported by a sandy matrix can be observed in the upper part of the torrent. At the lower part, boulders become gravels of a few tens of centimetres in general (Fig. 2.13).

The morphology of the torrent should also be noted, as it displays a straight stretched and elongated path. The vegetation consists of bushes and grass in the upper part of the catchment and presents small trees and shrubs in the lower part.

Figure 2.12: Perspective of Sant Nicolau's landscape viewed in Google™Earth.

On the 25th–26th of May 2008, a shallow landslide induced by heavy rainfall provoked a debris flow in Sant Nicolau torrent. The flow propagated down the steep upper part (Fig. 2.5), without significant erosion or deposition. The contact made by the bedrock and colluvium was observed and highlighted major scouring. Within the colluvium lateral levees had formed. The flow remained confined in the torrent, blocked the access road of the national park and deposited most of the material on the fan.

Figure 2.13: On the fan, where Sant Nicolau's debris flow induced clear lobes of deposition.

2.2.2. Morphologic analysis

The literature on debris-flow hazard provides examples of geomorphological characterisation of debris flows (e.g. Di Crescenzo & Santo 2005). However, only few researches focus on the Eastern Pyrenees (Gallart & Clotet 1988; Corominas *et al.* 2002). That is why two aspects of the five events described herein are analysed: one at catchment scale and the other focussing on the initiation area.

At catchment scale, magnitude (total volume) and area were assessed for each event based on field observations, aerial pictures and topographical maps. Figure 2.14a displays their relationship. Limits of occurrence published by D'Agostino & Marchi (2001) were added. These limits were defined using data on debris flows from 130 catchments observed in the Eastern part of the Italian Alps.

A study of the initiation zone is proposed in Figure 2.14b. In order to do so, the initiation point is defined, while two cases are recognised: 1) When the debris flow originates from a landslide, the initiation point is chosen as the headscar; 2) When the debris flow originates from bed fluidization, the initiation point is chosen as the beginning of the "channelization zone" (as defined in Di Crescenzo & Santo 2005). For both concerned catchments (Portaîné and Riu Runer), this point coincides with a significant scouring.

Figure 2.14a shows a positive trend: the magnitude of debris flows increases as the catchment area increases. Moreover, it appears that all the events described in this study fit within the limits published by D'Agostino & Marchi (2001). It may seem that the geographical position of the catchment does not quantitatively influence volume versus catchment area relationship. Nevertheless, further investigation is needed to confirm this regional relationship due to the large scattering of the data. The hazard study of Pyrenean catchments could be greatly enhanced by the use of such a relationship. The determination of a catchment area could lead to a range in the preliminary estimation of the event's magnitude, and could pledge for an optimised mitigation.

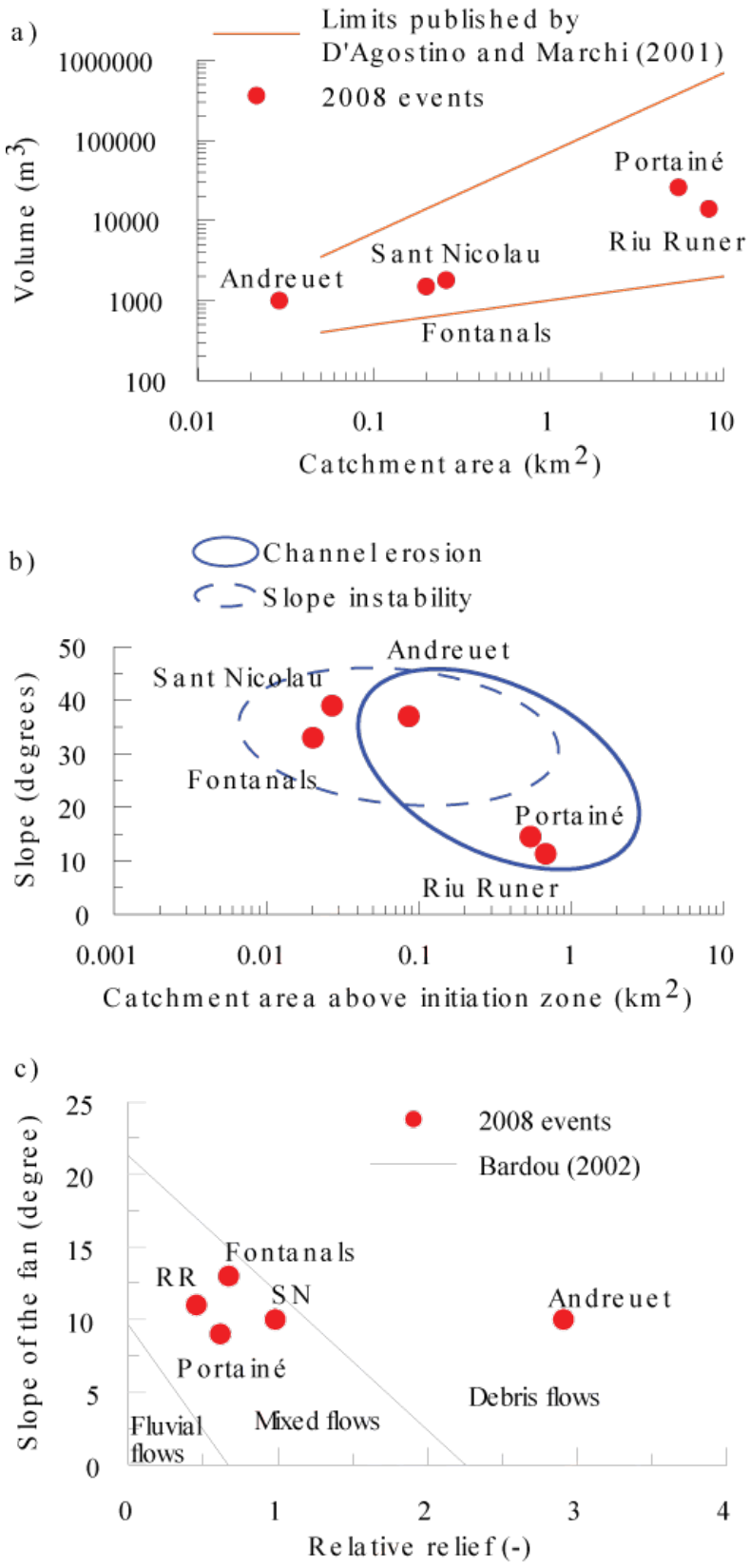

Figure 2.14: Geomorphological relationships. a) Volume versus catchment area, b) slope versus catchment area above initiation zone – Channel erosion and slope instability's clusters follow VAW (1992) and Zimmermann *et al.* (1997), and c) slope of the fan versus relative relief (Melton 1965).

When the slope at the initiation is plotted against the catchment area above this initiation zone, a negative correlation seems to emerge. VAW (1992) and Zimmermann *et al.* (1997) worked on this correlation for debris flows in the Swiss Alps, and defined and published two clusters of points shown in Figure 2.14b. The first cluster gathers the events initiated by a slope failure. It lies at a small catchment area above the initiation zone (<0.1 km^2) and at a rather large slope angle (over 27°). A second cluster is emphasized and includes both in-channel formed debris flows. Although overlapping, the clusters shown in Figure 2.14b incorporate all described events. Only Andreuet position remains ambiguous as it belongs to both clusters.

The difference in elevation of a catchment is divided by the square root of its area, his was mentioned first by Melton (1965), and is referred to as the relative relief (or Melton ratio/number). Different authors have used it since, emphasizing the relationship between the catchment morphology and the characterisation of the process of building up the fan (Jackson *et al.* 1985; Brochot & Marchi 2000; Bardou 2002). Figure 2.14c shows the relationship between the relative relief of the catchment and the slope of the fan. In the past, the study of this relationship permitted to differentiate fluvial fans from debris-flow fans (Kostaschuk *et al.* 1986). Limits found in Bardou (2002) are depicted. Catchments and fans where the 2008 debris flows occurred are shown in relation to these limits. It appears that only Andreuet's catchment and fan fit within the debris-flow zone that Bardou (2002) highlighted; the other four are to be found in the mixed zone. The French Alps (Maurienne region) served as a base for the establishment of Bardou's limits, which have been edited comparing his Swiss dataset (Valais region) with that of Brochot & Marchi (2000). Undoubtedly limits have to be adapted for the Eastern Pyrenees.

All of these results show that the geomorphological studies of catchments and corresponding fans are not sufficient when investigating the impact of debris-flow on the landscape. Many parameters, regarding land use, geology, and occurrences of wild fires for instance, should also be considered (Liu *et al.* 2002; Di Crescenzo & Santo 2005).

2.3. Events Database: toward an inventory

2.3.1. Extent

The Central-Eastern Pyrenees is subject to debris flows, as the year 2008 shows. It is evident that the number of occurrences is very low compared to other mountainous environments, but nonetheless high-risk spots exist. It is presented in the Introduction the study area at a large scale, and above is revealed some of the most recent events that struck the study area. Debris flows in the area are generally scarcely reported, and their study is unfortunately not compulsory or generalized. For this reason an attempt in order to start an inventory of past debris-flow events was realised, as only isolated inventories existed before this study started. Moreover, considering the large extent of the study area, it is not realistic to consider the whole study area for the inventory and thus four zones have been identified: Berga, Northwest Catalonia (NWCat), Andorra and Mollo (Fig. 2.15).

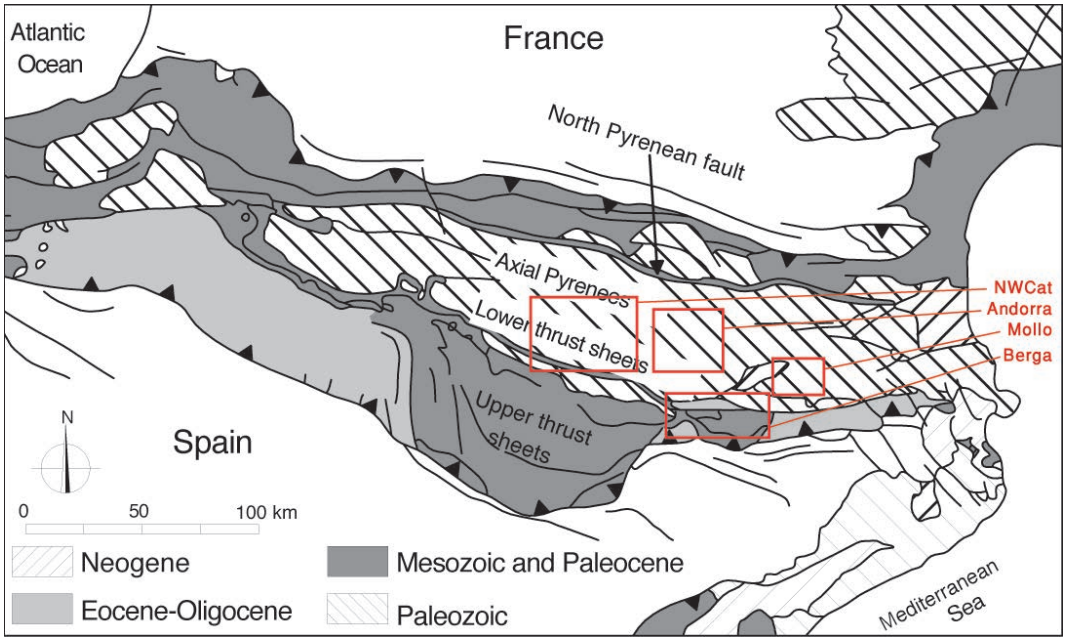

Figure 2.15: Pyrenean geological context (After ECORS team 1988). In red are highlighted the study areas.

Berga majorly lies within the pre-Pyrenees. NWCat, Andorra and Mollo fall into the Axial Pyrenees. These zones cover over 4000 km^2 and have been defined to represent typical environments of the Central-Eastern Pyrenees, where debris flows have been triggered in the past. The exact geographical coordinates of each zone are given in Figure 2.16.

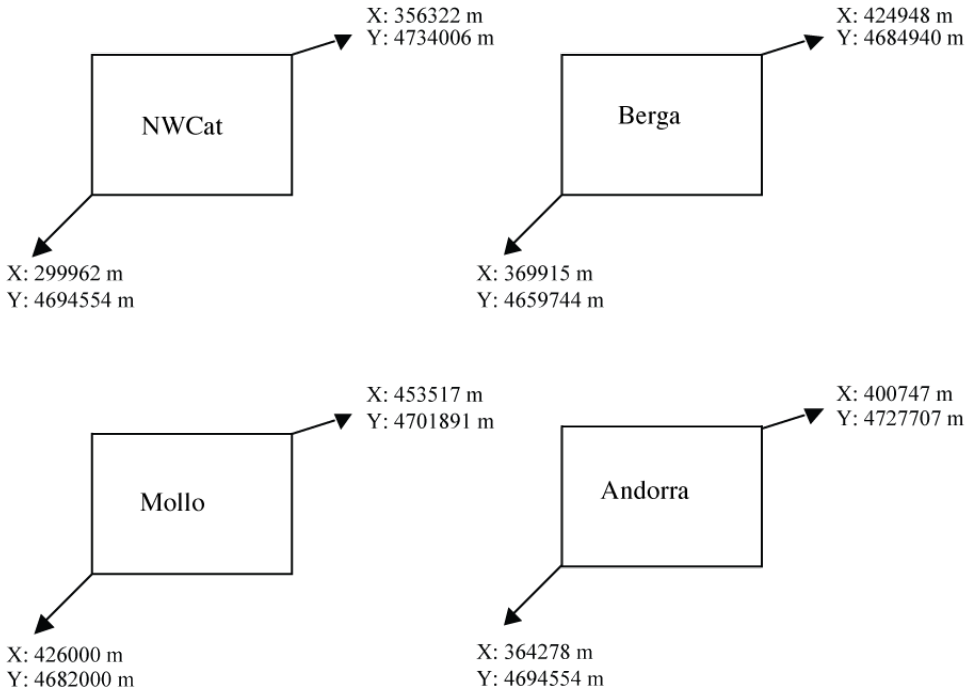

Figure 2.16: Geographical coordinates of the zones.

2.3.2. Criteria and methods applied

Due to the non-systematic reconnaissance of debris flows in Central-Eastern Pyrenees, most debris-flow events are not reported. Therefore an inventory of past debris flows is needed. The debris flows giving rise to the reactive catchments have been gathered. This has been collated and digitalized from past studies or analyses, aerial pictures, surveys and contemporary interactive surveys. No information on the mean of trigger is sought nor reported in this

thesis. The mean of elaboration of the inventory spreading over 4 zones (Fig. 2.15 and 2.16) is explained and detailed in this section, and are reported in Table 2.2. As Guzzetti *et al.* (2006) highlighted, a multi-temporal (landslides) inventory seems to produce better results than clustering the (landslides) events in time intervals and studying (the susceptibility) within these intervals. The inventory elaborated for this thesis follows these guidelines and no temporal distinction is considered or shown in this thesis.

Table 2.2: Source of information in the elaboration of the inventory. See text for references to OrtoXpres 1.0 and existing field data.

		Aerial pictures analysed	
	Existing field data or inventories	*Google™Earth and OrtoXpres 1.0 2008-2009*	*Standard aerial pictures 1975/76 and 1982/84*
Berga	Clotet & Gallart (1984), Baeza (1994)	X	X
Mollo	Portilla (2010)		
NWCat	nd	X*	X
Andorra	nd	X	

* and OrtoXpres 1.0 for aerial pictures of 1956/1957.

Debris flows in Berga's zone were determined using an existing database (Clotet & Gallart 1984; Baeza 1994) and contemporary images provider. The existing database shows different erosional processes. A filter was necessary and only debris flows involving at least 1000 m^3 of material were kept in this zone, after preliminary analysis. Aerial pictures from 2008, visible in Google™Earth, were used to determine where unreported debris flows could have occurred. Criteria

such as vegetation's change in the landscape, landslide scar(s), clear visibility of a torrent/gully/stream where roughness could be assessed or presence of potential deposition fans were considered (Fig. 2.17 and figures of landscape's perspectives of 2008 cases). Based on Guthrie & Evans (2007) the time period considered by these criteria ranges from 50 to 100 years.

In Mollo's zone, an unusually high intensity of rainfall in 1940 caused a great flood and many surficial slope failures, some of them developing into debris flows (Parde 1941). An analysis of these failures by the interpretation of 1956/57 aerial pictures permitted the determination of the debris flows related to this event (Portilla 2010). These debris flows are used to determine the reactive catchments. No more recent information was obtained for this zone.

Figure 2.17: Example of a criterion for debris-flow track's reconnaissance (white arrow), here visualized in Google™Earth.

In NWCat's zone, Google™Earth proved useful to analyse 2008 aerial pictures. Together with the criteria enumerated above, it allowed traces of debris flows

activity to be recognized in the landscape. In addition to this, more sets of aerial pictures available for this zone were consulted. On one hand aerial pictures from flights in 1975/76 and 1982/84 (black and white) were studied. On the other hand the Catalan Cartographic Institute (ICC), through the Internet application OrtoXpres 1.0 (URL: www.ortoxpres.cat/client/icc/) shares online aerial pictures from 1956/57 for the zone. Both sources of information were used.

Eventually debris flows in Andorra's zone have been determined by 1) a compilation of events coming from the interpretation of aerial pictures taken between 2003 and 2008 (Google™Earth) through the criteria aforementioned and 2) the compilation of historic debris flows that occurred in the zone, through the study of reports encompassing past events.

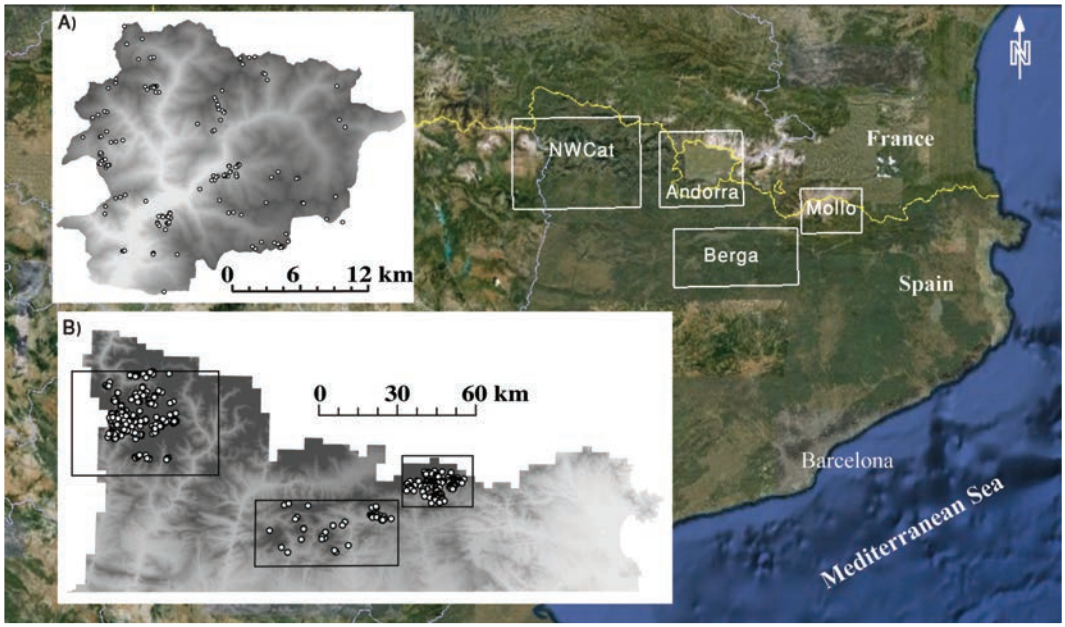

Figure 2.18: Debris-flow inventory. A) DEM view of Andorra and B) DEM view of NWCat, Berga and Mollo. A and B show debris flows (white points) used in this study for each zone. For the DEM, the darker the terrain, the higher the elevation.

In Berga, a total of 55 debris flows were recognised; in Mollo 181 debris flows were reported; in NWCat 298 debris flows have been identified; and in Andorra

157 debris flows have been digitalized. It leads to a final total of 691 debris flows spreading over the four zones defined. Figure 2.18 accounts for the localisation of the 691 debris flows encountered, each represented by a point over the digital elevation model (DEM) in a GIS.

The term reactive has been extracted from the medical jargon and is understood as showing a response to a stimulus. In this thesis, the response is a debris flow, and the stimulus is an adequate rainfall event. When clear signs of debris-flow activity were witnessed or reported, reactivity was assigned to its corresponding catchment. Debris flows are known to be able to travel great distances and the chance that one may exit its native catchment exists, but the study focuses on the source catchments (where the debris flows occurred) and doesn't account for its runouts.

2.4. Conclusion

Research on debris flow has only marginally been performed in the Pyrenees and associated hazard has mostly been neglected. That is why it was proposed in the first part of this chapter the study of five debris flows, which occurred in 2008 in the Central-Eastern Pyrenees. The second part focuses on the elaboration of a debris-flow inventory in the study area.

Debris flows triggered by landslide(s) encountered in 2008 display a high slope at the scar (over 25°) and a small catchment area above the initiation zone (less than 0.1 km^2). In-channel generated debris flows, on the contrary, show a large catchment area above the initiation zone (close to 1 km^2) and a lower slope angle (less than 15°). There also seems to exist a positive correlation between catchment area and debris flow volume, as witnessed in other mountain ranges. The distinction between both debris-flow types is however, hardly achievable when only taking into account simple geomorphological parameters, such as relative relief and fan's slope. Finally, the fact that the data from the Central-Eastern Pyrenees fit the relationships validated for the European Alps tends to

pledge for an interregional standardization of the susceptibility analysis of such hazards.

The inventory taken into account into this thesis is the result of a multi-sourced approach. Either extracted from past studies or encountered during aerial pictures surveys (digital or numerical), 691 debris flows serve as a base for the susceptibility analysis carried out in Chapter 4. Uncertainties certainly arise when tools such as Google™Earth are used in distinguishing debris-flow activity from fluvial activity, or in inferring that a landslide developed into a debris flow. However, one must keep in mind that erosional processes are continuous, from flood to avalanches encompassing debris flows and landslide. The inventory thus developed doesn't account for the trigger of debris flow, nor does it account for its runout. Debris-flow features widely recognized were considered when no past studies could ascertain the presence of one. A detailed study of these "debris-flow points", especially on the field, could stress the level of accuracy and point out the weaknesses of such techniques.

CHAPTER 3 ANALYSIS OF HEADWATERS MORPHOMETRY

3.1. Introduction

Chapter 3 accounts for an analysis of headwaters morphometry of the Central-Eastern Pyrenees based on geomorphology, emphasizing morphological parameters. Similar studies have already been performed at catchment scale (Obi Reddy *et al.* 2004; Ehsani & Quiel 2008), and Kompani-Zare *et al.* (2011)'s work in Iran identified 146 1st-order catchments and investigated 9 morphometric factors. Increasing the scale and the number of parameters, it is proposed the study of the 1st-order catchments as well as 2nd-order catchments, over almost a third of the south-facing Pyrenean range. This chapter will give an insight into the distinction between both order catchments. This distinction is based on simple fluvio-morphological parameters, when comparisons between the 1st-order and 2nd-order catchments are not its scope. Being able to characterize catchments in mountainous Central-Eastern Pyrenees was aimed for, from landscape's fluvio-morphological analysis, given that the literature lacks such information for the study area. Moreover it has to be apprehended as a contextualisation of the work, which is tackled in chapter four of this thesis.

After having presented the unit at which the work was carried out, this chapter explains the methodology used in order to gather sufficient information through

GIS techniques. GIS data is transferred into original results via histograms, frequency's curves and bi-dimensional relationships and eventually attempts at distinguishing a regional pattern through the study area, which is outlined in the Introduction.

3.2. Study unit

It is to be understood that in this chapter the watershed is an ensemble of catchments. The South-facing part of the Pyrenees has been divided into 8 units following the pre-existing and common regional extents of 8 watersheds, covering the equivalent of the Catalan Pyrenees and including Andorra (Fig 3.1): Fluvia (Flu); Garona (Gar); Llobregat (Llo); Noguera Pallaresa (NP); Noguera Ribagorçana (NR); Segre (Seg); Ter (Ter) / Valira (Val).

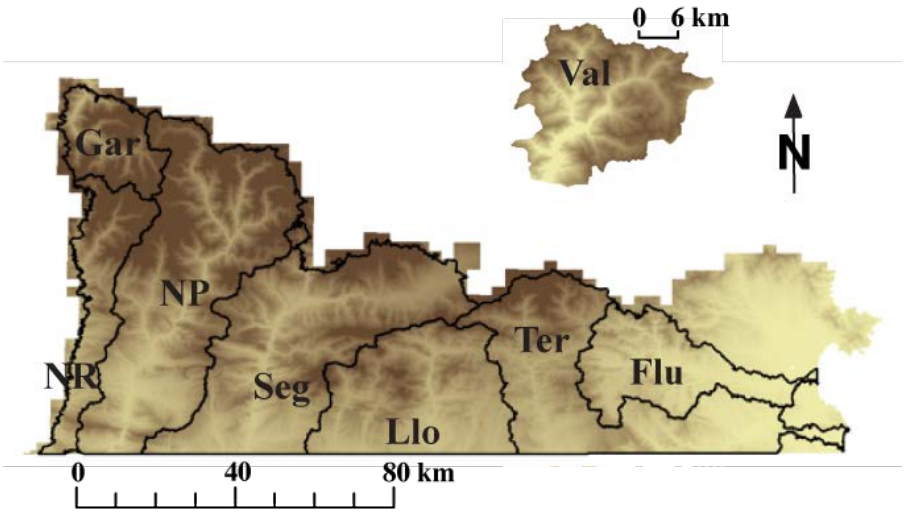

Figure 3.1: Extent's limits of the 8 studied watersheds in the DEM (dark, high elevation; light, low elevation): See text for abbreviations.

Table 3.1 shows the 8 watersheds mean values of total area, number of catchments, and mean area and mean elevation per catchment. Values for 1st-order and 2nd-order catchments are reported.

The 8 watersheds combined cover an area of 11,233 km^2. In each watershed, 1st-order and 2nd-order catchments have been defined and serve as a base for the extraction of parameters. The description of stream orders can be found in the first chapter (see Fig. 1.9).

Garona and Valira are clearly high-mountain watersheds with the highest elevations, which are generally attributed to the Axial Pyrenees. However, Fluvia and Ter have the lowest mean elevations, although they mainly fall within the Axial Pyrenees. Llobregat, Segre, Noguera Pallaresa and Noguera Ribagorçana spread over both Axial and pre-Pyrenees, to different extents.

Table 3.1: Area, number of catchments, and mean area and mean elevation per catchment of the 8 studied watersheds, individually and combined. Abbreviations of the watersheds are found below in the text.

	Total area (km^2)	*Number of catchments (# (%))*		*Mean area per catchment (km^2)*		*Mean elevation per catchment (m asl)*	
		1st-order	*2nd-order*	*1st-order*	*2nd-order*	*1st-order*	*2nd-order*
Flu	973.38	265 (8.8)	55 (8.4)	2.32	11.18	530	527
Gar	552.07	131 (4.3)	26 (3.9)	2.26	9.90	1973	2004
Llo	1519.00	423 (14.1)	91 (13.9)	2.20	10.09	1144	1160
NP	2688.94	713 (23.7)	162 (24.7)	2.29	9.70	1541	1538
NR	768.94	211 (7.1)	41 (6.3)	2.25	10.42	1529	1507
Seg	2414.05	632 (21.1)	146 (22.3)	2.32	10.75	1337	1332
Ter	1867.06	517 (17.2)	109 (16.7)	2.25	10.42	944	966
Val	450.28	113 (3.7)	25 (3.8)	2.31	11.68	2208	2153
All	11233.7	3005 (100)	655 (100)	2.28	10.36	1293	1299

3.3. Methodology

The general methodology is presented below focusing on 1) how to recreate the unit of study from a digital elevation model, 2) a presentation of the morphological information (parameters) to be gathered and 3) how to assign this information to the study unit.

Appendix 1 shows a manual of the GIS methodology, step by step, complementing the following description. Figure 3.2 accounts for the general methodology necessary for the elaboration of the analysis carried out in this thesis. It is to be noted that susceptibility models and maps are tackled in the following chapter.

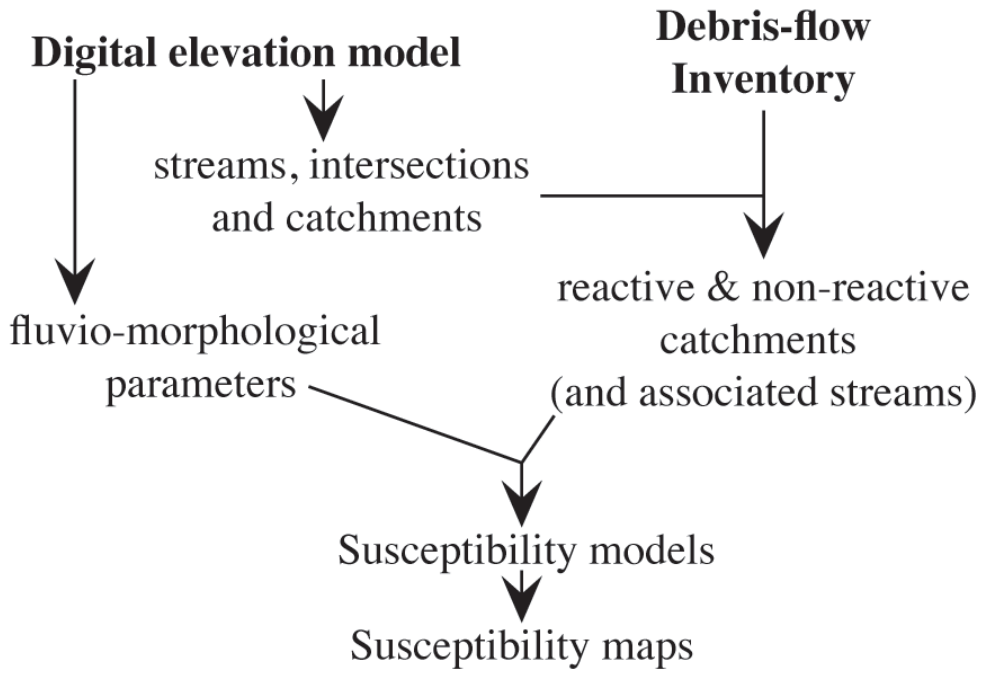

Figure 3.2: Methodology's flowchart.

3.3.1. Digital elevation model analysis

Landscape can be recreated through a 5x5m digital elevation model (DEM) in a geographical information system (GIS) (obtained from digitalizing contours using existing maps). The DEM of the study area was used to discretize the landscape and extract headwater catchments.

Imperfections of the DEM were filled and flow direction and flow accumulation commands followed. The next step consisted of editing streamlines, and catchment polygons. Definition of streams needs a minimum drainage area for initiating the stream, which was set at 1 km^2; for this reason no catchment has a drainage area inferior to this value. The literature specialized in GIS studies provides numerous studies concerning the initiation of streams and the minimum contributing area to consider, in order to localize the "best starting point" of a stream (Montgomery & Dietrich 1988, 1989; Tarboton *et al.* 1991; Tarboton & Ames 2001). The problem is mainly related to the stream density (or stream-area ratio) affecting the representation of the drainage network. In this work, the minimum contributing area is arbitrarily fixed, based on the information collected in the database. Similar studies have been carried out using smaller minimum drainage area for initiating streams, but the study area considered revealed smaller than the one considered herein (Carrara 1991). Streamlines were then processed as drainage lines. Aggregated upstream catchments were generated and eventually catchments were digitalized. Considering the number of catchments created, special attention needs to be given throughout the elaboration of the database on the identity of catchments and streams.

The analysis of the landscape is generally performed using DEM land surface representation. Features like slope, curvature and flow accumulation are obtained through DEM processing. However, some issues should be taken into account.

On the background of geometrical parameters like slope, flow direction or aspect there are several complex concerns. As a simplified explanation of the problem,

consider the slope. In a DEM, every cell has 8 neighbours. In most of the cases these 8 neighbours are not sharing a planar surface. A planar surface is defined by at least 3 points. Consequently, for a single cell, 14 different choices of slopes are available. The problem is not trivial and many results are possible. Similar issues could be described for the flow direction or flow accumulation computation. These problems have been widely analysed (Tarboton 1997; Wilson & Gallant 2000; Pike 2002).

Concerning the analysis carried out in this work, the most relevant choice was to use the O'Callaghan & Mark (1984) approach (formally D8). This approach however, has several limitations. For instance, it is not capable of modelling the divergence of a flow in ridge areas. However, it accurately captures the basin area, which is the main concern for the target of this thesis. The flow accumulation is performed using the Jenson & Domingue (1988) algorithm and the slope's computation follows the Burrough & McDonell (1998) approach.

All along the process, keeping clear the "identity" of catchments and streams is of crucial importance, otherwise confusion (between the catchments) may easily arise.

3.3.2. Parameters description

1st-order and 2nd-order catchments are the unit of this thesis and support a series of fluvio-morphological parameters (Table 3.2) applied to either both of the spatial features: catchments (polygons) and streams (lines). Their minimum contributing area is set up at 1 km^2. Polygons and lines were derived from the DEM. Information was gathered thanks to topography, slope, stream order and orientation (aspect) raster files through the use of the zonal statistic tool and zonal geometry tool (both being a command of "Spatial Analyst").

Table 3.2: List of analysed parameters applied to 1st-order and 2nd-order catchments. dH is the difference in elevation H_{max}-H_{min}.; L is the catchment's length.

Parameter	*Abbreviation*	*Units*	*Equations*	*Applied to*
Area	A	km^2	(-)	Catchment
Perimeter	P	km	(-)	Catchment
Maximum elevation	H_{max}	m asl	(-)	Catchment
Minimum elevation	H_{min}	m asl	(-)	Catchment
Mean elevation	H_M	m asl	(-)	Catchment
Mean slope	S_M	Degrees	(-)	Catchment
Orientation	O	degrees (N-S)	(-)	Catchment
Average slope	S_{ave}	degrees	(-)	Stream
200 m slope	S_{200}	degrees	(-)	Stream
Outlet slope	S_E	degrees	(-)	Stream
Length	L_S	m	(-)	Stream
Melton ratio	MR	dimensionless	$dH/\sqrt{A}$	Catchment
Form factor	FF	dimensionless	A/L^2	Catchment
Basin elongation	BE	dimensionless	$2\sqrt{A}/L\sqrt{\pi}$	Catchment
Lemniscate ratio	LR	dimensionless	$L^2 \cdot \pi/4A$	Catchment

It is necessary to create slope stream order and orientation rasters. This again has to be done with the DEM itself in order to attain the topographic information regarding each cell. Everything is done thanks to the spatial analyst command. However, the use of the "zonal statistic tool" is not possible because of the overlapping of catchments (Fig. 1.9). Certain catchments are overlapping others,

due to the way catchments are defined: 2nd-order catchments contain at least one 1st-order catchment, and so on. The raw tool would have calculated the information desired, only in the association of the two 1st-order catchments instead of assessing it for each 1st-order catchment individually. Thus a change in the original code of the "zonal statistic tool" was done allowing calculations over overlapping catchments. Besides, the "zonal geometry tool" has also been used for this study, and its original code sufficed.

The area of each catchment is calculated, taking into account the number of cells making up the catchment and their size (5*5 meters), as well as the perimeter. The results focus on 1st- and 2nd-order catchments. The choice was constrained to these two orders: catchments of higher orders are too few, and not representative enough of mountainous environments and related headwaters. Maximum, minimum and mean elevations for each catchment were defined based on the topographical data from the DEM. The mean of the catchments slope was achieved, but averaging the slope's value of each pixel, which makes up the catchment's polygon. The same logic is applied to the catchment's mean orientation. In addition, every catchment has been extrapolated to an ellipsoid, giving us the best-fit catchment's width and length (length, L, is used for the calculations of morpho-hydrological ratios – see Table 3.2).

The streams within each catchment have also been investigated. First, the length for each stream's segment contained within a catchment has been computed, knowing that the stream starts when the drainage area has reached 1 km^2. Besides its length, different stream's slopes have been calculated. The slope of every pixel making up the entire stream, from the head to the intersection, divided by the number of pixel is referred to as the average slope. Two other slopes have also been gathered for the study. The 200 m slope follows the same idea as the average slope, except that it was achieved over 200 m starting from the intersection (or outlet of the catchment) and going upstream. Asides from this the outlet slope considers the slope of the stream's segment running for 50 m from the intersection and going upstream.

Morpho-hydrological ratios have often been used to characterize catchments (references in Zavoianu 1978). These ratios are often easy to determine and imply few parameters. Four of them are considered herein: Melton ratio or ruggedness number is an index of average catchments slope (Melton 1965); basin elongation compares the longest dimension of the basin to the diameter of a circle of the same area as the basin (Schumm 1956); form factor gives information about the shape of a catchment (Horton 1932); lemniscate ratio is a measure of how closely the catchment's shape approaches a lemniscate (Chorley 1957).

3.4. Results

The results presented below are visualized through histograms and bi-dimensional relationships. During this work, statistics of the different parameters have also been gathered, although not documented nor considered in this chapter. However, they are presented in Appendix 2. They are consultable in a desire to complement the information provided by the following results, and present general statistical information, such as standard deviation, parameter-by-parameter, for 1st-order and 2nd-order catchments.

3.4.1. Histograms

Histograms bins are not constant in Figure 3.3, Figure 3.4 and Figure 3.5. They have automatically been determined to best fit the data (Shimazaki & Shinomoto, 2007a, b). The lower number of bins for the 2nd-order catchments is a consequence of a lower occurrence of 2nd-order catchments (Table 3.1).

3.4.1.1. Catchments

Figure 3.3 shows a series of histograms. The cumulative curve is displayed on top of the histogram. Divided between 1st-order catchments and 2nd-order catchments, this series concerns elevations (maximum and minimum), mean

slope, mean orientation, perimeters and areas. These parameters are related to the catchments.

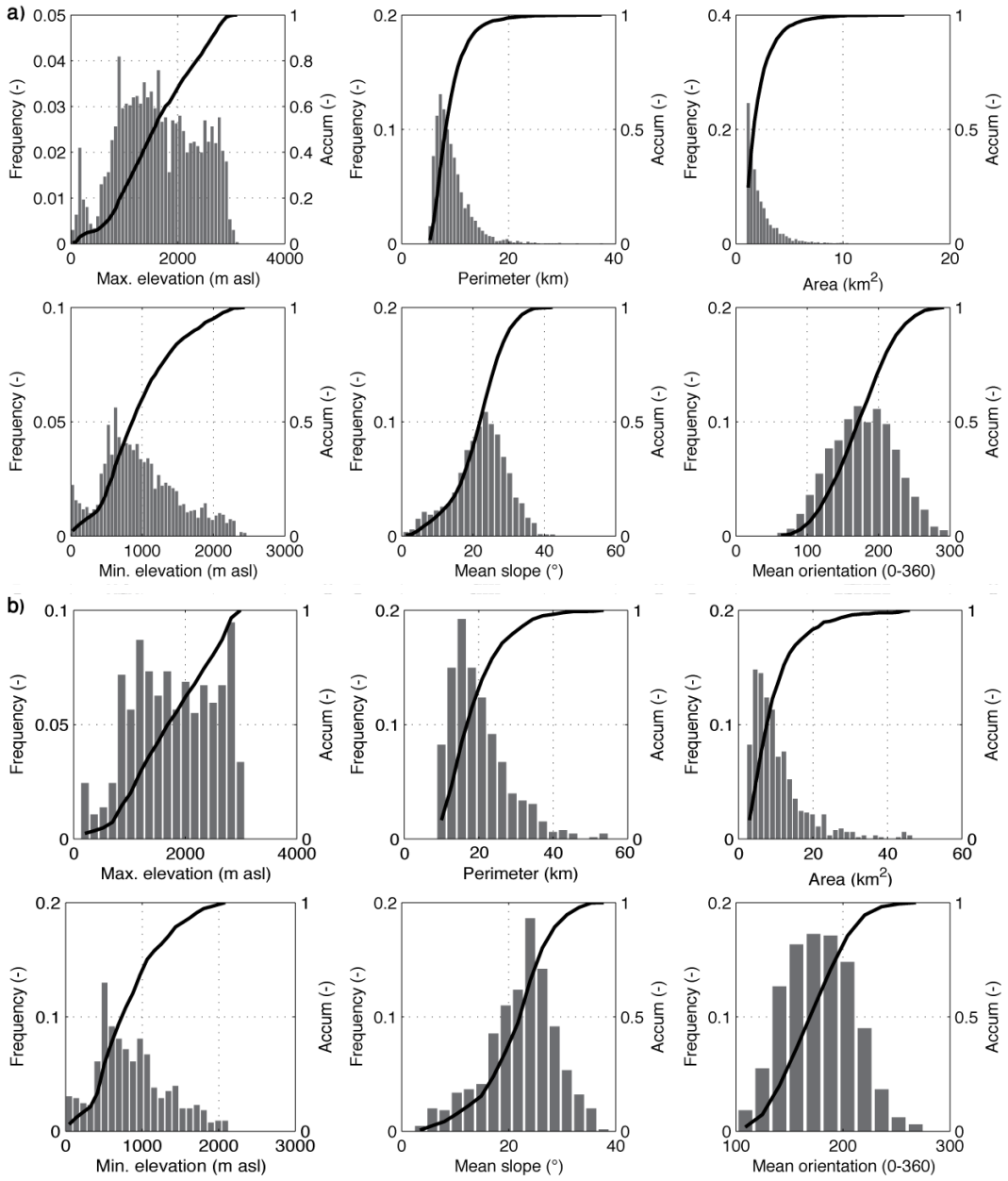

Figure 3.3: Histograms and accumulative curves showing parameters for a) 1st-order and b) 2nd-order catchments of all watersheds.

The maximum elevation and minimum elevation histograms (Fig. 3.3) display a similar trend for catchments of both orders. For the maximum elevation, ranges spread from 0 to just over 3000 m asl for both order catchments; for minimum elevation, 1st-order catchments values range from 0 to 2500 m asl when the 2nd-order catchments range from 0 and to just over 2000 m asl. The shape of the cumulative curve changes, depending on the parameter. For the maximum elevation, the cumulative curve presents the 1st-order catchments, three clear inflection points (200, 400 and 1800 m asl) with a total cumulating abruptly reached. For the minimum elevation, the first inflection point is hardly distinguishable (same value as for maximum elevation). In addition to this the cumulative curve's maximum is reached more smoothly. In the 2nd-order catchments, the maximum elevation's cumulative curve shows two inflection points (400 and near 3000 m asl), and again finishes abruptly. Regarding minimum elevation, two inflections points are seen on the cumulative curve (around 400 and 2500 m asl) and the shape of the curve is similar of that of 1st-order catchments.

Area and perimeter are closely related, either for 1st-order or 2nd-order catchments. Lathrop & Peterson (1992) also acknowledged this relationship, which helps validate the data. It was no surprise that the histograms also accounts for this validation. Perimeters are found between 5 to 38 km for 1st-order catchments, and from just below 10 to 55 km for 2nd-order catchments. The minimum area's value visualized for both orders catchments is due to the way they are defined in the GIS; a minimum of 1 km^2 of drainage area is used for defining streams, and catchments as well. Thus, areas, starting at 1 km^2, reach 14 and 45 km^2 respectively for 1st-order and 2nd-order catchments, these values being coherent with past studies in the Pyrenees (Portilla *et al.* 2010 – Chapter 2). The cumulative curve's also shows the similarity in their relationship. One inflection point characterises the cumulative curves of both these parameters. Perimeter's inflection points are localised for 1st-order and 2nd-order catchments respectively at 15 and 30 km; area's inflection points at 5 and 17 km^2. Values for both parameters increase with the order.

The slope's mean cumulative curves show two inflection points for both orders: one around 17 degrees (°) and another one at 30°. From the same curve, more than half of 1st-order catchments have a mean elevation over 20°, and this value tends to increase with 2nd-order catchments. Their range of value, somewhat wider for the 1st-order catchments, also differentiates 1st-order and 2nd-order catchments. For 1st-order catchments, values reach more than 40°, when this value is only nearly reached for 2nd-order catchments.

The Pyrenean range has a global orientation toward WNW-ESE. The histograms of the catchments mean orientation recognise this trend. Moreover, the symmetry is striking, centred toward 170° (South being 180°) and for both orders, two inflection points are seen on the cumulative curve: 120 and 240° for 1st-order catchments, and again 120 and 220° for 2nd-order catchments. The range is less wide for 2nd-order than for 1st-order catchments, just as observed for the mean slope.

Differences between 1st-order and 2nd-order catchments are scarce when looking at this first series of parameters, related to classic morphometry. Safe for parameters related to size (area and perimeter), values show similarities that offer little distinctions between 1st-order and 2nd-order catchments. Headwater catchments tend to be seemingly described by either both orders.

3.4.1.2. Streams

Figure 3.4 shows histograms related to a series of parameters extracted for each stream running within a defined 1st-order or 2nd-order catchment. The parameters studied here are length, average slope, 200 m slope, and outlet slope (Table 3.2). All those parameters are related to streams and again the cumulative curve is represented above the histograms.

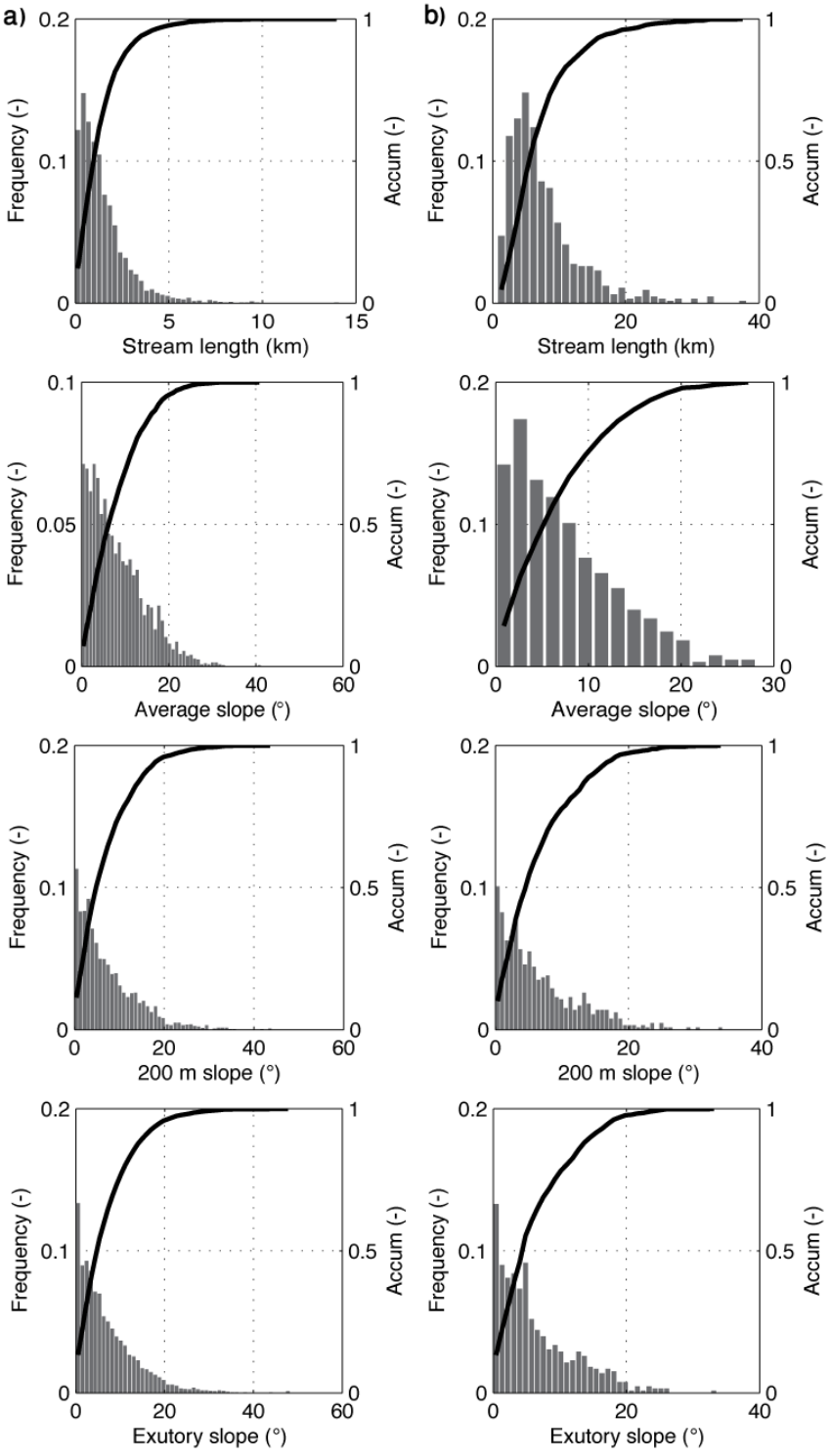

Figure 3.4: Histograms and cumulative curves showing parameters a) for 1st-order and b) 2nd-order streams of all watersheds.

Stream length unsurprisingly increases with the order of the catchment where the stream is found. For 1st-order catchments, the maximum value reached is 14

km, and their isolation on the histogram could show the exceptional character of a few catchments. The cumulative curve, showing one inflection point, allows redefining another maximum obtained where the curve is flattening near the top. A value of 10 km emerges when length is considered. It is to be noted that more than half of the 1st-order catchments have a stream length superior to 1 km when, for the 2nd-order catchments, it nears 5 km. The isolated maximum closes 40 km, with less dispersion toward the maximum values than for the 1st-order catchments.

Stream slopes have also been defined over 200 m upward, from their first intersection. Called the 200 m slope, the histograms show that for the 1st-order catchments the isolated maximum is over 40° and the secondary maximum nears 35°. Slightly more than half of those streams are under 5° over the last 200 meters. This value drops to 4° when 2nd-order catchments are considered, and the maximum is less than 30° (34° for the isolated maximum).

1st-order and 2nd-order catchment outlet slopes have maximums more pronounced than for all the other parameters. From 35° (non-isolated, 1st-order), it drops to 25° (2nd-order). (For the isolated maximum, 47° is reached for 1st-order, and it closes 35° for 2nd-order catchments). Regardless of the order, the cumulative curve gives between 5° and 5.5° for a 50% accumulation.

When the streams are studied through the series of parameters presented above, the better distinction is found for the outlet slope, which is computed over a short distance. The distinction is poor when the stream is considered over a large distance. On top of that, the stream's length is dependant on the order, just like areas and perimeters, and likely to be biased by the 1 km^2 threshold used while defining the catchments.

3.4.1.3. Morpho-hydrological ratios

Morpho-hydrological ratio histograms and cumulative curves are shown in Figure 3.5. Melton ratio, form factor, basin elongation and lemniscate ratio have been investigated and values are reported.

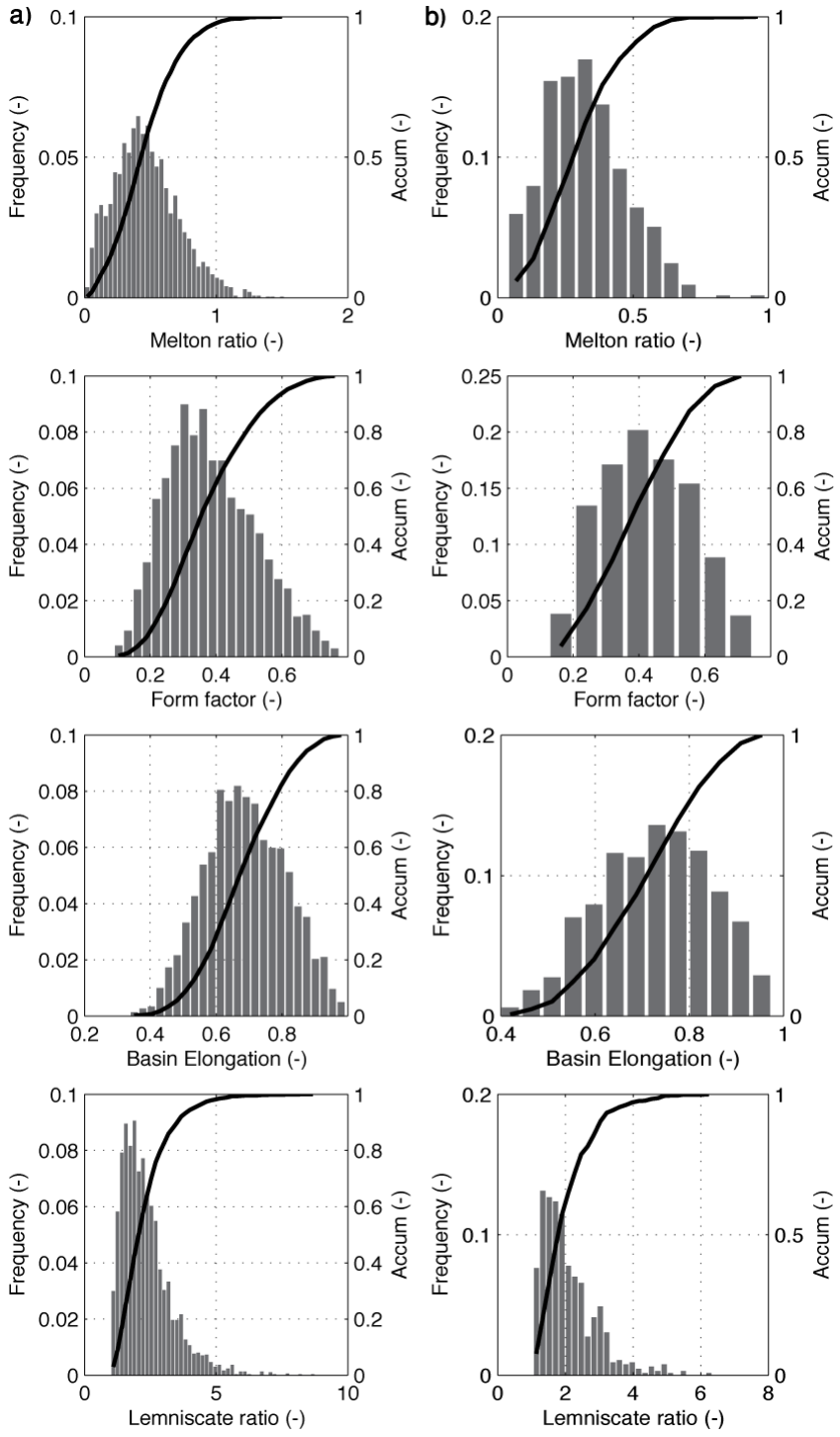

Figure 3.5: Histograms and cumulative curves showing hydrological ratios for a) 1st-order and b) 2nd-order catchments for all watersheds.

The Melton ratio (or ruggedness number) histogram for 1st-order catchments shows values reaching 1.5 as maximum, with a non-negligible portion over 1.0.

Half of the 1st-order catchments have a Melton ration over 0.4. For the 2nd-order catchments, maximum values are not exceeding 1.0, and half of the 2nd-order catchments have a Melton ratio lower than 0.3. Due to its definition (Table 3.2), it is normal to find an isolated maximum, just like it was for areas. Compared to other dataset gathered in the European and Southern Alps, the range of Melton ratio's values is coherent with past studies, although displaying less extreme high values (Bardou 2002; Welsh & Davies 2010). The role of the minimum area for defining the catchments on the Melton ratio's values is to be clarified, and could explain the values somewhat smaller observed in the study area.

Form factor's maximum values are found around 0.8, and minimum values appear around 0.1. In both cases 0.4 seems to be the limit of the 50% accumulation when looking at the cumulative curve. The difference between catchments of 1st and 2nd order resides in the range, slightly less wide for 2nd-order catchments.

Basin elongation's histograms are again very similar for both orders. Starting at 0.3 (1st-order catchments) and 0.4 (2nd-order catchments), the maximum values do not reach 1.0. In both cases, half of the catchments have a basin elongation just under 0.7.

The Lemniscate ratio, due to its definition (Table 3.2), presents histograms showing a minimum of 1.0. Again, the presence of an isolated and a secondary maximum is visible, again due to its equation based on parameters previously highlighting such a feature. For the 1st-order catchments, the isolated maximum is found at 8.5, when the secondary maximum seems to be close to 7.2. In respect of 2nd-order catchments, these values are nearing 6 (isolated maximum) and 5 (secondary). The shift towards the left, observed here for the maximum values, can also be seen when looking at the cumulative curve; half of the 1st-order catchments have lemniscate ratios below 2.1, and this value drops to 1.8 for 2nd-order catchments.

These ratio histograms mostly show little difference between orders. Basin elongation and form factor seem to be independent on the order, and remain almost unchanged, regardless the order of the catchments. On the other hand, Melton ratio and Lemniscate ratio offer a wider range of values, and thus a better way to differentiate trends between catchments of different orders. However, for all parameters, the cumulative curve's shape is unchanged through orders, showing two inflection points (Melton ratio, Form factor and basin elongation) or just one (lemniscate ratio).

3.4.2. Bi-dimensional comparisons

In this section, some parameters are compared thanks to the edition of bi-dimensional graphs. Figure 3.6 shows six of these relationships taking into account the Pyrenean 1st-order catchments. The data is the same, as used for the histograms presented above. When a correlation was obtained, a trend line is shown together with its equation and the R^2-value (or coefficient of determination, used to describe how well a regression line fits a set of data) (Fig. 3.6 a,b,c). Otherwise, the graphs remain free of this information (Fig. 3.6 d,e,f). The parameters used are maximum and mean elevations, stream length, Melton ratio, area and mean orientation. In Appendix 3 can be found the same relationships for 2nd-order catchments.

When the Melton ratio is plotted against the maximum elevation, it appears that the highest Melton ratio's values are found at a higher elevation (Fig. 3.6a). The ruggest catchments are found at high elevations. In Figure 3.6a, the best-fitting trend line is following a power law. The data could possibly be bracketed between two lines: an upper bound and a lower bound. Although these bounds are not drawn in Fig. 3.6a, they are clear from the graph.

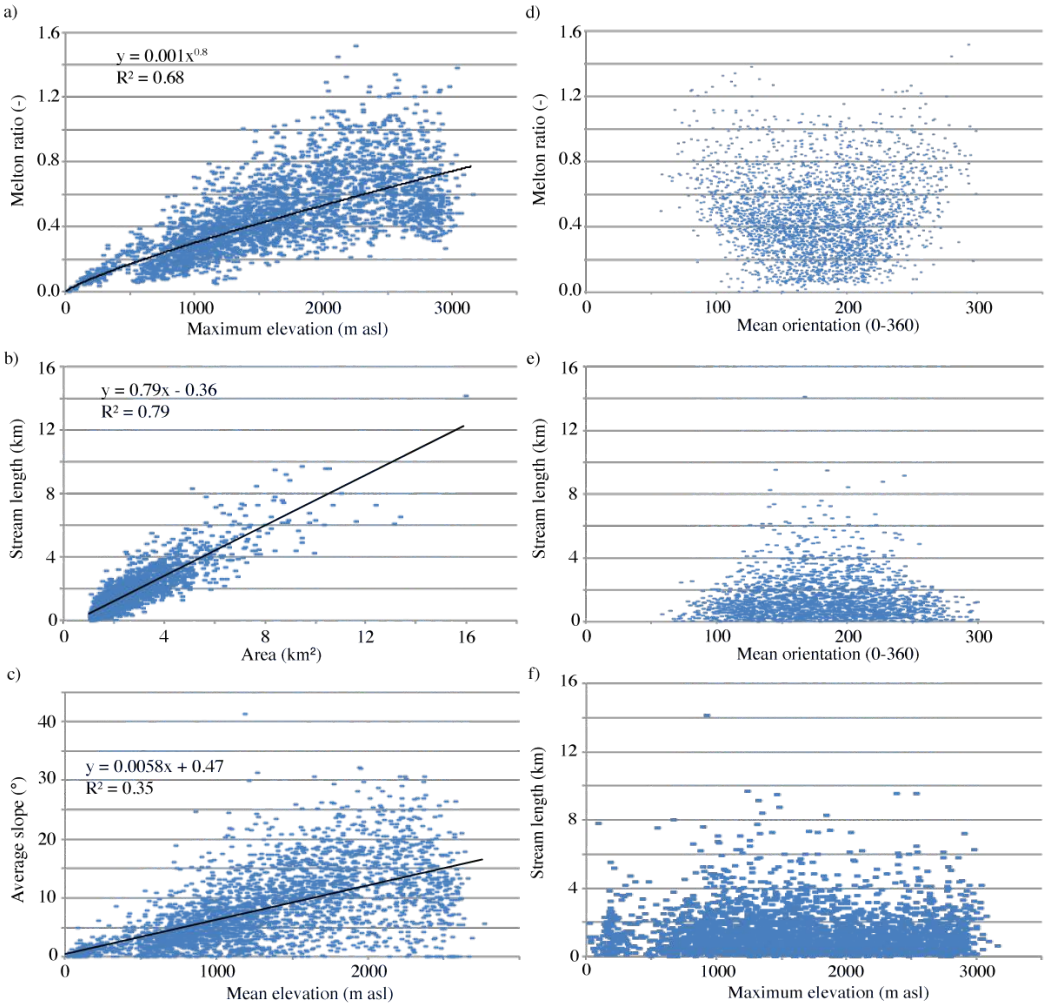

Figure 3.6: Bi-dimensional relationships shown for 1st-order catchments of all watersheds; a) Melton ratio vs. max elevation; b) stream length vs. area; c) average slope vs. mean elevation; d) Melton ratio vs. mean orientation; e) stream length vs. mean orientation; f) stream length vs. max elevation.

Figure 3.6b shows the relationship that exists between area and stream length (or drainage lines). Solyom & Tucker (2007) use this relationship in their work, which refers to Strahler (1952) and his extensive analysis of erosional topography. The R^2-value is relatively high (almost 0.8) for this relationship best characterised by a linear trend line. In Leopold (1964), the same relationship is shown on a logarithmic scale, based on the work of Hack (1957). Rivers like the Ganges, the Rio Grande or the Nile, together with 31 other river basins, are plotted. The results concern much bigger areas and lengths than presented herein. The authors highlight a linear trend in their logarithmic scale between those two parameters, meaning that when compared to Fig 3.6b, the trend line

should follow a power law. Here, however, the trend line is linear on a linear scale. Hack (1957), and then Leopold (1964) have studied one end of the spectrum, with high values of catchments orders (in fact, the highest order possible); the other end is presented here with 1st- and 2nd-order catchments. The relationship could be linear near the beginning where values are low, and then become a power law, as values get higher. When the graph is edited for the 2nd-order catchments, it appears that the best fitting trend line is a power law (R^2-value equal to 0.49), when the linear trend gives one R^2-value equal to 0.47 (Appendix 3). It seems to confirm the change of the trend line with the change of values range.

Mean elevation and (streams) average slopes are plotted in Fig. 3.6c. The best-fitting trend line is a linear relationship and gives a low R^2-value. Figure 3.6c shows that the highest slopes are found at higher elevations, but the range of slope values is wider, given a certain high elevation; encountering a flat portion stream is also likely at high elevations. To a lesser extent, Melton ratio behaves likewise (the Melton ratio is by some way a representation of the catchment's slope).

Figure 3.6 also shows the mean orientation compared to the Melton ratio (d) and the stream length (e). The scatters are opposite; For the Melton ratio, it is seen that the maximum values are found at the edge of the scatter, the catchments are therefore rugger when not facing the general orientation; As for the stream lengths, highest values are found for an orientation more consistent with the general trend of the range, as shown in the histogram.

The last graph presented in Figure 3.6 is an example of two parameters that are not correlated in any way (f). The stream length does not seem to be influenced by the elevation. Long streams can be found over the entire spectrum of elevations, and vice versa. It highlights the importance of the choice of the parameters in any study.

3.4.3. Regional distinctions

The Pyrenees are commonly compartmented into two main morpho-structural regions: the Axial Pyrenees and the pre-Pyrenees, which have been highlighted based on geology and tectonics. Figure 3.7 shows the frequency curves for three parameters, considering the 2nd-order catchments: area (Fig. 3.7a), mean elevation (Fig. 3.7b) and Melton ratio (Fig. 3.7c). 2nd-order catchments relationships and parameters were chosen for the readability of their graphs, as the same relationships for 1st-order catchments are very similar in trend. Table 3.1 gives a general distinction between watersheds in terms of mean values, when Figure 3.7 actually graphically shows these distinctions evolutions.

In case of a poor regionalisation, cumulative curves watersheds are hardly distinguishable between each other, as shown for area (Fig. 3.7a). The trends are similar, regardless of the watershed. A same value of area can be found in every watershed. The same comment applies also to perimeters, stream slopes, stream lengths or lemniscate ratios.

Figure 3.7b is an example of a clear regionalisation. Based on mean elevation, it can be clearly distinguished and presents three trends. A first trend is defined by the cumulative curves of Fluvia and Ter (to a lesser extent) with a high frequency at low mean elevation decreasing with increasing mean elevation. A second trend is recognised when frequency increases with increasing mean elevation and the maximum in frequency found at high mean elevations, as exemplified by Garona and Valira's cumulative curves. Eventually, lying between these two trends, other watersheds cumulative curves are found. A distinction between these watersheds could be attempted, based on frequency at high elevations, using Noguera Pallars and Noguera Ribagorçana in one hand, and Llobregat and Segre in the other, could be seen as displaying two distinct behaviours. Other elevations (maximum and minimum) cumulative curves follow a similar trend and induce similar distinctions.

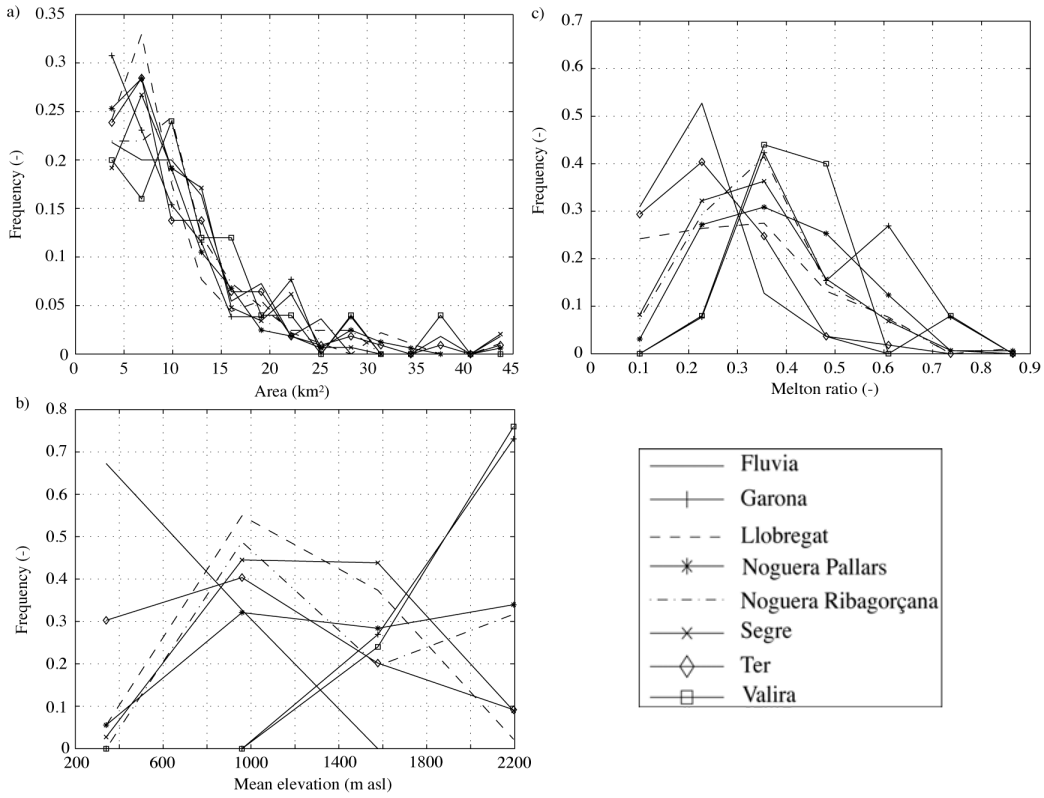

Figure 3.7: Frequency curves of a) area, b) mean elevation and c) Melton ratio, for all 2nd-order catchments.

As for the Melton ratio cumulative curves (Fig. 3.7c), all show a similar general trend: increase until a maximum and then a slow decrease. However, distinctions are possible in the light of the maximums position and the frequency at low Melton ratio's values. Fluvia and Ter cumulative curves display a maximum at very low Melton ratio's values (0.22). On the other hand, the other watersheds present a similar maximum in Melton ratios around 0.35. Out of these watersheds, two of them display a second maximum; for Garona the second maximum is found just over 0.6 in Melton ratio, and it is found around 0.74 for Valira. To be noted that those two watersheds cumulative curves are the only ones being null at low Melton ratio's values.

Garona, and Valira, could form one unique entity given the presented data. And Fluvia and Ter would be part of the last and lowest entity (low elevation and Melton ratio being representative). The rest of the watersheds would form the

middle entity, given the previous remarks. If an attempt is made at naming these three entities, and identify the major behaviour of fluvio-morphological parameters for each watershed, one could distinguish between high-mountain, medium-mountain and low-mountain environments watersheds.

The comparison with the distinction giving Axial and pre-Pyrenees, based on geology offers differences with the one presented herein. The Axial Pyrenees exhibits watersheds that give very different geomorphological behaviours (Fluvia and Garona for example). If Valira and Garona are considered typical of high-mountain headwaters watersheds, then the Axial Pyrenees cannot account for a high-mountain environment only whereas, the regionalisation based on fluvio-morphological parameters could better differentiate headwaters catchments and thus environments.

The data gathering was carried out at a given cell-size and with certain parameters. This chapter provides a description, sought by the means set up by the parameters. Not the statistical study of these parameters, nor the effect of a change in the cell-size. However, further investigation is required to precisely assess if a regionalisation is possibly hinted with the use and study of fluvio-morphological parameters. A statistical study looking at an ensemble of parameters would better refine the extent of such regionalisation and better emphasize at what scale would the regionalisation be optimized. Although high- and low-mountain environments are graphically distinguished, it could help apprehending and explaining the pre-Pyrenees and the disparities observed for the medium-mountain environment. It is shown here that using two common parameters, a distinction between Central-Eastern Pyrenean headwaters catchments is recognised at a defined scale.

3.5. Conclusion

The morphometric analysis of Central-Eastern Pyrenean and Andorran catchments and streams has benefited from GIS techniques. A series of fluvio-

geomorphological parameters has been identified. Those parameters are related to either catchments or corresponding streams. As outlined, the methodology renders possible the gathering of information necessary in order to obtain treatable data and the assessment of the different parameters values. They were investigated for Central-Eastern Pyrenean headwaters, more precisely catchments and streams of 1st and 2nd-order, following Strahler (1952).

Some of the parameters gathered at catchment's scale such as, area and perimeter are directly affected by the choice of the minimum draining area defined to draw (digitalise) the catchments in the GIS (equal or superior to 1 km^2). Others are not, likely to offer little changes in parameter values between orders like for the different elevations tackled in this thesis or the mean orientation. In addition, values gathered in this study agree with past studies showing that the 1-km^2 limit is not dramatically altering the values of the parameters. Streams and the slope's values gathered, at the outlet and going upstream have also been obtained. More dispersion in the stream's slopes occurs when the portion of stream is small: more dispersion is witnessed for outlet slope than for 200m slope. However, isolated values are found at the maximum end of the spectrum, which tend to pledge for the existence of abnormal catchments. Further studies could help explain their existence and geomorphological meaning. Morpho-hydrological ratio values mainly evolve in a similar way, as the parameters defining them. The values again are coherent with past studies, thus minimising the effect of the change in the minimum draining area defining each catchment.

Some parameters have been crossed, and bi-dimensional relationships are presented in the light of previous works. Being a power law relationship in Leopold (1964), the relationship between stream length and area is reported for great rivers fluvial systems, such as the Nile's one. The Central-Eastern Pyrenean headwater catchments represent the other end of the spectrum, and highlight the behaviour of the relationship near its origin point. Concerning the 2nd-order catchments of the study area, power law and linear regression equally best describe the relationship (similar R^2-value in both cases). However, it was

showed that a linear regression best fit, the relationship, for 1st-order catchments. The evolution of the relationship, from a linear to a power law behaviour as order increases, needs further investigation. Although acknowledged, comparing similar data to showed trends could reveal itself constraining. As Leopold (1964) pointed out, all the analysis depends on when you start to define a catchment. This study has been carried out with a minimum draining area of 1 km^2, in a unique geological and climatic setup. However, just as shown in this chapter, relationships can overpass these limitations and are recognised globally.

An attempt at recognising Axial Pyrenees and pre-Pyrenees through fluvio-morphological parameters is conducted. Divided into Axial Pyrenees and pre-Pyrenees based on geology and tectonics, it appears that this distinction seems hardly verifiable when fluvio-morphological parameters are investigated in the Central-Eastern Pyrenees. However, recognition of entities different from Axial and pre-Pyrenees is observed. Three entities seem to emerge from mean elevation and Melton ratio's frequency's curves study for all of the 2nd-order catchments. This first attempt needs further comparisons and studies.

Large-scale morphometric studies are scarce and the Pyrenees offers only a few studies of that kind, principally focusing on a little number of parameters at catchment scale. By this contribution a detailed geomorphometric analysis is attempted based on a consistent number of Central-Eastern Pyrenean headwaters catchments. Although this needs further refining, these results can thus serve as a base for, naming but one susceptibility assessment of natural hazards involving fluvial components such as debris flows (Su & Cui 2009) or flash floods, where geomorphology's role could be further understood next to climate and geology.

CHAPTER 4 SUSCEPTIBILITY ANALYSIS

4.1. Introduction

The main goal of this chapter is to elaborate a debris-flows susceptibility analysis at catchment scale, using the fluvio-morphological parameters, likely to be reproduced in remote areas with little knowledge about the physics of the erosional processes and without additional data but a digital elevation model. Another goal was to produce easily understandable results and apprehensible by non-experts. In order to achieve it, the applicability of data mining techniques was investigated.

Data mining techniques have the advantage to permit the treatment of a large quantity of data and, regressions equations and classification trees simplify the vision given to results (Wan *et al.* 2008; 2009). Trees are not common in literature focusing on debris flows, whereas matrices are well documented (Fawcett 2006; Frattini *et al.* 2010). Supporting modelling results and assessing robustness of the models are facilitated by these techniques as success and prediction rate curves are easily gathered (e.g. Santacana *et al.* 2003). Care is nonetheless necessary when interpreting these statistical results, given the likelihood of the complexity (Blahut *et al.* 2010).

The information presented in this chapter has been gathered thanks to 1) the machine learning software WEKA (Waikato Environment for Knowledge Analysis) developed at the University of Waikato (New Zealand), which is available under GNU General Public license (version 3-6-4), 2) numerical computing environment Matlab, developed by MathWorks™ (version 7.12) and 3) Excel from Microsoft™ (version Office Mac 2011). When the analysis required algorithms (codes) that did not exist, Dr. Vicente Medina programmed them into Matlab; WEKA and EXCEL were standardly used (with no change of existing codes).

The following sections explain the learning process that is considered in this thesis. 1) It focuses on the different sets (training and test sets) and methods, before presenting the models used. 2) The cost matrix is defined. It is a necessary step, explained by the fact that the ratio of reactive/non-reactive catchments is unbalanced; 78 reactive catchments in front of 944 non-reactive (1st-order catchments) and 52 in front of 226 (2nd-order catchments). In fact, it results in a learning process indirectly biased towards the most frequent class (non-reactivity). Data mining procedures provide tools to reduce this parasitic effect: The standard is to introduce a cost in the misclassification of certain class, applying a cost matrix (Witten *et al.* 2011). 3) The models and their results are presented in the coming paragraphs.

The structure of the work follows the classical approach used in data mining research (e.g. Witten *et al.* 2011): 1) Procedures and algorithms are run in order to obtain knowledge as a consequence of a learning process, 2) the knowledge is tuned/optimized, 3) the resulting knowledge is validated with the test set and 4) performance and credibility of the models are explained and evaluated. Eventually the susceptibility maps for each model is displayed, for both training and test sets. All the results are presented for the two study units: 1st-order and 2nd-order catchments.

4.2. Selection of datasets

When data mining techniques are considered, the method implies the creation of two sets of data. First, the training set (or learning set) will serve in the development and building of the models. Then the test set (or validation set) is used in order to confront the models. Both sets are described below. The list of the parameters, together with their abbreviations, is found in Chapter 3, as well as the methodology related to GIS and their extraction from it.

4.2.1. Training set

The training set spreads over three test sites: Berga, NWCat and Mollo (see Chapter 2 for test sites' description and Fig. 2.15 for their location). It covers a total area of 4156 km^2: 1386 for Berga, 547 for Mollo and 2223 for NWCat.

Table 4.1: Main characteristics, per catchment, of the three test areas of the training set (normal font), with "all" being the recapitulation of the whole training set. Percentages shown are relative to the training set. Number of reactive catchments and number of debris-flow tracks are also shown.

	Number of catchments (# (%))	*Mean area per catchment (km^2)*	*Mean elevation per catchment (m asl)*	*Number of reactive catchments (# (%))*	*Number of debris flows (#)*
1st-order catchments					
Berga	457 (45)	2.27	1380	20 (26)	36
Mollo	119 (11)	2.21	1712	33 (42)	139
NWCat	446 (44)	2.32	1942	25 (32)	76
All	1022 (100)	2.29	1664	78 (100)	251
2nd-order catchments					
Berga	113 (50)	11.32	1331	12 (23)	16
Mollo	27 (12)	12.69	1613	13 (25)	138
NWCat	86 (38)	11.07	1985	27 (52)	109
All	226 (100)	11.69	1643	52 (100)	263

Regarding 1st-order catchments, the training set consists of 1022 catchments, including 78 reactive catchments (Table 4.1). When 2nd-order catchments are considered, 226 catchments compose the training set, with 52 reactive catchments (Table 4.1). These training sets are not mixed and treated separately all along the analysis.

4.2.2. Test set

The test set, which is made up from the Principality of Andorra (Fig. 2.15), includes 113 1st-order catchments with 41 reactive catchments; and 25 2nd-order catchments, including 18 reactive catchments, compose the other test set. It spreads over 468 km^2 (Table 4.2). The test sets are not used in the models elaboration (but in testing them), and account for the models applicability.

Table 4.2: Main characteristics, per catchment, of the three test areas of the test set. Number of reactive catchments and number of debris-flow tracks are also shown.

	Number of catchments (#)	*Mean area per catchment (km^2)*	*Mean elevation per catchment (m asl)*	*Number of reactive catchments (#)*	*Number of debris flows (#)*
1st-order catchments	113	2.31	2208	41	91
2nd-order catchments	25	11.68	2152	18	102

4.3. Statistic

Details about the statistical tables that permitted to plot the following results can be found in Appendix 4. They are consultable in a desire to complement the information provided by the following results, and present general statistical

information, such as standard deviation, parameter-by-parameter, zone–by-zone, for 1st-order and 2nd-order catchments.

4.3.1. 1st-order catchments

Basic statistic relationships, under the form of bi-dimensional combinations of fluvio-morphological parameters, gathered thanks to GIS techniques form the backbone of this section (see chapter 3 for the methodology related to the extraction of the parameters). The objective of this preliminary task was to gain preliminary trends and knowledge about the distinction between reactive and non-reactive catchments, in order to acquire simple rules that could pledge for the necessity to use more powerful tools, such as those provided by data mining techniques.

The results obtained generally coincide well with published data regarding area (Rickenmann 1999; Welsh & Davies 2010), altitude (Blahut *et al.* 2010), mean slope of catchments (Rickenmann & Zimmermann 1993; Jakob & Hungr 2005), or Melton ratio (Portilla *et al.* 2010; Welsh & Davies 2010).

Figure 4.1 depicts relationships showing four bi-dimensional combinations. Distinction between reactive and non-reactive catchments based on fluvio-morphological parameters is not straightforward, as both classes of catchments are never found gathered or clustered: a given value on the X-axis (or Y-axis) shows both non-reactive and reactive catchments. However, thresholds emerge, capable of clustering the reactive catchments class. 11 km^2 in area (Fig. 4.1a), 20° in mean slope (Fig. 4.1a), 6 km in stream length (Fig. 4.1b), O.25 in Melton ratio (Fig. 4.1b) or 1500 m asl in maximum elevation (Fig. 4.1c) could restrain the spatial occurrence of reactive catchments, although a little number of reactive catchments are not respecting these simple rules of occurrence.

Some parameters show extremums values for debris-flow occurrence (e.g.: area, elevations, Melton ratio) when other better highlight clusters (e.g.: form factor, slope).

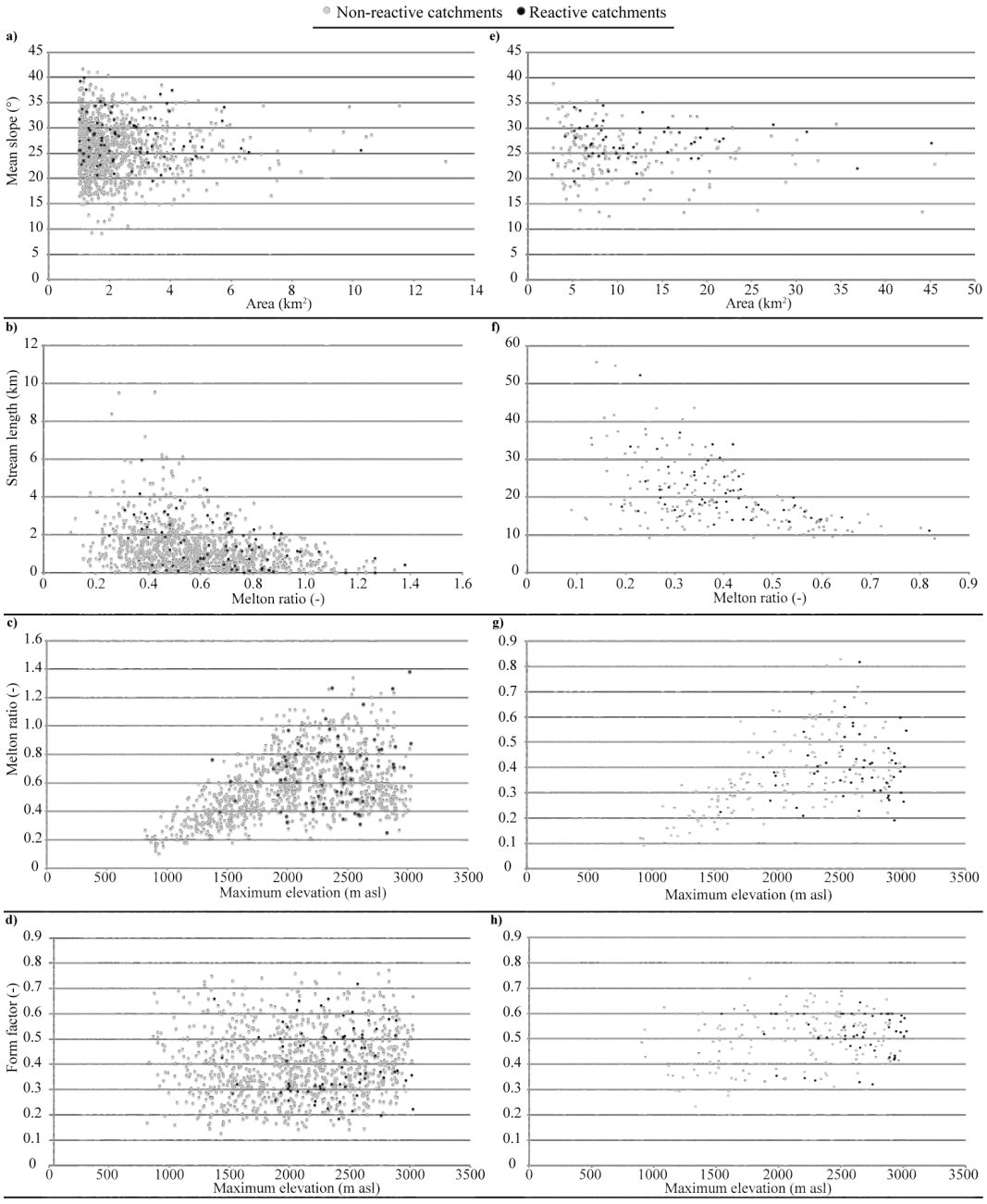

Figure 4.1: Bi-dimensional combinations showing non-reactive catchments (grey points) and reactive catchments (black points). Left column is for 1st-order catchments and right column for 2nd-order catchments: a) & e) Mean slope as a function of area; b) & f) Stream length as a function of Melton ratio; c) & g) Melton ratio as a function of maximum elevation; d) & h) Form factor as a function of maximum elevation.

4.3.2. 2nd-order catchments

Figure 4.1 also displays bi-dimensional relationships for 2nd-order catchments. The most striking difference obviously resides in the number of occurrences (Table 4.1). Then, a shift is observed in the minimum values for area and stream length toward a higher value. The Melton ratio diminishes as compared to 1st-order catchments. The maximum elevation suffers little change; and the range in form factor is less wide.

The shift in values for area and stream length is easily understood taking into account that 2nd-order catchments are by definition bigger than 1st-order catchments (Fig. 3.2). Always more than one 1st-order catchment, if not always at least 2 1st-order catchments compose a 2nd-order catchment. Leopold (1964) emphasized these relationships in the middle of the past century.

The elevation considered in Figure 4.1 (maximum elevation) is little affected by the change in order. In both cases it roughly spreads from 1000 to 3000 m asl (Fig. 4.1g or h). This value is directly dependent on the geographical zone where data is issued from (Berga, NWCat and Mollo).

As a consequence of these latest two points, the Melton ratio diminishes with the order for reactive catchments. The link with the mean slope is logical, as Melton ratio is a representation of the slope's gradient (Chapter 3); thus the range of mean slope applicable to reactive catchments diminishes as well.

Regarding the form factor, a decrease in the range of values for reactive catchments is stated. From 0.2 to 07, it changes from 0.3 to 0.65. At this point, one might have noticed a suspicious line at form factor equal to 0.6, formed by about fifteen reactive catchments. Only coincidence can be called upon to give a logical explanation.

However, just like for 1st-order catchments, extremums' or clusters' patterns in the data's relationships are found again for 2nd-order catchments. Thus no general rules can be straightforwardly highlighted. For this reason data mining

and statistical techniques were applied to both the 1st-order and 2nd-order catchments' training sets and are discussed in the following sections.

4.4. Cost matrix

The idea of a matrix as it is in this thesis is exemplified in Figure 4.2. It applies to the cost matrix developed in this section, as well as the other matrices shown in this chapter. It should be pointed out, that in this thesis, the main class is the reactive class; that is why it is defined as "positive" and non-reactive class is defined as "negative". Figure 4.5 uses the terms positive (reactive) and negatives (non-reactive) in context.

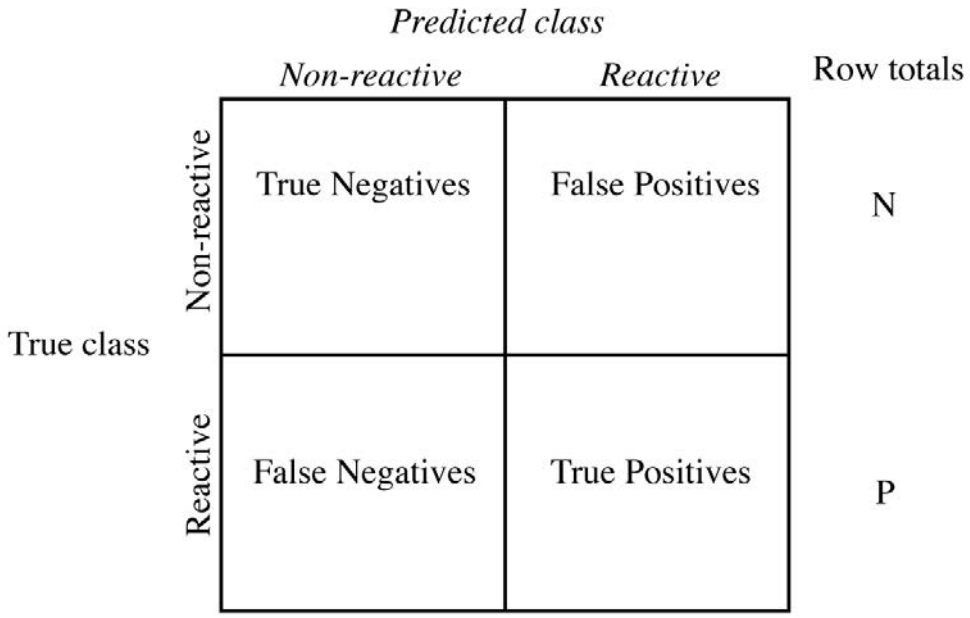

Figure 4.2: Matrix model as used and later reported in this work, after Fawcett 2006. N is the total of non-reactive in the true class; P is the total of reactive in the true class.

4.4.1. Definition

To select and use the cost matrix in this work, a comprehensive sensitivity analysis was carried out using the CART algorithm, which will be explained later. Of course defining the cost matrix suffers the influence of the selected tool for the computations, but it is supposed to be suitable for the rest of the analysis.

The selected choice to solve the stratification problem is to introduce a cost matrix in the training processes. The open question regards in the different costs used in the matrix. What should be kept in mind is that the safety requirements should increase the cost of a false negative (reactive catchment classified as non-reactive). The costs matrix are used all along the learning process, in all the proposed algorithms the cost matrix is introduced to address the stratification problem.

The selected choice, as previously stated, in order to address the stratification problem is the addition of a misclassified cost matrix. This matrix penalizes the misclassification of the database instances. From the practical point of view these matrices include a diagonal null, meaning the cost of the correctly classified instances is null. The remaining elements are arbitrary defined, with the aim of breaking classification isotropy.

Therefore, the problem becomes to define the anisotropy degree, i.e. the values of the non-diagonal matrix elements. In this case, the target of the matrices' introduction is to increase the influence of the reactive catchments. Hence, the ratio of misclassified reactive catchment value to the non-reactive one is to be high. However, by how much is there a change is an open question.

There is no standard procedure to fix these values. The procedure used in this work will be described in the following. The selected tool to test the different misclassification's cost values is the classification tree, and more specifically the CART tree (classification and regression tree) is the classifier chosen (Breiman *et al.* 1984; Breiman *et al.* 1995).

Several key elements should be mentioned before going deeper into the mathematical representation of the problem. Firstly there is the overfitting problem that is to say that the learning process suffers an excessive adaptation to the training dataset. The obtained classifier fully captures the available instances in the database. It means that the parasite errors, (always) existing in datasets, are fitted as well. This masks the accuracy in the predictor or knowledge obtained from the training process. To overcome this difficulty, the classical approach is pruning algorithms, which rely upon validation techniques: The cross-validation method is a common validation technique. The second issue to address is the fact that the selected cost matrix should be strong enough to guarantee anisotropy in the influence of the classes (reactive vs. non-reactive).

All these elements should be included in what is called an "objective function" that should be kept to a minimum. With the purpose of introducing the practical problem, the classification tree cost should be first used. It is defined as the sum, over all terminal nodes of the estimated probability of a node, times the cost of a node. The cost of a node is the sum of the misclassification costs of the observations in that node.

In Figure 4.3a & 4.3b the results are presented for 1st-order catchments. The independent variables are first, the reactive catchments' misclassification cost and, second, the selected pruning level used for optimizing the classifier. The range of the first variable is [1, 50] for 1st-order catchments, which means that the lowest possible cost of an error in reactive catchment is 1, and the maximum considered is 50. For 2nd-order catchments, this range changes to [1, 30] (Fig. 4.3c and 4.3d). The misclassification cost for the non-reactive catchments is fixed to 1. The cost should not be out of this range, due to the fact that the ratio of reactive/non-reactive catchments is 8.2% for 1st-order catchments and 30% for 2nd-order catchments.

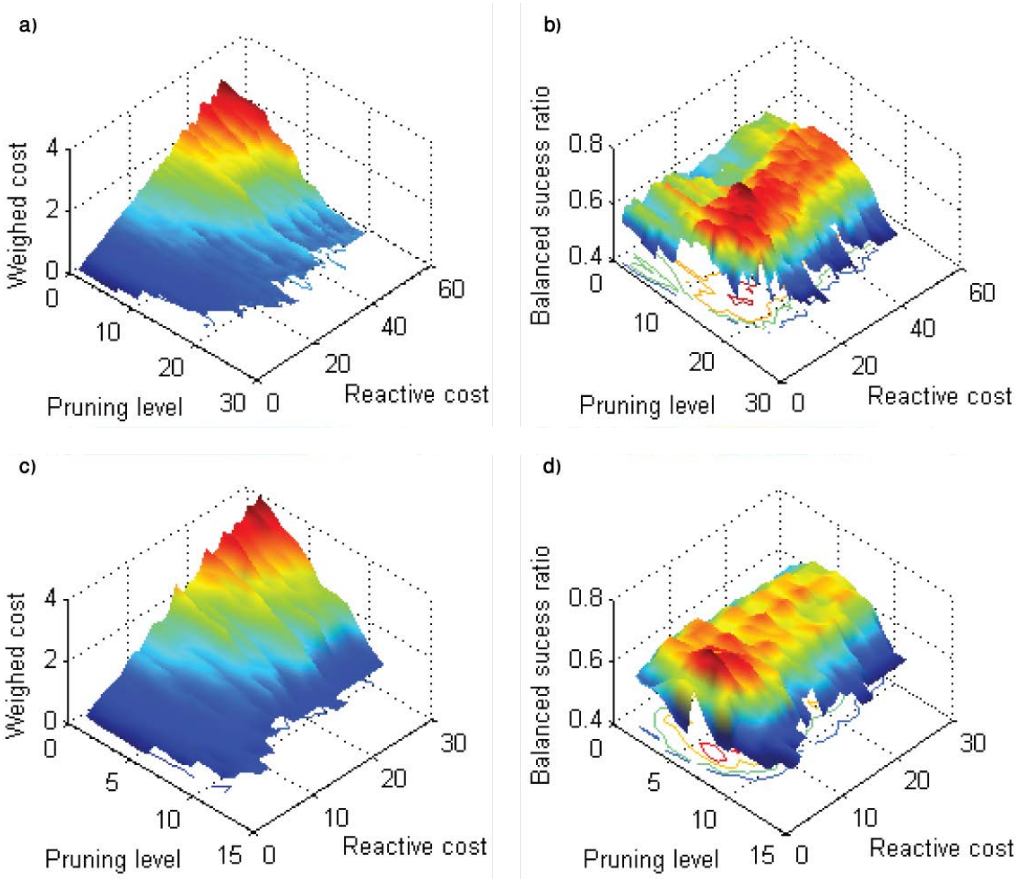

Figure 4.3: Classification tree cost as a function of cost matrix and pruning level (a & c). Balanced success ratio of the classification tree as a function of cost matrix and pruning level (b & d). a) & b) are related to 1st-order catchments and c) & d) to 2nd-order catchments.

The pruning level range depends on the constructed tree. It is at most equal to the number of levels of the tree. The result presented in the z-axis is the so-called classification tree cost and is plotted as "Weighted cost". So the procedure to construct the graph is:

1) Fix a cost matrix,

2) Compute the classification tree,

3) Calculate tree cost for every pruning level (overfitting reduction).

As shown in Figures 4.3a and 4.3c the result is not profitable. The tree cost is computed explicitly using the cost matrix. Consequently the obtained result strongly depends on the cost value, and that is represented in Figures 4.3a and 4.3c. If the reactive cost is high, then the tree cost is also high. There exist lots of minimums for these results (in blue in Figure 4.3) that the domain boundary always contains.

Therefore a new alternative approach is to be used. In this case what is proposed is to assign an equal weight to the success in both the reactive catchments' classification and the non-reactive catchments' classification. To do so a new index, the BSR (Balanced success ratio), only designed for the purpose of this analysis, is defined as:

$$BSR = \frac{1}{2}\,(TPR + TNR) \tag{4.1}$$

with TPR the "True Positive Rate" and TNR the " True Negative Rate".

Equation 4.1 expresses the averaged value in the classification of reactive and non-reactive catchments. Of course this index is arbitrary defined, based on the idea to obtain an index that balances the influence of each class. The key point is that the TPR is computed using the 78 reactive catchments classification success (or 52 for 2nd-order catchments) and the TNR is computed through the classification result of the 944 non-reactive catchments (or 226 for 2nd-order catchments). The results for this index are presented in Figure 4.3b and 4.3d. At the bottom of the graph (x-y plan) the levels curves are shown, although barely visible.

It is important to state that the cross-validation process used to evaluate the classification success has a random component in the folds construction. For every index realization the results are slightly different, so what is presented in

the graph is just a snapshot of the possible results. Cross-validation process is later explained in the chapter.

This index (Eq. 4.1) should be maximized and what is important for our purposes is that the index has a global maximum. After different runs it seems that the maximum is located in the cost range [11, 16] for 1st-order catchments. The required pruning level is around 15-16. For 2nd-order catchments the cost range is [4, 5] and the pruning level is found around from 5 to 7. In this analysis the main concern is the cost value, so the optimization/pruning issue of the trees is later analysed in this chapter.

The maximum is below 0.7, so the best expected success in classification using this kind of tree is below 70% (or 0.7). For 2nd-order catchments, this value is 0.75, meaning the best success is no more than 75%. It is interesting to note that, just like it was previously commented, the ratio between reactive and non-reactive catchments is 8.2%. Therefore the number of reactive catchments should be increased 12.1 times in order to balance the number of non-reactive catchments. The cost value 12 represents, in some sense, this scenario, and falls inside the range of the optimum cost. Obviously this result could be expected once the optimization index was defined searching the balance between both, reactive and non-reactive classes. Although a cost value equal to 12 plays a relevant role in the process, there were similar runs where the optimal value was achieved using cost equal to 15, so both values are candidates. The same logic applies to the 2nd-order catchments, safe that the ratio reactive over non-reactive is 30%, meaning a balance equalling 3.3, cost equal to 4 representing in some way this scenario.

Both values (for each order of catchments) were used in all the analysis and the best fit was kept. The profiles obtained in Figure 4.3b and 4.3d for the reactive catchments misclassification cost value equal to 12 (1st-order catchments) and 4 (2nd-order catchments) are presented in Figure 4.4. On the left (Fig. 4.4a and 4.4c) is found the “Weighted cost” and on the right (Fig. 4.4b and 4.4d) the

"Balanced Success Ratio". The effect of the pruning is clear, and the graphs confirm the existence of maximums and minimums.

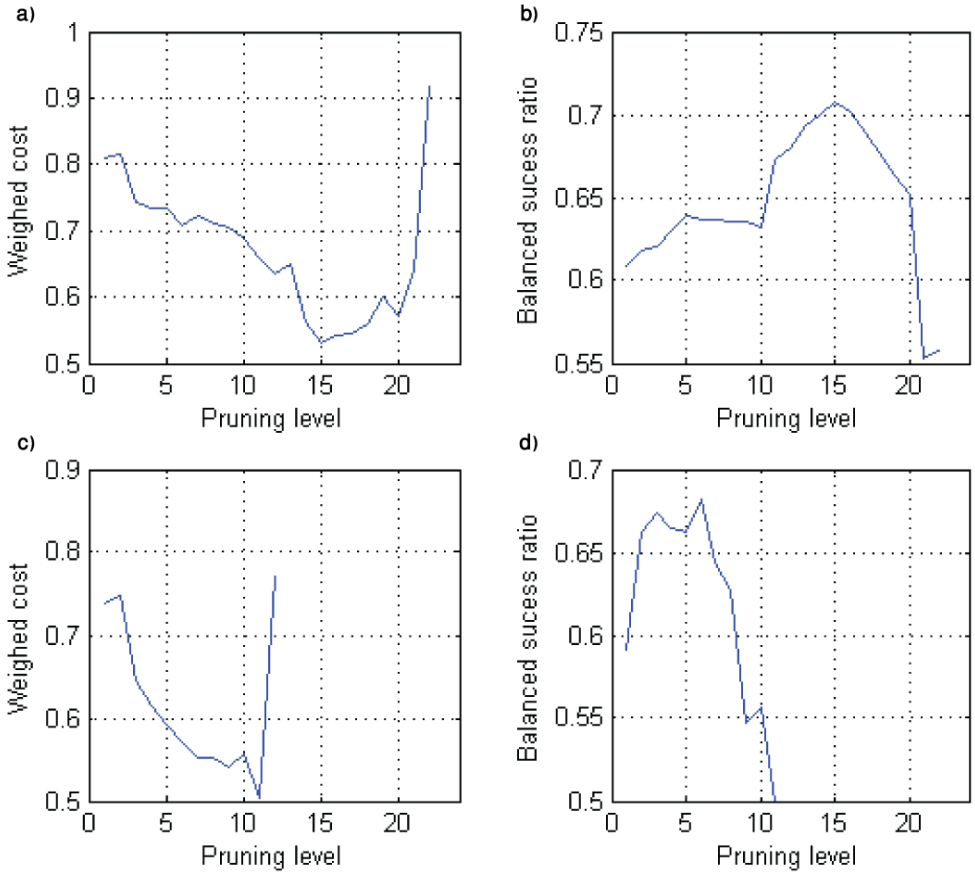

Figure 4.4: Weighted cost and BSR vs. pruning level: a) & b) for 1st-order catchments (cost value equal to 12); c) & d) for 2nd-order catchments (cost value equal to 4).

4.4.2. Cost matrix analysis

A link exists between, what has been presented and the standard cost curves (Witten & Frank, 2005). The analysis that was conducted considers a "Balanced Success Ratio", which involves using in equal form the reactive class and the non-reactive class. This type of analysis, done discarding explicitly the cost matrix, is similar to the one performed for the cost curves (there exists another cost curves family that explicitly consider the cost matrix and where the horizontal axes

variable is "probability cost function"). The result formed by this type of analysis is shown in Figure 4.5.

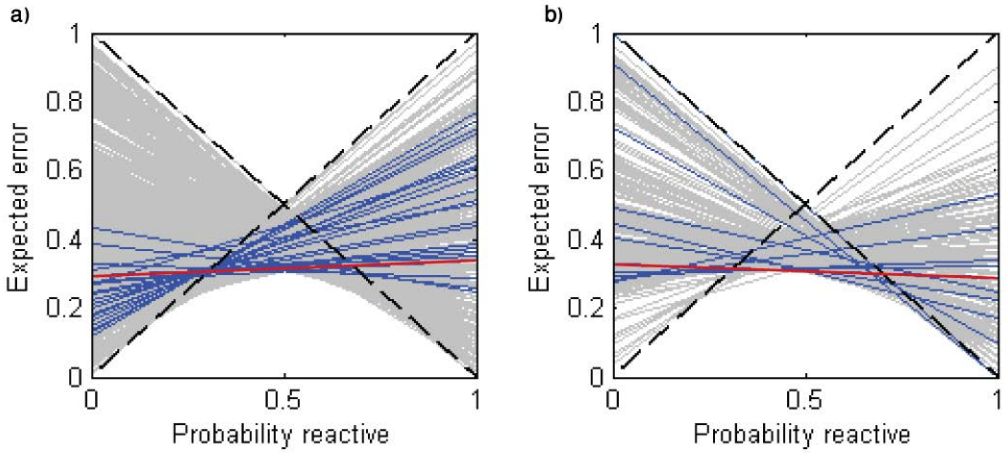

Figure 4.5: Cost curve for the whole range of test (grey color): a) 1st-order catchments; b) 2nd-order catchments. The curves corresponding to the optimal cost are in blue color. The dashed black lines are the extreme classifiers (always reactive and always non-reactive). In red are displayed the two curves the closest to the horizontal.

The horizontal axis of Figure 4.5 corresponds to the reactive percentage in the dataset sample. Every grey line corresponds to a point in the mesh defined by [cost range] x [pruning level]. Every point in Figure 4.3 matches one line in Figure 4.5. If in our data set, 100% of the instances are reactive, the probability value will be 1 and the error in our classifier will be equal to FNR. On the other hand, if the probability value is 0 the error will be equal to FPR. So the intersection on the left axis is the FPR (False Positive Rate) of the classifier, and the intersection with the right axis is the FNR (False Negative Rate). Hence, both values could be considered as "errors". And it can account for a measure of "success".

The optimum classifier is the one that minimizes the error for the whole probability values, which means the classifier corresponding to the closest line to

the horizontal axis. In order to select the best fit, the area between the line and the axis is considered.

The blue lines in Figure 4.5 represent classifiers corresponding to the selected cost (reactivity misclassification equal to 12 for Fig. 4.5a; and reactivity misclassification equal to 4 for Fig. 4.5b), and every line symbolizes the different pruning levels. It is possible to see that the optimum line in the graph corresponds to this family. The best line has the coordinates [0, 0.28] and [1, 0.33] for 1st-order catchments, and, [0, 0.286] and [1, 0.283] for 2nd-order catchments.

From the theory forming the background of cost curves, it is possible to establish that the valid application's range of the classifier is the length contained between the two black dashed lines. So, to apply the classification tree, the test dataset should contain between 30% and 70% of reactive catchments (probability value between [0.3, 0.7] for 1st-order catchments and [0.28, 0.72] for 2nd-order catchments). Beyond this constrain our classifier is useless because it is worse than the extreme classifiers (always reactive and always non-reactive) represented by the dashed black lines.

The main conclusion of this analysis is related to the accuracy of the expected classification. Considering all the possible cost matrices and pruning levels (optimization) none of the possible classifiers will obtain a success rate over 65-70% (error of 30%) for 1st-order catchments and over 70-75% (error of 25%) for 2nd-order catchments. So, respectively for 1st-order and 2nd-order catchments, the absolute ceiling of this classifier (CART) in accuracy is around 65% and 70% (prediction success rate).

Of course all the previous analysis suffers influence of the selected tool for the computations (CART tree), but it is supposed to be suitable for the different data mining tools used in this work.

4.5. Data mining classifiers

Three classifiers were selected to process the training sets to learn knowledge from it. First, a logistic regression was determined. Second, two classification trees were considered: C4.5 (J48) and CART.

The procedure is presented by default with its details for 1st-order catchments. Concerning the 2nd-order catchments, for which the procedures and logic remain the same, only the final product (optimized model) is shown and commented.

4.5.1. Logistic regression

Traditionally, the first choice to fit data is a linear regression. It is an excellent and simple method, although it only considers linearity. If the data exhibits nonlinear relations, the fitted straight line will not accurately reproduce the data behaviour. However linear models are the first approach to analyse multiple data problems.

The targeted attribute in this learning process is reactivity, which is a nominal/binary attribute. However, the standard scope of linear models is a numeric attributes, thus this technique should be adapted. For every class in the attribute a linear regression is carried out, considering value equal to 1 for members and 0 for instances not belonging to the class. This way a linear regression is obtained for every class, and they could be considered as a membership functions. This procedure is known as multi-response linear regressions and details can be found in Witten *et al.* (2011).

The inconsistency of this method stands in the fact that the membership functions should be in the range between 0 and 1. This constrain does not exist in the linear regression's procedure and consequently the expected result could be out of the range. To address this issue the logistic regressions (LR) was preferred (Landwehr *et al.* 2005; Witten *et al.* 2011). The theoretical basis of logistic regressions is simple and the result can be represented by the function:

$$f(z) = \frac{1}{1+e^{-z}} \tag{4.2}$$

with $$z = w_0 + w_1 a_1 + \cdots + w_k a_k$$

where a_i are the attribute values and w_i are the attribute weights. In conclusion, Eq. (4.2) could be considered as a membership function (Zadeh 1965).

The first try was run for the construction algorithm using the 1st-order catchments' training set without any tuning and without using the cost matrix. The obtained logistic regression is as follows:

$$\begin{aligned} z = {} & -2.6455 + 0.00123\, Hmax - 0.00085\, Hmin + 0.11379\, MR \\ & + 0.00188\, SM + 0.00185\, O + 0.12799\, A - 0.10574\, L - 0.00003\, P \\ & - 0.17712\, BE - 0.11440\, LR + 0.06086\, Se - 0.07900\, S200 \\ & + 0.00340\, Save \end{aligned} \tag{4.3}$$

Abbreviations of the parameters are listed and viewable in Chapter 3.

The resulting confusion matrix is shown in Table 4.3a, these results are extremely poor because the cost matrix was not used. This is not a consequence of the lack of optimization. If optimization algorithms were used, the attempt of applying the algorithm to the training set results in simple and irrelevant knowledge, i.e.:

$$z = -1.3611 + 0.00066\, Hmax \tag{4.4}$$

Considering that in the logistic regression the threshold is supposed to be in the form f(z)=0.5, the regression could be reinterpreted as:

$$f(z) = 0.5 \rightarrow z = 0.0\,, \tag{4.5}$$
$$0.0 = -1.3611 + 0.00066\,Hmax \;\longrightarrow Hmax = \frac{1.3611}{0.00066} = 2052.72$$

All the catchments having a maximum elevation over 2052 m asl are reactive is a conclusion of Equation 4.5, which shows the weakness of this process. The confusion matrix for this training set is the same as in Table 4.3a.

When the cost matrix is used with a value of 12, the weighted logistic regression can be expressed as:

$$\begin{aligned} z = {} & -0.9220 + 0.00137\,Hmax - 0.00103\,Hmin + 0.28304\,MR \\ & - 0.00297\,SM + 0.00105\,O + 0.21793\,A - 0.10705\,L - 0.00006\,P \\ & - 0.60802\,BE - 0.18096\,LR + 0.05579\,Se - 0.06914\,S200 \\ & + 0.00565\,Save + 0.24360\,FF \end{aligned} \tag{4.6}$$

Using this regression the success in reactive catchments classification was clearly improved at the sacrifice of the non-reactive ones (Table 4.3b).

Linear regressions have a great handicap: the maximum complexity is one coefficient per input variable. Therefore, the maximum freedom degree in the tuning process is the number of input variables plus one. Another important point is that input variables are not normalized. It means that the coefficient value does not provide information about the relative importance of each

variable. This non-optimized version of the fitting curve is applied to the corresponding test set and the confusion matrix is presented in Table 4.3c.

Table 4.3: Confusion matrices in relation to the logistic regression, for 1st-order catchments: a) Confusion matrix obtained for the training set; b) Confusion matrix obtained for the weighted training set; c) Success in test set using the weighted non optimized logistic regression.

a)

	Non-reactive	*Reactive*
Non-reactive	**944**	**0**
Reactive	**78**	**0**

b)

	Non-reactive	*Reactive*
Non-reactive	**649**	**295**
Reactive	**21**	**57**

c)

	Non-reactive	*Reactive*
Non-reactive	**41**	**31**
Reactive	**15**	**26**

Optimization of the logistic regression

The resulting equation should also be optimized in order to be useful for sets different from the training one, to reduce the influence of overfitting.

A tenfold cross-validation is applied to the weighted logistic regression obtained in the previous sections. Cross-validation means to divide randomly the training set in 10 parts of similar size, run the classifier 10 times with each part and average the error estimates to get an overall error estimate (Witten *et al.* 2011). The new optimized regression equation obtained after a tenfold cross-validation is:

$$z = -1.84110 + 0.00078\,Hmax - 0.00044\,Hmin + 0.71571\,MR - 0.00735\,SM + 0.00105\,O + 0.15465\,A - 0.07577\,L - 0.14204\,LR + 0.04088\,Se - 0.05077\,S200 + 000356\,Save \quad (4.7)$$

The confusion matrix for this training set is presented in Table 4.4a. The results are slightly worse than the ones obtained using the non-optimized regression in the training set. But this was the target due to the overfitting problem. Finally, when this optimized regression is applied to the test set and the obtained confusion matrix (Table 4.4b) is compared to the results obtained for the non-optimized version of the regression (Table 4.3c), results are improved.

Table 4.4: Confusion matrices in relation to the logistic regression, for 1st-order catchments: a) Confusion matrix for the weighted set after optimization; b) Success in test set after optimization.

a)

	Non-reactive	*Reactive*
Non-reactive	**633**	**311**
Reactive	**23**	**55**

b)

	Non-reactive	*Reactive*
Non-reactive	**41**	**31**
Reactive	**12**	**29**

2^{nd}-order catchments

The results presented here are corresponding to a cost equal to 5 as defined earlier. Equation 4.8 shows the result obtained using the training set, when 2nd-order catchments are considered. The equation was achieved after optimization of the model, following the same method as introduced for 1st-order catchments:

$$z = -2.87794 + 0.00121\,Hmax + 0.00026\,Hmin - 0.01068\,Sm - 0.00436\,O + 0.02053\,L + 53.06599\,FF - 0.48506\,BE + 0.00857\,Se - 0.01464\,S200 - 0.01041\,Save \quad (4.8)$$

The confusion matrices for both training and test sets are found in, respectively, Tables 4.5a and 4.5b. Bearing in mind that the very different number of instances

available for 2nd-order catchments, results are very complicated to compare with the ones previously determined for 1st-order catchments with the format offered by confusion matrices. For this reason, a section later in this chapter is dedicated to the comparison between the different models and orders of catchments.

Table 4.5: Confusion matrices in relation to the logistic regression, for 2nd-order catchments: a) Confusion matrix for the weighted set after optimization; b) Success in test set after optimization.

a)

	Non-reactive	*Reactive*
Non-reactive	**102**	**72**
Reactive	**10**	**42**

b)

	Non-reactive	*Reactive*
Non-reactive	**1**	**6**
Reactive	**2**	**16**

4.5.2. Classification trees

Two algorithms were used to construct the classification tree: CART and C4.5 (J48), thus giving two resulting trees (Breiman *et al.* 1984; Breiman *et al.* 1995). Gini's Diversity index (Gini 1912) was selected as a splitting method: it defines the order in which questions are reported in the trees.

The optimal size of the final tree is an important issue in considering a decision tree algorithm. Overfitting the training data and poorly generalizing to new samples are often due to a tree that is too large. On the other side an excessively small tree may not capture and thus lack important structural information about the sample. However, telling where a tree's algorithm should stop is a tricky task. It is impossible to tell whether adding a single extra node will dramatically decrease the error or not. "Horizon effect" is the name of this well-known problem. A common strategy to overcome the problem is 1) growing the tree until each node contains a small number of instances and 2) pruning it in order to remove the nodes that do not provide additional information. Pruning 1) reduces the complexity of the final classifier, 2) better predicts the accuracy by

the reduction of overfitting (which is a common problem in data mining and consists of finding patterns in the training set which are not present in the general set) and 3) eliminates classifier's sections likely to be based on noisy or erroneous data (which could be associated to the principle of regionalization).

4.5.2.1. C4.5 (J48)

A preliminary result is shown to highlight the limitation of the training set used in the tree's construction. If the C4.5 tree is constructed using the raw training set without cost matrix, the resulting tree includes 7 leaves and 13 nodes (Fig. 4.6). Table 4.6a illustrates its confusion matrix.

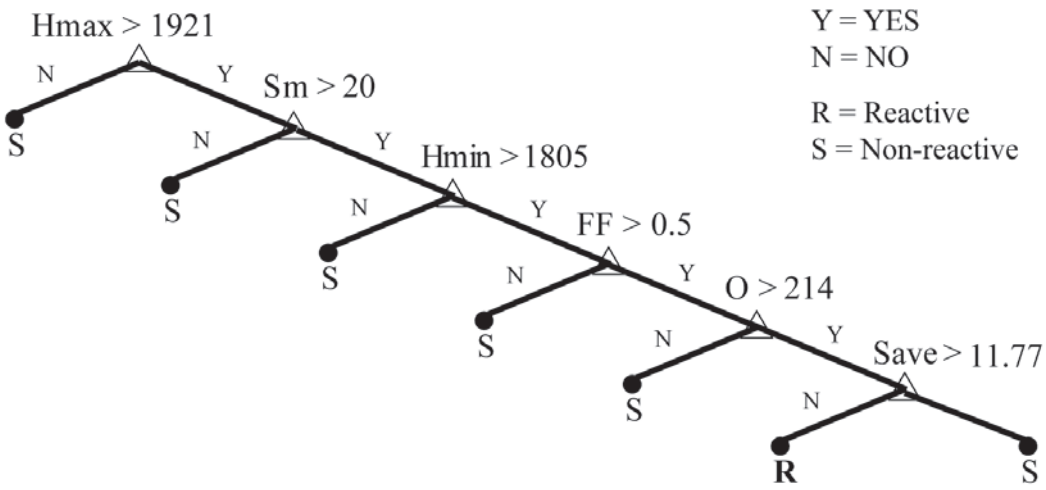

Figure 4.6: Classification tree J48 constructed with the raw 1st-order set and with no optimization of the algorithm. Leaves with a non-null probability of reactivity are not reported. Abbreviations of the parameters are listed in in Chapter 3.

Looking from a reactivity class point of view, the results shown in the confusion matrix are poor (Table 4.6a). The unbalanced rate of reactive/non-reactive catchments is partial to the non-reactive catchments. It results in a tree better at predicting non-reactive catchments and poorly capturing the reactive ones. From a susceptibility point of view, a good capture of the reactive catchments is

preferable. The light weight of the reactive catchments inside the training set (when the cost matrix is not applied) provokes the tree to exhibit only one leaf belonging to the reactive class.

A remedy for this is the use of the cost matrix. A cost of 15 for the FN has been chosen to carry out the analysis. The resulting tree has 48 leaves and 95 nodes, being more complex in order to capture reactive catchments particularities. The tree is not shown due to its complexity. The confusion matrix obtained for this unpruned tree considered the weighted 1st-order catchments' training set (Table 4.6b). Before the optimization, the results obtained on the corresponding test set are obviously poor (Table 4.6c). The sensibility regarding the reactive catchments should be improved and justifies the following optimization.

Table 4.6: Confusion matrices related to the C4.5 classifier, for 1st-order catchments: a) Confusion matrix obtained for the training raw set; b) Confusion matrix obtained for the unpruned tree done and training raw set using weighted database; c) Success in test set using the unpruned tree.

a)

	Non-reactive	*Reactive*
Non-reactive	**941**	**3**
Reactive	**78**	**0**

b)

	Non-reactive	*Reactive*
Non-reactive	**851**	**93**
Reactive	**0**	**78**

c)

	Non-reactive	*Reactive*
Non-reactive	**59**	**13**
Reactive	**34**	**7**

Optimization of C4.5 (J48)

The tuning algorithm uses a tenfold cross-validation method to optimize the C4.5 tree. The resulting pruned and weighted tree has 14 leaves and 27 nodes (Fig. 4.7). Its confusion matrix is visible in Table 4.7a.

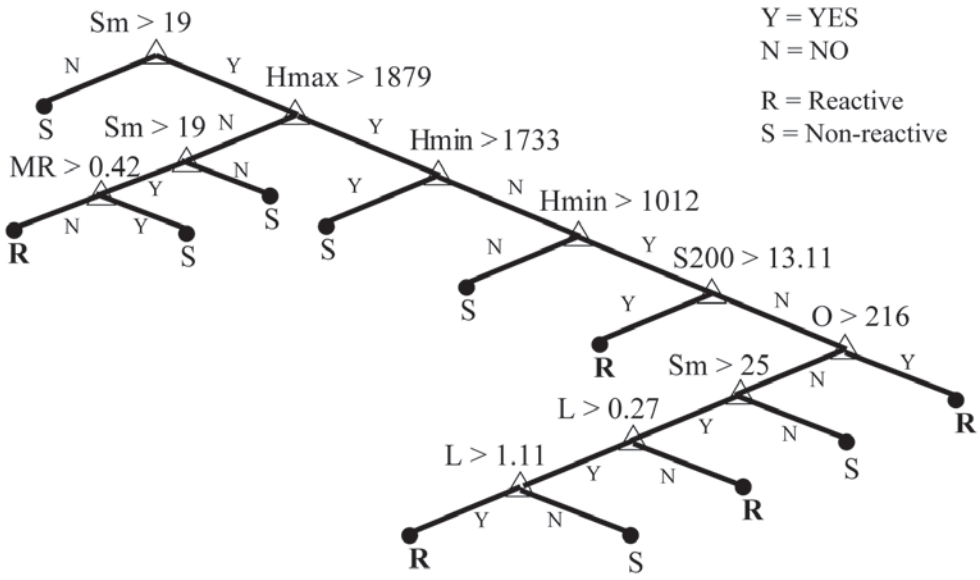

Figure 4.7: Pruned version of the classification tree obtained using the C4.5 algorithm for the weighted 1st-order training set.

Comparing these results and those obtained using the unpruned tree, it is clear that the results are slightly worse, as expected after reducing overfitting. Once the tree has been pruned using the cross-validation it is applied to the test set (Table 4.7b). The results should be compared to the ones obtained before optimization (Table 4.6c). There is a general increase of accuracy while success in classifying the reactive catchments has been improved, and the accuracy for the non-reactive ones has been reduced.

Table 4.7: Confusion matrices related to the C4.5 classifier, for 1st-order catchments: a) Confusion matrix for the pruned tree obtained with the weighted set; b) Success in test set using the pruned tree.

a)

	Non-reactive	*Reactive*
Non-reactive	**586**	**358**
Reactive	**8**	**70**

b)

	Non-reactive	*Reactive*
Non-reactive	**52**	**20**
Reactive	**27**	**14**

2nd-order catchments

The tree defined by processing the training set composed of the 2nd-order catchments is shown in Figure 4.8. The cost applied to the reactive catchments is equal to 4. Figure 4.8 displays 5 leaves and 9 nodes, and is much simpler than the one exhibited in Figure 4.7. Maximum elevation, form factor, average slope and area are the parameters the model retained in the construction of its tree.

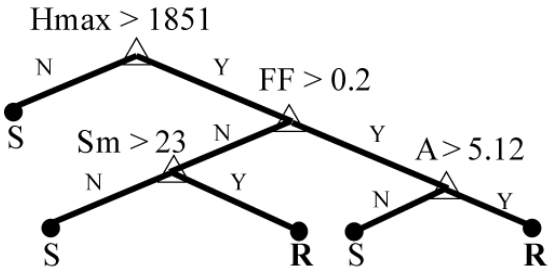

Figure 4.8: Pruned version of the classification tree obtained using the C4.5 algorithm for the weighted 2nd-order catchments training set.

The confusion matrix in relation to the training set is found in Table 4.8a and the test set's confusion matrix is in Table 4.8b. Again, the models obtained for the 2nd-order catchments' training set are compared to each other and to each model defined for 1st-order catchments in the following section.

Table 4.8: Confusion matrices related to the C4.5 classifier, for 2nd-order catchments: a) Confusion matrix for the pruned tree obtained with the weighted set; b) Success in test set using the pruned tree.

a)

	Non-reactive	*Reactive*
Non-reactive	**95**	**79**
Reactive	**2**	**50**

b)

	Non-reactive	*Reactive*
Non-reactive	**2**	**5**
Reactive	**5**	**13**

4.5.2.2. CART

The CART algorithm provides, from the start a weighted unpruned tree. It is constructed by applying the cost matrix using a value of 12. There are 161 nodes and 81 leaves making up this tree, which is not plotted due to its complexity.

Table 4.9: Confusion matrices in relation to the C4.5 classifier, for 1st-order catchments: a) Confusion matrix for the unpruned CART tree obtained using the weighted set; b) Success in test set using the unpruned CART tree.

a)

	Non-reactive	*Reactive*
Non-reactive	**898**	**46**
Reactive	**0**	**78**

b)

	Non-reactive	*Reactive*
Non-reactive	**65**	**7**
Reactive	**37**	**4**

It is clear that the accuracy in classifying the training set is high (Table 4.9a), when the test set gives very poor results (Table 4.9b). From the susceptibility point of view the result is unacceptable, justifying the following optimization.

Optimization of CART

A tenfold cross-validation is applied to the training set. It is then necessary to determine the most efficient level of pruning for the tree. A comprehensive sensitivity analysis was carried out and from this, an optimum range level was defined, comprised between 13 and 16. In this analysis it is fixed to 15.

In the following, the pruned tree (Fig. 4.9) served as a base for a tenfold cross-validation. The corresponding confusion matrix is collected in Table 4.10a, when the results concerning the test set are presented in Table 4.10b. Due to the high weight assigned to reactive catchments, the resulting classification tree better performs for reactive catchments and presents low accuracy for non-reactive catchments.

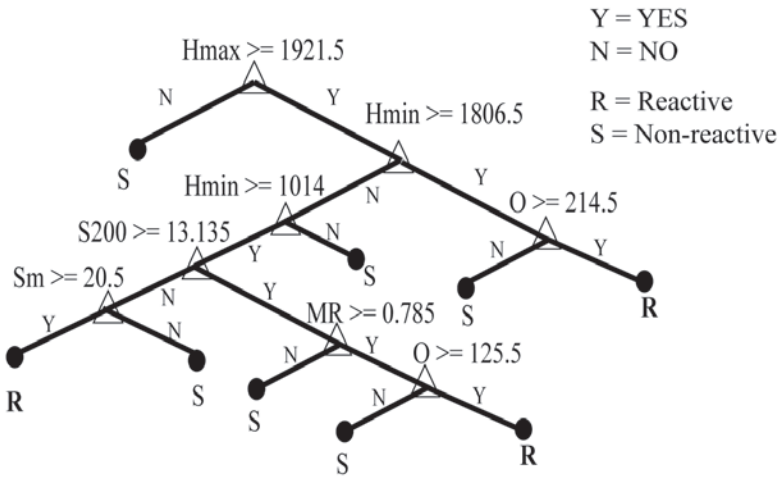

Figure 4.9: Optimized CART classification tree after pruning at level 15 for the 1st-order catchments.

Table 4.10: Confusion matrices in relation to the C4.5 classifier, for 1st-order catchments: a) Confusion matrix for the weighted set using the pruned CART tree; b) Success in test set.

a)

	Non-reactive	*Reactive*
Non-reactive	**683**	**261**
Reactive	**27**	**51**

b)

	Non-reactive	*Reactive*
Non-reactive	**39**	**33**
Reactive	**25**	**16**

2nd-order catchments

The cost used here is equal to 5. The optimized CART classification tree has 11 leaves and 21 nodes (Fig. 4.10). Table 4.11 shows the confusion matrices for both training (Table 4.11a) and test (Table 4.11b) sets.

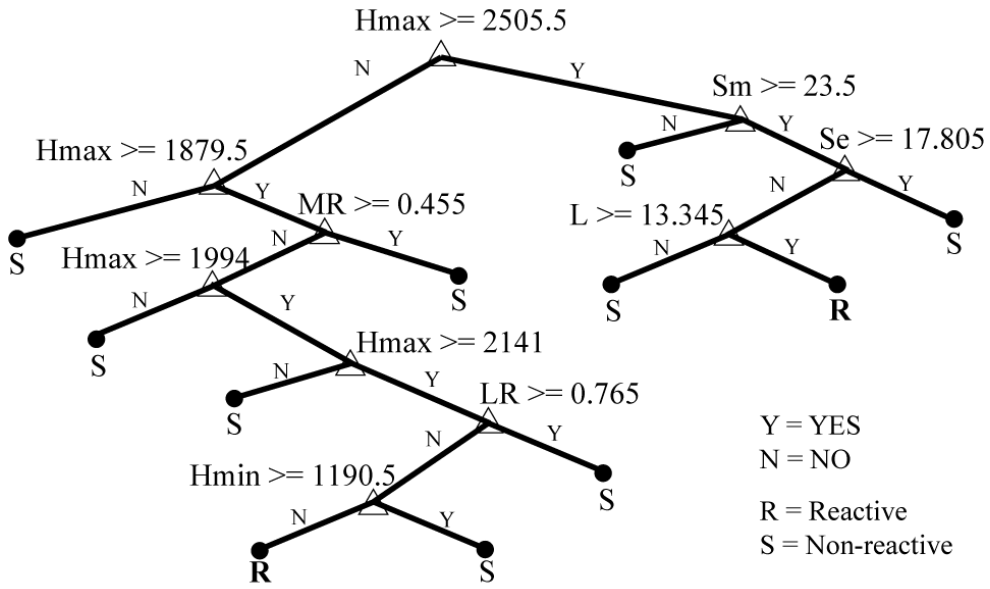

Figure 4.10: Optimized CART classification tree for 2nd-order catchments.

The model fits well with the training set, at least better than for the C4.5 model or even better than the logistic regression. However, when the results for the data set are considered, one has to accept the poor results offered by this model, when compared to the other models' results, which are compiled and evaluated in the next paragraph.

Table 4.11: Confusion matrices in relation to the C4.5 classifier, for 2nd-order catchments: a) Confusion matrix for the weighted set using the pruned CART tree; b) Success in test set.

a)

	Non-reactive	*Reactive*
Non-reactive	**138**	**36**
Reactive	**3**	**49**

b)

	Non-reactive	*Reactive*
Non-reactive	**1**	**6**
Reactive	**1**	**17**

4.6. Evaluation and credibility

4.6.1. Definition of measuring performances indexes

There are several factors that affect the success of the classification process. The main factors conditioning the learning algorithm performance include: (1) Class distribution (the rate between different classes involved in the classification), (2) cost of misclassification (cost matrix is user defined, so there is no guarantee on that), (3) size of training and test sets and (4) selected algorithm.

In order to qualitatively analyse the performance in learning process several standard indexes are selected. The performance indexes are; confusion matrix, precision, recall, F-measure, success rate and weighted success rate. Confusion matrices are already known, and the different new indexes are defined below (cf: Fig. 4.2):

$$Precision = \frac{TP}{TP+FP} \tag{4.9}$$

$$Recall = \frac{TP}{TP+FN} \tag{4.10}$$

$$F - measure = \frac{2TP}{2TP+FP+FN} \tag{4.11}$$

$$Success\ rate = \frac{TP+TN}{TP+FP+TN+FN} \tag{4.12}$$

$$Weighted\ success\ rate = \frac{W_{TP}TP+W_{TN}TN}{W_{TP}TP+W_{FP}FP+W_{TN}TN+W_{FN}FN} \tag{4.13}$$

Table 4.12: Performance in terms of indexes calculated taking into account test sets' results for a) 1st-order reactive catchments' class, b) 1st-order non-reactive catchments' class, c) 2nd-order reactive catchments' class and d) 2nd-order non-reactive catchments' class. In italics are highlighted reactive catchments.

	Logistic regression	C4.5	CART
a)			
Precision	*0.483*	*0.412*	*0.298*
Recall	*0.707*	*0.341*	*0.359*
F-measure	*0.574*	*0.373*	*0.326*
Success rate	*0.619*	*0.584*	*0.477*
Weighted sucess rate	*0.690*	*0.381*	*0.383*
b)			
Precision	0.774	0.658	0.609
Recall	0.569	0.722	0.542
F-measure	0.656	0.689	0.574
Sucess rate	0.619	0.584	0.477
Weighted sucess rate	0.690	0.381	0.383
c)			
Precision	*0.345*	*0.316*	*0.800*
Recall	*0.750*	*0.692*	*0.666*
F-measure	*0.473*	*0.434*	*0.727*
Success rate	*0.680*	*0.600*	*0.640*
Weighted sucess rate	*0.835*	*0.683*	*0.658*
d)			
Precision	0.885	0.857	0.400
Recall	0.575	0.552	0.571
F-measure	0.697	0.671	0.470
Sucess rate	0.680	0.600	0.640
Weighted sucess rate	0.835	0.683	0.658

Based on Table 4.12, for 1st-order catchments, the results show that the logistic regression is the best, although the C4.5 classification tree has better performance for some specific indexes related to the non-reactive class. For 2nd-order catchments, the performance globally gets better. The logistic regression remains the "best" model when the test sets are used in the validation. It is to be noted, that the weighting will influence the database. For 1st-order catchments, it induces a decrease in the weighted success rate (compared to the success rate) for both trees when the logistic regression is improved.

For 2nd-order catchments, all models have its weighted success rate increase. As a general conclusion it can be stated that the global performance when 1st-order catchments are considered does not exceed 70%; for 2nd-order catchments, it never exceeds 84%.

4.6.2. Measuring relative performance

The main difference between what has been seen in the previous section (4.6.1) and what is performed here is the fact that the comparison presented here is carried out using the training set. It does not consider the results obtained with the test sets. Analysing both performances is not redundant. The test sets also suffer overfitting, and thus the best fit on the test sets does not account for the global best fit. Three approaches are presented below: (1) area under curve, (2) lift chart and (3) threshold curves. The different approaches all aim at helping and defining the best model of fit.

4.6.2.1. AUC – Area under curve

A classical approach to measure the performance of a model was considered: The receiver operating characteristics (ROC). Each point on a ROC curve represents a classifier, obtained using different threshold values for a method (considering that the classifier used is probabilistic and not deterministic).

Changes in the optimization's algorithm, sample distributions or cost matrix could be represented also in the ROC curve, as shown in Figure 4.11. In the following, ROC curves are constructed measuring the success in the classification. In Figure 4.11a, the comparison results for the three classifiers taking into account 1st-order catchments are presented. The area under the ROC-curve, called AUC, for the logistic regression is 0.694, for the C4.5 tree is 0.659 and for the CART tree is 0.675. When 2nd-order catchments are considered, the AUC values evolve. The logistic regression's AUC increases to 0.747. For the C4.5 tree, it slightly decreases to 0.630. And for the CART tree the AUC slightly increases to 0.698.

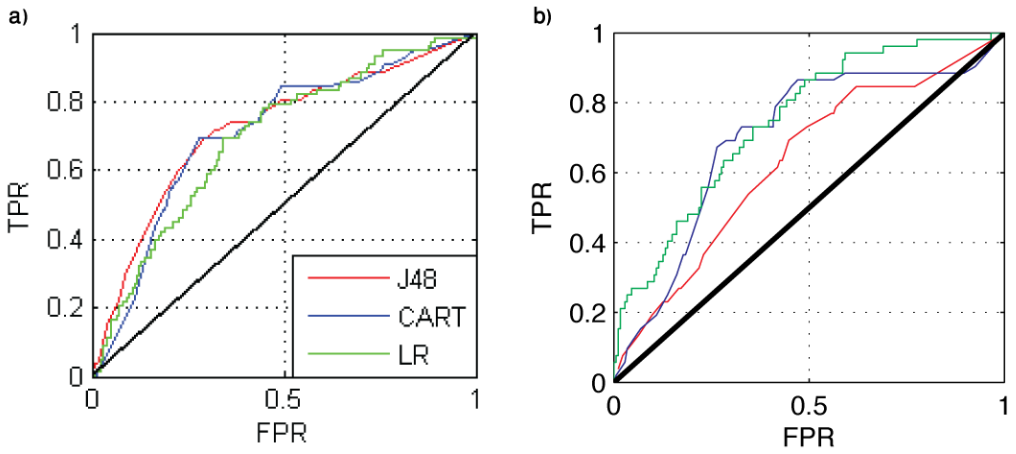

Figure 4.11: ROC curves, for the optimized models, determined with the training sets a) for 1st-order catchments and b) for 2nd-order catchments.

When these results are compared to existing AUC values, defined for susceptibility analysis, the results are low (Carrara *et al.* 2008; Frattini *et al.* 2010). For instance, Frattini *et al.* (2010) reports AUC ranging from 0.64 to 0.84 for five different models (four statistical models – including a logistic regression – and a physically-based model). Without entering the details, reasons why such a difference can occur is linked to 1) the study's unit, at which the assessment is done (and thus the scale) and 2) the theme behind the choice of the parameters, together with the choice of the parameters. For instance, between 17 and 41 parameters have been used to mount the 5 models previously mentioned (24 for the logistic regression), at small terrain units (slope unit and grid cell) over 300 km^2. The parameters are related to lithology, structure, geomorphology, morphometry, microclimate and land cover.

Alternative to AUC

Alternatively, instead of showing the evolution of one classifier (through a curve, like Fig. 4.11), the graph allowing the AUC to be determined can also show the result of a classifier as a point, which in that case corresponds to one classifier. It uses the final matrices fixed earlier, and can be applied to both training and test sets.

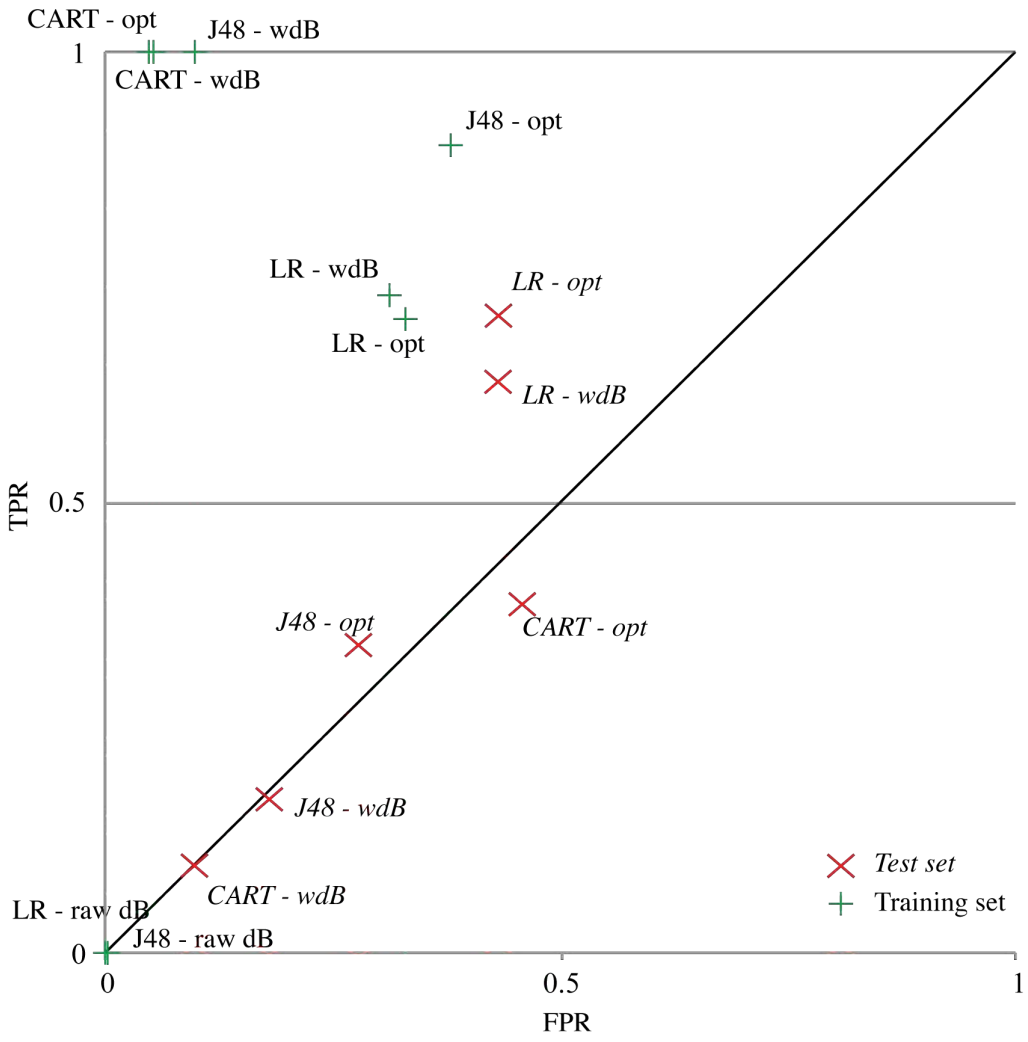

Figure 4.12: ROC graph presenting all the classifiers obtained for the 1st-order catchments' sets classified in two families (training and testing sets) – raw dB stands for "non weighted set", wdB for "weighted set", and opt for "optimized".

Figure 4.12 shows this alternative viewing and all the classifiers encountered for the analysis of the 1st-order catchments. The format of such graphs allows showing in one graph the results for training sets together with the results for test sets, whether the sets are weighted or not and whether the algorithms are optimized or not. The more clustered the results (of a same classifier), the better the classifier.

Conventionally a classifier has a better performance if it lies in the upper left corner of the graph (Fawcett 2006). For instance the optimized CART tree (Fig.

4.12) is excellent when the training set is considered, but when the testing set is considered the results are largely unacceptable.

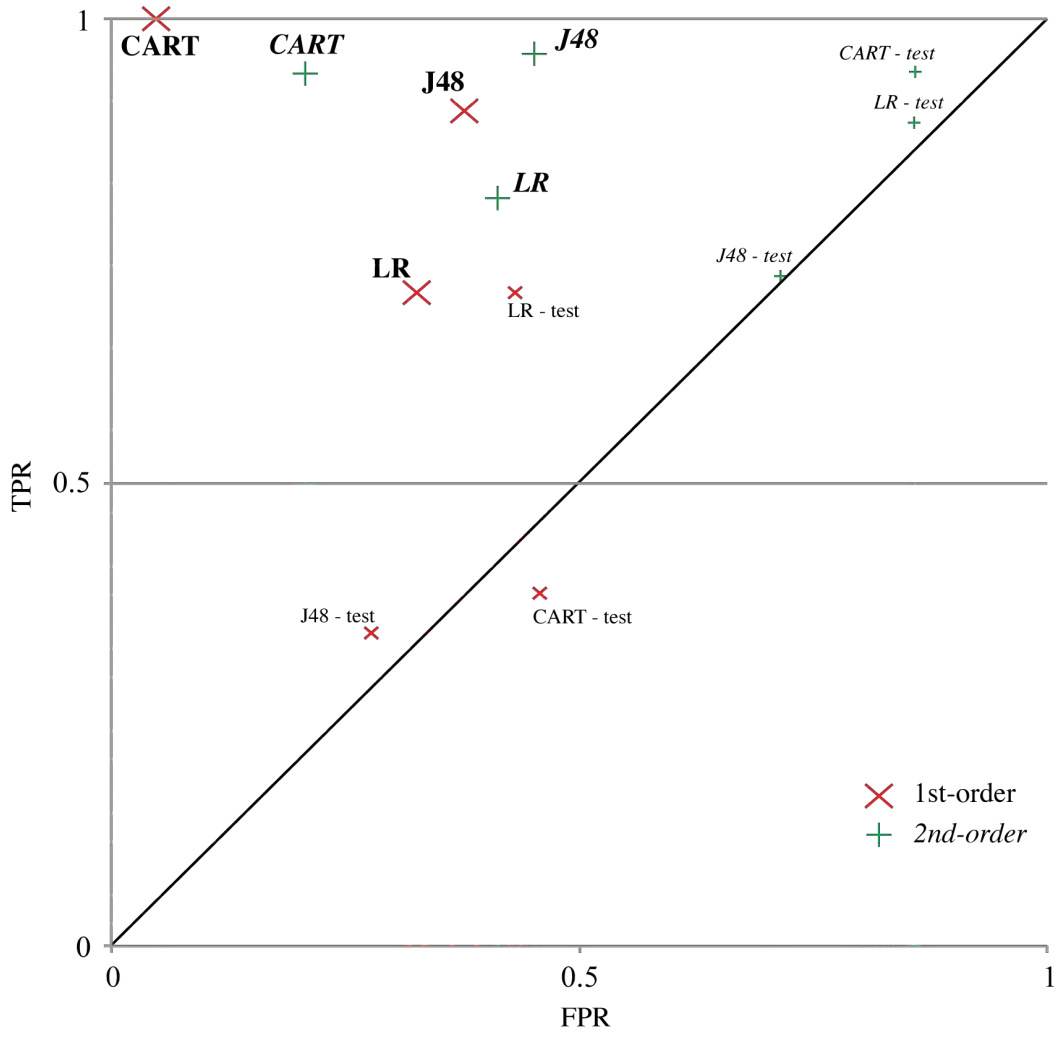

Figure 4.13: ROC graphs presenting the optimized models for both sets and both orders.

Besides showing the evolution of the classifiers through the analysis of the 1st-order catchments' training sets, the format of the graph was kept for showing the ending classifiers for both 1st-order and 2nd-order catchments. Figure 4.13 shows the three optimized classifiers (LR, J48, CART) for both training and test sets. It

permits the visualization of the three classifiers studied here, with the distinctions between the two orders that this study focuses on. From Figure 4.13, it is possible to see that both FPR and TPR increase with the order for the logistic regression, both trees lose performance with the order.

4.6.2.2. Lift chart

Lift is a measure of the effectiveness (or performance) of a predictive model calculated as the ratio between the results obtained with and without the predictive model (or the targeted response divided by the average response). Cumulative gains and lift charts are visual aids for measuring model performance. The greater the area between the lift curve and the baseline, the better the model will be. The lift curve can also be considered a variation of the ROC curves. Further reading and details about lift and its analysis can be seen in data mining literature (e.g.: Witten *et al.* 2011).

The lift curve could be applied when a probability value is obtained from the classification tool. The first hypothesis is that all the records belong to the successful class. The results of the classification are sorted using the probability, and the success of the classifier is evaluated. Two graphs are generally plotted for the classification trees: the first is the sample size against the TP, the second is the sample size against the lift. The lift is computed as sample precision over the full dataset precision.

In Figure 4.14, only the "sample size against the lift" graphs for the three classifiers are presented. For the 1st-order catchments, the maximum lift is obtained for the C4.5: it displays the maximum value for lift, but also the maximum area under the curve displayed. The behaviour of classification trees and logistic regression is completely different, the first ones have a clear maximum, but the logistic regression does not behave like this and possess a logarithmic shape.

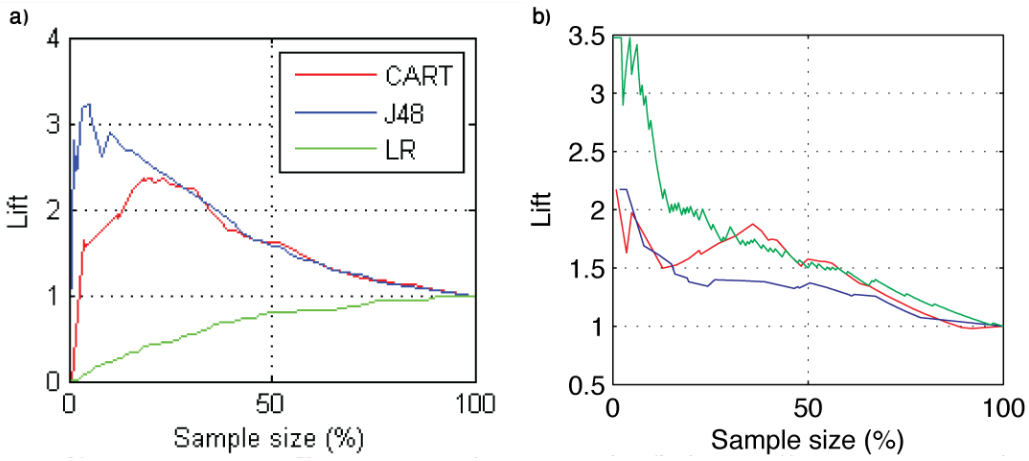

Figure 4.14: Lift comparison of optimized LR, C4.5 (J48) tree and CART tree for the training sets; a) 1st-order catchments and b) 2nd-order catchments.

For 2nd-order catchments, the maximum lift is reached for the logistic regression. The behaviour witnessed for 1st-order catchments' logistic regression is lost with 2nd-order catchments' logistic regression; this has been duly noted within this study.

The way to interpret Figure 4.14 can necessitate an explanation. The sample size is plotted versus the lift. Lift may be understood as an improvement in the results by choosing wisely a certain subset, like processing the model willingly putting an order on the instances (for this reason, probability values are necessary; it can be ordered). Let's consider the logistic regression's curve for 1st-order catchments. Lift and sample size increase together. The model learns from every new input in the subset. As for CART, still in Figure 4.14a, the model stops to learn when about 25% of the instances. C4.5 stops to learn even quicker.

4.6.2.3. Threshold curves

The last performance comparison is achieved through the threshold curves. These curves relate the probabilistic result of the classifier to the success in the classification. The constructed trees as well as the logistic regression include a probabilistic output. By default the class classification threshold is fixed in 0.5.

Values over it are "react" (reactive or positive) and below are considered "non-react" (non-reactive or negative).

In a tree's terminal node, the probability is defined as "react instances"/("Non react instances" + "react instances"). In the logistic regression the probability output is straight; the coefficients are fitted in order to obtain 0.5 as a class threshold.

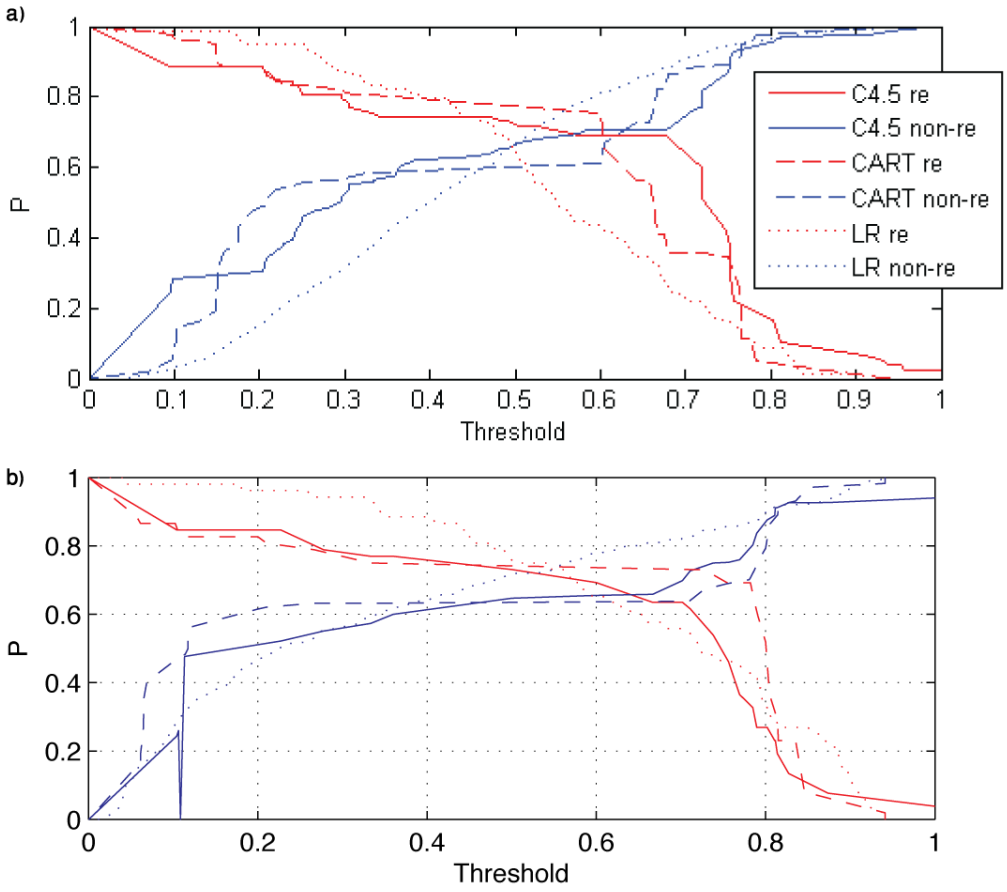

Figure 4.15: Threshold curves for optimized C4.5, CART and LR classifiers with training sets a) 1st-order catchments and b) 2nd-order catchments. "Re" stands for "reactive and "non-re" for "non-reactive".

Of course the presence of a cost matrix modifies the probability computation providing higher weight to the "react" instances. In Figure 4.15 the curves are

presented. The values are already corrected using the cost matrix used for the construction of the classifiers.

It should be noticed that the best results for the trees are obtained when moving the threshold slightly from 0.5 (1st-order) to 0.55 (2nd-order catchments). For C4.5, the threshold was roughly 0.55 for 1st-order catchments, and changed to 0.65 for 2nd-order catchments. As for CART, .the threshold is 0.62 for 1st-order catchments and almost reaches 0.8 for 2nd-order catchments. The best success rates visualized in Figure 4.15 hardly exceed 70%, as foreseen in the preliminary part of the analysis.

4.7. Susceptibility maps

Results are previously reported in terms of performance and other ratios. Susceptibility assessments are not easily used and difficult to understand for whom the tests are for. On the contrary, susceptibility maps are a common output for hazard assessments. Figure 4.16 shows the susceptibility maps for the 1st-order catchments, resulting from the three models, for each zone of the training set (Berga, NWCat and Mollo) and for the test set (Andorra); Figure 4.17 shows the same maps but for the 2nd-order catchments. Catchments are represented as follows: in white are predicted non-reactive catchments, in grey are predicted reactive catchments, and outlined in black are proven reactive catchments. A good map is a map when all (or most of) the black-outlined polygons are shaded in grey and not in white, when all (or most of) the grey-shaded polygons are outlined in black, and when white polygons remain white.

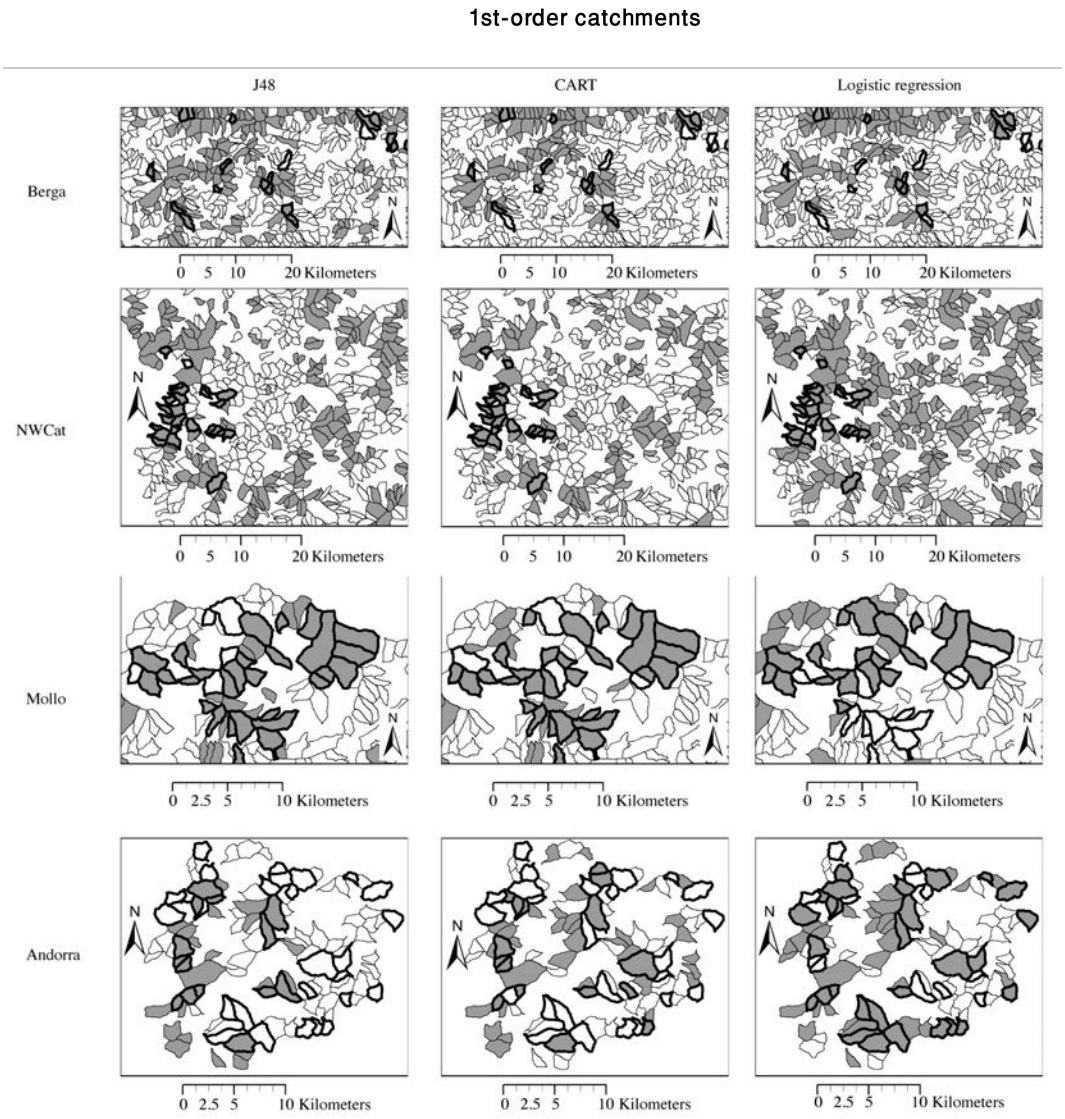

Figure 4.16: Susceptibility maps of the 1st-order catchments' training and test set. Catchments filled in grey are reactive catchments resulting from the models. Catchments filled in white are non-reactive catchments resulting from the models. Catchments with black contour are the reactive catchments present in the dataset when catchments without contour are the non-reactive catchments in the dataset.

For 1st-order catchments in NWCat, CART and LR models predict the proven reactive catchments well, but it is also easily visualized that CART predicts less reactive catchments than LR. In Andorra, LR also produces more reactive catchments than CART. But it also better predicts the proven reactive catchments. Figure 4.16 is a good example of the spatial variability of predicted

patterns within a study area due to statistical techniques (Sterlacchini *et al.* 2011).

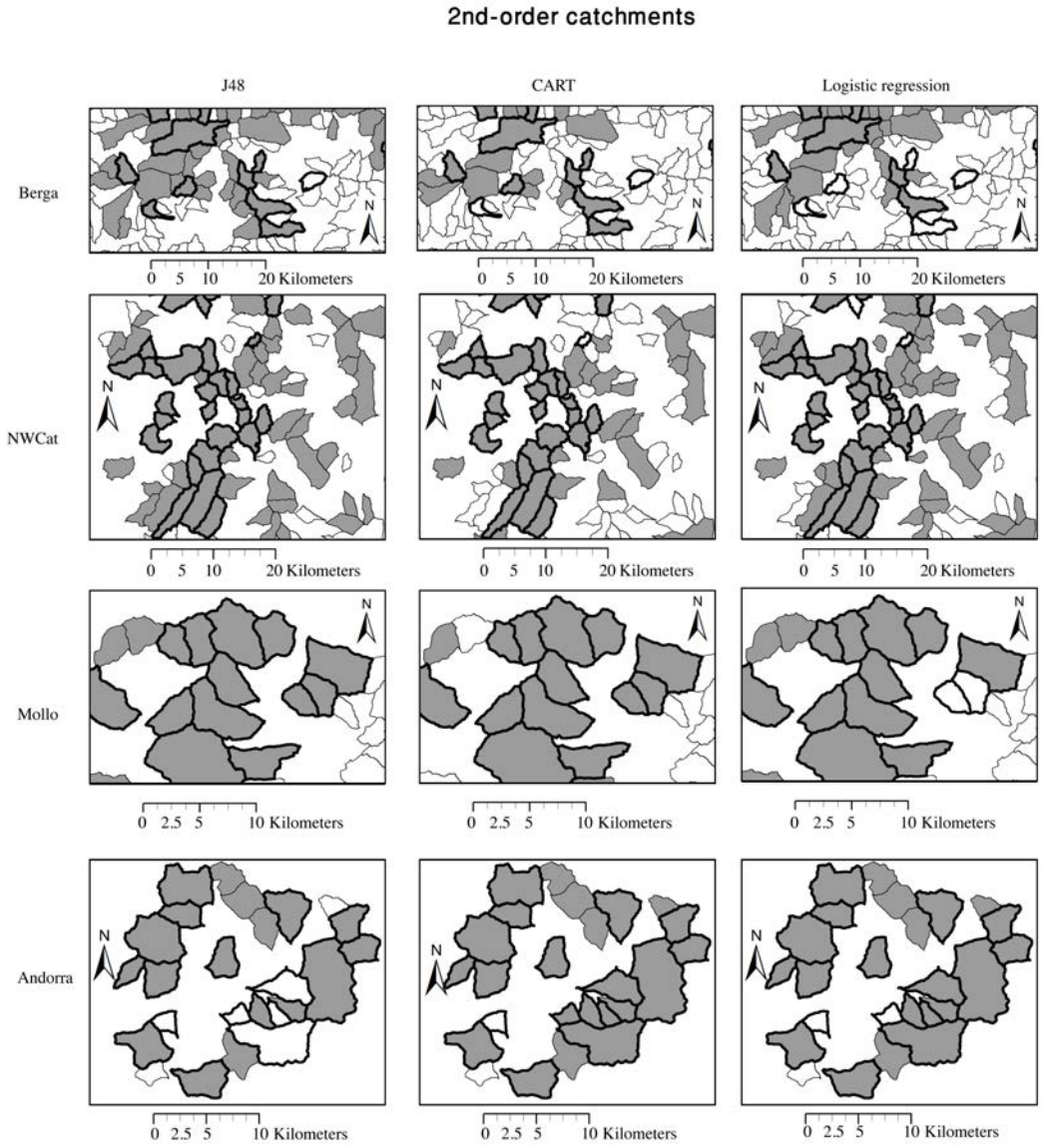

Figure 4.17: Susceptibility maps of the 2nd-order catchments' training and test set. Catchments filled in grey are reactive catchments resulting from the models. Catchments filled in white are non-reactive catchments resulting from the models. Catchments with black contour are the reactive catchments present in the dataset when catchments without contour are the non-reactive catchments in the dataset.

When multiple susceptibility maps are edited, the evaluation of the spatial agreement between these maps helps the hazard assessment users, in choosing the most suitable map (in other words the model that has the best prediction). Sterlacchini *et al.* (2011) estimated how much 13 predictions differed from one to another, which aimed at finding the best model. Determining a best model used is a difficult task. In this study, it is affected by the division of the training set in three zones and the use of a test set, all displaying different morphological characteristics of reactive catchments due to parameters purposely not envisaged in this study (like lithology and sediment availability). For this reason the best regional model is the one giving the higher level of performance in Andorra (the test set) although, other models may reveal more accurate in a specific zone (Fig. 4.16 and 4.17).

Combinations and superimpositions are also an idea to which the research led, although they are not tackled in this thesis. On one hand, a confidence index can be given to each model. On the other hand, susceptibility maps can be superimposed. The intersections of reactive catchments defined by the models could be compared to the catchments that appeared as reactive with the combination of the algorithms.

Eventually, the proximity in the performance of the two models discussed makes the two models interchangeable depending on the task and the objectives sought. If one wants to organize a field campaign in search for debris flows, CART is more appropriate as it identifies less FP (false positives). Otherwise, logistic regressions better fit hazard studies, which could benefit from them.

4.8. Conclusion

Based on 78 reactive catchments and 944 non-reactive catchments of order 1 (52 and 226 for catchments of order 2), the statistical models suffer from overfitting, encouraged by the unbalanced ratio of the number of reactive over non-reactive catchments. Introducing a cost matrix is necessary to overcome the

problem, as to weight the database. Moreover, it appears that applying the results to test sets generally gives poor matching. Optimizing the algorithms permits to better export the models to a test set. Among the models tested here, the logistic regression gives better results than decision trees when a test set is considered. The decision trees are better at extracting rules from a training set but are hardly applicable to a test set, even after optimization.

Generally it emerges that increasing the size of the GIS unit (from 1st-order to 2nd-order) enables the models to better predict the susceptibility. Indexes and other performance's analyses pledge so. However, a simple remark needs to be made: during the computations of the catchments, the maximum order encountered was 5. There were only a few of them, but all were reactive. The models if treating 5th-order catchments, would probably come with an incredible performance at finding reactive catchments because all the catchments are reactive, no matter the parameters chosen. Size does matter and that is why the study only focuses on 1st- and 2nd-order catchments.

Inherent limitations of our approach include the omission of parameters recognized to play a relevant role in debris-flow susceptibility assessment. Geology, vegetation and especially sediment availability are generally closely related to debris-flow spatial occurrence. However it is strongly believed that incorporating such information would benefit the results obtained from the models.

The validation of the models is a necessary step, which in our case revealed them to give poor results. The pertinence of the test set is an issue that plays a direct role on the validation's results. In our case, Andorra, high mountain environment, has been chosen for validation of the models, which have been computed based on not only high mountain environments, but also on medium mountain environments like encountered in the pre-Pyrenees. The test set should reflect the same environments as encountered in the training dataset. Regionalization is influencing the validation results. The study of this influence is out of the scope of this thesis, but should be considered in future studies.

Simple methodologies leading to the gathering of the study unit and the different sets, reproducibility of the work and straightforward understanding of the results have been sought throughout this analysis. It best suits places where little information is available, is addressed to entities dealing with debris-flow hazards having a small number of facilities or sources of information, and is a first step toward a regional risk assessment, which would need further studies to improve the errors estimates of the models. Drawbacks involved in this study may explain the rather poor success rate obtained, which could be attenuated by further refine the parameters or the unit of study or the inventory.

CHAPTER 5 MAGNITUDE-FREQUENCY RELATIONSHIP

5.1. Introduction

In the framework of any hazard assessment, the notion of time is crucial and compulsory. “How often” and “how much” are questions often considered when the notion of time is sought. The chapter gives an outlook on how to achieve an answer to this consideration. The most documented way of answering it for geological hazards like debris flows is done through the elaboration of a magnitude-frequency relationship, which is presented in the corresponding state-of-the-art (Chapter 1).

In order to document the Magnitude-Frequency (M-F) relationship for the debris flows, two scales have been reviewed. The first part of this chapter stresses the elaboration of M-F relationship at local scale. The example of a torrent (El Rebaixader), known to have suffered many debris-flow events in the past, lacks any clear description/study of these events. Dendrochronological tools have permitted to recollect information of its past activity. The second part of this chapter emphasizes the same relationship, but at regional scale. It is shown in this chapter how aerial pictures can be used to report M-F relationship at regional scale, over the national park of Aigüestortes, lying in the Axial Pyrenees (cf. study area in Introduction).

The goals of this chapter are: 1) to apply a local-scaled study's methodology, 2) to stress the importance and relevance of aerial picture studies at regional scale, 3) to report M-F relationships at both local and regional scale for the study area and 4) to show that dendrochronological tools and aerial pictures studies can be used together in a debris-flow hazard assessment, allowing to encompass different scales, and thus giving a broad first idea on how to characterize frequency and magnitude of debris flows in the study area.

5.2. Local analysis at El Rebaixader

Few attempts have been made so far in the estimation of the magnitude of debris-flow events using dendrogeomorphology. One approach combining tree-ring and relative dating was tested in a Pyrenean catchment (Tordò creek, Eastern Pyrenees, in Corominas & Moya 2010). It showed debris flows develop in periglacial deposits and accumulate in a valley bottom. Here, the method is extended to another Pyrenean site, the Rebaixader creek, in order to start a local study of magnitude and frequency of debris flows and to check the method in a different setting: a debris fan.

5.2.1. El Rebaixader

Rebaixader torrent is a tributary of the Noguera Ribagorçana river and lies in the high reach of the basin, about 10 km South of the atlantic-mediterranean water divide (Fig. 5.1). The bedrock consists of Palaeozoic meta-sedimentary rocks from the Axial Zone of the Pyrenees, which were folded during the Hercynian and Alpin orogenies. Tills overtopping the bedrock were deposited during the Upper Pleistocene by a glacier that occupied the Noguera Ribagorçana valley (Vilaplana 1983). Deglaciation resulted in destabilization of the steep slopes developed during the Last Glacial cycle, giving rise to landslide activity.

Rebaixader's catchment lies between 2479 and 1225 m asl. Its catchment's area has an extent of 0.7 km^2, and its length 2.6 km. The mean slope of the catchment is 28°. The head zone has a semi-circular scar culminating at 1725 m asl (Fig.

5.1). The debris fan has the apex at 1325 m asl and the bottom at 1225 m asl, at the confluence with the river Noguera Ribagorçana. The channel linking the source zone and the fan is 630 m long. The fan has a radius of 370 m, an area of 0.082 km^2 and a mean slope just over 15°.

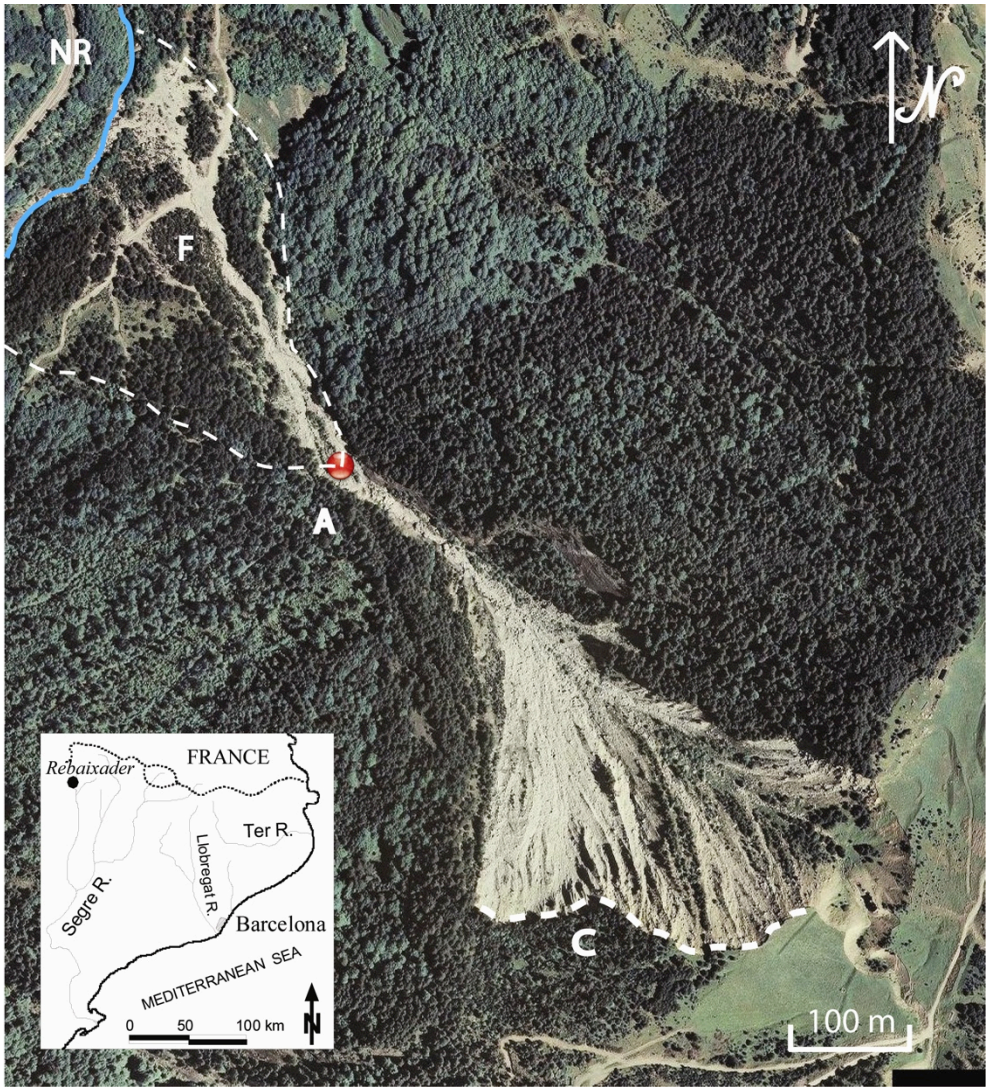

Figure 5.1: Aerial view of the Rebaixader creek. The inset shows the location of the site. C: head zone; F: debris fan; A: fan apex; NR: Noguera Ribagorçana river.

The fan was built up by debris flows and displays a complex ensemble of deposits, which are mostly colonised by a forest of Pinus Sylvestris. Rebaixader

has recently been monitored (summer 2010). Geophones and an ultrasonic device have been set up to control occurrence and discharge of debris flows. A meteorological station is also currently operating to control rainfall conditions (Hürlimann *et al.* 2011).

5.2.2. Methodology

5.2.2.1. Magnitude

The magnitude of debris flows is conventionally expressed as its volume of deposition. However, assessing the volume of past debris flows from fieldwork can prove complicated. Past studies have emphasized the relationship between volume and area of debris-flow deposits (Iverson et al. 1998; Berti & Simoni 2007; Scheidl & Rickenmann 2009). The magnitude can thus be assessed by 1) delimiting the surficial extent of the deposit and 2) extrapolating to an estimate of the volume deposited.

Nevertheless, at sites where debris flows are recurrent, as in a debris cone, new debris-flow events may remove evidences of earlier ones by eroding or overlapping them. As a consequence, several parts of a debris-flow deposit can be found at present separated by younger deposits or by a channel scoured by a more recent event. These remnants should be identified as corresponding to the same event. To do this, sediments deposited by debris flows were differentiated using relative dating criteria, and were grouped into relative-age classes and, eventually, assembled by correlation in depositional units (DU). The term depositional unit is used for a set of deposits included in a relative-age class and can be regarded as accumulated by a debris-flow event. The definition of the depositional units is necessary for estimating debris-flow magnitude and age (Corominas & Moya 2010).

At the Rebaixader creek, the fan is the place of preferential deposition of debris flows developed in the site. A series of criteria has been used in order to distinguish between different depositional units accounting for its development: maximum size of trees (diameter and height), lichen's cover on boulders making

up the DU and cross-cutting relationships. Each depositional unit has developed different cohorts of trees and lichen development covering the fan to different extents (Fig. 5.2).

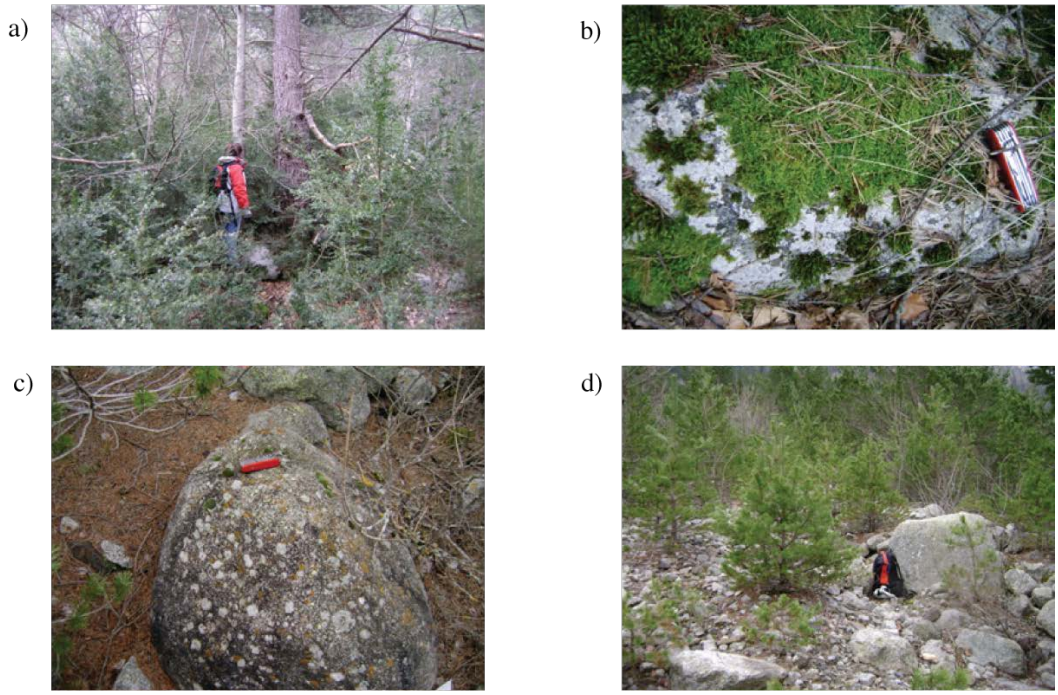

Figure 5.2: Examples of relative age characteristics shown by different depositional units in the Rebaixader debris fan. a) and b) show DU 7 trees and lichen assemblages; c) shows lichens for DU 5; d) exhibits trees as found on DU 3.

In Rebaixader, assessing the size of past debris flows is rendered very difficult due to the superimposition of depositional units. The magnitude of debris flows is conventionally expressed in volume, but can also be determined in terms of area of event deposits. The site dictated the use of area of deposits (of depositional units, more exactly) to express the debris-flow magnitude; this is because the low relief in the fan surface made very difficult the estimation of the deposits thickness.

5.2.2.2. Frequency

Once the number and extent of the depositional units were determined for the site, the numerical dating was carried out by means of dendrochronology.

Two types of tree-ring dating elements were found at the site: trees wounded by debris flows and trees colonizing the depositional unit's surface. Wounds' dating was carried out by counting the number of rings having straddled over the scar. It gives the number of years passed since the tree was injured, and, therefore allows an exact dating of debris flow occurrence, with an accuracy of a growing season (Fig. 5.3).

Figure 5.3: Example of a wedge permitting to date a scar found on a tree.

The age of trees colonizing depositional units gave a minimum age for the corresponding debris-flow events. There is a time-span between the new surface's formation and the colonization by trees. The time for colonizing a newly formed surface, ecesis time or colonization time gap, is highly variable and depends upon a wide variety of controlling factors (Schroder 1978).

To obtain the age of colonizing trees two techniques have been used, depending on the apparent age of the trees:

1) For old or mature trees, a core of the biggest trees (likely to represent the oldest tress) was extracted and the rings counted when visible (see Fig. 5.4 for tool). The minimum age for the event, which produced the surface (herein: DU), is given by the germination date of the oldest tree.

2) For young trees, conifers not taller than human height, another technique (more direct and easily applicable) is used. It is based on the fact that the number of branch whorls of a young conifer indicates the tree age (Schweingruber 1990); 371 young pines were dated by this method.

Obtaining the tree's age from cores has several shortcomings. First, the sampling height should be as close to ground level as possible in order to hit the oldest tree-ring of the tree (e.g. Grissimo-Mayer 2003). The higher the sampling height, the greater the number of tree-rings formed before the tree reaches this height. This is called the sampling height growth time (SHGT). A sampling height common for all trees is hardly achievable as it depends on the access to the tree. In this study, sampling heights ranged from 0.5 to 1.4 m. Second, cores may not reach the pith (which is the oldest part of a tree radius). Thus, results given by this technique are subject to approximations, as Schroder (1978) emphasized.

In order to get the most exact age, a series of corrections have been realised. When the pith was not hit and inner growth ring arcs were visible, the geometric model proposed in Duncan (1989) was used to estimate the number of rings between the last visible ring and the virtual pith. Details and limits of the method are not discussed here and can be found in the reference above. This method is not applicable to all cores as arcs are not always visible. 23 cores are concerned with this method.

Figure 5.4: Swedish increment borer (or increment borer): a) the auger and the handle (in orange); b) the extractor; c) the full borer in action. The nomenclature follows that of Grissimo-Mayer (2003).

The colonization time gap (CTG) can be defined as including the germination lag time (GLT) and the breast height growth time (BHGT) (following Pierson 2007) or the sampling height growth time (SHGT) if the samples were taken close to the ground. Because the cores were sampled as close from the ground as possible, the BHGT is considered as null or sufficiently small to be considered as null. The GLT is highly dependent on the local conditions (as mentioned above) and has not been studied for Pinus Sylvestris in the study site. Pierson (2007) found that for a mixed population of conifers, the GLT had a mean value of 6 years. Although this gap has only been taken as guidance for the Rebaixader creek, it was not applied to obtain tree ages.

A minimum age for each depositional unit was finally obtained after applying the age-corrections to samples and using the age of the oldest tree colonizing the unit.

5.2.3. Results

5.2.3.1. Debris-flow depositional units and magnitude

Using these different features, seven depositional units have been recognized on Rebaixader's fan. Below is their description:

- The first depositional unit recognized (DU 1) corresponds to the currently active channel. No vegetation is found and lichens have not covered boulders yet.

- DU 2 is made up of small trees scarcely distributed; lichens do not colonize the boulders.

- DU 3 exhibits trees of medium size (up to human size) with an increase in the density, and boulders covered by lichens; coverage estimated to range from 5 to 10 %.

- DU 4's trees are between 2 and 3 m high with a diameter varying between 5 to 10 cm. Boulders are covered with lichens (15-20%) and moss (scarcely). To be noted is the accumulation of organic matter (twigs, spikes, leaves…) on the ground.

- DU 5 shows a dense cohort of trees with diameter closing 10 cm and as high as 4 m. Very similar to DU 4, the difference resides in the assemblage of lichens found on the boulders. Lichens (white and yellow) cover 30-40 % of them, and moss less than 5%. Ground remains covered with organic matter.

- DU 6's trees exceed 4 m, and diameters range from 15 to 25 cm. Their density decreases compared to DU 5. The boulders are covered by 5-10 % of moss, the rest being almost entirely covered by both lichens. Organic matter is still found on the ground.

- DU 7, which is the oldest depositional unit encountered, has the biggest trees, reaching 50 cm in diameter, with a high density. Yellow lichens disappear leaving the boulders covered by moss (25-30%) and white lichens. Organic matter still covers the ground, and in places has extended over boulders.

The establishment of the different DU encountered on site has permitted to evaluate the minimum extent of a series of debris flows that occurred in Rebaixader (Fig. 5.5 and Table 5.1). Appendix 5 shows the field results, consisting of 2 descriptive tables, one for the trees and the other for the wounds, and a sample's location map.

Table 5.1: Area and age of depositional units of Rebaixader fan.

DU (#)	*Area (m^2)*	*Number of sampled trees (#)*	*Wound age (years)*	*Age of the oldest colonizing tree (years)*	*DU age*	
					Years old	*Dendrochronological year*
1	2116	-	-	-	0	active
2	611	162	11	7	11	1997-98
3	2092	147	14	11	14	1994-95
4	1098	62	-	21	21	1987-88*
5	4157	4	-	25	25*	1983-84*
6	6168	15	-	51	51*	1957-58*
7	4528	17	-	71	71*	1937-38*

* Minimum age.

As it can be observed in Figure 5.5, a portion of the fan has not been mapped. It can be explained by the facts that few trees are colonising the area and that the surface is covered by grass, probably the remnant of a human/agricultural activity having cleared the initial surface from its characteristics.

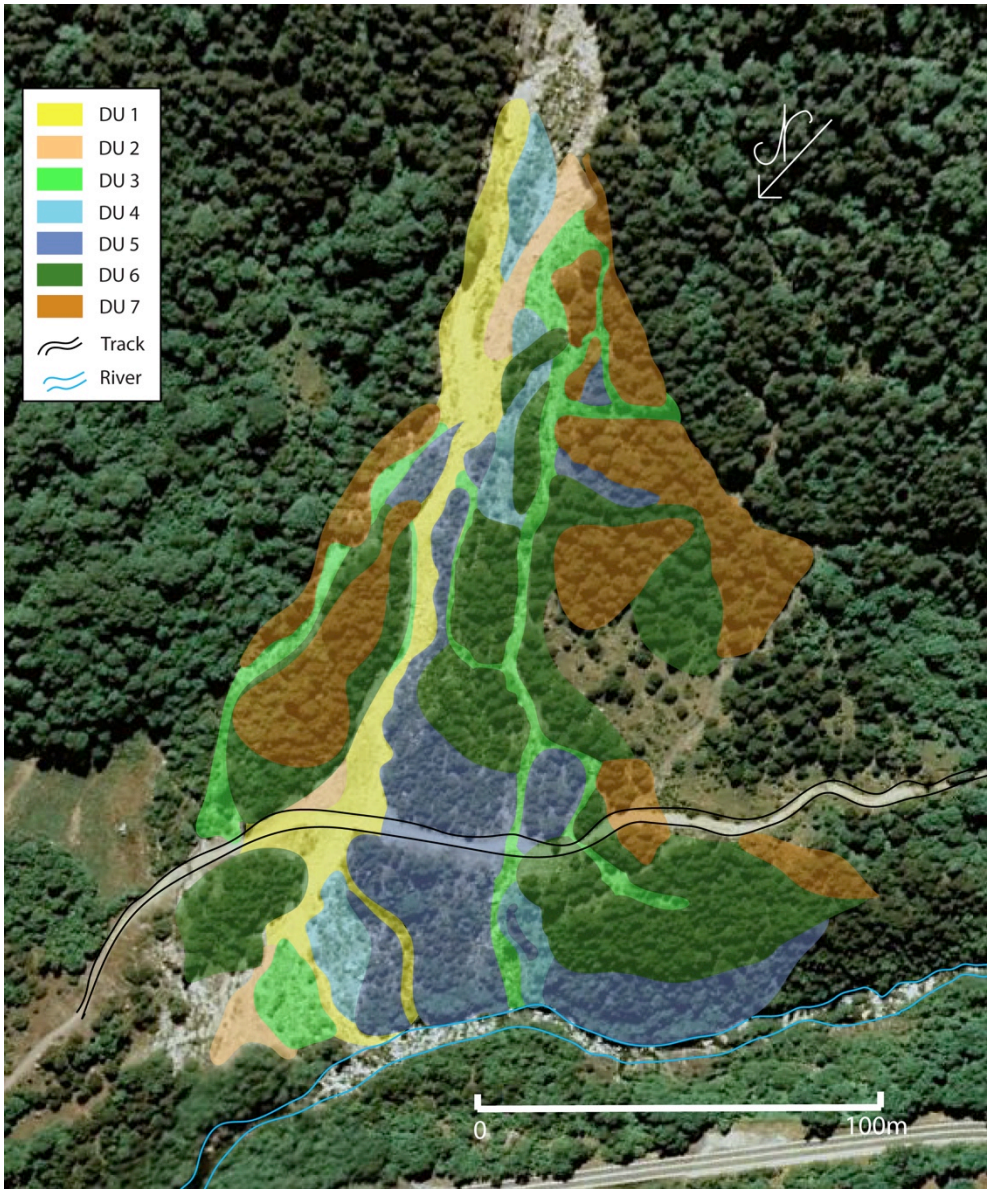

Figure 5.5: Map of debris-flow depositional units at the Rebaixader fan.

5.2.3.2. Age of depositional units and magnitude-frequency of debris flows

Table 5.1 shows the dating results corresponding to the depositional units. The reduced number of wounded trees that has been sampled provided the exact age for only two DU (DU2 and DU3). For the older units (DU4 to DU7) a minimum age was obtained. Minimum ages from colonizing trees were also obtained for DU2 and DU3. The comparison of minimum and exact ages for these units suggests that Pinus Sylvestris needs at least 3 years to colonize a new debris-flow deposit.

The tree-ring record at Rebaixader fan spans the last 70 years. Seven units were deposited within this time span. From these numbers, an average return period for debris flows, of about 9 years, can be obtained. The area of the deposits ranged from 600 to 6200 m^2. However, the frequency of debris flows seems to be higher for the last 25 years (Table 5.1) with a return period of 5 years.

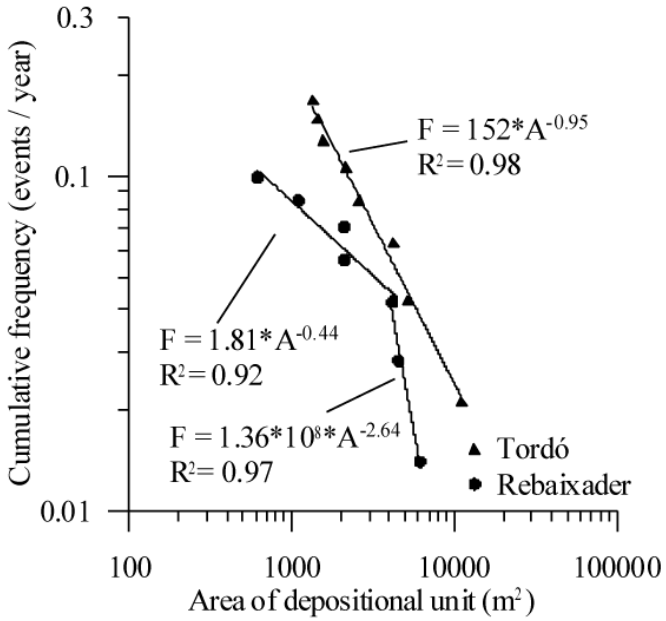

Figure 5.6: Magnitude-Cumulative Frequency curve (logarithmic scaled axes) for the Rebaixader creek. The curve corresponding to another site studied in the Eastern Pyrenees (Tordó Torrent) is also shown (data from Corominas & Moya 2010).

Figure 5.6 shows the magnitude-cumulative frequency (MCF) relationship of debris flows at Rebaixader fan. Landslide MCF relationships is usually fitted by a right line (in logarithmic scales) (Corominas & Moya 2008). The MCF curve fit to the Rebaixader data is, however, strongly nonlinear, or more exactly bilinear. Certainly, the points corresponding to the five smaller depositional units can be fit with a line with a gentler slope than the three bigger ones. Frequency for theses smaller magnitudes is notoriously lower in Rebaixader than in the other site studied in the Pyrenees (Tordó torrent). A decrease in the slope of the MCF curve is also commonly reported for other sites and for different types of landslides (Corominas & Moya, 2008). This flattening of the curve, so-called rollover effect, is usually considered as the consequence of an under-recording of small events. In the Rebaixader fan, deposits of some small-magnitude debris flows can and have been totally buried by younger events of a larger magnitude. Actually low debris-flow frequency obtained for the period, older than the year 1983-84 (Table 5.1), can result from an overlapping of small-magnitude debris flows. It should be noted that the two older depositional units (DU6 and DU7) also have the maximum extent.

A shortcoming inherent to tree-ring dating can also explain an under-recording of small debris flows. Accuracy of tree-ring dating is usually of a year, although obviously lower if only minimum ages are obtained. This means that events occurring within a same year cannot be differentiated, and that the assessed depositional units may actually be formed by several debris flows. Relative dating does not permit to distinguish events occurred in a same year, unless cross-cutting relationships were produced.

5.3. Regional analysis at the Aigüestortes national park

The main purpose of the present study focuses on the definition of a first estimate of the debris flow M–F relationship in an area of the Central Pyrenees at regional scale. Additionally, the results are compared with other studies carried out worldwide.

5.3.1. Settings

The study area covers about 384 km^2 and is located within and around the "Aigüestortes i Estany de Sant Maurici" (or shortly Aigüestortes) national park in the Central Pyrenees, Spain (Fig. 5.7). The national park is characterized by a high mountain relief, with elevations between about 1300 and almost 3000 m asl.

From a geological point of view, the study area is situated in the Axial Pyrenees (Muñoz 1992). The basement consists almost entirely of igneous and metamorphic Palaeozoic rocks formed and tectonised during the Hercynian orogeny and further deformed during the Alpine orogeny. The bedrock is covered by colluvium and tills. Colluvial deposits reach a thickness of a few meters in some low order catchments, and glacial deposits can locally present a thickness of several tens of meters.

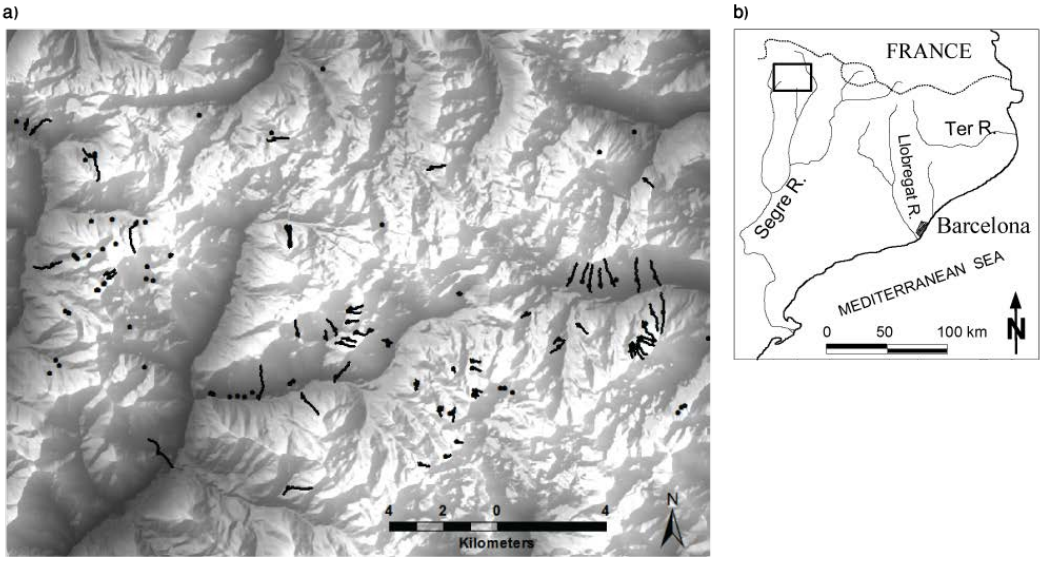

Figure 5.7: a) Debris-flows inventory. The situations of the 116 affected torrents are indicated by dots, while some selected debris-flow tracks are given by lines. For the DEM, the darker the terrain, the lower the elevation. b) Location of the national park in the Central Pyrenees.

The climate in the study area is influenced by three factors: the vicinity of the Mediterranean Sea, the west winds from the North Atlantic and the orographic effects of the Pyrenean mountain range (Novoa 1984, Cuadrat & Pita 1997). There are two typical rainfall patterns, which can trigger debris-flow activity (Hürlimann *et al.* 2003): 1) Short duration, high intensity rainfalls related to convective summer storms, and 2) moderate intensity rainfall during autumn/winter lasting for several days or weeks and affecting large areas.

5.3.2. Methodology

The methodology includes three main parts: 1) the interpretation of aerial photographs, 2) the digitalization in a GIS, and 3) the analysis of the inventory data.

5.3.2.1. Interpretation of aerial photographs

The debris-flow inventory was built by the interpretation of several sets of aerial photographs covering a time span of 53 years. The details on the different datasets are listed in Table 5.2 and the explanation of their interpretation follows.

Three types of photo-interpretation were applied due to different datasets: 1) standard interpretation of paper aerial photographs using a mirror stereoscope, 2) the two-dimensional interpretation of digital ortho-photos, and 3) the three-dimensional interpretation of digital ortho-photos.

Standard photo interpretation was applied to the printed pairs of aerial photos of 1975 and 1982. In contrast, the 1956/57 aerial photographs were analysed using the ortoXpres 1.0 application created by the Cartography Institute of Catalonia. In ortoXpres 1.0, the digitized and geo-referenced 1956/57 aerial photos can be visualised and directly compared with an extended cartography database consisting of topographic maps and recent ortho-photos. Thus, the interpretation of the 1956/57 aerial photographs was called two-dimensional. At last, the detailed aerial photos between 2004 and 2009 were analysed by the

Google™Earth software application. Google™Earth displays the colour aerial photos in three-dimensional views and facilitates a detailed interpretation.

Table 5.2: Aerial photographs analysed

Year	*Type **	*Scale or pixel size*	*Source*
1956/1957	Digitalized (b&w)	1:33000	OrtoXpres 1.0
1975	Paper (b&w)	1:18000	ICC
1982	Paper (b&w)	1:22000	ICC
2004	Digital (col)	50 cm	Google™ Earth
2005	Digital (col)	50 cm	Google™ Earth
2008	Digital (col)	50 cm	Google™ Earth
2009	Digital (col)	25 cm	Google™Earth

* b&w: black and white; col: colour

It must be stated that the 1975 and 1982 datasets were unfortunately not covering all the study area, respectively 45% and 95%.

A separate inventory map was created for each year listed in Table 5.2 and finally an overall inventory was generated. The separate inventories were created by the observation of different types of morphologic features and changes in the aerial photos. The debris-flow activity in a catchment or torrent channel was generally characterized by one of the following features (similarly to Chapter 2): 1) observation of the deposit in the accumulation zone, 2) observation of deep erosion and/or lateral levees along the debris-flow track, 3) changes and damages in the vegetation, and 4) widening or migration of the debris-flow channel.

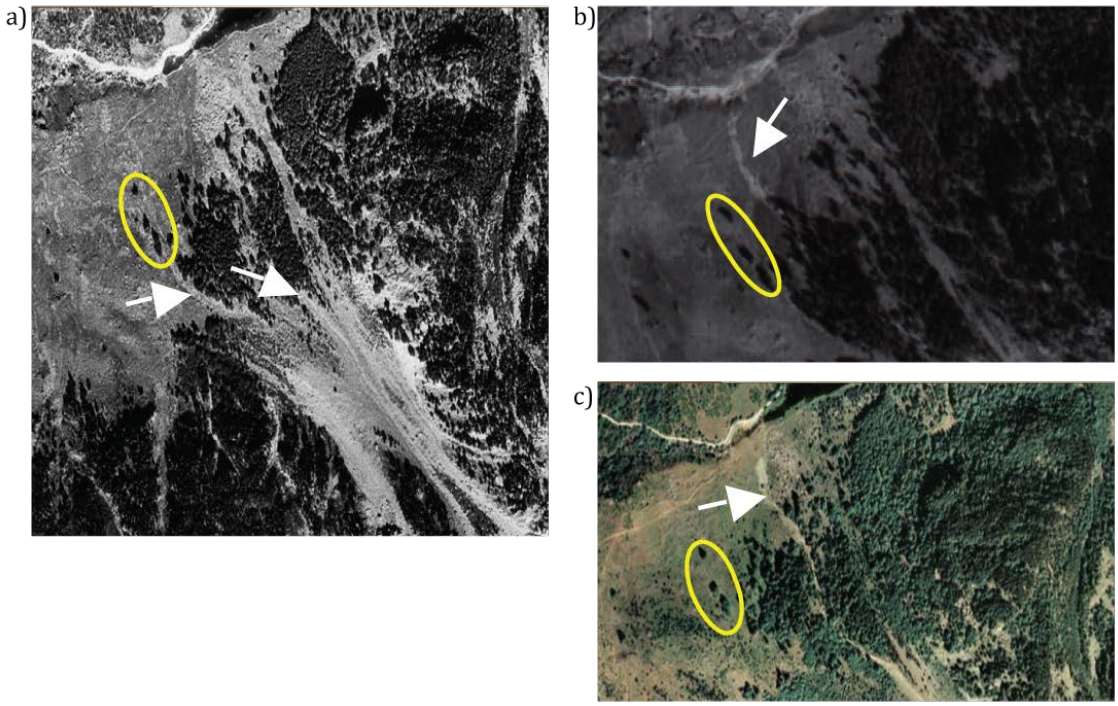

Figure 5.8: Examples of debris-flow activity at one specific catchment. a) 1956/57 digitalized aerial photo, b) 1975 scanned aerial photo, c) 2008 ortho-photo. Arrows indicated debris-flow tracks or deposits. Ellipses show trees to give some reference points.

Examples of changes related to debris-flow activity in a specific catchment are shown in Figure 5.8. In spite of the distinct scales and quality of the aerial photos, differences in morphology and vegetation are clearly visible between the different years.

A comparison of the three-dimensional view in Google™Earth and an oblique photograph is given in Figure 5.9 for the same event, as illustrated in Figure 5.6. The comparison of the two views shows the usefulness of Google™Earth, which can represent debris-flow activity rather well. However, it must be stated that the 2008 ortho-photo used in Google™Earth is characterized by a very good resolution (0.5 m pixel size). Only, such a high-quality aerial photograph may enable the coherent interpretation of morphologic changes by Google™Earth.

The experience showed that applications like Google™Earth are perfect tools for a fast and simple detection and digitalization of debris-flow activity in remote

areas, but they should not replace field surveys, when detailed observations are required.

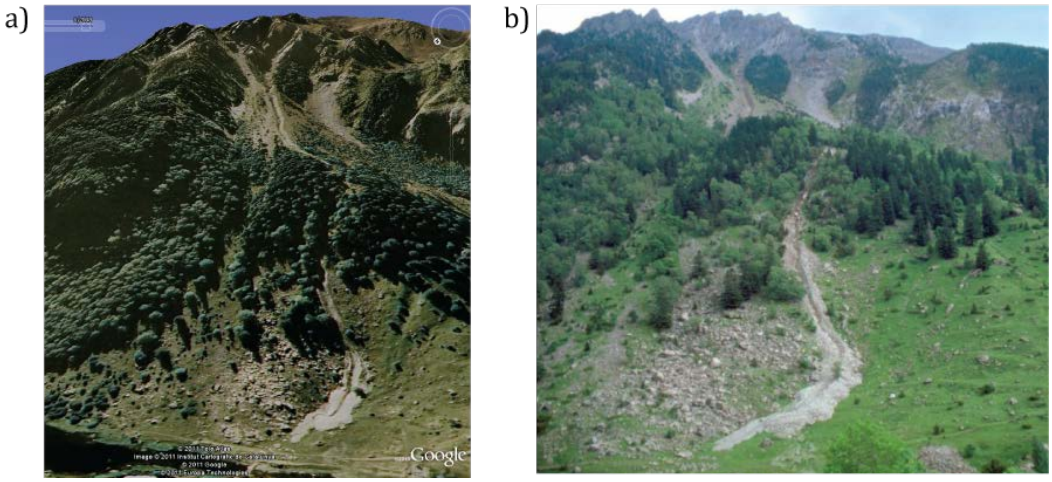

Fig 5.9: Three-dimensional view of the catchment shown in Figure 5.6. a) Google™Earth view of the 2008 ortho-photo and b) oblique photo taken during field observation in 2003 (photograph: P. Oller, Geological Institute of Catalonia).

5.3.2.2. Digitalization in a GIS and classification of the inventory data

When a debris-flow event was detected, the area affected by the event was digitized in a GIS over the base of the current coloured ortho-photos at a scale of 1:5000.

The magnitude of the events are generally determined by the area of the accumulation zone, A. Then the volume, V, was estimated by available formulae (see e.g. Scheidl & Rickenmann 2009). The correlation between accumulation area and volume is generally expressed by:

$$A = \alpha . V^{2/3} \tag{5.1}$$

where **α** is an empirically derived, dimensionless coefficient, which commonly ranges between 6 and 45 for debris flow (Scheidl & Rickenmann 2009). Finally, 19 as **α**-value was selected in this study to estimate the volume, because such a value may best match for granular debris flows.

It must be stated that the debris-flow deposit was not always clearly visible (e.g. hidden by forest, in a shadow area of the aerial photograph etc.) or was located inside the torrent channel. Then, additional parameters, like the erosion length inside the channel, were used to estimate the magnitude.

Finally, five different magnitude classes were defined (Table 5.3). The magnitudes of the debris flows detected in the Central Pyrenees are evidently smaller than events observed in other mountain ranges, such as the European Alps and the Canadian Coast Ranges (Jakob 2005b). As it will be described below, there were only 3 debris flows (out of almost 200) with a volume exceeding 10000 m^3.

Table 5.3: Classes of debris-flow magnitude applied in this study.

Class	*Area of accumulation zone (m^2)*	*Volume * (m^3)*
Very large	>4000	>3055
Large	2200-4000	1246-3055
Medium	1300-2200	566-1246
Small	700-1300	224-566
Very small	<700	<224

* Estimated by Eq. (5.1) and with 19 as α-value.

5.3.3. Results

5.3.3.1. General aspects

A total of 194 debris flows were detected in 116 different torrents. These numbers provide a spatial density of 0.5 events per square kilometre or 0.3 torrents with debris-flow activity per square kilometre for the time span analysed.

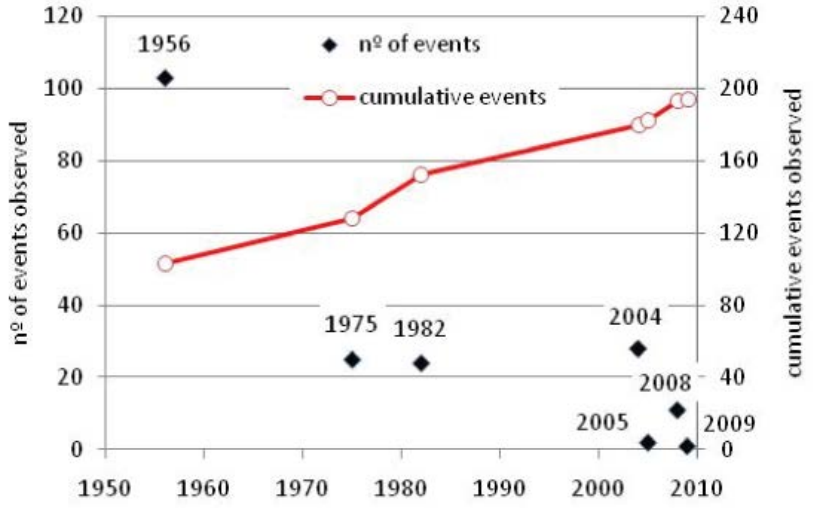

Figure 5.10: Number of debris flows observed in each dataset. Year of the datasets are given as labels.

Almost half of the debris flows were observed in the oldest aerial photographs of 1956/57 (Fig. 5.10). This fact may be related to the 1937 flood episode, which is described in historic archives and other landslide studies (Corominas & Alonso 1984, Balasch 2008). The 1937 flood episode was one of the most catastrophic that has affected the Central Pyrenees during the XXth century. Most of debris flows identified in the 1956/57 photographs are likely to be related to the 1937 flood episode. The remaining cases may have been triggered by intense but localised rainstorms that occurred between 1937 and 1956/57.

The observed debris-flows depositional areas range from ~200 m^2 up to 35000 m^2, which correspond to volume estimates of ~35 m^3 and ~80000 m^3 applying Equation 5.1. More than half of the magnitudes correspond to the classes small and very small and only about 10% of the debris flows belong to the class very large (Fig. 5.11). Figure 5.11 does reject the hypothesis of a significant increase or decrease of magnitude over the time span analysed in this study.

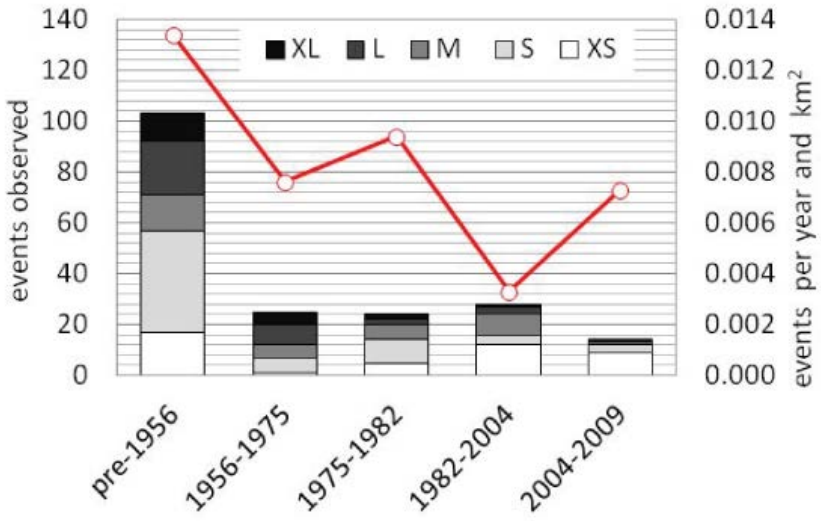

Figure 5.11: Debris flows observed within time intervals. Stacked columns indicate number of events separating different magnitudes. Line shows the number of events normalized per area and year.

Figure 5.9 also includes information on the frequency of events along the time span analysed. Since the photo sets of 1972 and 1982 do not cover the entire study area, the frequency was normalized by the area analysed. The events prior to 1956 were associated with a time span of 25 years, which would characterize the time interval for debris-flow detection through aerial photographs. The assumption of 25 years might be subjective, but the resulting normalized frequency curve represents rather well the two largest historic flood events of the Pyrenees (1937 and 1982).

5.3.3.2. Magnitude-Frequency relationship

The MCF relationship was established incorporating the area of the debris flow (in m^2) and selecting a total time span of 78 years (53 + 25 years). The resulting MCF curve is illustrated in Figure 5.12a. In order to complete the analysis, the MCF relationship is also visualized for debris-flow volumes. Equation 5.1 was used to extrapolate the volumes from the areas and the resulting curve is illustrated in Figure 5.12b.

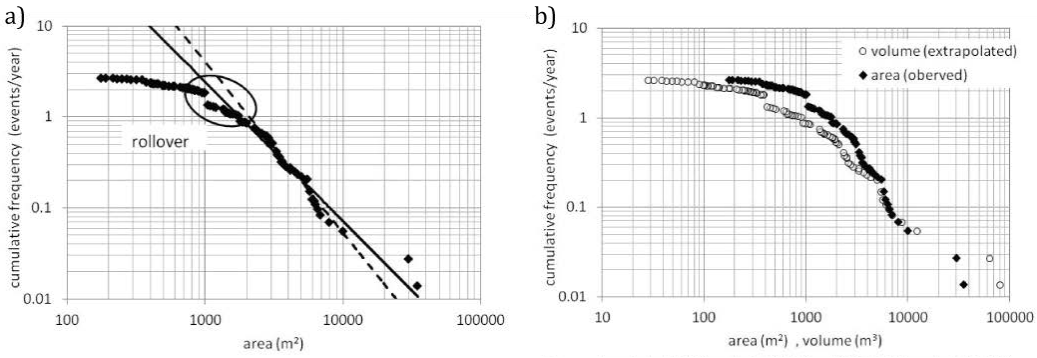

Figure 5.12: a) Magnitude- cumulative frequency curves obtained from the inventory data. Solid line represents Eq. 5.2; dashed line shows Eq. 5.3, which excludes the two outliers. b) Magnitude is represented by area observed and also by volume estimated by Eq. 5.1.

A rollover effect is visible distinguishing two groups of events: smaller and larger than about 1000-2000 m^2. Such a rollover in M-F relationships has been observed in many studies (e.g. Stark & Hovius 2001; Guzzetti *et al.* 2002; Guthrie & Evans 2004) or even above at local scale.

Regarding the events of our dataset with areas larger than 2000 m^2, the MCF relationship, can be represented by a power law:

$$F_{cum} = 9.4 \times 10^5 \times M^{-1.53} \quad (5.2)$$

where the magnitude M is defined as the debris-flow area.

The slope of the power law relation, which is given by the constant b in the general form of the MCF relationship (Eq. 1.1), fits very well the value obtained from the database on debris slides and debris flows on Vancouver Island, Canada (b = 1.6; Guthrie *et al.* 2004).

If the two outliners (represented by areas of 1000 and 35000 m^2) are neglected, the power law can be expressed as:

$$F_{cum} = 1.76 \times 10^6 \times M^{-1.88} \quad (5.3)$$

This equation gives a slightly better R^2-value (R^2 = 0.98) than the one obtained by Equation 5.2, where R^2 was 0.95. The higher slope (b = 1.88) better fits the results from the dataset on debris flows and debris avalanches at the West Coast of British Columbia, Canada (Hungr *et al.* 2008).

The comparison between the Pyrenean and Canadian datasets reveals that the magnitude of the debris flows in the Central Pyrenees is generally smaller than the one observed for the two Canadian studies. This conclusion is also supported by the fact that the rollover defined by Guthrie & Evans (2004) is at 10000 m^2, which corresponds to a value about one order of magnitude larger than the one determined in this thesis.

5.4. Comparison between local and regional scales

This final paragraph compiles and analyses the different relationships linking frequency and magnitude that are presented in this thesis: Rebaixader and

Aigüestortes national park's data, as well as Tordó and another interpretation of Rebaixader found in Aizpiri Garcia (2010).

The other interpretation provided by Aizpiri Garcia (2010) only differs from the interpretation provided earlier in this chapter in the estimation of the depositional units' areas. When the areas are strictly confined to the present extent in the original interpretation, Aizpiri Garcia (2010) assumes an extrapolation of the area, based on aerial pictures (1957 and 1975). The results are shown in Table 5.4.

Table 5.4: Extrapolation of Rebaixader's depositional units extent, based on Aizpiri Garcia (2010).

DU (#)	*Area (m^2)*
DU 1	2093
DU 2	1679
DU 3	4652
DU 4	4428
DU 5	8582
DU 6	13701
DU 7	24770

Figure 5.13 represents the MCF curves at local scale as well as at regional scale. In red, Rebaixader's results are presented; Aigüestortes national park's data are shown in blue; in black is Tordó; and in green is given Aizpiri Garcia (2010)'s interpretation of Rebaixader. Again, magnitude is expressed as area of depositional units and frequency as events per year. Trend lines are also shown, as well as their equations.

Trend lines and related equations shown in Figure 5.13 are different to that defined earlier in this chapter: the slope of the trend line is generally flatter. The trend lines in Figure 5.13 take into consideration the whole set of data and the

relationships are regarded as a unique linear relationship. Earlier in this chapter, trend lines were defined considering the bilinear shape of the relationships induced by the rollover effect, which is disregarded in the edition of Figure 5.13's trend lines.

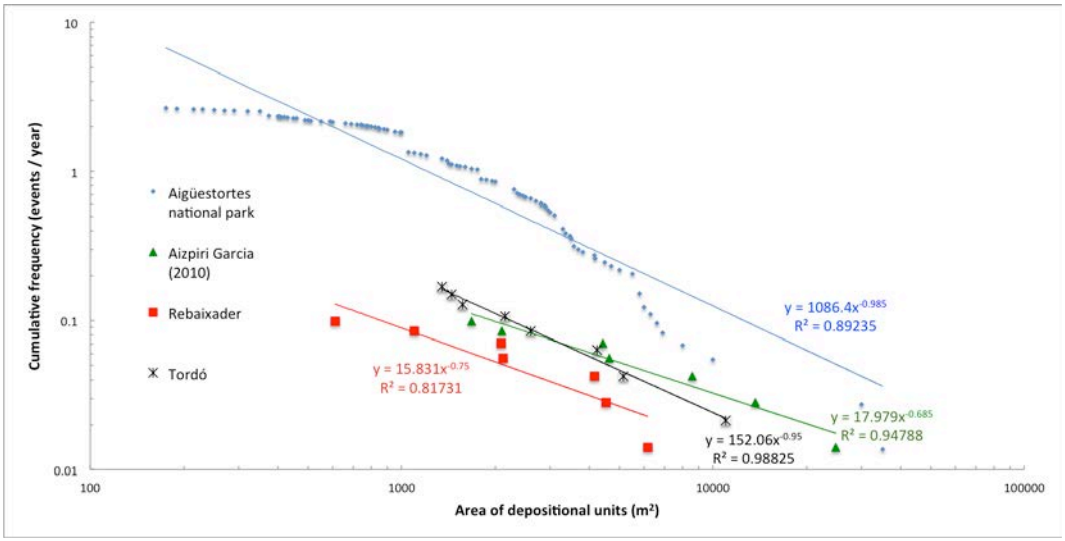

Figure 5.13: Recapitulative MCF graph, for local scale (Rebaixader, in red; Tordó, in black; Re-interpretation of Rebaixader (Aizpiri Garcia (2010)), in green) and regional scale (Aigüestortes national park, in blue).

The general trends are similar for both scales; the curves could be easily superimposable. A point of inflection is visible near 2000-3000 m^2, which corresponds to the expression of the rollover effect defined earlier in this chapter. It is to be noted that for the regional relationship, this rollover effect is somehow attenuated, compared to that of local one. At the highest frequency, the curve is relatively flat and gets vertical as it reaches large areas, with this transition (roll-over) seen round 3000 m^2.

However, for a given frequency, differences in the area of depositional units are possible. For instance, for a frequency of 1 events per 10 years (0.1 in the graph), the area is close to 600 m^2 for Rebaixader, when it corresponds to 6000 m^2 for

the Aigüestortes national park: a ratio of 10 is witnessed. Likewise, a depositional unit's area of 1000 m^2 can have a frequency close to 1.5 for the regional relationship and approximately 0.09 for the Rebaixader (original interpretation).

These differences can be related to the degree in precision of the estimates of the depositional units. When defined from field studies, these estimates are thought to better correspond to the actual dynamics of the processes than studies performed through the survey of aerial pictures (obtainable at certain dates only). Moreover, local and regional relationships are hard to compare due to the effect of the scale of the analysis: at regional scale there is more probability to observe large events, just like there is more probability to observe small events at local scale. Similarities between the MCF relationships in shape and trend edited for the Central-Eastern Pyrenees, for both regional and local scales, have also been recognized in past studies (Guthrie & Evans 2004).

This is the first time that a study of the Central-Eastern Pyrenees led to the elaboration of various MCF relationships at different scales and coinciding with past studies.

5.5. Conclusion

5.5.1. Local scale

Magnitude and frequency of past debris flows that left a trace on Rebaixader's fan were worked out. Within the last 70 years, at least 7 debris flows were great enough to create new colonisable surfaces for vegetation. And in the time study, several debris flows of smaller intensity occurred (Hürlimann *et al.* 2011).

When compared to another Pyrenean site, it appears that Rebaixader's activity is lesser than expected by the aspect of the fan. However, the methodology suffers limitations and estimates that are likely to bias the analysis:

- The area making up the DU's area is to be understood as the DU's area visible in 2009. No extrapolation has been done, therefore, clearly underestimating this parameter.

- The trees ages require the pith to be hit when coring. Because it is not always achieved, we have used a geometric model to add the rings missing between the sample and the pith. This method implies a constant ring width, when nothing proves it is.

- The colonisation time gap (CTG) of Pines in the Pyrenees has not been investigated. 3 years were chosen based on field data. This value needs further investigation.

- DU4 has benefited from several dating techniques used herein. Using branch whorls, a maximum age of 21 years was found, and an average over 60 trees was calculated (13.5 years). Furthermore, the biggest tree found on this DU was cored. A minimum age of 13 years was determined, coring the biggest tree does not necessarily mean to date the oldest.

- Debris flows can remain undetected by the approach used here if they occur with a high frequency (greater than on event per year).

This study of debris-flow frequency and magnitude represents a step forward in the understanding of Pyrenean debris-flow hazard. Therefore, coupled with the study of the susceptibility of Pyrenean landscapes to debris flows the work, presented herein, would fulfil the requirements of a debris-flow hazard assessment in the Pyrenees.

Little information is available on the subject, at both catchment and regional scales. More case studies are needed in order to better compare the current dataset and provide accurate analysis and knowledge to communities and stakeholders whose interests are related to debris flows.

5.5.2. Regional scale

At regional scale, this chapter's second part supports the conclusions of previous studies: interpretations of aerial photographs are a useful methodology to determine a M-F relationship at regional scale; especially in remote mountain areas, where detailed historical data on debris-flow occurrence are usually missing.

The use of Google™Earth and other web-based applications, which visualize aerial photographs in a geo-referenced mode, made possible a fast and straightforward creation of an inventory.

National parks are perfect test areas for studies dealing with geomorphologic processes, because human activity is very or totally restricted.

A total of 194 debris flows were detected in the aerial photographs analysed. The time window of these photographs covers 53 years (from 1956/57 to 2009). However, 25 years prior to the oldest photo set was selected to include debris-flow activity observed in the 1956/57 aerial photographs. This assumption is rather subjective, but coincides with field observations and dendrochronological studies carried out in the same area.

The resulting M-F relationship was compared to data obtained from other regional studies. This comparison showed that our relationship from the Pyrenees coincides rather well with studies from other mountain ranges (Coastal British Columbia, Canada). Nevertheless, the magnitudes of the Pyrenean debris flows seem to be smaller than the ones observed in Canada.

As a general and global conclusion, it can be stated that the M-F relationships reported here, at both local and regional scale, support the idea that debris-flow temporal occurrences can be tackled by two easy, but different techniques, enlightening that geological processes are better apprehended when multi-disciplinary visions are joined.

CONCLUSION

General aspects

The landscape of the Central-eastern Pyrenees has served as a base in the elaboration of this thesis. Statistical susceptibility models and magnitude-frequency relationships form the core of this debris-flow hazard assessment.

Mountainous environments are places of intense erosion due to unpredictable weather climates (or something like this). The peaks shape is the result of climatic sculpting ever since the climate fluctuates. Rainfall, snow, thawing (and even solar radiations) erode the surface of the lithosphere, which is also affected by the mantle's palpitations. Together they bring down mountains and shape the Earth surfaces, at a pace depending on the influence of one over the other.

Erosional processes are numerous; generally chemistry (molecular structures' alteration) and physics (gravity) are used to distinguish two main types of erosion. This thesis focuses on one of the gravity-driven processes, which is common in mountainous environments.

Debris flows are formed when water mixed with products of erosion travel down torrents and gullies. Water and debris (material ranging in size from clay to boulders and possibly incorporating organic matter like trees) in adequate proportion (40-80% in debris) can reshape the surface and leave traces in the

landscape, some typical of the specific physical properties. Their occurrence and recurrence within a torrent leads debris-flow studies to be conducted over small areas (local scale), often united under the term catchment. In this thesis the debris-flow assessment's scale is regional, which drove the author to tackle debris flows through catchments in reference to the landscape.

The topography and morphometry of catchments are a common data source, easily gatherable and proved useful in past debris-flow studies. Statistics is used to analyse the information. It links geomorphology and data mining techniques to calculate the debris-flow susceptibility. In this same landscape, debris flows leave traces, which can be analysed through dendrochronological techniques and aerial picture comparisons, and help to determine the frequency and magnitude of occurrence.

Specific outcomes

Reconnaissance

Summary

5 debris flows that occurred in the Central-Eastern Pyrenees from 2008 have been studied as an introduction to this assessment. In-channel and landslide-triggered debris flows display different geomorphological characteristics and the data fits the relationships validated for the European Alps. It is after the study of these few examples that an inventory was started, based on past studies and/or aerial pictures. 691 debris-flow tracks through which debris flows are thought to have travelled form this inventory.

Discussion

Inventory

The problem here is linked to the trigger of debris flows. The dynamics are different from one kind to another. A unique inventory where all kinds of debris

flows are represented was elaborated for this thesis. This unique inventory is one of the reasons why prediction rates of the models are low when compared to the literature providing examples. These studies usually take into consideration one type of debris flows - often landslide-triggered debris flows, as landslides are more easily found in the landscape than debris-flow traces left by in-channel debris flows. It offers a somewhat homogeneity in the results however, it simplifies the complexity of the landscape's truth.

The physical behavior of the process and consequences on the landscape were more important than the trigger. Although, there are numerous triggers, the process remains the same at the end, and thus the choice of not clustering the debris flows depending on the trigger was retained. Clearly the inventory suffers from its assemblage. Ideally each type of debris flow should have a corresponding hazard assessment with a specific inventory.

Field studies

Study of geological hazards implies the study of the environment where hazards can be witnessed. Field studies are in fact the backbone of hazards studies. However, field studies can reveal complicated the gathering of data and are not meant to change soon. The pressure exerted on land by the population growth leads to a development of the urbanization over dangerous, unsuitable places like colluvium fans, scarce flat areas in mountainous environments that may prove of scientific interest. In the case of erosional processes in mountainous environments, urbanization is responsible for an always-increasing number of people or infrastructure at risk. Although, a study like the one presented in the thesis aims at protecting Societies by explaining the processes likely to have an impact on them, that they will have to face, urbanization too often neglects such studies and prefers to rely on economical prospects. By doing so, natural systems are disturbed, sometimes for ever (a catchment can be one of the systems). Studies of such systems can be biased compared to natural systems. The case of Port-Ainé is an interesting example, as the ski resort activities are thought to have a role in local debris-flow activity (change in the material transit – skiers

exert pressure on the snow and soil and displace material when skiing). Another case encountered in the Pyrenees is Riu Runer, which shows in the upper part of the catchment an aqueduct that connects 2 different catchments. The non-natural input of water in Riu Runer catchment is thought to be responsible for the intense erosion witnessed in the upper part. This erosion could be linked to the abnormally large debris flow of 2008. Anthropogenic activity should never be under-estimated, when geological hazards are considered.

Morpho-fluvial analysis

Summary

Thanks to GIS techniques, Central-Eastern Pyrenean and Andorran 1st- and 2nd-order catchments (following Strahler's system) have been edited, considering that a drainage line initiates when the drainage area reaches 1km^2 as a minimum. A series of 14 fluvio-morphological parameters describes either the catchment's polygon or the stream (drainage line) within a catchment. The 1km^2 threshold's choice directly influences the catchments' area and perimeter. On the contrary, parameters like the different elevations or the orientation offer little difference from one order to the other. Values encountered agree with past studies, which show that the 1km^2 threshold does not significantly alter the values of the parameters and the comparison is appropriate. Streams through their associated parameters tend to show that the outlet is a place of great dispersion in the slopes' values, which smoothen as larger segments of streams are looked at. Morpho-hydrological ratios are also coherent with past studies.

Leopold (1964) shows the relationship between stream length and area, which in his opinion are best fitted by a power law. The data from the Central-Eastern Pyrenees confirm this trend, but it emerges from the data that the linear regression describes best the relationship for headwaters.

Discussion

Study unit

The inventory elaborated takes into account the track of a debris flow, any point from its presumed initiation point to its depositional area, based on the recurrence of the phenomenon. The occurrence of debris flows can be assessed, which is not always the case for the frequency or the number of occurrences. A specific example: when a landslide scar was seen together with what seemed a corresponding depositional area, checking for the actual link between scar and depositional areas demands field investigations. This was not realistic, given the number of torrents to analyse. It is for this reason that the usual study unit, which is the point of initiation of the phenomenon, was discarded for this study. A direct consequence is a limitation in the number of comparable data. Another one was to rethink the study unit at which the work would be conducted.

From the beginning the idea was to incorporate a hydrological component to this work. Catchments are a common unit of study in hydrology. In general debris-flow cases, catchments are the whole study area. In this thesis catchments are the study unit. The advantage of such a unit is its ease of determination through GIS. Moreover, it was possible to simply overlap the information relative to the inventory to that of the catchments.

The historic way of apprehending catchments is to divide them into orders. In this study 1st- and 2nd-order catchments have been considered. Higher orders were not investigated because 1) their numbers were too few to support the statistics, 2) past studies showed that the size of 3rd-order (and above) catchments is in general too big to be compared to data from existing studies and 3) ultimately high ordered catchments present traces of debris-flow occurrences (it makes increase the spatial probability of encountering a debris flow).

Stream initiation and catchments

The main issue regarding the methodology concerns, the GIS manipulations, and more precisely the threshold of 1 km^2 for the stream's initiation. This value is not a constant in catchment studies but it is recognized as a rather usable threshold in delimitating drainage network. The choice of this value has a direct influence on the results, especially since it plays a role on catchments' form. Area, perimeter and stream length have a clear minimum. Changing the 1-km^2 threshold would mean a change in these minimums, confirming the threshold's influence.

In addition, great care is to be taken when comparing these catchments to other studies, especially to that of local studies. In review, lets consider the 5 catchments from Chapter 2 and compare them to the catchments from Chapter 3. 3 catchments out of 5, all the landslide-triggered debris-flow catchments, have larger areas, below the thresholds used in Chapter 3 and 4. For this reason, the threshold used in delimitating the drainage network should be thought, as well as considering the study's scale.

In this thesis, the work on the inventory and susceptibility was conducted at regional scale, as the need was to cover a large area and catchments like the 3 mentioned above, were thought to be too small to be considered a study unit. Experience and past studies have proved this choice correct: 1) calculations' times have proved extremely long due to the number of catchments (a larger number of catchments may have been lethal to the calculations) and 2) comparisons are enabled: catchments' data's range given after the use of the 1-km^2 threshold coincide well with catchments' data from other studies dealing with debris-flow occurrences.

Parameter selection

Occurrence of debris flows is recognized to be governed by environmental factors such as climate or geology. In fact, for a debris flow to develop, it needs

water and material. The water comes from the rainfall, and the material from the erosion of the bedrock. Logically, if one wants to parameterize debris-flow occurrence, it should encompass debris availability (either from the torrent's bed and potentially from banks' destabilizations or landslides) and rainfall delivery. However, simple as it looks, debris (or sediment) availability is still under investigation as its incorporation into debris-flow occurrence's models is poorly understood.

However, the angle on which to tackle debris flows is wide. Morphometry of the debris-flow event (at local scale) and/or of the debris-flow landscape (at regional scale) is often used in bypassing the complexity of sediment availability in susceptibility models. In this thesis 14 parameters were chosen to reflect the morphometry of the landscape (with catchments as study units) through a fluvial point of view. Given that debris-flow process makes the transition between mass movements and fluvial activity, the susceptibility models presented in this thesis are based on the fluvial aspects of debris flows for this reason.

In the series of parameters studied in this thesis, there is missing a very important factor in debris-flow occurrence, Geology. Geology often plays an important role in debris-flow occurrences, and especially on debris-flow triggers. The nature of the bedrock is often responsible for the availability of material degraded by erosion and present (or likely to be found) in the torrent. In the author's opinion, geology is on the same level as rainfall: it could be seen as primary factors. The approach considered in this thesis is centred on secondary factors, already showing the effects of past erosional processes. However, including geology to the parameters' list could lead the models to increase their performance.

About the parameters, there is an aspect of the data that need to be discussed. In the models presented in Chapter 4, data are presented in terms of related units (e.g.: area in square kilometres, slopes in degrees). For some parameters (like for elevations) keeping the data in the original unit could make difficult the application of the models to other landscapes, as it emphasizes the regional

differences. To overcome this difficulty and optimize the likelihood of a foreign application of the models, it could be considered to have all the data bracketed between 0 and 1. Other issues may arise from this hypothesis, like how to define the maximum area or elevation or slope (should it be relative or absolute maximum?) and how to tackle parameters like orientation.

Susceptibility analysis

Summary

Now that the inventory is ready and the study units' background is validated, the data can be cross-referenced, in 4 zones forming the training set for three of them and the test set for one. From that, in the training set, 78 out of 1022 catchments were reactive for the 1st-order catchments, and 52 out of 278 for the 2nd-order catchments. The un-balanced ratio of reactive over non-reactive catchments leads to overfitting, which is a common issue with statistical models. A cost matrix, which acts as to 1) weight the database and 2) give an equal weight to reactive and non-reactive catchments, is applied in order to overcome the problem.

The validation of the models was achieved by opposing the models to a test set. The results are better when the models are optimized. Out of the three models (C4.5, CART and logistic regression) the logistic regression is more efficient for the 1st-order catchments when the CART gives better results for the 2nd-order catchments. When compared to other studies, performance of the models are low, not exceeding 75% and can be compared to 0.86 for instance in Frattini *et al.* (2012). This can be partly explained by the choice of parameters, their numbers, or the use of a test set. This issue is one of the themes that are explored in the discussion below. Nonetheless data mining proved useful in tackling the data. At the end, 14 parameters and a performance summiting 75% can only lead to improvement.

Discussion

The idea behind models can be very different from one model to the other. Digital models can be made of sand and water, in a laboratory or even outside. Statistical models arrange data (often numbers) and extract relationships between them. Physically based models require computer programming and equations accounting for the physics of the phenomenon. Depending on which direction you want the investigation to go in order to support the subject, there is always a suitable model to mount.

In the case of regional assessments, which often means considerable amount of data to treat, statistical models are recurrent. In this thesis, the models are based on data mining techniques. These techniques are rather novel for debris-flow susceptibility assessment and perhaps more study on its applicability is needed. However, it allowed the author to develop, from the available data, both the statistical analysis and learning machines.

The elaboration of the learning machines is a demanding task, which implies a consequent knowledge of the techniques. However, it is shown in this thesis that a considerable amount of data can be treated, thanks to those techniques and that the results are easily understandable and applicable.

Many different data mining algorithms on which to base a model are available. The choice of the models, the logistic regression and the two decision trees (C4.5 and CART), are based on trial runs. The easiness of the mounting of the model and understandability of the results were an issue in the final choice. The idea was to confront different models, all based on statistics, and data mining offered a lot of possibilities. It is not impossible for a model that has not been investigated in this thesis, to present a better performance.

When it comes to statistical analysis and data mining techniques, one has to be aware that different trials from the same model, mounted with the same data, can present different performances. The difference in the results depends on the algorithms used. Generally the data used to mount the models are used in a

random order and thus, every trial is different. This is the reason why a general truth extracted from statistical models, is often illusory. Talking about a trend would be more adequate.

Magnitude-frequency relationships

Summary

The notion of hazard assessment implies to assess the susceptibility and the debris-flow frequency. In this thesis the magnitude-cumulative frequency relationship is reported at local and regional scale. At local scale, dendrochronological techniques revealed 7 debris flows within 70 years, which in turn shaped the vegetation's clusters at Rebaixader creek. At regional scale, aerial pictures' comparison, from 1956/7 to 2009, of the national park of Aigüestortes highlighted 194 debris flows. They permitted to work out a regional magnitude-cumulative frequency relationship, which coincide well with other mountain ranges. The comparison between both -local and regional - relationships seems to pledge for a general over-estimation in the frequency. However, both relationships are similar in shape, and also fit other studies' results.

In a nutshell, debris-flow hazard assessment can only be studied through the subtle association of scientific disciplines dealing with the contact lithosphere/atmosphere, from inorganic rocks to organic vegetation.

Discussion

In this thesis, the vegetation was used to study the frequency of occurrence of debris flows. The aim is to gather sufficient information about the surface on which it grows, to determine the oldest trees and thus, assess the minimum age of the creation of the surface. Tree cores and branch whorls' counting, when cores were not obtainable, like when they are too small, were used. These techniques aim at give an absolute age, as opposed to relative age when ages are

given in relation to undated features (Chevalier 2008) to the trees and thus to the surface where it grows.

When the pith of the tree (centre of the tree) is reached, tree cores can provide an (minimum) absolute age. Otherwise, when the centre of the tree is not visible on the core, the use of a geometrical model is used to estimate the missing rings and re-estimate the age of the tree. This technique implies the use of an increment borer, which is a precision tool that requires experience, care and knowledge in its use. Cores are extracted from the tree, then dried, and finally mounted and polished. Once polished, the rings can be counted from the mounted core. Complications can arise such as, breaking the borer, or jamming it or blocking it in the trees, due to the intense pressures within the tree trunk. Hitting the pith is not always the case and require due care and attention. Generally, different cores should be taken from the same trees, preferably at 90° one from the other (in two different directions) as close to the ground as possible. It surely demands more time for gathering/preparing/treating the data but it minimizes the approximation in the age's estimate.

Cores are a great source of information as it shows all the environmental conditions the trees have suffered. For this reason, applying it to natural hazards, which are likely to cause the tree a certain stress and thus change its growing processes have already proved useful. That being said, cores also show general climatic change, droughts/flood, insect attacks and other changes that can be correlated between trees over large areas. In order to differentiate general stresses from stresses due to erosional activity, it is recommended not only to core trees within the study area, but also outside the study area: trees in a close proximity to the study area are to be used as references. In the case of debris flows, trees having experienced one are as important as trees let free of it. Basically, one needs to know the surrounding's background in order to determine traces of anomalies in the rings' pattern.

Counting branch whorls is a harmless technique for the young trees, but the domain of applicability is somewhat not clear. Usually it applies to pines no taller

than 2m (maximum). At this point it is important to remember that, the size of the trees is dependent on the quality of the soil the tree gathers its nutrients from. So the criterion of the size is not good to rely on. Nonetheless counting branch whorls gave coherent results for the population of trees encountered in this thesis/study.

Beside these two techniques, another one was used and consists of dating a scar visible on the bark of a tree. This is often the case with debris flows: impacts from boulders/rocks flowing down with the flow with trees present on the flow's trajectory can leave scars on a tree. These scars can be studied in order to determine the number of rings that have grown over the scar and thus the age of the scar. This technique is to be used carefully. As a wedge is needed, a small section of the tree carefully cut away with an axe. A bad estimation in the extraction of the wedge can be lethal to the tree. There is also another important point to consider when extracting a wedge; the possibility that more than one flow can be responsible for the scaring. It is for these reasons that due care and attention is needed in the field while gathering the wedges and interpreting them.

Using the vegetation to study the frequency of erosional processes is common but all the studies are dependent on the vegetation present on site. Not all the vegetal clusters can support dating techniques used here; maybe only part of the cluster is appropriate to the dating or maybe vegetation cannot be found. The site often dictates the use of one technique over another one. The means of study must be thought of in the full knowledge of the study area. In the case of this thesis, 1) debris-flow consequences in the landscape are known to affect the vegetation at risk, and 2) the techniques have permitted to extract as much information as it was possible, from the landscape, in order to gather silent witnesses and optimise their study.

Overall outcomes

This thesis is a debris-flow hazard assessment. It uses a morpho-fluvial point of view for the characterization of the catchments encountered. Statistical techniques, data mining techniques, have been chosen to treat the data and mount susceptibility models. Eventually, a study showing the link between frequency and magnitude is withdrawn.

The examples of debris flows from 2008 showed that the reconnaissance of debris flows is crucial in any debris-flow hazard assessment. It also shows the first step toward an inventory of past debris flows, on which to base susceptibility models and future predictions. 691 tracks were found in 4 zones of the study area.

The unit at which the work was conducted, catchments of order 1 and order 2, are detailed, which aims at presenting headwaters' morphometry. The 14 different parameters used for the hazard assessment and a first series of statistical results regarding catchments' morphometry can be found. The idea was to present the environment in which the work was conducted, as well as to add a morphological context.

The next step is the analysis of the susceptibility or spatial occurrences of debris flows. Datasets used and models developed are detailed, and the results are presented. Evaluation and credibility of the models are investigated, and their performance is measured in order to choose the best model. The logistic regression gives the best results, with performances in AUC closing 70% for 1st-order catchments and 0.75 for 2nd-order catchments.

Finally, the relationship between magnitude and frequency is provided at both local and regional scales. For the local scale, the Rebaixader torrent and its fan were chosen. The site is known in the area for displaying a complex fan where different depositional surfaces representing different debris flows are recognized using dendrochronological methods. For the regional scale, a study of

aerial pictures of the national park of Aigüestortes allowed to construct and further detail the magnitude-frequency relationship for the Central-Eastern Pyrenees.

Research outlook

Inventory

The inventory created for the study conducted in this thesis concentrates on debris flows. Their origin is not reported, only their occurrence serves as its base.

In the future the inventory has a vocation to be developed and new events can be added. If no new events are added, a close look at the events already in the inventory could be considered in order to gain more local data about these events, and maybe refine the inventory. In addition, not only debris flows could be studied, and the inventory could also benefit from the presence of various erosional processes. The aim at developing the inventory could be to further stress the main variables/parameters in the initiation/propagation/deposition sequences of erosional processes at local scale. Other themes than the morpho-fluvial one used in this thesis could also be considered in broadening the ensemble of data.

Ultimately the comparison between the inventory developed in this thesis and other existing inventories could prove useful in studying the impact of regionalization upon debris-flow occurrence. The same approach could be kept for other erosional processes if necessary.

Morpho-fluvial statistics

While conducting this thesis, over 3000 catchments of order 1 and 650 of order 2 have been defined and the series of parameters extracted, Chapter 3 presents the information. This presentation was sought to be simple and focuses on

straightforward relationships. However, the whole set of results found in Appendix 2 provide lots of information that was not presented given the framework of the work sought and that might proved relevant and useful in future statistical work conducted over the same area.

GIS manipulation

GIS manipulations that led to the digitalization of the catchments had to be done step by step, which was time consuming. It appeared that errors are likely to occur between steps. All along the GIS process it was thought that developing a code in which the different steps would be ordered and executed. Time would be gained and errors due to inadequate manipulations of the GIS files avoided. Creating such an automated package (of the codes to be written) would permit to spend more time gathering data instead of processing them.

Models vs. parameters

In this thesis, 14 parameters and 3 models were used to study the susceptibility of the landscape toward debris flows. The choice of the parameters and of the models led to the results presented here, but other sets were gatherable.

The list of the parameters used in this thesis is substantial, 14. The next step of the study would be the study of the same models with a new list of parameters. The new list would obviously be based on the existing parameters but would be shortened. To do so, an evaluation of the most important parameters would be needed and could be carried out. The author recommends not choosing more than 5 parameters as a start.

The general theme tackled in this thesis could be compared to other themes of parameters. Instead of focusing on morpho-fluvial parameters, similar studies could focus on other themes like geology. The bedrock, the percentage of glacial deposits, presence of (active) faults, and original ratios issued from the literature could serve as a base for a new theme. Since the theme tackled in this thesis is clearly oriented toward a fluvial aspect, the next logical theme would be one

based on geology and material in order to complement the morpho-fluvial susceptibility models.

The susceptibility models developed in this thesis are based on data mining techniques. These techniques are numerous, thus the possibility to develop other models exists, and so does the comparison between the models. A study focusing on data mining techniques specifically applied to debris flows in the Central-eastern Pyrenees could permit to further refine the results presented in this thesis and increase the general knowledge of the application of data mining techniques to hazard assessment.

Regionalization

The regionalization's issue is an important issue in exporting the models to other landscapes. Each mountain range is different, in elevation, in geology, in orientation. What may appear as a maximum in the Pyrenees (3028 m asl as maximum elevation) is far from being the maximum of other range (compared to 4807 m asl for the Alps). For this reason, the idea to cluster the data between 0 and 1, no matter what the parameter is, could remedy this difficulty.

Future work could focus on different landscapes and/or mountain ranges. So far, the work presented in this thesis has been applied to insular environments: Amami island and Nagasaki's region in Japan (thanks to Pr. Shinji EGASHIRA for the data and R. Roy Gallart for the computations). Unsurprisingly, results were not outstanding, but it is a first step to the application outside the Pyrenees. Moreover, the volcano La caldera de la Taburiente (National park of la Taburiente, Isla de la Palma) was chosen to apply the models to the catchments inside the caldera and study the results, which are still under process.

These two new environments are a first step toward the understanding of the effect of regionalization on debris-flow hazard assessment. However, a first step implies many more, and the issue demands further research.

BIBLIOGRAPHY

Aizpiri Garcia, R. (2010) - Frecuencia de las de corrientes de derrubios y su relación con la pluviometria: Aplicación a la cuenca El Rebaixader (Pirineo Central). *Minor thesis, UPC-BarcelonaTech*, 83 pp. (in Spanish).

Alcoverro, J., Corominas, J. & Gomez, M. (1999) - The Barranco de Arás flood of 7 August 1996 (Biescas, Central Pyrenees, Spain). *Eng. Geol.*, 51: 237-255.

Alestalo, J. (1971) - Dendrochronological interpretation of geomorphic processes. *Fennia*, 105: 1-140.

Ames, A. P., Rafin, E. B., Van Dirk, R. & Crosby, B. (2009) - Estimation of stream channel geometry in Idaho using GIS-derived watershed characteristics. *EMSOFT*, 24: 444-448.

Aulitzky, H. (1980) – Preliminary two-fold classification of debris torrents. *Interpraevent*, Bad Ischl, Austria, 4: 285-309 (translated to English by G.Eisbacher).

Bacchini, M. & Zannoni, A. (2003) - Relations between rainfall and triggering of debris-flow: case study of Cancia (Dolomites, Northeastern Italy). *Nat Hazard Earth Syst Sci*, 3: 71-79.

Baeza, C. (1994) - Evaluación de las condiciones de rotura y la movilidad de los deslizamientos superficiales mediante el uso de técnicas de análisis multivariante. PhD thesis, *Universitat Politècnica de Catalunya*, Barcelona, Spain (in Spanish).

Baeza, C. & Corominas, J. (2001) - Assessment of shallow landslide susceptibility by means of multivariate statistical techniques. *Earth Surf. Proc. Land.*, 26, 1251–1263.

Baeza, C., Lantada, N. & Moya, J. (2010) - Validation and evaluation of two multivariate statistical models for predictive shallow landslide susceptibility mapping of the Eastern Pyrenees (Spain). *Environ Earth Sci*, 61: 507-523.

Balasch, J. (2008) - Les riuades del segle XX al Pallars Sobirà: 1907, 1937 i 1982. Barcelona, Generalitat de Catalunya: 240 pp. (in Catalan).

Bardou, E. (2002) - Méthodologie de diagnostic des laves torrentielles sur un bassin versant. *Ph.D. thesis*, *Ecole Polytechnique de Lausanne*, 188 pp. (in French).

Bathurst, J. C., Burton, A., Clarke, B. G. & Gallart, F. (2006) - Application of the SHETRAN basin-scale, landslide sediment yield model to the Llobregat basin, Spanish Pyrenees. *Hydrol. Process.*, 20, 3119–3138.

Bathurst, J. C., Moretti, G., El-Hames, A., Begueria, S. & Garcia-Ruiz, J. M. (2007) - Modelling the impact of forest loss on shallow landslide sediment yield, Ijuez river catchment, Spanish Pyrenees. *Hydrol. Earth Syst. Sci.*, 11 (1): 569-583.

Berti, M. & Simoni, A. (2005) - Experimental evidences and numerical modeling of debris flows initiated by channel runoff. *Landslides*, 2: 171-182.

Berti, M. & Simoni, A. (2007) - Prediction of debris flow inundation areas using empirical mobility relationships. *Geomorphology*, 90: 144-161.

Bhagwat, T. N., Shetty, A. & Hegde, V. S. (2011) - Spatial variation in drainage characteristics and geomorphic instantaneous unit hydrograph (GIUH); implications for watershed management - A case study of the Varada River basin, Northern Karnataka. *Doi: 10.1016/j.catena.2011.05.007*.

BigDataNerd (2011) – Introduction to data mining, types of data mining techniques. *BigDataNerd's blog*. 25/06/2011. URL: http://bigdatanerd.wordpress.com/2011/06/25/introduction-to-data-mining-types-of-data-mining-techniques./: last access 15/01/2013.

Blahut, J., van Westen, C.J. & Sterlacchini, S. (2010) - Analysis of landslide inventories for accurate prediction of debris-flow source areas. *Geomorphol*, 119: 36-51. doi:10.1016/j.geomorph.2010.02.017.

Bollschweiler, M., Stoffel, M., Ehmisch, M. & Monbaron, M. (2007) - Reconstructing spatio-temporal patterns of debris-flow activity using dendrogeomorphological methods. *Geomorphology*, 87: 337-351.

Bollschweiler, M., Stoffel, M. & Schneuwly, D.M. (2008) - Dynamics in debris-flow activity on a forested cone – A case study using different dendroecological approaches. *Catena*, 72: 67-78.

Bovis, M.J. & Jakob, M. (1999) - The role of debris supply conditions in predicting debris flow activity. *Earth Surf. Process. Landforms,* 24: 1039-1054.

Brardinoni, F. & Church, M. (2004) - Representing the landslide magnitude–frequency relation: Capilano River basin, British Columbia. *Earth Surf. Process. Landforms*, 29: 115-124.

Brayshaw, D. & Hassan, M. A. (2009) – Debris flow initiation and sediment recharge in gullies. *Geomorphol.*, 109: 122-131. doi:10.1016/j.geomorph.2009.02.021

Breiman, L., Friedman, J., Olshen, R. & Stone, C. (1984) - Classification and regression trees. *Chapman and Hall*.

Breiman, L., Friedman, J., Olshen, R., Stone, C., Steinberg, D. & Colla, P. (1995) - Cart: Classification and regression trees. *Chapman and Hall*.

Brochot, S. & Marchi, L. (2000) - Les cônes de déjection torrentiels dans les Alpes françaises. Morphométrie et processus de transport solide torrential. *Revue de géographie alpine*, 88: 23-38 (in French).

Burrough, P. A. & McDonell, R. A. (1998) - Principles of Geographical Information Systems. *Oxford University Press*, New York: 190 pp.

Cammeraat, L. H. (2002) - A review of two strongly contrasting geomorphological systems within the context of scale. *Earth Surf. Process. Landforms*, 27: 1201-1222.

Cannon, S.H., Kirkham, R.M. & Parise, M. (2001) - Wildfire-related debris-flow initiation processes, Storm King Mountain, Colorado. *Geomorphol.*, 39: 171–188.

Carrara, A., Cardinali, M., Detti, R., Guzzetti, F., Pasqui, V. & Reichenbach, P. (1991) - GIS techniques and statistical models in evaluating landslide hazard. *Earth Surf. Process. Landforms*, 16: 427-445.

Carrara, A., Crosta, G. & Frattini, P. (2008) - Comparing models of debris-flow susceptibility in the alpine environment. *Geomorphol.*, 94: 353-378. doi:10.1016/j.geomorph.2006.10.033.

Catani, F., Casagli, N., Ermini, L., Righini, G. & Menduni, G. (2005) - Landslide hazard and risk mapping at catchment scale in the Arno River basin. *Landslides*, 2: 329-342. doi: 10.1007/s10346-005-0021-0.

Chen, C.-Y. & Yu, F. C. (2011) - Morphometric analysis of debris flows and their source areas using GIS. *Geomorphol.*, 129: 387-397. doi:10.1016/j.geomorph.2011.03.002.

Chevalier, G. G., Davies, T. R. H. & McSavaney, M. (2009) - The prehistoric Mt Wilberg rock avalanche, Westland, New Zealand. *Landslides*, 6: 253-262.

Chorley, R. J. (1957) - Illustrating the laws of morphometry. *Geological magazine*, 94: 140-150.

Chorley, S. A. (1966) - The application of statistical methods to geomorphology. *In: Chorley, S.A. (ed.) Essays in Geomorphology*. Elsevier, New York: 275-387.

Chung, C. F. & Fabbri, A. G. (2003) - Validation of spatial prediction models for landslide hazard mapping. *Nat Hazards*, 30 (3): 451-472.

Clotet, N. & Gallart, F. (1984) - Inventari de degradacions de vessants originades pels aiguats de novembre de 1982, a les altes conques del Llobregat i Cardener. *Servei Geològic de la Generalitat de Catalunya*, Barcelona, Spain (in Spanish).

Coe, J. A., Godt, J. W., Baum, R. L., Buckman, R. C. & Michael, J. A. (2004) - Landslide susceptibility from topography in Guatemala. *In: Lacerda, Ehrlich, Fontoura, Sayao (Eds), Landslides evaluation and stabilization, Proceedings 1Xth Symp. On Landslides*. Balkema, Leiden, 69-78.

Coehlo-Netto, A. L., Avelar, A. S., Fernandes, M. C. & Lacerda, W. A. (2006) - Landslide susceptibility in a mountainous geoecosystem, Tijuca Massif, Rio de Janeiro: The role of morphometric subdivision of the terrain. *Geomorphol.*, 87: 120-131.

Corominas, J. & Alonso, E. (1984) - Inestabilidad de laderas en el Pirineo Catalan. Tipología y causas. *In ETSECCPB (ed), Inestabilidad de laderas en el Pirineo*. Barcelona: C.1-C.53 (in Catalan).

Corominas, J., Moya, J. & Hürlimann, M. (2002) - Landslide rainfall triggers in the Spanish Eastern Pyrenees. *Proceedings of the 4th EGS Plinius Conference*, Mallorca, Spain.

Corominas, J. & Moya, J. (2008) - A review of assessing landslide frequency for hazard zoning purposes. *Engineering Geology*, 102: 193-213.

Corominas, J. & Moya, J. (2010) - Contribution of dendrochronology to the determination of magnitude frequency relationships for landslides. *Geomorphol*., 124: 137-149.

Costa, J. E. (1984) – Physical geomorphology of debris flows. In Costa, J. E., Fleisher, P. J. (Eds*): Developments and Applications in Geomorphology*, Springer-Verlag, Heidelberg, 268-317.

Coussot, P. & Meunier, M. (1996) - Recognition, classification and mechanical description of debris flows. *Earth Sci. Rev.*, 40: 209-227.

Cruden, D. M. & Varnes, D. J. (1996) - Landslide types and processes. In: Turner, A. K. & Schuster, R. L. (ed) *Landslides: investigation and mitigation*, pp 36–75.

Cuadrat, J. & Pita, M. (1997) - Climatologia. *Ediciones Catedra*, Madrid: 496 (in Spanish).

D'Agostino, V. & Marchi, L. (2001) - Debris flow magnitude in the Eastern Italian Alps: Data collection and analysis. *Phys. Chem. Earth Pt. C*, 26(9): 657-663.

Davies, T. R. H. (1986)- Large debris flows: A macro-viscous phenomenon. *Acta Mechanica*, 63: 161-178.

Deb, S. K. & El-Kadi, A. I. (2009) - Susceptibility assessment of shallow landslides on Oahu, Hawaii, under extreme-rainfall events. *Geomorphol.*, 108: 219-233. doi:10.1016/j.geomorph.2009.01.009.

Di Crescenzo, G. & Santo, A. (2005) - Debris slides-rapid earth flows in the carbonate massifs of the Campania region (Southern Italy): morphological and morphometric data for evaluating triggering susceptibility. *Geomorphol.*, 66: 255–276.

Dragut, L., Eisank, C. & Strasser, T. (2011) - Local variance for multi-scale analysis in geomorphometry. *Geomorphol.*, 130: 162-172.

Duncan, R.P. (1989) - An evaluation of errors in tree age estimates based on increment cores in Kahikatea (Dacrycarpus Dacrydioides). *New Zealand Natural Sciences*, 16: 31-37.

ECORS Pyrenees Team (1988) - The ECORS deep reflection seismic survey across the Pyrenees. *Nature*, 331: 508-510.

Ehsani, A. H. & Quiel, F. (2008) - Geomorphometric feature analysis using morphometric parameterization and artificial neural networks. *Geomorphol.,* 99: 1-12.

Ellen, S. D., Mark, R. K., Cannon, S. H. & Knifong, D. L. (1993) - Map of debris-flow hazard in the Honolulu District of Oahu, Hawaii. *Open File Report. U.S. Geological Survey*: 93–213.

EPIDOR (2006) – Le bassin de la Dordogne. *Bassin Dordogne, Information debits*. URL: http://www.debits-dordogne.fr/index.php?id=2: last access 16/01/2013.

Erkeling, G., Reiss, D., Hiesinger, H. & Jaumann, R. (2010) - Morphologic, stratigraphic and morphometric investigations of valley networks in eastern Libya Montes, Mars: Implications for the Noachian/Hesperian climate change. *Doi: 10.1016/j.epsl.2009.08.008*.

Fawcett, T. (2006) - An introduction to ROC analysis. *Pattern Recognit. Lett.*, 27: 861-874.

Félix, G. & Thomas, N. (2004) - Relation between dry granular flow regimes and morphology of deposits: Formation of levées in pyroclastic deposits. *Earth Planet. Sci. Lett.*, 221 (1-4): 197-213.

Fell, R., Corominas, J., Bonnard, C., Cascini, L., Leroi, E., Savage, W. Z. on behalf of the JTC-1 Joint Technical Committee on Landslides and Engineered Slopes (2008) - Guidelines for landslide susceptibility, hazard and risk zoning for land use planning. *Eng. Geol.*, 102: 85-98.

Fitzgerald, P. G., Muñoz, J. A., Coney, P. J. & Baldwin, S. L. (1999) - Asymmetric exhumation across the Pyrenean orogen: implications for the tectonic evolution of a collisional orogeny. *Earth Planet. Sci. Lett.*, 173(3): 157-170.

Font, M., Amorese, D. & Lagarde, J.-L. (2010) - DEM and GIS analysis of the stream gradient index to evaluate effects of tectonics: The Normandy intraplate area (NW France). *Geomorphol.,* 119: 172-180.

Frattini, P., Crosta, G. & Carrara, A. (2010) - Techniques for evaluating the performance of landslide susceptibility models. *Eng. Geol.*, 111: 62-72.

Fuchs, S., Kaitna, R., Scheidl, C. & Hübl, J. (2008) - The application of risk concept to debris flow hazards. *Geomechanics and Tunnelling,* 1 (2): 120-129. doi: 10.1002/geot.200800013.

Gallart, F. & Clotet, N. (1988) - Some aspects of the geomorphic processes triggered by an extreme rainfall event: The November 1982 flood in The Eastern Pyrenees. *Catena Supp.*, 13: 79-95.

Garcia-Ruiz, J. M., Arnaez, J., Begueria, S., Seeger, M., Marti-Bono, C., Regüés, D., Lana-Renault, N. & White, S. (2005) - Runoff generation in an intensively

disturbed, abandoned farmland catchment, Central Spanish Pyrenees. *Catena*, 59: 79-92.

Gentile, F., Bisantino, T. & Trisorio Liuzzi, G. (2008) - Debris flow risk analysis in South Gargano watersheds (Southern Italy). *Nat. Hazards*, 44: 1-17.

Gini, C. (1912) - Variabilità e mutabilità, *C. Cuppini*, Bologna, 156 pages. Reprinted in Memorie di metodologica statistica (1955), *Ed. Pizetti, E. & Salvemini, T.*, Rome (in Italiano).

Glade, T. (2005) - Linking debris flow hazard assessments with geomorphology. *Geomorphol.*, 66: 189-213.

Godt, J. W. & Coe, J. A. (2007) - Alpine debris flows triggered by a 28 July 1999 thunderstorm in Central Front Range, Colorado. *Geomorphol.*, 84: 80-97.

Grissimo-Mayer, H. D. (2003) - A manual and tutorial for the proper use of an increment borer. *Tree-ring Research*, 59 (2): 63-79.

Guinau, M., Pallas, R. & Vilaplana, J. M. (2005) - A feasible methodology for landslide susceptibility assessment in developing countries: A case-study of NW Nicaragua after Hurricane Mitch. *Eng. Geol.*, 80: 316-327.

Guthrie, R.H. & Evans, S.G. (2004) - Analysis of landslide frequencies and characteristics in a natural system, coastal British Columbia. *Earth Surf. Process. Landforms*, 29: 1321-1339.

Guzzetti, F., Carrara, A., Cardinali, M. & Reichenbach, P. (1999) - Landslide hazard evaluation: an aid to a sustainable development. *Geomorphol.*, 31: 181-216.

Guzzetti, F., Malamud, B. D., Turcotte, D. L. & Reichenbach, P. (2002) - Power-law correlations of landslide areas in central Italy. *Earth Planet. Sci. Lett.,* 195: 169-183.

Guzzetti, F., Reichenbach, P., Cardinali, M., Galli, M. & Ardizzone, F. (2005) - Probabilistic landslide hazard assessment at the basin scale. *Geomorphol.*, 72: 272-299.

Guzzetti, F., Reichenbach, P., Ardizzone, F., Cardinali, M. & Galli, M. (2006) - Estimating the quality of landslide susceptibility models. *Geomorphol.*, 81:166–184.

Hack, J. T. (1957) - Studies of longitudinal stream profiles in Virginia and Maryland. *U.S. Geol Survey Prof. Paper*, 294-B: 45-97.

Horton, R. E. (1932) - Drainage basin characteristics. *Transactions of the American Geophysical Union*, 13: 350-361.

Horton, R. E. (1945) - Erosional development of streams and their drainage basin: hydrophysical approach to quantitative morphology. *Geol. Soc. Am. Bull.*, 56: 275–370.

Hungr, O., Morgan, G. C. & Kellerhals, R. (1984) - Quantitative analysis of debris torrent hazards for design of remedial measures. *Can. Geotech. J.*, 21: 663-677.

Hungr, O., Evans, S. G. & Hazzard, J. (1999) - Magnitude and frequency of rock falls and rock slides along the main transportation corridors of southwestern British Columbia. *Can. Geotech. J.*, 36: 224-238.

Hungr, O., Evans, S. G., Bovis, M. J. & Hutchinson, J. N. (2001) - A review of the classification of landslides of the flow type. *Environ. Eng. Geosci.*, 3: 221-238.

Hungr, O., McDougall, S., Wise, M. & Cullen, M. (2008) - Magnitude-frequency relationships of debris flows and debris avalanches in relation to slope relief. *Geomorphol.*, 96: 355-365.

Hungr, O., Leroueil, S. & Picarelli, L. (2012) - Varnes classification of landslide types, an update. *In: XI international symposium on landslides and engineered slopes*, Banff, Canada: 47–58.

Hürlimann, M., Corominas, J., Moya, J. & Copons, R. (2003) - Debris-flow events in the Eastern Pyrenees. Preliminary study on initiation and propagation. *In Eds. D. Rickenmann & C. Chen, 3rd Int. Conf. on Debris-Flow Hazards Mitigation*, Millpress, Davos: 115-126.

Hürlimann, M., Copons, R., & Altimir, J. (2006) - Detailed debris flow hazard assessment in Andorra: A multidisciplinary approach. *Geomorphol.*, 78: 359-372.

Hürlimann, M., Abancó, C., Moya, J., Raïmat, C. & Luis-Fonseca R. (2011) - Debris-flow monitoring stations in the Eastern Pyrenees. Description of instrumentation, first experiences and preliminary results. *In R. Genevois, D. Hamilton & A. Prestininzi (eds), 5th Int. Conf. on Debris-Flow Hazards Mitigation*, Padua, Italy: 553-562.

Hutchinson, J. N. (1988) – General report: morphological and geotechnical parameters of landslides in relation to geology and hydrogeology. *In Bonnard, C. (Eds). Fifth International Symposium on Landslides*, Volume 1, A. A. Balkema / Rotterdam / Brooklield: 3-136.

ICC, Institut Cartográfic de Catalunya (2003) - Mapa geológic de Catalunya, 1:250000. Barcelona.

ISDR, International Strategy for Disaster Reduction (1999) - International decade for natural disaster reduction: successor arrangements. *Report of the General Secretary*. http:/www.unisdr.org/

Iverson, R. H. (1997) - The physics of debris flows. *Rev. Geophys.*, 35 (3): 245-296.

Iverson, R. H., Schilling, S. P. & Vallance, J. W. (1998) - Objective delineation of lahar-inundation hazard zones. *GSA bulletin*, 110 (8): 972-984.

Jackson, L. E., Kostaschuk, R. A. and MacDonald, G. M. (1985) - Identification of debris flow hazard on alluvial fans in the Canadian rocky mountains. *Eng. Geol.*, 7: 115–124.

Jakob, M. (2005a) - A size classification for debris flows. *Eng. Geol.*, 79: 151-161.

Jakob, M. (2005b) - Debris flow hazard assessment. *Eds Jakob M. and Hungr O., Debris flow hazard assessments and related phenomena*. Springer Verlag, Heidelberg: Chapter 17, 411-443.

Jakob, M. & Hungr, O. (2005) - Debris-flow hazards and related phenomena. *Springer,* Berlin: 739 pp.

Jakob, M. & Friele, P. (2010) - Frequency and magnitude of debris flows on Cheekye River, British Columbia. *Geomorphol.*, 114: 382-395.

Jenson, S. K. & Domingue, J. O. (1988) - Extracting topographic structure from digital elevation data for geographic information system analysis. *Photogramm. Eng. Remote Sensing*, 54 (11): 1593–1600.

Jordan, G., Meijninger, B. M. L., Van Hinsbergen, D. J. J., Meulenkamp, J. E. & van Dijk, P. M. (2005) - Extraction of morphotectonic features from DEMs: Development and applications for study areas in Hungary and NW Greece. *Int. J. of Appl. Earth Obs. and Geoinfo.,* 7 (3): 163-182. doi: 10.1016/j.jag.2005.03.003.

Kar, G., Kumar, A. & Singh, R. (2009) - Spatial distribution of soil hydro-physical properties and morphometric analysis of a rainfed watershed as a tool for sustainable land use planning. *Agricultural Water Management*, 96 (10): 1449-1459. doi: 10.1016/j.agwat.2009.05.003.

Kiel, A., Berking, J., Mügler, I., Schütt, B., Schwalb, A. & Steeb, P. (2010) - Hydrological and geomorphological basin and catchment characteristics of Lake Nam Co, South-Central Tibet. *Quat. Int.*, 218 (1-2): 118-130. doi: 10.1016/j.quaint.2009.02.022.

Kompani-Zare, M., Soufi, M., Hamzehzarghani, H. & Dehghani, M. (2011) - The effect of some watershed, soil characteristics and morphometric factors on the relationship between the gully volume and length in Fars Province, Iran. *Catena*, 86: 150-159. doi: 10.1016/j.catena.2011.03.008.

Kostaschuk, R. A., MacDonald, G. M. & Putnam, P. E. (1986) - Depositional process and alluvial fan-drainage basin morphometric relationships near Banff, Alberta, Canada. *Earth Surf. Process. Land.*, 11: 471-484.

Lana-Renault, N. & Regüés, D. (2009) - Seasonal patterns of suspended sediment transport in an abandoned farmland catchment in the Central Spanish Pyrenees. *Earth Surf. Process. Land.*, 34 (9): 1291-1301. doi: 10.1002/esp.1825.

Landwehr, N., Hall, M. & Frank, E. (2005) - Logistic model trees. *Machine Learning*, 59: 161-205.

Lathrop, R. G. & Peterson, D. L. (1992) - Identifying structural self-similarity in mountainous landscapes. *Landscape Ecology*, 6 (4): 233-238.

Leopold, L. B., Wolman, M. G. & Miller, J. P. (1964) - Fluvial processes in Geomorphology. *W. H. Freeman and Company*, San Francisco.

Lin, Z. & Ogushi, T. (2006) - DEM analysis on longitudinal and transverse profiles of steep mountainous watersheds. *Geomorphol.*,, 78 (1-2): 77-79. doi: 10.1016/j.geomorph.2006.01.017.

Liu, X., Yue, Z. Q., Tham, L. G. & Lee, C. F. (2002) - Empirical assessment of debris flow risk on a regional scale in Yunnan Province, southwestern China. *Environ. Manage.*, 30: 249–264.

Lopez-Vicente, M., Navas, A. & Machin, J. (2009) - Geomorphic mapping in endorheic catchments in the Spanish Pyrenees: An integrated GIS analysis of karstic features. *Geomorphol.*, 111 (1-2): 38-47. doi: 10.1016/j.geomorph.2008.03.014.

Lynn, G. (2005) - Macrogeomorphology and Erosional History of the Post-Orogenic Pyrenean Mountain Belt. *Ph.D. thesis, University of Edinburgh*, Edinburgh: 388 pp.

Malamud, B. D., Turcotte, D. L., Guzzetti, F. & Reichenbach, P. (2004) - Landslide inventories and their statistical properties. *Earth Surf. Process. Landforms*, 29: 687-711.

Martín, V. J. & Olcina, C. J. (2001) - Climas y Tiempos de España. *Eds Alianza S.A.*, Madrid: 258 pp (in Spanish).

Melelli, L. & Taramelli, A. (2004) - An example of debris-flows hazard modeling using GIS. *Nat. Hazard Earth Syst. Sci*., 4: 347-358.

Melton, M. A. (1965) - The morphologic and paleoclimatic significance of alluvial deposits in southern Arizona. *J. Geol.*, 73: 1-38.

Montgomery, D. R. & Dietrich, W. E. (1988) - Where do channels begin? *Nature,* 336: 232–234.

Montgomery, D. R. & Dietrich, W. E. (1989) - Source areas, drainage density, and channel initiation. *Water Resour. Res.*, 25: 1907–1918.

Muñoz, A. (1992) - Evolution of a continental collision belt: ECORS-Pyrenees crustal balanced cross-section. *Eds McClay K.R., Thrust Tectonics*, Chapman & Hall: 235-246.

Napieralski, J., Harbour, J. & Li, Y. (2007) - Glacial geomorphology and geographic information systems. *Earth-Sci. Rev.*, 85 (1-2): 1-22. doi:10.1016/j.earscirev.2007.06.003.

Ng, K. Y. (2006) - Landslide locations and drainage network development: A case study of Hong Kong. *Geomorphol., 76 (1-2): 229-239.* doi:10.1016/j.geomorph.2005.10.008.

Novoa, M. (1984) - Precipitaciones y avenidas extraordinarias en Cataluña. *Eds ETSECCPB, Inestabilidad de laderas en el Pirineo*. Barcelona: I.1.1-I.1.15.

O'Callaghan, J. F. & Mark, D. M. (1984) - The extraction of drainage networks from digital elevation data. *Comp. Vis. Graph Image Process.*, 28(3): 323–344.

Obi Reddy, G. P., Maji, A. K. & Gajbhije, K. S. (2004) - Drainage morphometry and its influence on landform characteristics in a basaltic terrain, Central India – a remote sensing and GIS approach. *J. Appli. Earth Obs. Geoinfo., 6 (1): 1-16.* doi:10.1016/j.jag.2004.06.003.

Okunishi, K. & Suwa, H. (2001) - Assessment of debris-flow hazards of alluvial fans. *Nat. Hazard*, 23: 259-269.

Parde, M. (1941) - La formidable crue d'octobre 1940 dans les Pyrénées-Orientales. *Rev. Geog. Pyré. et du Sud-Ouest*, 12: 237-279 (in French).

Peña, J. C., Aran, M., Cunillera, J. & Amaro, J. (2011) - Atmospheric circulation patterns associated with strong wind events in Catalonia. *Nat. Hazards Earth Syst. Sci.*, 11: 145-155.

Perucca, L. P. & Angilieri, Y. E. (2011) - Morphometric characterization of del Molle Basin applied to the evaluation of flash floods hazard, Iglesia Department, San Juan, Argentina. *Quat. Int.,* 233 (1): 81-86. doi:10.1016/j.quaint.2010.08.007.

Phillips, C. J. & Davies, T. R. H. (1991) - Determining rheological parameters of debris flow material. *Geomorphol*., 4: 101-110.

Pierson, T. C. & Scott, K. M. (1985) - Downstream dilution of a lahar: Tansition from debris flow to hyperconcentrated streamflow. *Water Resour. Res.*, 21: 1511-1524.

Pierson, T. C. & Costa, J. E. (1987) - A rheological classification of subaerial sediment-water flows. *Geol. Soc. Am. Rev. Eng. Geol.,* 7: 1-12.

Pierson, T. C. (2007) - Dating young geomorphic surfaces using age of colonizing Douglas fir in southwestern Washington and northwester Oregon, USA. *Earth Surf. Process. Landforms*, 32: 811-831.

Pike, R. J. (2002) - A bibliography of terrain modeling (geomorphometry), the quantitative representation of topography. *USGS Open file*, report 02-465.

Portilla, M. (2010) - Análisis del campo de densidad de movimientos en masa del área Molló-Queralbs. *Internal report BarcelonaTech – UPC* (in Spanish).

Portilla, M., Chevalier, G. G. & Hürlimann, M. (2010) - Description and analysis of the debris flows occurred during 2008 in the Eastern Pyrenees. *Nat. Hazards Earth Syst. Sci.*, 10: 1635-1645.

Remaître, A. (2006) – Morphologie and dynamique des laves torrentielles: Application aux torrents des Terres Noires du basin de Barcelonette (Alpes du Sud). *Ph.D. thesis, University of Caen/Basse-Normandie*, Caen: 487 pp.

Remondo, J., Gonzalez, A., Diaz de Teran, J. R., Cendrero, A., Fabbri, A. & Chung, C.-J. F. (2003) - Validation of Landslide Susceptibility Maps; Examples and Applications from a Case Study in Northern Spain. *Nat. Hazards*, 30: 437-449.

Rickenmann, D. & Zimmermann, M. (1993) - The 1987 debris flows in Switzerland: documentation and analysis. *Geomorphol.*, 8: 175-189.

Rickenmann, D. (1995) - Beurteilung von Murgängen [Assessment of debris flows]. Schweizer Ingenieur und Architekt, 48: 1104–1108 (in German).

Rickenmann, D. (1997) - Sediment transport in Swiss torrents. *Earth Surf. Process. Landforms*, 22: 937-951.

Rickenmann, D. (1999) - Empirical relationships for debris flows. *Nat. Hazards*, 19: 47-77.

Santacana, N., Baeza, B., Corominas, J., Paz, A. D. & Marturiá, J. (2003) - A GIS-based multivariate statistical analysis for shallow landslide susceptibility mapping in La Pobla de Lillet area (Eastern Pyrenees, Spain). *Nat. Hazards*, 30: 281-295.

Scheidl, C. (2009) - Prediction of debris-flow mobility and deposition fan. *Ph.D. thesis, University of Natural Resources and Applied Life Sciences*, Vienna: 183 pp.

Scheidl, C. & Rickenmann, D. (2009) - Empirical prediction of debris-flow mobility and deposition on fans. *Earth Surf. Process. Landforms*, 35 (2): 157-173.

Schroder, J.F. (1978) - Dendrogeomorphological analysis of mass movement on table Cliffs Plateau, Utah. *Quaternary Research*, 9: 168-185.

Schumm, S. A. (1956) - The evolution of drainage systems and slopes in badlands at Perth Amboy, New Jersey. *Bull. Geol.Soc. Am*, 67: 597-646.

Schweingruber, F.H., Eckstein, D., Serre-Bachet, F. & Bräker, O.U. (1990) - Identification, presentation and interpretation of event years and pointer years in dendrochronology. *Dendrochronologia*, 8: 9-38.

Seeger, M., Errea, M.-P., Begueria, S., Marti, C., Garcia-Ruiz., J. M. & Arnaez, J. (2004) - Catchment soil moisture and rainfall characteristics as determinant factors for discharge/suspended sediment hysteretic loops in a small headwater catchment in the Spanish Pyrenees. *J. Hydrol.*, 288: 299-311.

Shimazaki, H. & Shinomoto, S. (2007a) - A method for selecting the bin size of a time histogram. *Neural Computation*, 19 (6): 1503-1527.

Shimazaki, H. & Shinomoto, S. (2007b) - A recipe for optimizing a time-histogram. *Advances in NIPS*, 19: 1289-1296.

Solyom, P. B. & Tucker, G. E. (2007) - The importance of the catchment area–length relationship in governing non-steady state hydrology, optimal junction angles and drainage network pattern. *Geomorphol.*, 88: 84-108.

Staley, D. M., Wasklewicz, T. A. & Blaszczynski, J. S. (2006) - Surficial patterns of debris flow deposition on alluvial fans in Death Valley, CA using airborne laser swath mapping data. *Geomorphol.*, 74 (1-4): 152-163. doi:10.1016/j.geomorph.2005.07.014.

Stark, C.P. & Hovius, N. (2001) - The characterization of landslide size distributions. *Geophys. Res. Lett.*, 28: 1091-1094.

Sterlacchini, J., Ballabio, C., Blahut, J., Masetti, M. & Sorichetta, A. (2011) - Spatial agreement of predicted patterns in landslide susceptibility maps. *Geomorphol.*, 125: 51-61.

Stoffel, M., Bollschweiler, M. & Hassler, G.-R. (2006) - Differentiating past events on a cone influenced by debris-flow and snow avalanche activity – a dendrogeomorphological approach. *Earth Surf. Process. Landforms*, 31: 1424-1437.

Stoffel, M. & Bollschweiler, M. (2008) - Tree-ring analysis in natural hazards research – an overview. *Nat. Hazards Earth Syst. Sci.*, 8: 187-202.

Strager, M. P., Fletcher, J. J., Strager, J. M., Yuill, C. B., Eli, R. N., Todd Penny, J. & Lamont, S. J. (2010) - Watershed analysis with GIS: The watershed characterization and modeling system software application. *Comput. Geosci.,* 36 (7): 970-976. doi: 10.1016/j.cageo.2010.01.003.

Strahler, A. N. (1952) - Hypsometric (area-altitude) analysis of erosional topography. *GSA Bulletin*, 63 (11): 1117-1142.

Strahler, A. N. (1957) - Quantitative analysis of watershed geomorphology. *Transactions of the American Geophysical Union*, 8 (6): 913–920.

Su, F. & Cui, P. (2009) - GIS-Based Susceptibility Mapping and Zonation of Debris Flows Caused by Wenchuan Earthquake. *In: Conf. on Information Engineering and Computer Science,* Wuhan, China. doi: 10.1109/ICIECS.2009.5364077.

Tarboton, D. G., Bras, R. L. & Rodriguez-Iturbe, I. (1991) - On the extraction of channel networks from digital elevation data. *Hydrol. Process.*, 5: 81–100.

Tarboton, D. G. (1997) - A new method for the determination of flow directions and contributing areas in grid digital elevation models. *Water Resour. Res.*, 33 (2): 309–319.

Tarboton, D. G. & Ames, D. P. (2001) - Advances in the mapping of flow networks from digital elevation data. *World Water and Environmental Resources Congress*. ASCE, Orlando, FL.

Teixell, A. (1998) - Crustal structure and orogenic material budget in the west-central Pyrenees. *Tectonics*, 17: 395-406.

Varnes, D. J. (1954) - Landslide types and processes. In: Eckel, E.B. (eds). *Lanslides and Engineering Practice*. Special Report 28, Highway Research Board, National Academy of Sciences, Washington DC.: 20-47.

Varnes, D. J. (1978) - Slope movement types and processes. In: Landslides Analysis and Control. National Academy of Sciences, Washington D.C. *Transp. Res. Board Spec. Rep.*, 176: 11-33.

VAW: Murgänge (1992) - Dokumentation und Analyse. *Eds Versuchsanstalt für Wasserbau, Hydrologie und Glaziologie*, ETH Zürich, unpublished, 97.6: 620 pp (in German).

Vilaplana, J.M. (1983) - Quaternary Glacial Goelogy of Alta Ribagroça Basin (Central Southern Pyerenees). *Acta Geológica Hispánica*, 18: 217-233.

Wan, S., Lei, T. C., Huang, P. C. & Chou, T. Y. (2008) - The knowledge rules of debris flow event: A case study for investigation Chen Yu Lan River, Taiwan. *Eng. Geol.*, 98: 102-114.

Wan, S. & Lei, T. C. (2009) - A knowledge-based decision support system to analyze the debris-flow problems at Chen-Yu-Lan River, Taiwan. *Knowl.-based Syst.,* 22: 580-588. doi:10.1016/j.knosys.2009.07.008.

Welsh, A. & Davies, T. R. H. (2010) - Identification of alluvial fans susceptible to debris-flow hazards. *Landslides,* 8: 183-194. doi: 10.1007/s10346-010-0238-4.

White, S., Garcia-Ruiz, J. M., Marti, C., Alvera, B. & Del barrio, G. (1996) - Sediment transport in a high mountain catchment in the Central Spanish Pyrenees. *Phys. Chem. Earth*, 22 (3-4): 377-380.

Wilson, J. P. & Gallant, J. C. (2000) - Terrain analysis: principles and applications. *Wiley*, London.

Witten, I.H., Frank, E. & Hall, M. A. (2011) - Data Mining: Practical machine learning tools and techniques. *Morgan Kaufmann*, Burlington, 3rd Ed.: 629 pp.

Zadeh, L. A. (1965) – Fuzzy sets. *Information and Control*, 3: 338-353.

Zavoianu, I. (1978) - Morphometry of drainage basins. *Elsivier*, Amsterdam, NL.

Zimmermann, M., Mani, P. Gamma, P., Gsteiger, P., Heiniger, O. & Hunziker, G. (1997) - Murganggefahr und Klimaänderung – ein GIS-basierter Ansatz. *Eds Schlussbericht NFP 31*, ETH Zürich: 161 pp. (in German).

APPENDICES

Appendix 1: ArcGIS methodology of headwaters catchments' digitalization

Appendix 2: Statistical results of 1st-order and 2nd-order catchments present in the study zones.

Appendix 3: Bi-dimensional relationships for all 655 2nd-order catchments.

Appendix 4: Statistical results for training and test sets.

Appendix 5: Dendrochronological field data.

Appendix 1: ArcGIS methodology of headwaters catchments' digitalization

- Fill Sinks

Terrain processing / DEM Manipulation / Fill Sinks.

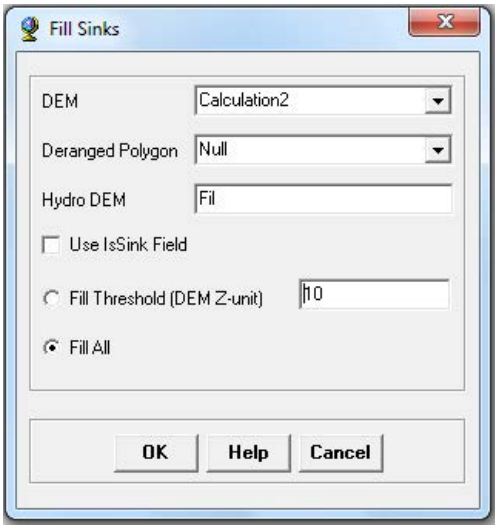

- Flow Direction

Terrain Processing / Flow Direction.

- Flow Accumulation

Terrain Processing / Flow Accumulation.

- Stream Definition

Terrain Processing / Stream Definition.

A second window will pop up, and this is where the threshold is needed.

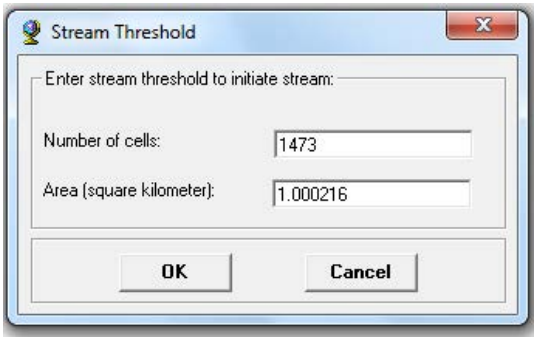

- Stream Link

Terrain Processing / Stream Segmentation.

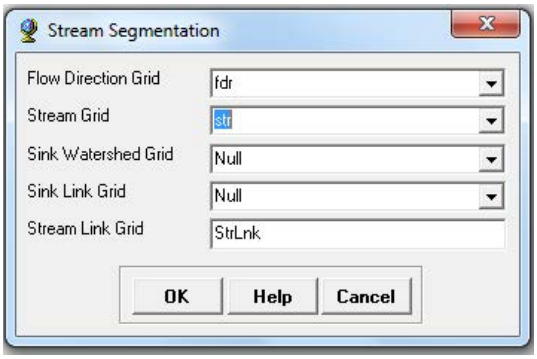

- Catchment Grid Delineation

Terrain Processing / Catchment Grid Delineation.

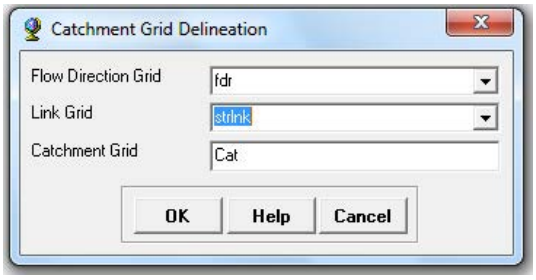

- Catchment Polygon Processing

Terrain Processing / Catchment Polygon Processing.

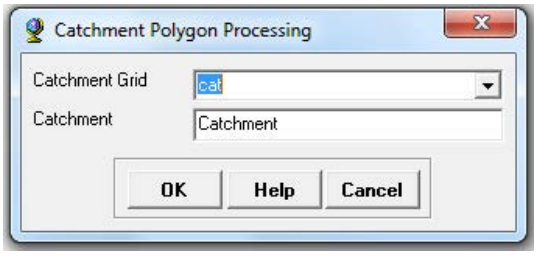

- Drainage Line Processing

Terrain Processing / Drainage Line Processing.

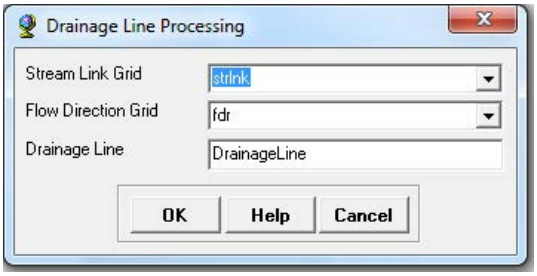

- Adjoint Catchment Processing

Terrain Processing / Adjoint Catchment Processing.

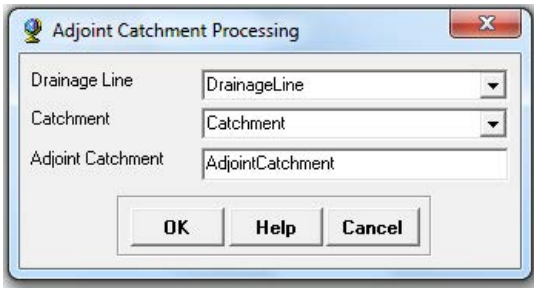

- Stream Order

Spatial Analyst tools / Hydrology / Stream Order.

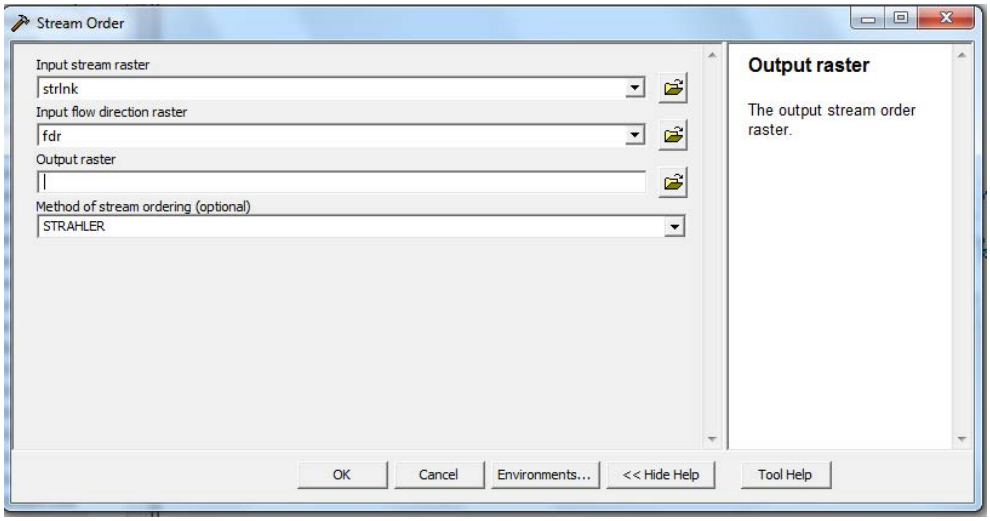

Note: the method of stream ordering is to be set up to Strahler.

- Aspect

Spatial Analyst tools / Surface Analysis / Aspect.

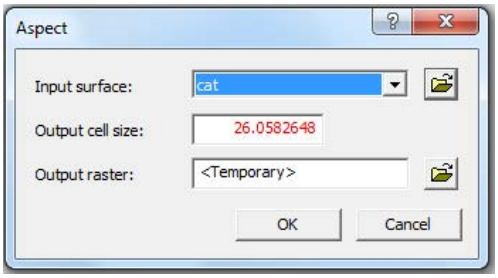

- Slopes

Spatial Analyst tool / Surface Analysis / Slope.

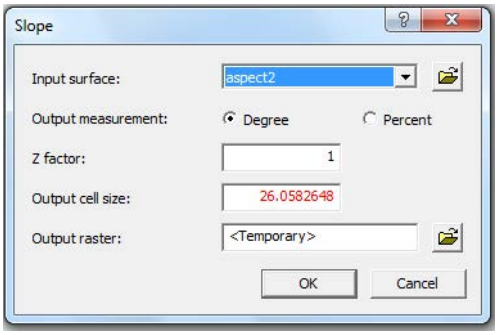

- Running Slope

Toolbars / customize / Commands Tab / COS tools / Running Slope.

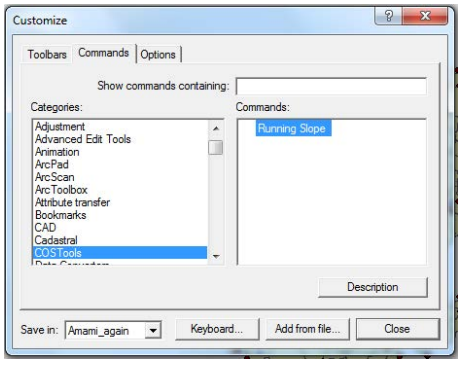

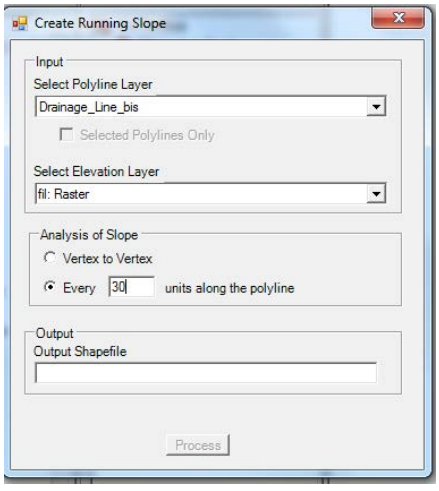

- From-Node-to-Node

Now, what we want to do is to delimit the slope of each basin. The next tool defines the point at the beginning of the basin.

Firstly, we create a new shape file called Nodes, and then we apply the From-node-to-node tool.

It creates a 3-point line. The middle point is not our interest. So, go to attribute table and delete all except the points with valence 1 (middle points have valence equal to 3).

- Import batchpoint

HEC-GeoHMS / Basin Processing / Import Batchpoint.

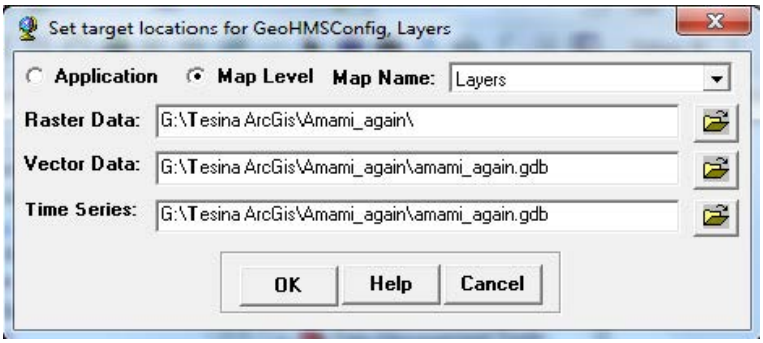

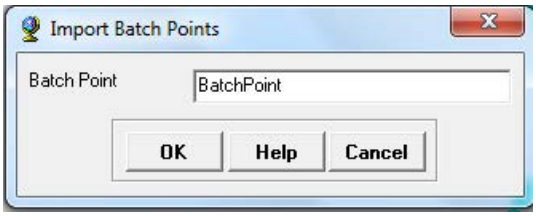

Note: we input all the nodes as batchpoint.

- Watershed processing and batch watershed delineation

Arc Hydro Tools 9 / Watershed Processing, and, Batch Watershed Delineation.

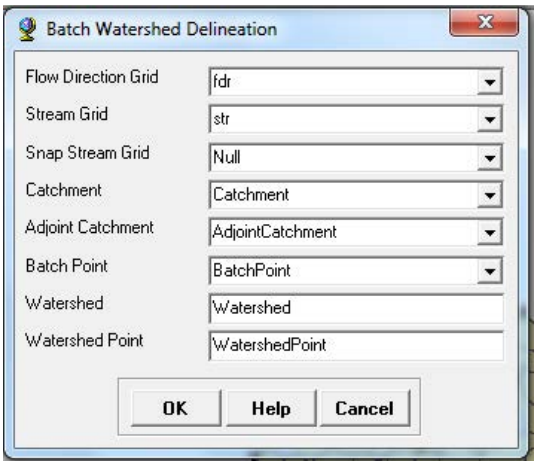

Appendix 2: Statistical results of all the catchments present in the study area.

1st-order catchments.

Maximum elevation (m asl)			
Count	3.01E+03	*Skewness*	-9.87E-03
Mean	1.63E+03	*Skewness Standard Error*	4.46E-02
Mean LCL	1.60E+03	*Kurtosis*	2.13E+00
Mean UCL	1.66E+03	*Kurtosis Standard Error*	8.92E-02
Variance	5.36E+05	*Alternative Skewness (Fisher's)*	-9.87E-03
Standard Deviation	7.32E+02	*Alternative Kurtosis (Fisher's)*	-8.66E-01
Mean Standard Error	1.34E+01	*Coefficient of Variation*	4.50E-01
Minimum	4.41E+00	*Mean Deviation*	6.15E+02
Maximum	3.14E+03	*Second Moment*	5.36E+05
Range	3.14E+03	*Third Moment*	-3.87E+06
Sum	4.89E+06	*Fourth Moment*	6.13E+11
Sum Standard Error	4.01E+04	*Median*	1.59E+03
Total Sum Squares	9.57E+09	*Median Error*	3.05E-01
Adjusted Sum Squares	1.61E+09	*Percentile 25% (Q1)*	1.07E+03
Geometric Mean	1.40E+03	*Percentile 75% (Q2)*	2.23E+03
Harmonic Mean	8.92E+02	*IQR*	1.16E+03
Mode	#N/A	*MAD*	5.67E+02
Mean elevation (m asl)			
Count	3.01E+03	*Skewness*	1.87E-01
Mean	1.29E+03	*Skewness Standard Error*	4.46E-02
Mean LCL	1.27E+03	*Kurtosis*	2.22E+00
Mean UCL	1.32E+03	*Kurtosis Standard Error*	8.92E-02
Variance	4.09E+05	*Alternative Skewness (Fisher's)*	1.87E-01
Standard Deviation	6.40E+02	*Alternative Kurtosis (Fisher's)*	-7.84E-01
Mean Standard Error	1.17E+01	*Coefficient of Variation*	4.95E-01
Minimum	2.31E+00	*Mean Deviation*	5.33E+02
Maximum	2.75E+03	*Second Moment*	4.09E+05
Range	2.75E+03	*Third Moment*	4.90E+07
Sum	3.89E+06	*Fourth Moment*	3.71E+11
Sum Standard Error	3.51E+04	*Median*	1.21E+03
Total Sum Squares	6.26E+09	*Median Error*	2.67E-01
Adjusted Sum Squares	1.23E+09	*Percentile 25% (Q1)*	8.08E+02
Geometric Mean	1.07E+03	*Percentile 75% (Q2)*	1.77E+03
Harmonic Mean	5.90E+02	*IQR*	9.67E+02
Mode	#N/A	*MAD*	4.71E+02
Minimum elevation (m asl)			
Count	3.01E+03	*Skewness*	5.21E-01
Mean	9.68E+02	*Skewness Standard Error*	4.46E-02
Mean LCL	9.46E+02	*Kurtosis*	2.77E+00
Mean UCL	9.91E+02	*Kurtosis Standard Error*	8.92E-02
Variance	2.80E+05	*Alternative Skewness (Fisher's)*	5.21E-01
Standard Deviation	5.29E+02	*Alternative Kurtosis (Fisher's)*	-2.31E-01
Mean Standard Error	9.66E+00	*Coefficient of Variation*	5.47E-01
Minimum	4.00E-02	*Mean Deviation*	4.25E+02
Maximum	2.46E+03	*Second Moment*	2.80E+05
Range	2.46E+03	*Third Moment*	7.72E+07
Sum	2.91E+06	*Fourth Moment*	2.17E+11
Sum Standard Error	2.90E+04	*Median*	8.89E+02
Total Sum Squares	3.66E+09	*Median Error*	2.21E-01
Adjusted Sum Squares	8.42E+08	*Percentile 25% (Q1)*	5.98E+02
Geometric Mean	7.68E+02	*Percentile 75% (Q2)*	1.29E+03
Harmonic Mean	7.67E+01	*IQR*	6.95E+02
Mode	4.34E+02	*MAD*	3.37E+02

Melton ratio (-)

Count	3.01E+03	*Skewness*	5.80E-01
Mean	4.70E-01	*Skewness Standard Error*	4.46E-02
Mean LCL	4.60E-01	*Kurtosis*	3.24E+00
Mean UCL	4.80E-01	*Kurtosis Standard Error*	8.92E-02
Variance	5.85E-02	*Alternative Skewness (Fisher's)*	5.80E-01
Standard Deviation	2.42E-01	*Alternative Kurtosis (Fisher's)*	2.46E-01
Mean Standard Error	4.41E-03	*Coefficient of Variation*	5.15E-01
Minimum	3.63E-03	*Mean Deviation*	1.92E-01
Maximum	1.52E+00	*Second Moment*	5.85E-02
Range	1.51E+00	*Third Moment*	8.20E-03
Sum	1.41E+03	*Fourth Moment*	1.11E-02
Sum Standard Error	1.33E+01	*Median*	4.46E-01
Total Sum Squares	8.40E+02	*Median Error*	1.01E-04
Adjusted Sum Squares	1.76E+02	*Percentile 25% (Q1)*	2.94E-01
Geometric Mean	3.97E-01	*Percentile 75% (Q2)*	6.17E-01
Harmonic Mean	2.85E-01	*IQR*	3.23E-01
Mode	#N/A	*MAD*	1.59E-01

Mean slope (°)

Count	3.01E+03	*Skewness*	-4.11E-01
Mean	2.21E+01	*Skewness Standard Error*	4.46E-02
Mean LCL	2.18E+01	*Kurtosis*	3.01E+00
Mean UCL	2.24E+01	*Kurtosis Standard Error*	8.92E-02
Variance	5.42E+01	*Alternative Skewness (Fisher's)*	-4.11E-01
Standard Deviation	7.36E+00	*Alternative Kurtosis (Fisher's)*	1.12E-02
Mean Standard Error	1.34E-01	*Coefficient of Variation*	3.33E-01
Minimum	3.63E-01	*Mean Deviation*	5.79E+00
Maximum	4.31E+01	*Second Moment*	5.42E+01
Range	4.28E+01	*Third Moment*	-1.64E+02
Sum	6.64E+04	*Fourth Moment*	8.84E+03
Sum Standard Error	4.04E+02	*Median*	2.28E+01
Total Sum Squares	1.63E+06	*Median Error*	3.07E-03
Adjusted Sum Squares	1.63E+05	*Percentile 25% (Q1)*	1.79E+01
Geometric Mean	2.04E+01	*Percentile 75% (Q2)*	2.71E+01
Harmonic Mean	1.68E+01	*IQR*	9.14E+00
Mode	#N/A	*MAD*	4.58E+00

Mean orientation (0-360)

Count	3.01E+03	*Skewness*	1.53E-02
Mean	1.78E+02	*Skewness Standard Error*	4.46E-02
Mean LCL	1.76E+02	*Kurtosis*	2.51E+00
Mean UCL	1.80E+02	*Kurtosis Standard Error*	8.92E-02
Variance	1.95E+03	*Alternative Skewness (Fisher's)*	1.53E-02
Standard Deviation	4.41E+01	*Alternative Kurtosis (Fisher's)*	-4.87E-01
Mean Standard Error	8.05E-01	*Coefficient of Variation*	2.48E-01
Minimum	5.67E+01	*Mean Deviation*	3.62E+01
Maximum	2.98E+02	*Second Moment*	1.95E+03
Range	2.41E+02	*Third Moment*	1.32E+03
Sum	5.36E+05	*Fourth Moment*	9.53E+06
Sum Standard Error	2.42E+03	*Median*	1.78E+02
Total Sum Squares	1.01E+08	*Median Error*	1.84E-02
Adjusted Sum Squares	5.85E+06	*Percentile 25% (Q1)*	1.46E+02
Geometric Mean	1.72E+02	*Percentile 75% (Q2)*	2.10E+02
Harmonic Mean	1.66E+02	*IQR*	6.42E+01
Mode	#N/A	*MAD*	3.21E+01

Area (km2)

Count	3.01E+03	*Skewness*	2.59E+00
Mean	2.28E+00	*Skewness Standard Error*	4.46E-02
Mean LCL	2.22E+00	*Kurtosis*	1.32E+01
Mean UCL	2.35E+00	*Kurtosis Standard Error*	8.92E-02
Variance	2.18E+00	*Alternative Skewness (Fisher's)*	2.59E+00
Standard Deviation	1.48E+00	*Alternative Kurtosis (Fisher's)*	1.02E+01
Mean Standard Error	2.69E-02	*Coefficient of Variation*	6.47E-01
Minimum	1.00E+00	*Mean Deviation*	1.03E+00
Maximum	1.59E+01	*Second Moment*	2.18E+00
Range	1.49E+01	*Third Moment*	8.34E+00
Sum	6.86E+03	*Fourth Moment*	6.28E+01
Sum Standard Error	8.10E+01	*Median*	1.80E+00
Total Sum Squares	2.22E+04	*Median Error*	6.16E-04
Adjusted Sum Squares	6.55E+03	*Percentile 25% (Q1)*	1.31E+00
Geometric Mean	1.97E+00	*Percentile 75% (Q2)*	2.70E+00
Harmonic Mean	1.77E+00	*IQR*	1.40E+00
Mode	1.10E+00	*MAD*	5.97E-01

Stream length (km)

Count	3.01E+03	*Skewness*	2.23E+00
Mean	1.44E+00	*Skewness Standard Error*	4.46E-02
Mean LCL	1.39E+00	*Kurtosis*	1.13E+01
Mean UCL	1.50E+00	*Kurtosis Standard Error*	8.92E-02
Variance	1.73E+00	*Alternative Skewness (Fisher's)*	2.23E+00
Standard Deviation	1.32E+00	*Alternative Kurtosis (Fisher's)*	8.36E+00
Mean Standard Error	2.40E-02	*Coefficient of Variation*	9.11E-01
Minimum	5.00E-03	*Mean Deviation*	9.42E-01
Maximum	1.41E+01	*Second Moment*	1.73E+00
Range	1.41E+01	*Third Moment*	5.07E+00
Sum	4.34E+03	*Fourth Moment*	3.40E+01
Sum Standard Error	7.21E+01	*Median*	1.10E+00
Total Sum Squares	1.15E+04	*Median Error*	5.49E-04
Adjusted Sum Squares	5.20E+03	*Percentile 25% (Q1)*	5.33E-01
Geometric Mean	9.44E-01	*Percentile 75% (Q2)*	1.94E+00
Harmonic Mean	4.19E-01	*IQR*	1.40E+00
Mode	#N/A	*MAD*	6.45E-01

Perimeter (m)

Count	3.01E+03	*Skewness*	2.14E+00
Mean	9.33E+03	*Skewness Standard Error*	4.46E-02
Mean LCL	9.19E+03	*Kurtosis*	1.10E+01
Mean UCL	9.47E+03	*Kurtosis Standard Error*	8.92E-02
Variance	1.02E+07	*Alternative Skewness (Fisher's)*	2.14E+00
Standard Deviation	3.19E+03	*Alternative Kurtosis (Fisher's)*	7.97E+00
Mean Standard Error	5.83E+01	*Coefficient of Variation*	3.42E-01
Minimum	4.96E+03	*Mean Deviation*	2.30E+03
Maximum	3.77E+04	*Second Moment*	1.02E+07
Range	3.27E+04	*Third Moment*	6.97E+10
Sum	2.80E+07	*Fourth Moment*	1.14E+15
Sum Standard Error	1.75E+05	*Median*	8.56E+03
Total Sum Squares	2.92E+11	*Median Error*	1.33E+00
Adjusted Sum Squares	3.06E+10	*Percentile 25% (Q1)*	7.16E+03
Geometric Mean	8.90E+03	*Percentile 75% (Q2)*	1.06E+04
Harmonic Mean	8.56E+03	*IQR*	3.44E+03
Mode	7.20E+03	*MAD*	1.56E+03

Form factor (-)

Count	3.01E+03	*Skewness*	4.21E-01
Mean	3.84E-01	*Skewness Standard Error*	4.46E-02
Mean LCL	3.79E-01	*Kurtosis*	2.60E+00
Mean UCL	3.90E-01	*Kurtosis Standard Error*	8.92E-02
Variance	1.81E-02	*Alternative Skewness (Fisher's)*	4.21E-01
Standard Deviation	1.34E-01	*Alternative Kurtosis (Fisher's)*	-4.01E-01
Mean Standard Error	2.45E-03	*Coefficient of Variation*	3.50E-01
Minimum	8.97E-02	*Mean Deviation*	1.10E-01
Maximum	7.75E-01	*Second Moment*	1.80E-02
Range	6.85E-01	*Third Moment*	1.02E-03
Sum	1.15E+03	*Fourth Moment*	8.46E-04
Sum Standard Error	7.37E+00	*Median*	3.67E-01
Total Sum Squares	4.98E+02	*Median Error*	5.60E-05
Adjusted Sum Squares	5.42E+01	*Percentile 25% (Q1)*	2.85E-01
Geometric Mean	3.60E-01	*Percentile 75% (Q2)*	4.77E-01
Harmonic Mean	3.35E-01	*IQR*	1.93E-01
Mode	#N/A	*MAD*	9.39E-02

Basin Elongation (-)

Count	3.01E+03	*Skewness*	3.53E-02
Mean	6.89E-01	*Skewness Standard Error*	4.46E-02
Mean LCL	6.83E-01	*Kurtosis*	2.48E+00
Mean UCL	6.94E-01	*Kurtosis Standard Error*	8.92E-02
Variance	1.52E-02	*Alternative Skewness (Fisher's)*	3.54E-02
Standard Deviation	1.23E-01	*Alternative Kurtosis (Fisher's)*	-5.23E-01
Mean Standard Error	2.25E-03	*Coefficient of Variation*	1.79E-01
Minimum	3.38E-01	*Mean Deviation*	1.01E-01
Maximum	9.93E-01	*Second Moment*	1.52E-02
Range	6.55E-01	*Third Moment*	6.59E-05
Sum	2.07E+03	*Fourth Moment*	5.68E-04
Sum Standard Error	6.75E+00	*Median*	6.84E-01
Total Sum Squares	1.47E+03	*Median Error*	5.13E-05
Adjusted Sum Squares	4.55E+01	*Percentile 25% (Q1)*	6.02E-01
Geometric Mean	6.77E-01	*Percentile 75% (Q2)*	7.80E-01
Harmonic Mean	6.66E-01	*IQR*	1.78E-01
Mode	#N/A	*MAD*	8.86E-02

Lemniscate ratio (-)

Count	3.01E+03	*Skewness*	1.57E+00
Mean	2.34E+00	*Skewness Standard Error*	4.46E-02
Mean LCL	2.30E+00	*Kurtosis*	6.90E+00
Mean UCL	2.38E+00	*Kurtosis Standard Error*	8.92E-02
Variance	9.13E-01	*Alternative Skewness (Fisher's)*	1.57E+00
Standard Deviation	9.56E-01	*Alternative Kurtosis (Fisher's)*	3.90E+00
Mean Standard Error	1.74E-02	*Coefficient of Variation*	4.08E-01
Minimum	1.01E+00	*Mean Deviation*	7.17E-01
Maximum	8.76E+00	*Second Moment*	9.13E-01
Range	7.74E+00	*Third Moment*	1.37E+00
Sum	7.04E+03	*Fourth Moment*	5.75E+00
Sum Standard Error	5.24E+01	*Median*	2.14E+00
Total Sum Squares	1.92E+04	*Median Error*	3.99E-04
Adjusted Sum Squares	2.74E+03	*Percentile 25% (Q1)*	1.65E+00
Geometric Mean	2.18E+00	*Percentile 75% (Q2)*	2.76E+00
Harmonic Mean	2.04E+00	*IQR*	1.11E+00
Mode	#N/A	*MAD*	5.42E-01

Outlet slope (°)

Count	3.01E+03	*Skewness*	1.58E+00
Mean	6.98E+00	*Skewness Standard Error*	4.46E-02
Mean LCL	6.71E+00	*Kurtosis*	6.60E+00
Mean UCL	7.26E+00	*Kurtosis Standard Error*	8.92E-02
Variance	4.17E+01	*Alternative Skewness (Fisher's)*	1.59E+00
Standard Deviation	6.46E+00	*Alternative Kurtosis (Fisher's)*	3.61E+00
Mean Standard Error	1.18E-01	*Coefficient of Variation*	9.25E-01
Minimum	0.00E+00	*Mean Deviation*	4.95E+00
Maximum	4.82E+01	*Second Moment*	4.17E+01
Range	4.82E+01	*Third Moment*	4.27E+02
Sum	2.10E+04	*Fourth Moment*	1.15E+04
Sum Standard Error	3.54E+02	*Median*	5.12E+00
Total Sum Squares	2.72E+05	*Median Error*	2.69E-03
Adjusted Sum Squares	1.25E+05	*Percentile 25% (Q1)*	2.22E+00
Geometric Mean	4.34E+00	*Percentile 75% (Q2)*	1.01E+01
Harmonic Mean	1.46E+00	*IQR*	7.92E+00
Mode	0.00E+00	*MAD*	3.53E+00

200m slope (°)

Count	3.01E+03	*Skewness*	1.42E+00
Mean	7.11E+00	*Skewness Standard Error*	4.46E-02
Mean LCL	6.84E+00	*Kurtosis*	5.48E+00
Mean UCL	7.39E+00	*Kurtosis Standard Error*	8.92E-02
Variance	4.12E+01	*Alternative Skewness (Fisher's)*	1.42E+00
Standard Deviation	6.42E+00	*Alternative Kurtosis (Fisher's)*	2.49E+00
Mean Standard Error	1.17E-01	*Coefficient of Variation*	9.03E-01
Minimum	0.00E+00	*Mean Deviation*	5.00E+00
Maximum	4.40E+01	*Second Moment*	4.12E+01
Range	4.40E+01	*Third Moment*	3.77E+02
Sum	2.14E+04	*Fourth Moment*	9.31E+03
Sum Standard Error	3.52E+02	*Median*	5.19E+00
Total Sum Squares	2.76E+05	*Median Error*	2.68E-03
Adjusted Sum Squares	1.24E+05	*Percentile 25% (Q1)*	2.32E+00
Geometric Mean	4.45E+00	*Percentile 75% (Q2)*	1.03E+01
Harmonic Mean	1.58E+00	*IQR*	8.01E+00
Mode	0.00E+00	*MAD*	3.56E+00

Average slope (°)

Count	3.01E+03	*Skewness*	9.55E-01
Mean	8.03E+00	*Skewness Standard Error*	4.46E-02
Mean LCL	7.76E+00	*Kurtosis*	3.62E+00
Mean UCL	8.29E+00	*Kurtosis Standard Error*	8.92E-02
Variance	3.90E+01	*Alternative Skewness (Fisher's)*	9.56E-01
Standard Deviation	6.25E+00	*Alternative Kurtosis (Fisher's)*	6.23E-01
Mean Standard Error	1.14E-01	*Coefficient of Variation*	7.78E-01
Minimum	0.00E+00	*Mean Deviation*	5.07E+00
Maximum	4.12E+01	*Second Moment*	3.90E+01
Range	4.12E+01	*Third Moment*	2.33E+02
Sum	2.41E+04	*Fourth Moment*	5.51E+03
Sum Standard Error	3.42E+02	*Median*	6.65E+00
Total Sum Squares	3.11E+05	*Median Error*	2.61E-03
Adjusted Sum Squares	1.17E+05	*Percentile 25% (Q1)*	3.01E+00
Geometric Mean	5.37E+00	*Percentile 75% (Q2)*	1.19E+01
Harmonic Mean	2.24E+00	*IQR*	8.85E+00
Mode	0.00E+00	*MAD*	4.13E+00

2nd-order catchments.

Max. elevation (m asl)			
Count	*6.55E+02*	*Skewness*	-1.17E-01
Mean	*1.79E+03*	*Skewness Standard Error*	9.53E-02
Mean LCL	*1.72E+03*	*Kurtosis*	2.03E+00
Mean UCL	*1.86E+03*	*Kurtosis Standard Error*	1.90E-01
Variance	5.45E+05	*Alternative Skewness (Fisher's)*	-1.17E-01
Standard Deviation	7.38E+02	*Alternative Kurtosis (Fisher's)*	-9.72E-01
Mean Standard Error	2.88E+01	*Coefficient of Variation*	4.13E-01
Minimum	1.22E+02	*Mean Deviation*	6.33E+02
Maximum	3.07E+03	*Second Moment*	5.44E+05
Range	2.95E+03	*Third Moment*	-4.70E+07
Sum	1.17E+06	*Fourth Moment*	6.00E+11
Sum Standard Error	1.89E+04	*Median*	1.76E+03
Total Sum Squares	2.45E+09	*Median Error*	1.41E+00
Adjusted Sum Squares	3.56E+08	*Percentile 25% (Q1)*	1.19E+03
Geometric Mean	1.59E+03	*Percentile 75% (Q2)*	2.45E+03
Harmonic Mean	1.28E+03	*IQR*	1.26E+03
Mode	9.91E+02	*MAD*	6.14E+02
Mean elevation (m asl)			
Count	6.55E+02	*Skewness*	1.44E-01
Mean	1.30E+03	*Skewness Standard Error*	9.53E-02
Mean LCL	1.24E+03	*Kurtosis*	2.15E+00
Mean UCL	1.36E+03	*Kurtosis Standard Error*	1.90E-01
Variance	3.77E+05	*Alternative Skewness (Fisher's)*	1.44E-01
Standard Deviation	6.14E+02	*Alternative Kurtosis (Fisher's)*	-8.50E-01
Mean Standard Error	2.40E+01	*Coefficient of Variation*	4.73E-01
Minimum	3.16E+01	*Mean Deviation*	5.19E+02
Maximum	2.50E+03	*Second Moment*	3.77E+05
Range	2.47E+03	*Third Moment*	3.32E+07
Sum	8.51E+05	*Fourth Moment*	3.05E+11
Sum Standard Error	1.57E+04	*Median*	1.24E+03
Total Sum Squares	1.35E+09	*Median Error*	1.18E+00
Adjusted Sum Squares	2.47E+08	*Percentile 25% (Q1)*	8.25E+02
Geometric Mean	1.11E+03	*Percentile 75% (Q2)*	1.76E+03
Harmonic Mean	7.94E+02	*IQR*	9.36E+02
Mode	#N/A	*MAD*	4.49E+02
Min. elevation (m asl)			
Count	6.55E+02	*Skewness*	5.45E-01
Mean	8.53E+02	*Skewness Standard Error*	9.53E-02
Mean LCL	8.12E+02	*Kurtosis*	2.85E+00
Mean UCL	8.95E+02	*Kurtosis Standard Error*	1.90E-01
Variance	2.09E+05	*Alternative Skewness (Fisher's)*	5.46E-01
Standard Deviation	4.57E+02	*Alternative Kurtosis (Fisher's)*	-1.40E-01
Mean Standard Error	1.79E+01	*Coefficient of Variation*	5.36E-01
Minimum	0.00E+00	*Mean Deviation*	3.68E+02
Maximum	2.13E+03	*Second Moment*	2.09E+05
Range	2.13E+03	*Third Moment*	5.19E+07
Sum	5.59E+05	*Fourth Moment*	1.24E+11
Sum Standard Error	1.17E+04	*Median*	7.86E+02
Total Sum Squares	6.14E+08	*Median Error*	8.75E-01
Adjusted Sum Squares	1.37E+08	*Percentile 25% (Q1)*	5.26E+02
Geometric Mean	6.89E+02	*Percentile 75% (Q2)*	1.11E+03
Harmonic Mean	3.81E+02	*IQR*	5.85E+02
Mode	#N/A	*MAD*	2.80E+02

Melton ratio (-)

Count	6.55E+02	*Skewness*	4.91E-01
Mean	3.21E-01	*Skewness Standard Error*	9.53E-02
Mean LCL	3.08E-01	*Kurtosis*	3.19E+00
Mean UCL	3.35E-01	*Kurtosis Standard Error*	1.90E-01
Variance	2.21E-02	*Alternative Skewness (Fisher's)*	4.92E-01
Standard Deviation	1.49E-01	*Alternative Kurtosis (Fisher's)*	1.98E-01
Mean Standard Error	5.81E-03	*Coefficient of Variation*	4.63E-01
Minimum	3.60E-02	*Mean Deviation*	1.19E-01
Maximum	9.92E-01	*Second Moment*	2.21E-02
Range	9.56E-01	*Third Moment*	1.61E-03
Sum	2.10E+02	*Fourth Moment*	1.56E-03
Sum Standard Error	3.81E+00	*Median*	3.09E-01
Total Sum Squares	8.20E+01	*Median Error*	2.85E-04
Adjusted Sum Squares	1.45E+01	*Percentile 25% (Q1)*	2.12E-01
Geometric Mean	2.82E-01	*Percentile 75% (Q2)*	4.12E-01
Harmonic Mean	2.34E-01	*IQR*	2.01E-01
Mode	#N/A	*MAD*	9.84E-02

Mean slope (°)

Count	6.55E+02	*Skewness*	-4.96E-01
Mean	2.23E+01	*Skewness Standard Error*	9.53E-02
Mean LCL	2.17E+01	*Kurtosis*	3.12E+00
Mean UCL	2.29E+01	*Kurtosis Standard Error*	1.90E-01
Variance	4.23E+01	*Alternative Skewness (Fisher's)*	-4.97E-01
Standard Deviation	6.50E+00	*Alternative Kurtosis (Fisher's)*	1.31E-01
Mean Standard Error	2.54E-01	*Coefficient of Variation*	2.92E-01
Minimum	2.30E+00	*Mean Deviation*	5.11E+00
Maximum	3.89E+01	*Second Moment*	4.22E+01
Range	3.66E+01	*Third Moment*	-1.36E+02
Sum	1.46E+04	*Fourth Moment*	5.56E+03
Sum Standard Error	1.66E+02	*Median*	2.31E+01
Total Sum Squares	3.52E+05	*Median Error*	1.24E-02
Adjusted Sum Squares	2.76E+04	*Percentile 25% (Q1)*	1.85E+01
Geometric Mean	2.10E+01	*Percentile 75% (Q2)*	2.66E+01
Harmonic Mean	1.92E+01	*IQR*	8.07E+00
Mode	#N/A	*MAD*	4.03E+00

Mean orientation (0-360)

Count	6.55E+02	*Skewness*	1.60E-01
Mean	1.78E+02	*Skewness Standard Error*	9.53E-02
Mean LCL	1.75E+02	*Kurtosis*	2.70E+00
Mean UCL	1.81E+02	*Kurtosis Standard Error*	1.90E-01
Variance	9.94E+02	*Alternative Skewness (Fisher's)*	1.60E-01
Standard Deviation	3.15E+01	*Alternative Kurtosis (Fisher's)*	-2.97E-01
Mean Standard Error	1.23E+00	*Coefficient of Variation*	1.77E-01
Minimum	1.01E+02	*Mean Deviation*	2.58E+01
Maximum	2.76E+02	*Second Moment*	9.92E+02
Range	1.75E+02	*Third Moment*	4.99E+03
Sum	1.17E+05	*Fourth Moment*	2.65E+06
Sum Standard Error	8.07E+02	*Median*	1.77E+02
Total Sum Squares	2.14E+07	*Median Error*	6.03E-02
Adjusted Sum Squares	6.50E+05	*Percentile 25% (Q1)*	1.55E+02
Geometric Mean	1.75E+02	*Percentile 75% (Q2)*	2.01E+02
Harmonic Mean	1.72E+02	*IQR*	4.64E+01
Mode	#N/A	*MAD*	2.35E+01

Area (km2)

Count	6.55E+02	*Skewness*	2.05E+00
Mean	1.04E+01	*Skewness Standard Error*	9.53E-02
Mean LCL	9.70E+00	*Kurtosis*	8.51E+00
Mean UCL	1.10E+01	*Kurtosis Standard Error*	1.90E-01
Variance	5.28E+01	*Alternative Skewness (Fisher's)*	2.06E+00
Standard Deviation	7.27E+00	*Alternative Kurtosis (Fisher's)*	5.56E+00
Mean Standard Error	2.84E-01	*Coefficient of Variation*	7.01E-01
Minimum	2.20E+00	*Mean Deviation*	5.19E+00
Maximum	4.68E+01	*Second Moment*	5.28E+01
Range	4.46E+01	*Third Moment*	7.87E+02
Sum	6.79E+03	*Fourth Moment*	2.37E+04
Sum Standard Error	1.86E+02	*Median*	8.36E+00
Total Sum Squares	1.05E+05	*Median Error*	1.39E-02
Adjusted Sum Squares	3.46E+04	*Percentile 25% (Q1)*	5.42E+00
Geometric Mean	8.54E+00	*Percentile 75% (Q2)*	1.27E+01
Harmonic Mean	7.17E+00	*IQR*	7.28E+00
Mode	#N/A	*MAD*	3.35E+00

Stream length (km)

Count	6.55E+02	*Skewness*	1.88E+00
Mean	7.60E+00	*Skewness Standard Error*	9.53E-02
Mean LCL	7.10E+00	*Kurtosis*	7.66E+00
Mean UCL	8.10E+00	*Kurtosis Standard Error*	1.90E-01
Variance	2.99E+01	*Alternative Skewness (Fisher's)*	1.89E+00
Standard Deviation	5.47E+00	*Alternative Kurtosis (Fisher's)*	4.71E+00
Mean Standard Error	2.14E-01	*Coefficient of Variation*	7.20E-01
Minimum	7.10E-01	*Mean Deviation*	3.97E+00
Maximum	3.81E+01	*Second Moment*	2.99E+01
Range	3.74E+01	*Third Moment*	3.07E+02
Sum	4.98E+03	*Fourth Moment*	6.84E+03
Sum Standard Error	1.40E+02	*Median*	6.19E+00
Total Sum Squares	5.74E+04	*Median Error*	1.05E-02
Adjusted Sum Squares	1.96E+04	*Percentile 25% (Q1)*	3.89E+00
Geometric Mean	6.08E+00	*Percentile 75% (Q2)*	9.46E+00
Harmonic Mean	4.83E+00	*IQR*	5.58E+00
Mode	#N/A	*MAD*	2.62E+00

Perimeter (m)

Count	6.55E+02	*Skewness*	1.27E+00
Mean	1.99E+04	*Skewness Standard Error*	9.53E-02
Mean LCL	1.92E+04	*Kurtosis*	5.06E+00
Mean UCL	2.06E+04	*Kurtosis Standard Error*	1.90E-01
Variance	5.87E+07	*Alternative Skewness (Fisher's)*	1.27E+00
Standard Deviation	7.66E+03	*Alternative Kurtosis (Fisher's)*	2.08E+00
Mean Standard Error	2.99E+02	*Coefficient of Variation*	3.85E-01
Minimum	8.64E+03	*Mean Deviation*	5.91E+03
Maximum	5.49E+04	*Second Moment*	5.86E+07
Range	4.63E+04	*Third Moment*	5.71E+11
Sum	1.30E+07	*Fourth Moment*	1.74E+16
Sum Standard Error	1.96E+05	*Median*	1.81E+04
Total Sum Squares	2.98E+11	*Median Error*	1.47E+01
Adjusted Sum Squares	3.84E+10	*Percentile 25% (Q1)*	1.44E+04
Geometric Mean	1.86E+04	*Percentile 75% (Q2)*	2.38E+04
Harmonic Mean	1.75E+04	*IQR*	9.36E+03
Mode	#N/A	*MAD*	4.32E+03

Form factor (-)

Count	6.55E+02	*Skewness*	1.59E-01
Mean	4.26E-01	*Skewness Standard Error*	9.53E-02
Mean LCL	4.13E-01	*Kurtosis*	2.29E+00
Mean UCL	4.38E-01	*Kurtosis Standard Error*	1.90E-01
Variance	1.84E-02	*Alternative Skewness (Fisher's)*	1.60E-01
Standard Deviation	1.36E-01	*Alternative Kurtosis (Fisher's)*	-7.03E-01
Mean Standard Error	5.30E-03	*Coefficient of Variation*	3.19E-01
Minimum	1.24E-01	*Mean Deviation*	1.12E-01
Maximum	7.48E-01	*Second Moment*	1.84E-02
Range	6.24E-01	*Third Moment*	3.97E-04
Sum	2.79E+02	*Fourth Moment*	7.77E-04
Sum Standard Error	3.47E+00	*Median*	4.20E-01
Total Sum Squares	1.31E+02	*Median Error*	2.60E-04
Adjusted Sum Squares	1.21E+01	*Percentile 25% (Q1)*	3.21E-01
Geometric Mean	4.02E-01	*Percentile 75% (Q2)*	5.27E-01
Harmonic Mean	3.78E-01	*IQR*	2.06E-01
Mode	#N/A	*MAD*	1.02E-01

Basin Elongation (-)

Count	6.55E+02	*Skewness*	-1.73E-01
Mean	7.26E-01	*Skewness Standard Error*	9.53E-02
Mean LCL	7.15E-01	*Kurtosis*	2.39E+00
Mean UCL	7.37E-01	*Kurtosis Standard Error*	1.90E-01
Variance	1.44E-02	*Alternative Skewness (Fisher's)*	-1.73E-01
Standard Deviation	1.20E-01	*Alternative Kurtosis (Fisher's)*	-6.09E-01
Mean Standard Error	4.69E-03	*Coefficient of Variation*	1.65E-01
Minimum	3.97E-01	*Mean Deviation*	9.91E-02
Maximum	9.76E-01	*Second Moment*	1.44E-02
Range	5.79E-01	*Third Moment*	-2.99E-04
Sum	4.76E+02	*Fourth Moment*	4.96E-04
Sum Standard Error	3.08E+00	*Median*	7.31E-01
Total Sum Squares	3.55E+02	*Median Error*	2.30E-04
Adjusted Sum Squares	9.44E+00	*Percentile 25% (Q1)*	6.39E-01
Geometric Mean	7.16E-01	*Percentile 75% (Q2)*	8.19E-01
Harmonic Mean	7.05E-01	*IQR*	1.80E-01
Mode	#N/A	*MAD*	9.04E-02

Lemniscate ratio (-)

Count	6.55E+02	*Skewness*	1.54E+00
Mean	2.08E+00	*Skewness Standard Error*	9.53E-02
Mean LCL	2.01E+00	*Kurtosis*	6.15E+00
Mean UCL	2.15E+00	*Kurtosis Standard Error*	1.90E-01
Variance	6.48E-01	*Alternative Skewness (Fisher's)*	1.54E+00
Standard Deviation	8.05E-01	*Alternative Kurtosis (Fisher's)*	3.18E+00
Mean Standard Error	3.15E-02	*Coefficient of Variation*	3.87E-01
Minimum	1.05E+00	*Mean Deviation*	6.11E-01
Maximum	6.33E+00	*Second Moment*	6.47E-01
Range	5.28E+00	*Third Moment*	8.01E-01
Sum	1.36E+03	*Fourth Moment*	2.57E+00
Sum Standard Error	2.06E+01	*Median*	1.87E+00
Total Sum Squares	3.25E+03	*Median Error*	1.54E-03
Adjusted Sum Squares	4.24E+02	*Percentile 25% (Q1)*	1.49E+00
Geometric Mean	1.95E+00	*Percentile 75% (Q2)*	2.45E+00
Harmonic Mean	1.85E+00	*IQR*	9.55E-01
Mode	#N/A	*MAD*	4.54E-01

Outlet slope (°)			
Count	6.55E+02	*Skewness*	1.16E+00
Mean	6.49E+00	*Skewness Standard Error*	9.53E-02
Mean LCL	5.96E+00	*Kurtosis*	4.03E+00
Mean UCL	7.01E+00	*Kurtosis Standard Error*	1.90E-01
Variance	3.31E+01	*Alternative Skewness (Fisher's)*	1.17E+00
Standard Deviation	5.75E+00	*Alternative Kurtosis (Fisher's)*	1.05E+00
Mean Standard Error	2.25E-01	*Coefficient of Variation*	8.87E-01
Minimum	0.00E+00	*Mean Deviation*	4.59E+00
Maximum	3.36E+01	*Second Moment*	3.31E+01
Range	3.36E+01	*Third Moment*	2.21E+02
Sum	4.25E+03	*Fourth Moment*	4.41E+03
Sum Standard Error	1.47E+02	*Median*	4.91E+00
Total Sum Squares	4.92E+04	*Median Error*	1.10E-02
Adjusted Sum Squares	2.17E+04	*Percentile 25% (Q1)*	2.07E+00
Geometric Mean	3.96E+00	*Percentile 75% (Q2)*	9.65E+00
Harmonic Mean	1.19E+00	*IQR*	7.58E+00
Mode	0.00E+00	*MAD*	3.38E+00

200m slope (°)			
Count	6.55E+02	*Skewness*	1.28E+00
Mean	6.50E+00	*Skewness Standard Error*	9.53E-02
Mean LCL	5.97E+00	*Kurtosis*	4.63E+00
Mean UCL	7.03E+00	*Kurtosis Standard Error*	1.90E-01
Variance	3.36E+01	*Alternative Skewness (Fisher's)*	1.28E+00
Standard Deviation	5.80E+00	*Alternative Kurtosis (Fisher's)*	1.65E+00
Mean Standard Error	2.27E-01	*Coefficient of Variation*	8.92E-01
Minimum	0.00E+00	*Mean Deviation*	4.57E+00
Maximum	3.41E+01	*Second Moment*	3.36E+01
Range	3.41E+01	*Third Moment*	2.49E+02
Sum	4.26E+03	*Fourth Moment*	5.22E+03
Sum Standard Error	1.48E+02	*Median*	4.85E+00
Total Sum Squares	4.97E+04	*Median Error*	1.11E-02
Adjusted Sum Squares	2.20E+04	*Percentile 25% (Q1)*	2.14E+00
Geometric Mean	3.99E+00	*Percentile 75% (Q2)*	9.48E+00
Harmonic Mean	1.02E+00	*IQR*	7.34E+00
Mode	0.00E+00	*MAD*	3.23E+00

Average slope (°)			
Count	6.55E+02	*Skewness*	9.72E-01
Mean	7.31E+00	*Skewness Standard Error*	9.53E-02
Mean LCL	6.80E+00	*Kurtosis*	3.51E+00
Mean UCL	7.82E+00	*Kurtosis Standard Error*	1.90E-01
Variance	3.17E+01	*Alternative Skewness (Fisher's)*	9.74E-01
Standard Deviation	5.63E+00	*Alternative Kurtosis (Fisher's)*	5.27E-01
Mean Standard Error	2.20E-01	*Coefficient of Variation*	7.71E-01
Minimum	0.00E+00	*Mean Deviation*	4.54E+00
Maximum	2.81E+01	*Second Moment*	3.17E+01
Range	2.81E+01	*Third Moment*	1.73E+02
Sum	4.79E+03	*Fourth Moment*	3.53E+03
Sum Standard Error	1.44E+02	*Median*	5.96E+00
Total Sum Squares	5.58E+04	*Median Error*	1.08E-02
Adjusted Sum Squares	2.07E+04	*Percentile 25% (Q1)*	2.93E+00
Geometric Mean	4.96E+00	*Percentile 75% (Q2)*	1.07E+01
Harmonic Mean	1.63E+00	*IQR*	7.76E+00
Mode	0.00E+00	*MAD*	3.64E+00

Appendix 3: Bi-dimensional relationships for the 655 2nd-order catchments in the study area.

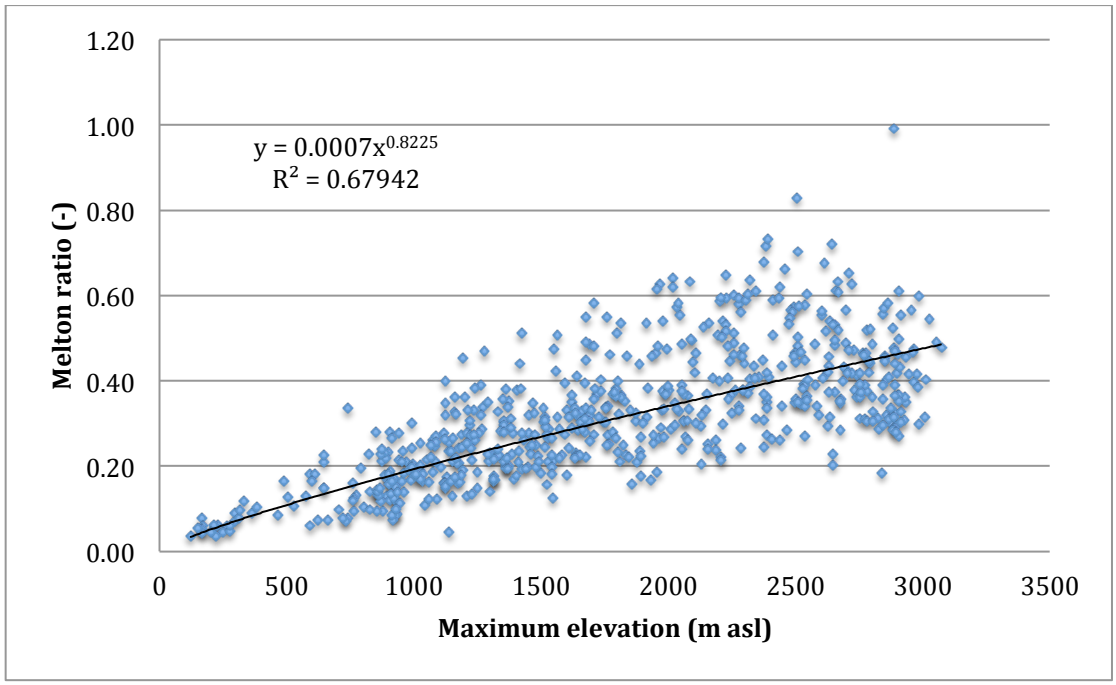
y = 0.0007x^0.8225
R² = 0.67942
Melton ratio (-)
Maximum elevation (m asl)
0.00
0.20
0.40
0.60
0.80
1.00
1.20
0
500
1000
1500
2000
2500
3000
3500

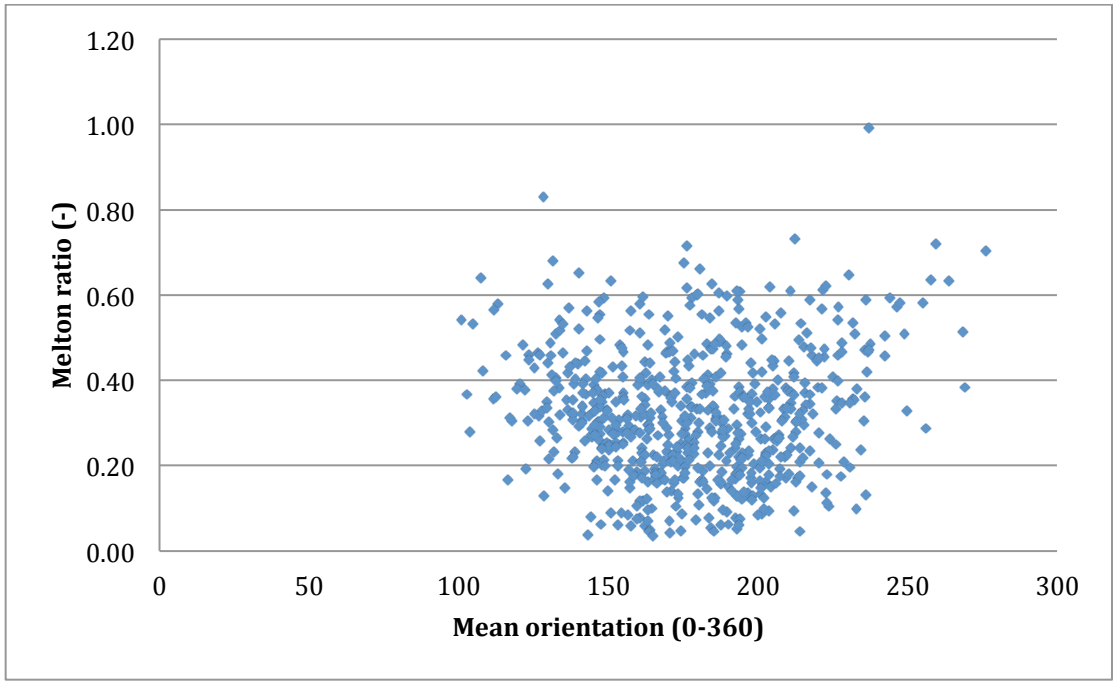
Melton ratio (-)
Mean orientation (0-360)
0.00
0.20
0.40
0.60
0.80
1.00
1.20
0
50
100
150
200
250
300

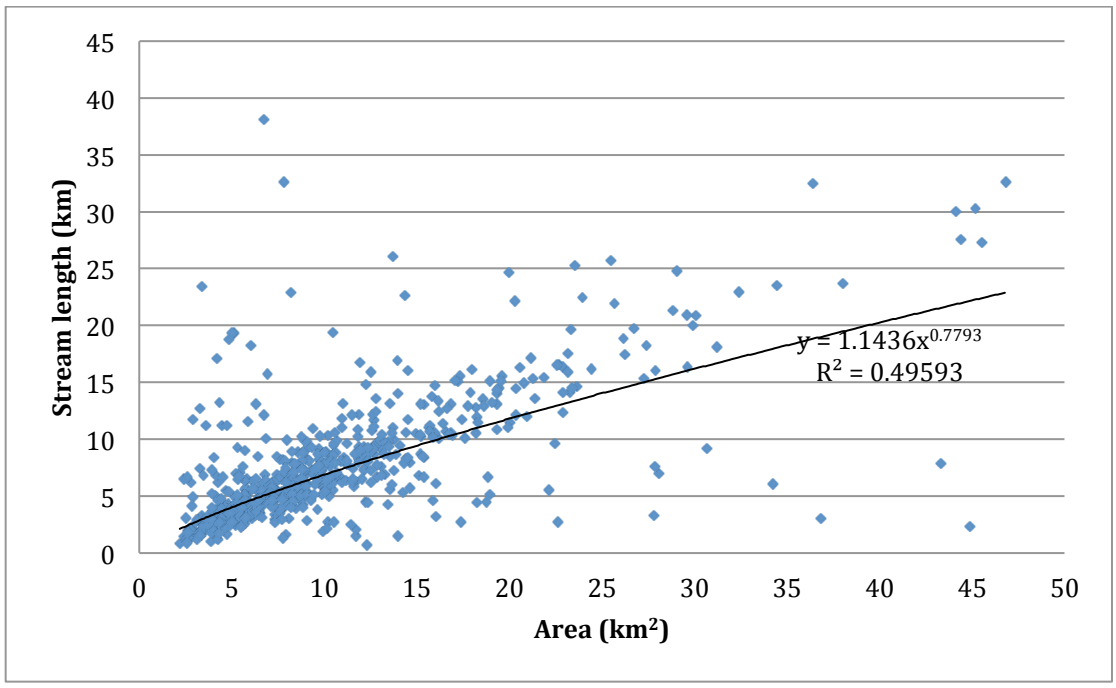
Stream length (km)
Area (km²)
y = 1.1436x^0.7793
R² = 0.49593
0
5
10
15
20
25
30
35
40
45
50

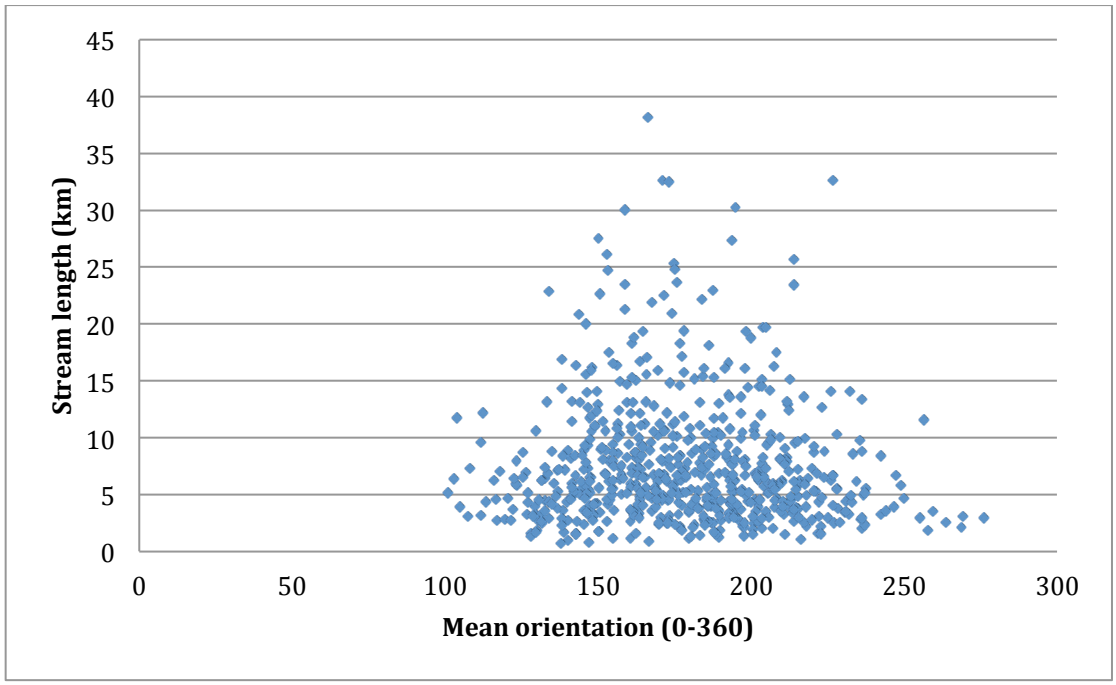
Stream length (km)
Mean orientation (0-360)
0
50
100
150
200
250
300

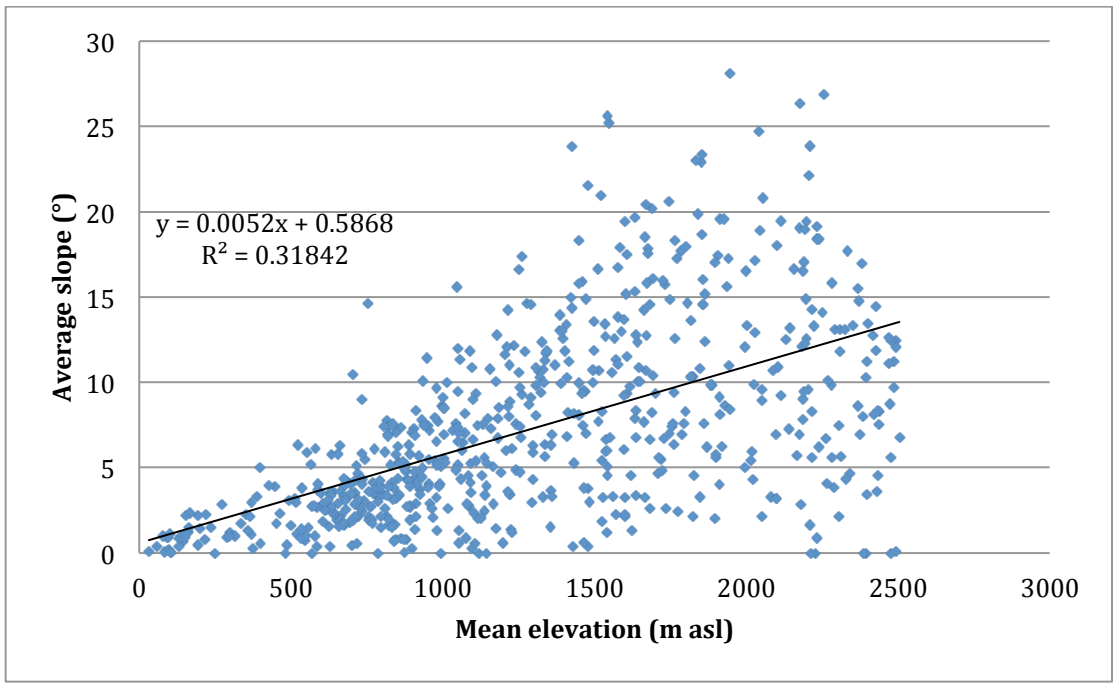
y = 0.0052x + 0.5868
R² = 0.31842
Average slope (°)
Mean elevation (m asl)
0
5
10
15
20
25
30
0
500
1000
1500
2000
2500
3000

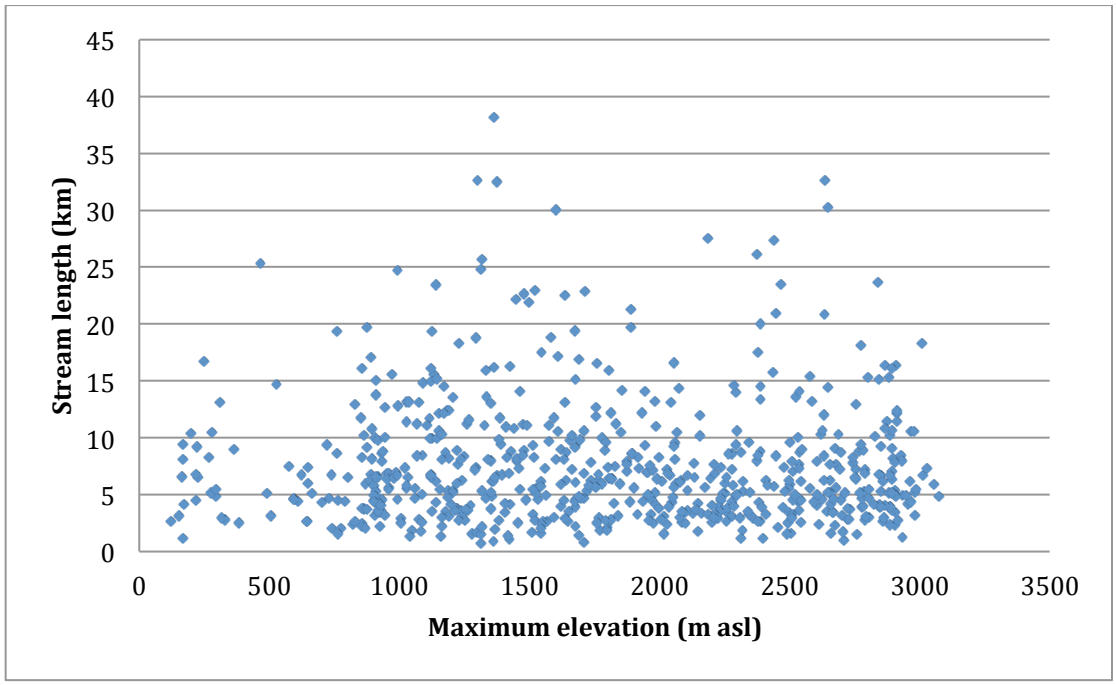
Stream length (km)
Maximum elevation (m asl)
0
5
10
15
20
25
30
35
40
45
0
500
1000
1500
2000
2500
3000
3500

Appendix 4: Statistical results for training and test sets.

1st-order catchments - Training set – Berga - all catchments.

Max. elevation (m asl)			
Count	457	*Skewness*	0.06031
Mean	1,763.10098	*Skewness Standard Error*	0.11396
Mean LCL	1,714.3386	*Kurtosis*	2.10497
Mean UCL	1,811.86337	*Kurtosis Standard Error*	0.22643
Variance	199,378.57034	*Alternative Skewness (Fisher's)*	0.0605
Standard Deviation	446.51828	*Alternative Kurtosis (Fisher's)*	-0.89165
Mean Standard Error	20.88724	*Coefficient of Variation*	0.25326
Minimum	816.22	*Mean Deviation*	378.23634
Maximum	2,648.32	*Second Moment*	198,942.29339
Range	1,832.1	*Third Moment*	5,351,210.2196
Sum	805,737.15	*Fourth Moment*	8.33106E+10
Sum Standard Error	9,545.47048	*Median*	1,707.6
Total Sum Squares	1,511,512,590.6375	*Median Error*	1.22457
Adjusted Sum Squares	90,916,628.07706	*Percentile 25% (Q1)*	1,430.8525
Geometric Mean	1,703.96767	*Percentile 75% (Q2)*	2,128.41
Harmonic Mean	1,642.39826	*IQR*	697.5575
Mode	#N/A	*MAD*	354.58
Mean elevation (m asl)			
Count	457	*Skewness*	0.24899
Mean	1,379.90184	*Skewness Standard Error*	0.11396
Mean LCL	1,340.17421	*Kurtosis*	2.30908
Mean UCL	1,419.62947	*Kurtosis Standard Error*	0.22643
Variance	132,340.85463	*Alternative Skewness (Fisher's)*	0.24981
Standard Deviation	363.78683	*Alternative Kurtosis (Fisher's)*	-0.6853
Mean Standard Error	17.01723	*Coefficient of Variation*	0.26363
Minimum	637.092	*Mean Deviation*	305.42599
Maximum	2,268.623	*Second Moment*	132,051.26852
Range	1,631.531	*Third Moment*	11,947,780.62559
Sum	630,615.1417	*Fourth Moment*	4.02646E+10
Sum Standard Error	7,776.87409	*Median*	1,330.722
Total Sum Squares	930,534,425.20725	*Median Error*	0.99768
Adjusted Sum Squares	60,347,429.71204	*Percentile 25% (Q1)*	1,110.5035
Geometric Mean	1,331.14199	*Percentile 75% (Q2)*	1,661.8065
Harmonic Mean	1,281.7602	*IQR*	551.303
Mode	#N/A	*MAD*	266.419
Min. elevation (m asl)			
Count	457	*Skewness*	0.57399
Mean	1,037.02952	*Skewness Standard Error*	0.11396
Mean LCL	1,005.54609	*Kurtosis*	3.11892
Mean UCL	1,068.51294	*Kurtosis Standard Error*	0.22643
Variance	83,113.68601	*Alternative Skewness (Fisher's)*	0.57589
Standard Deviation	288.29444	*Alternative Kurtosis (Fisher's)*	0.13347
Mean Standard Error	13.48585	*Coefficient of Variation*	0.278
Minimum	473.54	*Mean Deviation*	232.79302
Maximum	1,979.29	*Second Moment*	82,931.81799
Range	1,505.75	*Third Moment*	13,708,488.18878
Sum	473,922.49	*Fourth Moment*	2.14509E+10
Sum Standard Error	6,163.03128	*Median*	993.36
Total Sum Squares	529,371,452.4793	*Median Error*	0.79064
Adjusted Sum Squares	37,899,840.82109	*Percentile 25% (Q1)*	827.8525
Geometric Mean	997.99799	*Percentile 75% (Q2)*	1,243.6875
Harmonic Mean	959.77692	*IQR*	415.835
Mode	628.5	*MAD*	193.59

Melton ratio (-)

Count	457	*Skewness*	0.6834
Mean	0.51493	*Skewness Standard Error*	0.11396
Mean LCL	0.49258	*Kurtosis*	3.15262
Mean UCL	0.53729	*Kurtosis Standard Error*	0.22643
Variance	0.0419	*Alternative Skewness (Fisher's)*	0.68565
Standard Deviation	0.2047	*Alternative Kurtosis (Fisher's)*	0.16754
Mean Standard Error	0.00958	*Coefficient of Variation*	0.39754
Minimum	0.10372	*Mean Deviation*	0.16302
Maximum	1.11711	*Second Moment*	0.04181
Range	1.01339	*Third Moment*	0.00584
Sum	235.32507	*Fourth Moment*	0.00551
Sum Standard Error	4.37609	*Median*	0.48392
Total Sum Squares	140.28526	*Median Error*	0.00056
Adjusted Sum Squares	19.10825	*Percentile 25% (Q1)*	0.36738
Geometric Mean	0.47468	*Percentile 75% (Q2)*	0.62703
Harmonic Mean	0.43365	*IQR*	0.25965
Mode	#N/A	*MAD*	0.12966

Mean slope (°)

Count	457	*Skewness*	0.14327
Mean	24.74129	*Skewness Standard Error*	0.11396
Mean LCL	24.17786	*Kurtosis*	3.3111
Mean UCL	25.30471	*Kurtosis Standard Error*	0.22643
Variance	26.61838	*Alternative Skewness (Fisher's)*	0.14374
Standard Deviation	5.1593	*Alternative Kurtosis (Fisher's)*	0.32778
Mean Standard Error	0.24134	*Coefficient of Variation*	0.20853
Minimum	9.15218	*Mean Deviation*	3.98772
Maximum	41.01257	*Second Moment*	26.56014
Range	31.86039	*Third Moment*	19.61051
Sum	11,306.76888	*Fourth Moment*	2,335.7856
Sum Standard Error	110.29325	*Median*	24.56085
Total Sum Squares	291,882.0136	*Median Error*	0.01415
Adjusted Sum Squares	12,137.98206	*Percentile 25% (Q1)*	21.61186
Geometric Mean	24.17794	*Percentile 75% (Q2)*	27.73597
Harmonic Mean	23.56674	*IQR*	6.12412
Mode	#N/A	*MAD*	3.081

Mean orientation (0-360)

Count	457	*Skewness*	-0.03805
Mean	179.78816	*Skewness Standard Error*	0.11396
Mean LCL	175.53155	*Kurtosis*	2.61238
Mean UCL	184.04478	*Kurtosis Standard Error*	0.22643
Variance	1,519.28097	*Alternative Skewness (Fisher's)*	-0.03817
Standard Deviation	38.97795	*Alternative Kurtosis (Fisher's)*	-0.37865
Mean Standard Error	1.82331	*Coefficient of Variation*	0.2168
Minimum	74.17361	*Mean Deviation*	31.9784
Maximum	277.5351	*Second Moment*	1,515.9565
Range	203.36149	*Third Moment*	-2,245.8401
Sum	82,163.1911	*Fourth Moment*	6,003,575.65246
Sum Standard Error	833.2535	*Median*	179.2415
Total Sum Squares	15,464,761.42563	*Median Error*	0.1069
Adjusted Sum Squares	692,792.12205	*Percentile 25% (Q1)*	152.99148
Geometric Mean	175.3064	*Percentile 75% (Q2)*	209.0013
Harmonic Mean	170.49803	*IQR*	56.00983
Mode	#N/A	*MAD*	28.3075

Area (km2)

Count	457	*Skewness*	2.24184
Mean	2.27931	*Skewness Standard Error*	0.11396
Mean LCL	2.13295	*Kurtosis*	9.86428
Mean UCL	2.42567	*Kurtosis Standard Error*	0.22643
Variance	1.79625	*Alternative Skewness (Fisher's)*	2.24923
Standard Deviation	1.34024	*Alternative Kurtosis (Fisher's)*	6.95322
Mean Standard Error	0.06269	*Coefficient of Variation*	0.588
Minimum	1.00198	*Mean Deviation*	0.95489
Maximum	10.44433	*Second Moment*	1.79232
Range	9.44235	*Third Moment*	5.37931
Sum	1,041.64435	*Fourth Moment*	31.68798
Sum Standard Error	28.65108	*Median*	1.85858
Total Sum Squares	3,193.31807	*Median Error*	0.00368
Adjusted Sum Squares	819.08842	*Percentile 25% (Q1)*	1.37351
Geometric Mean	2.00885	*Percentile 75% (Q2)*	2.69478
Harmonic Mean	1.81712	*IQR*	1.32128
Mode	#N/A	*MAD*	0.59125

Stream length (km)

Count	457	*Skewness*	2.58843
Mean	1.37521	*Skewness Standard Error*	0.11396
Mean LCL	1.24226	*Kurtosis*	14.26902
Mean UCL	1.50815	*Kurtosis Standard Error*	0.22643
Variance	1.482	*Alternative Skewness (Fisher's)*	2.59697
Standard Deviation	1.21738	*Alternative Kurtosis (Fisher's)*	11.40654
Mean Standard Error	0.05695	*Coefficient of Variation*	0.88523
Minimum	0.0075	*Mean Deviation*	0.85244
Maximum	9.55379	*Second Moment*	1.47876
Range	9.54629	*Third Moment*	4.65461
Sum	628.46927	*Fourth Moment*	31.20251
Sum Standard Error	26.02451	*Median*	1.05114
Total Sum Squares	1,540.06819	*Median Error*	0.00334
Adjusted Sum Squares	675.79329	*Percentile 25% (Q1)*	0.5494
Geometric Mean	0.94427	*Percentile 75% (Q2)*	1.84202
Harmonic Mean	0.43578	*IQR*	1.29262
Mode	0.46877	*MAD*	0.58648

Perimeter (m)

Count	457	*Skewness*	2.20992
Mean	9,187.04595	*Skewness Standard Error*	0.11396
Mean LCL	8,862.1412	*Kurtosis*	11.34899
Mean UCL	9,511.9507	*Kurtosis Standard Error*	0.22643
Variance	8,851,579.19306	*Alternative Skewness (Fisher's)*	2.21721
Standard Deviation	2,975.16036	*Alternative Kurtosis (Fisher's)*	8.4543
Mean Standard Error	139.17213	*Coefficient of Variation*	0.32384
Minimum	5,080.	*Mean Deviation*	2,115.04733
Maximum	27,880.	*Second Moment*	8,832,210.3108
Range	22,800.	*Third Moment*	5.80071E+10
Sum	4,198,480.	*Fourth Moment*	8.85311E+14
Sum Standard Error	63,601.66422	*Median*	8,600.
Total Sum Squares	4.26079E+10	*Median Error*	8.15932
Adjusted Sum Squares	4,036,320,112.03501	*Percentile 25% (Q1)*	7,200.
Geometric Mean	8,810.59195	*Percentile 75% (Q2)*	10,280.
Harmonic Mean	8,500.16568	*IQR*	3,080.
Mode	#N/A	*MAD*	1,520.

Form factor (-)

Count	457	*Skewness*	0.32944
Mean	0.39498	*Skewness Standard Error*	0.11396
Mean LCL	0.38032	*Kurtosis*	2.32718
Mean UCL	0.40964	*Kurtosis Standard Error*	0.22643
Variance	0.01803	*Alternative Skewness (Fisher's)*	0.33053
Standard Deviation	0.13426	*Alternative Kurtosis (Fisher's)*	-0.66699
Mean Standard Error	0.00628	*Coefficient of Variation*	0.33992
Minimum	0.12789	*Mean Deviation*	0.11234
Maximum	0.75059	*Second Moment*	0.01799
Range	0.6227	*Third Moment*	0.00079
Sum	180.50664	*Fourth Moment*	0.00075
Sum Standard Error	2.87018	*Median*	0.37239
Total Sum Squares	79.51672	*Median Error*	0.00037
Adjusted Sum Squares	8.2199	*Percentile 25% (Q1)*	0.29425
Geometric Mean	0.37151	*Percentile 75% (Q2)*	0.49897
Harmonic Mean	0.34752	*IQR*	0.20472
Mode	#N/A	*MAD*	0.09511

Basin Elongation (-)

Count	457	*Skewness*	0.00214
Mean	0.69866	*Skewness Standard Error*	0.11396
Mean LCL	0.68536	*Kurtosis*	2.28442
Mean UCL	0.71195	*Kurtosis Standard Error*	0.22643
Variance	0.01482	*Alternative Skewness (Fisher's)*	0.00215
Standard Deviation	0.12173	*Alternative Kurtosis (Fisher's)*	-0.71022
Mean Standard Error	0.00569	*Coefficient of Variation*	0.17423
Minimum	0.40353	*Mean Deviation*	0.10151
Maximum	0.97759	*Second Moment*	0.01478
Range	0.57406	*Third Moment*	0.
Sum	319.28618	*Fourth Moment*	0.0005
Sum Standard Error	2.60222	*Median*	0.68858
Total Sum Squares	229.82819	*Median Error*	0.00033
Adjusted Sum Squares	6.75671	*Percentile 25% (Q1)*	0.61209
Geometric Mean	0.68777	*Percentile 75% (Q2)*	0.79706
Harmonic Mean	0.67658	*IQR*	0.18497
Mode	#N/A	*MAD*	0.09102

Lemniscate ratio (-)

Count	457	*Skewness*	1.24977
Mean	2.26002	*Skewness Standard Error*	0.11396
Mean LCL	2.1642	*Kurtosis*	4.71579
Mean UCL	2.35584	*Kurtosis Standard Error*	0.22643
Variance	0.76986	*Alternative Skewness (Fisher's)*	1.25389
Standard Deviation	0.87742	*Alternative Kurtosis (Fisher's)*	1.74795
Mean Standard Error	0.04104	*Coefficient of Variation*	0.38823
Minimum	1.04637	*Mean Deviation*	0.67343
Maximum	6.14107	*Second Moment*	0.76817
Range	5.0947	*Third Moment*	0.84143
Sum	1,032.82886	*Fourth Moment*	2.78274
Sum Standard Error	18.757	*Median*	2.10908
Total Sum Squares	2,685.26844	*Median Error*	0.00241
Adjusted Sum Squares	351.0552	*Percentile 25% (Q1)*	1.57856
Geometric Mean	2.11405	*Percentile 75% (Q2)*	2.67967
Harmonic Mean	1.98844	*IQR*	1.10112
Mode	#N/A	*MAD*	0.54153

Outlet slope (°)

Count	457	*Skewness*	1.27029
Mean	7.95374	*Skewness Standard Error*	0.11396
Mean LCL	7.27932	*Kurtosis*	4.75421
Mean UCL	8.62817	*Kurtosis Standard Error*	0.22643
Variance	38.13972	*Alternative Skewness (Fisher's)*	1.27448
Standard Deviation	6.17574	*Alternative Kurtosis (Fisher's)*	1.7868
Mean Standard Error	0.28889	*Coefficient of Variation*	0.77646
Minimum	0.E+0	*Mean Deviation*	4.74147
Maximum	36.23	*Second Moment*	38.05626
Range	36.23	*Third Moment*	298.2242
Sum	3,634.86	*Fourth Moment*	6,885.42832
Sum Standard Error	132.02217	*Median*	6.67
Total Sum Squares	46,302.4508	*Median Error*	0.01694
Adjusted Sum Squares	17,391.7129	*Percentile 25% (Q1)*	3.3825
Geometric Mean	5.74521	*Percentile 75% (Q2)*	10.81
Harmonic Mean	4.03921	*IQR*	7.4275
Mode	0.E+0	*MAD*	3.52

200m slope (°)

Count	457	*Skewness*	1.37184
Mean	7.91381	*Skewness Standard Error*	0.11396
Mean LCL	7.25202	*Kurtosis*	5.19977
Mean UCL	8.57559	*Kurtosis Standard Error*	0.22643
Variance	36.72354	*Alternative Skewness (Fisher's)*	1.37636
Standard Deviation	6.05999	*Alternative Kurtosis (Fisher's)*	2.23727
Mean Standard Error	0.28347	*Coefficient of Variation*	0.76575
Minimum	0.E+0	*Mean Deviation*	4.64335
Maximum	33.52	*Second Moment*	36.64318
Range	33.52	*Third Moment*	304.29339
Sum	3,616.61	*Fourth Moment*	6,981.84933
Sum Standard Error	129.54789	*Median*	6.57
Total Sum Squares	45,367.0883	*Median Error*	0.01662
Adjusted Sum Squares	16,745.93318	*Percentile 25% (Q1)*	3.53
Geometric Mean	5.8622	*Percentile 75% (Q2)*	11.0075
Harmonic Mean	4.30295	*IQR*	7.4775
Mode	0.E+0	*MAD*	3.43

Average slope (°)

Count	457	*Skewness*	0.94683
Mean	8.78864	*Skewness Standard Error*	0.11396
Mean LCL	8.17895	*Kurtosis*	4.05362
Mean UCL	9.39833	*Kurtosis Standard Error*	0.22643
Variance	31.16932	*Alternative Skewness (Fisher's)*	0.94995
Standard Deviation	5.58295	*Alternative Kurtosis (Fisher's)*	1.07848
Mean Standard Error	0.26116	*Coefficient of Variation*	0.63525
Minimum	0.E+0	*Mean Deviation*	4.41929
Maximum	29.89	*Second Moment*	31.10111
Range	29.89	*Third Moment*	164.22382
Sum	4,016.41	*Fourth Moment*	3,920.97938
Sum Standard Error	119.34981	*Median*	7.8
Total Sum Squares	49,512.0027	*Median Error*	0.01531
Adjusted Sum Squares	14,213.20776	*Percentile 25% (Q1)*	4.3325
Geometric Mean	6.94105	*Percentile 75% (Q2)*	11.84
Harmonic Mean	5.34052	*IQR*	7.5075
Mode	0.E+0	*MAD*	3.63

1st-order catchments - Training set – Berga - Reactive catchments.

Max. elevation (m asl)			
Count	20	*Skewness*	-0.47314
Mean	2,060.8945	*Skewness Standard Error*	0.48582
Mean LCL	1,851.30868	*Kurtosis*	2.13439
Mean UCL	2,270.48032	*Kurtosis Standard Error*	0.84119
Variance	136,226.97602	*Alternative Skewness (Fisher's)*	-0.5124
Standard Deviation	369.08939	*Alternative Kurtosis (Fisher's)*	-0.75613
Mean Standard Error	82.5309	*Coefficient of Variation*	0.17909
Minimum	1,376.27	*Mean Deviation*	301.9066
Maximum	2,603.13	*Second Moment*	129,415.62721
Range	1,226.86	*Third Moment*	-22,027,754.3264
Sum	41,217.89	*Fourth Moment*	3.57477E+10
Sum Standard Error	1,650.61792	*Median*	2,155.895
Total Sum Squares	87,534,035.3469	*Median Error*	23.12925
Adjusted Sum Squares	2,588,312.5443	*Percentile 25% (Q1)*	1,884.84
Geometric Mean	2,026.83717	*Percentile 75% (Q2)*	2,320.5
Harmonic Mean	1,990.27322	*IQR*	435.66
Mode	#N/A	*MAD*	233.135
Mean elevation (m asl)			
Count	20	*Skewness*	-0.15724
Mean	1,574.607	*Skewness Standard Error*	0.48582
Mean LCL	1,400.75377	*Kurtosis*	2.29462
Mean UCL	1,748.46023	*Kurtosis Standard Error*	0.84119
Variance	93,735.66327	*Alternative Skewness (Fisher's)*	-0.17029
Standard Deviation	306.16281	*Alternative Kurtosis (Fisher's)*	-0.54721
Mean Standard Error	68.46008	*Coefficient of Variation*	0.19444
Minimum	1,067.994	*Mean Deviation*	245.4649
Maximum	2,170.139	*Second Moment*	89,048.88011
Range	1,102.145	*Third Moment*	-4,178,319.44595
Sum	31,492.14	*Fourth Moment*	1.81957E+10
Sum Standard Error	1,369.20169	*Median*	1,639.595
Total Sum Squares	51,368,721.69114	*Median Error*	19.18591
Adjusted Sum Squares	1,780,977.60216	*Percentile 25% (Q1)*	1,459.436
Geometric Mean	1,544.80121	*Percentile 75% (Q2)*	1,801.975
Harmonic Mean	1,513.63031	*IQR*	342.539
Mode	#N/A	*MAD*	165.4675
Min. elevation (m asl)			
Count	20	*Skewness*	0.50085
Mean	1,179.818	*Skewness Standard Error*	0.48582
Mean LCL	1,032.6343	*Kurtosis*	2.33643
Mean UCL	1,327.0017	*Kurtosis Standard Error*	0.84119
Variance	67,182.90391	*Alternative Skewness (Fisher's)*	0.54241
Standard Deviation	259.19665	*Alternative Kurtosis (Fisher's)*	-0.4927
Mean Standard Error	57.95813	*Coefficient of Variation*	0.21969
Minimum	802.62	*Mean Deviation*	213.1828
Maximum	1,733.43	*Second Moment*	63,823.75872
Range	930.81	*Third Moment*	8,075,698.11235
Sum	23,596.36	*Fourth Moment*	9,517,379,545.86169
Sum Standard Error	1,159.16266	*Median*	1,111.45
Total Sum Squares	29,115,885.4368	*Median Error*	16.24274
Adjusted Sum Squares	1,276,475.17432	*Percentile 25% (Q1)*	949.76
Geometric Mean	1,153.72132	*Percentile 75% (Q2)*	1,385.06
Harmonic Mean	1,128.8006	*IQR*	435.3
Mode	#N/A	*MAD*	191.09

Melton ratio (-)

Count	20	*Skewness*	-0.14365
Mean	0.56416	*Skewness Standard Error*	0.48582
Mean LCL	0.47627	*Kurtosis*	2.104
Mean UCL	0.65204	*Kurtosis Standard Error*	0.84119
Variance	0.02395	*Alternative Skewness (Fisher's)*	-0.15557
Standard Deviation	0.15477	*Alternative Kurtosis (Fisher's)*	-0.79577
Mean Standard Error	0.03461	*Coefficient of Variation*	0.27434
Minimum	0.25177	*Mean Deviation*	0.12864
Maximum	0.79701	*Second Moment*	0.02276
Range	0.54524	*Third Moment*	-0.00049
Sum	11.28311	*Fourth Moment*	0.00109
Sum Standard Error	0.69216	*Median*	0.5979
Total Sum Squares	6.82057	*Median Error*	0.0097
Adjusted Sum Squares	0.45513	*Percentile 25% (Q1)*	0.42297
Geometric Mean	0.54191	*Percentile 75% (Q2)*	0.70128
Harmonic Mean	0.51741	*IQR*	0.27832
Mode	#N/A	*MAD*	0.14224

Mean slope (°)

Count	20	*Skewness*	0.64483
Mean	27.16963	*Skewness Standard Error*	0.48582
Mean LCL	24.86818	*Kurtosis*	3.61347
Mean UCL	29.47109	*Kurtosis Standard Error*	0.84119
Variance	16.42646	*Alternative Skewness (Fisher's)*	0.69833
Standard Deviation	4.05296	*Alternative Kurtosis (Fisher's)*	1.17246
Mean Standard Error	0.90627	*Coefficient of Variation*	0.14917
Minimum	19.56865	*Mean Deviation*	3.01535
Maximum	37.52913	*Second Moment*	15.60514
Range	17.96048	*Third Moment*	39.75078
Sum	543.39262	*Fourth Moment*	879.95273
Sum Standard Error	18.12537	*Median*	26.87394
Total Sum Squares	15,075.87971	*Median Error*	0.25398
Adjusted Sum Squares	312.10274	*Percentile 25% (Q1)*	24.51813
Geometric Mean	26.892	*Percentile 75% (Q2)*	29.21734
Harmonic Mean	26.62162	*IQR*	4.69921
Mode	#N/A	*MAD*	2.34961

Mean orientation (0-360)

Count	20	*Skewness*	0.28147
Mean	171.46616	*Skewness Standard Error*	0.48582
Mean LCL	154.48215	*Kurtosis*	1.82808
Mean UCL	188.45017	*Kurtosis Standard Error*	0.84119
Variance	894.58146	*Alternative Skewness (Fisher's)*	0.30483
Standard Deviation	29.90955	*Alternative Kurtosis (Fisher's)*	-1.15555
Mean Standard Error	6.68798	*Coefficient of Variation*	0.17443
Minimum	129.101	*Mean Deviation*	25.81781
Maximum	223.1142	*Second Moment*	849.85239
Range	94.0132	*Third Moment*	6,973.53102
Sum	3,429.3232	*Fourth Moment*	1,320,325.75353
Sum Standard Error	133.75959	*Median*	162.53415
Total Sum Squares	605,009.92828	*Median Error*	1.8743
Adjusted Sum Squares	16,997.04777	*Percentile 25% (Q1)*	150.2469
Geometric Mean	169.02165	*Percentile 75% (Q2)*	199.8419
Harmonic Mean	166.63504	*IQR*	49.595
Mode	#N/A	*MAD*	25.74795

Area (km2)

Count	20	*Skewness*	0.34227
Mean	2.62024	*Skewness Standard Error*	0.48582
Mean LCL	2.00736	*Kurtosis*	2.31858
Mean UCL	3.23311	*Kurtosis Standard Error*	0.84119
Variance	1.16488	*Alternative Skewness (Fisher's)*	0.37067
Standard Deviation	1.0793	*Alternative Kurtosis (Fisher's)*	-0.51596
Mean Standard Error	0.24134	*Coefficient of Variation*	0.41191
Minimum	1.01225	*Mean Deviation*	0.90013
Maximum	4.72858	*Second Moment*	1.10663
Range	3.71633	*Third Moment*	0.39845
Sum	52.40475	*Fourth Moment*	2.83943
Sum Standard Error	4.82676	*Median*	2.5517
Total Sum Squares	159.44559	*Median Error*	0.06763
Adjusted Sum Squares	22.1327	*Percentile 25% (Q1)*	1.74403
Geometric Mean	2.39893	*Percentile 75% (Q2)*	3.40785
Harmonic Mean	2.17534	*IQR*	1.66383
Mode	#N/A	*MAD*	0.84444

Stream length (km)

Count	20	*Skewness*	0.4694
Mean	1.66576	*Skewness Standard Error*	0.48582
Mean LCL	0.9461	*Kurtosis*	2.20043
Mean UCL	2.38542	*Kurtosis Standard Error*	0.84119
Variance	1.60618	*Alternative Skewness (Fisher's)*	0.50835
Standard Deviation	1.26735	*Alternative Kurtosis (Fisher's)*	-0.67003
Mean Standard Error	0.28339	*Coefficient of Variation*	0.76083
Minimum	0.06871	*Mean Deviation*	1.05249
Maximum	4.40335	*Second Moment*	1.52588
Range	4.33464	*Third Moment*	0.88475
Sum	33.31514	*Fourth Moment*	5.12325
Sum Standard Error	5.66778	*Median*	1.47304
Total Sum Squares	86.01244	*Median Error*	0.07942
Adjusted Sum Squares	30.51751	*Percentile 25% (Q1)*	0.65277
Geometric Mean	1.05478	*Percentile 75% (Q2)*	2.89674
Harmonic Mean	0.47765	*IQR*	2.24397
Mode	#N/A	*MAD*	1.12123

Perimeter (m)

Count	20	*Skewness*	0.65951
Mean	9,884.	*Skewness Standard Error*	0.48582
Mean LCL	8,358.79784	*Kurtosis*	3.40711
Mean UCL	11,409.20216	*Kurtosis Standard Error*	0.84119
Variance	7,214,298.94737	*Alternative Skewness (Fisher's)*	0.71424
Standard Deviation	2,685.9447	*Alternative Kurtosis (Fisher's)*	0.90339
Mean Standard Error	600.59549	*Coefficient of Variation*	0.27175
Minimum	5,960.	*Mean Deviation*	1,948.8
Maximum	16,760.	*Second Moment*	6,853,584.
Range	10,800.	*Third Moment*	1.18331E+10
Sum	197,680.	*Fourth Moment*	1.60037E+14
Sum Standard Error	12,011.90988	*Median*	9,800.
Total Sum Squares	2,090,940,800.	*Median Error*	168.31662
Adjusted Sum Squares	137,071,680.	*Percentile 25% (Q1)*	8,240.
Geometric Mean	9,549.4869	*Percentile 75% (Q2)*	11,800.
Harmonic Mean	9,224.79635	*IQR*	3,560.
Mode	#N/A	*MAD*	1,780.

Form factor (-)

Count	20	*Skewness*	0.44145
Mean	0.40709	*Skewness Standard Error*	0.48582
Mean LCL	0.32364	*Kurtosis*	1.98659
Mean UCL	0.49055	*Kurtosis Standard Error*	0.84119
Variance	0.0216	*Alternative Skewness (Fisher's)*	0.47808
Standard Deviation	0.14697	*Alternative Kurtosis (Fisher's)*	-0.94886
Mean Standard Error	0.03286	*Coefficient of Variation*	0.36101
Minimum	0.18356	*Mean Deviation*	0.12653
Maximum	0.6596	*Second Moment*	0.02052
Range	0.47603	*Third Moment*	0.0013
Sum	8.14186	*Fourth Moment*	0.00084
Sum Standard Error	0.65725	*Median*	0.35487
Total Sum Squares	3.72487	*Median Error*	0.00921
Adjusted Sum Squares	0.41038	*Percentile 25% (Q1)*	0.30233
Geometric Mean	0.3824	*Percentile 75% (Q2)*	0.51746
Harmonic Mean	0.359	*IQR*	0.21513
Mode	#N/A	*MAD*	0.09775

Basin Elongation (-)

Count	20	*Skewness*	0.22159
Mean	0.70888	*Skewness Standard Error*	0.48582
Mean LCL	0.63562	*Kurtosis*	1.92007
Mean UCL	0.78214	*Kurtosis Standard Error*	0.84119
Variance	0.01664	*Alternative Skewness (Fisher's)*	0.23998
Standard Deviation	0.12902	*Alternative Kurtosis (Fisher's)*	-1.03559
Mean Standard Error	0.02885	*Coefficient of Variation*	0.182
Minimum	0.48345	*Mean Deviation*	0.11148
Maximum	0.91642	*Second Moment*	0.01581
Range	0.43297	*Third Moment*	0.00044
Sum	14.17764	*Fourth Moment*	0.00048
Sum Standard Error	0.57697	*Median*	0.6714
Total Sum Squares	10.36653	*Median Error*	0.00808
Adjusted Sum Squares	0.31625	*Percentile 25% (Q1)*	0.62044
Geometric Mean	0.69777	*Percentile 75% (Q2)*	0.8117
Harmonic Mean	0.68679	*IQR*	0.19126
Mode	#N/A	*MAD*	0.09924

Lemniscate ratio (-)

Count	20	*Skewness*	0.70643
Mean	2.18772	*Skewness Standard Error*	0.48582
Mean LCL	1.73085	*Kurtosis*	3.22136
Mean UCL	2.6446	*Kurtosis Standard Error*	0.84119
Variance	0.64734	*Alternative Skewness (Fisher's)*	0.76505
Standard Deviation	0.80458	*Alternative Kurtosis (Fisher's)*	0.66118
Mean Standard Error	0.17991	*Coefficient of Variation*	0.36777
Minimum	1.19072	*Mean Deviation*	0.66666
Maximum	4.27861	*Second Moment*	0.61498
Range	3.08789	*Third Moment*	0.34069
Sum	43.75445	*Fourth Moment*	1.21831
Sum Standard Error	3.59818	*Median*	2.23396
Total Sum Squares	108.02214	*Median Error*	0.05042
Adjusted Sum Squares	12.29955	*Percentile 25% (Q1)*	1.539
Geometric Mean	2.05388	*Percentile 75% (Q2)*	2.75722
Harmonic Mean	1.92929	*IQR*	1.21822
Mode	#N/A	*MAD*	0.64302

Outlet slope (°)

Count	20	*Skewness*	0.63288
Mean	7.425	*Skewness Standard Error*	0.48582
Mean LCL	4.78532	*Kurtosis*	2.90561
Mean UCL	10.06468	*Kurtosis Standard Error*	0.84119
Variance	21.60941	*Alternative Skewness (Fisher's)*	0.68539
Standard Deviation	4.64859	*Alternative Kurtosis (Fisher's)*	0.24947
Mean Standard Error	1.03946	*Coefficient of Variation*	0.62607
Minimum	0.E+0	*Mean Deviation*	3.6405
Maximum	18.13	*Second Moment*	20.52894
Range	18.13	*Third Moment*	58.86649
Sum	148.5	*Fourth Moment*	1,224.5306
Sum Standard Error	20.78913	*Median*	7.55
Total Sum Squares	1,513.1912	*Median Error*	0.29131
Adjusted Sum Squares	410.5787	*Percentile 25% (Q1)*	4.16
Geometric Mean	6.04207	*Percentile 75% (Q2)*	10.05
Harmonic Mean	5.8148	*IQR*	5.89
Mode	8.8	*MAD*	3.305

200m slope (°)

Count	20	*Skewness*	0.31922
Mean	6.8065	*Skewness Standard Error*	0.48582
Mean LCL	4.60284	*Kurtosis*	2.5212
Mean UCL	9.01016	*Kurtosis Standard Error*	0.84119
Variance	15.06013	*Alternative Skewness (Fisher's)*	0.3457
Standard Deviation	3.88074	*Alternative Kurtosis (Fisher's)*	-0.25176
Mean Standard Error	0.86776	*Coefficient of Variation*	0.57015
Minimum	0.E+0	*Mean Deviation*	3.1715
Maximum	15.11	*Second Moment*	14.30712
Range	15.11	*Third Moment*	17.27487
Sum	136.13	*Fourth Moment*	516.07455
Sum Standard Error	17.35519	*Median*	6.765
Total Sum Squares	1,212.7113	*Median Error*	0.24319
Adjusted Sum Squares	286.14246	*Percentile 25% (Q1)*	4.33
Geometric Mean	5.69372	*Percentile 75% (Q2)*	9.5
Harmonic Mean	5.58548	*IQR*	5.17
Mode	7.57	*MAD*	2.63

Average slope (°)

Count	20	*Skewness*	0.47651
Mean	8.731	*Skewness Standard Error*	0.48582
Mean LCL	6.39316	*Kurtosis*	2.9097
Mean UCL	11.06884	*Kurtosis Standard Error*	0.84119
Variance	16.94997	*Alternative Skewness (Fisher's)*	0.51605
Standard Deviation	4.11703	*Alternative Kurtosis (Fisher's)*	0.25481
Mean Standard Error	0.9206	*Coefficient of Variation*	0.47154
Minimum	2.4	*Mean Deviation*	3.2289
Maximum	18.51	*Second Moment*	16.10247
Range	16.11	*Third Moment*	30.79019
Sum	174.62	*Fourth Moment*	754.4558
Sum Standard Error	18.41193	*Median*	9.045
Total Sum Squares	1,846.6566	*Median Error*	0.258
Adjusted Sum Squares	322.04938	*Percentile 25% (Q1)*	5.41
Geometric Mean	7.72782	*Percentile 75% (Q2)*	11.43
Harmonic Mean	6.65195	*IQR*	6.02
Mode	10.5	*MAD*	2.475

1st-order catchments - Training set – Mollo - all catchments.

Max. elevation (m asl)			
Count	119	*Skewness*	0.06973
Mean	2,076.19454	*Skewness Standard Error*	0.21991
Mean LCL	1,969.47901	*Kurtosis*	1.95709
Mean UCL	2,182.91007	*Kurtosis Standard Error*	0.42897
Variance	243,657.70161	*Alternative Skewness (Fisher's)*	0.07062
Standard Deviation	493.61696	*Alternative Kurtosis (Fisher's)*	-1.03593
Mean Standard Error	45.24979	*Coefficient of Variation*	0.23775
Minimum	1,166.74	*Mean Deviation*	411.77677
Maximum	2,909.58	*Second Moment*	241,610.1579
Range	1,742.84	*Third Moment*	8,280,613.39503
Sum	247,067.15	*Fourth Moment*	1.14246E+11
Sum Standard Error	5,384.72529	*Median*	1,990.99
Total Sum Squares	541,711,076.0939	*Median Error*	5.1988
Adjusted Sum Squares	28,751,608.79035	*Percentile 25% (Q1)*	1,734.4475
Geometric Mean	2,016.03399	*Percentile 75% (Q2)*	2,529.9825
Harmonic Mean	1,954.58005	*IQR*	795.535
Mode	#N/A	*MAD*	400.44
Mean elevation (m asl)			
Count	119	*Skewness*	0.30507
Mean	1,712.00393	*Skewness Standard Error*	0.21991
Mean LCL	1,613.07098	*Kurtosis*	2.0922
Mean UCL	1,810.93688	*Kurtosis Standard Error*	0.42897
Variance	209,414.53145	*Alternative Skewness (Fisher's)*	0.30897
Standard Deviation	457.61833	*Alternative Kurtosis (Fisher's)*	-0.89497
Mean Standard Error	41.9498	*Coefficient of Variation*	0.2673
Minimum	861.408	*Mean Deviation*	378.45639
Maximum	2,573.131	*Second Moment*	207,654.74547
Range	1,711.723	*Third Moment*	28,867,334.43177
Sum	203,728.4676	*Fourth Moment*	9.02166E+10
Sum Standard Error	4,992.02657	*Median*	1,625.649
Total Sum Squares	373,494,851.77478	*Median Error*	4.81966
Adjusted Sum Squares	24,710,914.71054	*Percentile 25% (Q1)*	1,392.60725
Geometric Mean	1,651.20538	*Percentile 75% (Q2)*	2,145.00475
Harmonic Mean	1,590.93577	*IQR*	752.3975
Mode	#N/A	*MAD*	322.717
Min. elevation (m asl)			
Count	119	*Skewness*	0.68703
Mean	1,312.42109	*Skewness Standard Error*	0.21991
Mean LCL	1,224.35741	*Kurtosis*	2.60594
Mean UCL	1,400.48477	*Kurtosis Standard Error*	0.42897
Variance	165,927.56868	*Alternative Skewness (Fisher's)*	0.69583
Standard Deviation	407.34208	*Alternative Kurtosis (Fisher's)*	-0.35897
Mean Standard Error	37.34099	*Coefficient of Variation*	0.31037
Minimum	616.4	*Mean Deviation*	327.36143
Maximum	2,253.8	*Second Moment*	164,533.21936
Range	1,637.4	*Third Moment*	45,851,908.5498
Sum	156,178.11	*Fourth Moment*	7.05457E+10
Sum Standard Error	4,443.57746	*Median*	1,211.27
Total Sum Squares	224,550,898.8453	*Median Error*	4.29015
Adjusted Sum Squares	19,579,453.10436	*Percentile 25% (Q1)*	1,014.3
Geometric Mean	1,253.29974	*Percentile 75% (Q2)*	1,577.465
Harmonic Mean	1,197.7721	*IQR*	563.165
Mode	1,211.27	*MAD*	227.54

Melton ratio (-)

Count	119	*Skewness*	0.60213
Mean	0.55457	*Skewness Standard Error*	0.21991
Mean LCL	0.51613	*Kurtosis*	2.89884
Mean UCL	0.59301	*Kurtosis Standard Error*	0.42897
Variance	0.03162	*Alternative Skewness (Fisher's)*	0.60984
Standard Deviation	0.17782	*Alternative Kurtosis (Fisher's)*	-0.05338
Mean Standard Error	0.0163	*Coefficient of Variation*	0.32065
Minimum	0.22331	*Mean Deviation*	0.14228
Maximum	1.03981	*Second Moment*	0.03136
Range	0.8165	*Third Moment*	0.00334
Sum	65.99384	*Fourth Moment*	0.00285
Sum Standard Error	1.93981	*Median*	0.52566
Total Sum Squares	40.32945	*Median Error*	0.00187
Adjusted Sum Squares	3.73125	*Percentile 25% (Q1)*	0.4229
Geometric Mean	0.52696	*Percentile 75% (Q2)*	0.66125
Harmonic Mean	0.49975	*IQR*	0.23835
Mode	#N/A	*MAD*	0.11716

Mean slope (°)

Count	119	*Skewness*	0.16587
Mean	24.18477	*Skewness Standard Error*	0.21991
Mean LCL	23.32712	*Kurtosis*	2.63729
Mean UCL	25.04242	*Kurtosis Standard Error*	0.42897
Variance	15.73792	*Alternative Skewness (Fisher's)*	0.16799
Standard Deviation	3.96711	*Alternative Kurtosis (Fisher's)*	-0.32626
Mean Standard Error	0.36366	*Coefficient of Variation*	0.16403
Minimum	15.98658	*Mean Deviation*	3.25218
Maximum	34.58064	*Second Moment*	15.60567
Range	18.59406	*Third Moment*	10.22553
Sum	2,877.98788	*Fourth Moment*	642.27651
Sum Standard Error	43.27601	*Median*	24.39371
Total Sum Squares	71,460.55594	*Median Error*	0.04178
Adjusted Sum Squares	1,857.07496	*Percentile 25% (Q1)*	20.86299
Geometric Mean	23.85901	*Percentile 75% (Q2)*	26.5877
Harmonic Mean	23.52995	*IQR*	5.72471
Mode	#N/A	*MAD*	2.87982

Mean orientation (0-360)

Count	119	*Skewness*	0.15232
Mean	171.24891	*Skewness Standard Error*	0.21991
Mean LCL	162.16939	*Kurtosis*	2.2832
Mean UCL	180.32843	*Kurtosis Standard Error*	0.42897
Variance	1,763.80434	*Alternative Skewness (Fisher's)*	0.15427
Standard Deviation	41.99767	*Alternative Kurtosis (Fisher's)*	-0.69568
Mean Standard Error	3.84992	*Coefficient of Variation*	0.24524
Minimum	87.28545	*Mean Deviation*	35.0433
Maximum	270.9428	*Second Moment*	1,748.98245
Range	183.65735	*Third Moment*	11,141.46123
Sum	20,378.62002	*Fourth Moment*	6,984,182.90221
Sum Standard Error	458.1405	*Median*	165.6967
Total Sum Squares	3,697,945.33125	*Median Error*	0.44232
Adjusted Sum Squares	208,128.91176	*Percentile 25% (Q1)*	140.82765
Geometric Mean	165.99465	*Percentile 75% (Q2)*	206.72708
Harmonic Mean	160.63279	*IQR*	65.89943
Mode	#N/A	*MAD*	33.6454

Area (km2)

Count	119	*Skewness*	2.28995
Mean	2.21582	*Skewness Standard Error*	0.21991
Mean LCL	1.89887	*Kurtosis*	10.31682
Mean UCL	2.53277	*Kurtosis Standard Error*	0.42897
Variance	2.14939	*Alternative Skewness (Fisher's)*	2.31929
Standard Deviation	1.46608	*Alternative Kurtosis (Fisher's)*	7.68599
Mean Standard Error	0.1344	*Coefficient of Variation*	0.66164
Minimum	1.0058	*Mean Deviation*	1.05173
Maximum	10.26843	*Second Moment*	2.13133
Range	9.26263	*Third Moment*	7.12529
Sum	263.68258	*Fourth Moment*	46.86487
Sum Standard Error	15.99305	*Median*	1.71925
Total Sum Squares	837.90138	*Median Error*	0.01544
Adjusted Sum Squares	253.62827	*Percentile 25% (Q1)*	1.20646
Geometric Mean	1.89647	*Percentile 75% (Q2)*	2.63988
Harmonic Mean	1.68367	*IQR*	1.43342
Mode	#N/A	*MAD*	0.5901

Stream length (km)

Count	119	*Skewness*	1.53006
Mean	1.21762	*Skewness Standard Error*	0.21991
Mean LCL	0.98851	*Kurtosis*	6.0474
Mean UCL	1.44672	*Kurtosis Standard Error*	0.42897
Variance	1.12301	*Alternative Skewness (Fisher's)*	1.54966
Standard Deviation	1.05972	*Alternative Kurtosis (Fisher's)*	3.23159
Mean Standard Error	0.09714	*Coefficient of Variation*	0.87033
Minimum	0.0075	*Mean Deviation*	0.80913
Maximum	5.98267	*Second Moment*	1.11358
Range	5.97517	*Third Moment*	1.79799
Sum	144.89647	*Fourth Moment*	7.49911
Sum Standard Error	11.56022	*Median*	0.94534
Total Sum Squares	308.9442	*Median Error*	0.01116
Adjusted Sum Squares	132.51575	*Percentile 25% (Q1)*	0.40534
Geometric Mean	0.78157	*Percentile 75% (Q2)*	1.79123
Harmonic Mean	0.29826	*IQR*	1.38589
Mode	#N/A	*MAD*	0.61569

Perimeter (m)

Count	119	*Skewness*	1.39518
Mean	8,622.52101	*Skewness Standard Error*	0.21991
Mean LCL	8,063.13281	*Kurtosis*	5.30435
Mean UCL	9,181.90921	*Kurtosis Standard Error*	0.42897
Variance	6,695,013.92964	*Alternative Skewness (Fisher's)*	1.41306
Standard Deviation	2,587.4725	*Alternative Kurtosis (Fisher's)*	2.45636
Mean Standard Error	237.19322	*Coefficient of Variation*	0.30008
Minimum	5,480.	*Mean Deviation*	2,001.41233
Maximum	19,760.	*Second Moment*	6,638,753.30838
Range	14,280.	*Third Moment*	2.3865E+10
Sum	1,026,080.	*Fourth Moment*	2.33779E+14
Sum Standard Error	28,225.99259	*Median*	7,760.
Total Sum Squares	9,637,408,000.	*Median Error*	27.25139
Adjusted Sum Squares	790,011,643.69748	*Percentile 25% (Q1)*	6,800.
Geometric Mean	8,296.03004	*Percentile 75% (Q2)*	9,810.
Harmonic Mean	8,018.01056	*IQR*	3,010.
Mode	6,240.	*MAD*	1,440.

Form factor (-)

Count	119	*Skewness*	0.63019
Mean	0.4024	*Skewness Standard Error*	0.21991
Mean LCL	0.37381	*Kurtosis*	3.00529
Mean UCL	0.43099	*Kurtosis Standard Error*	0.42897
Variance	0.01749	*Alternative Skewness (Fisher's)*	0.63827
Standard Deviation	0.13223	*Alternative Kurtosis (Fisher's)*	0.05769
Mean Standard Error	0.01212	*Coefficient of Variation*	0.32861
Minimum	0.17129	*Mean Deviation*	0.10533
Maximum	0.7734	*Second Moment*	0.01734
Range	0.6021	*Third Moment*	0.00144
Sum	47.88564	*Fourth Moment*	0.0009
Sum Standard Error	1.44249	*Median*	0.39736
Total Sum Squares	21.33248	*Median Error*	0.00139
Adjusted Sum Squares	2.06329	*Percentile 25% (Q1)*	0.31083
Geometric Mean	0.38146	*Percentile 75% (Q2)*	0.47574
Harmonic Mean	0.36107	*IQR*	0.16491
Mode	#N/A	*MAD*	0.08642

Basin Elongation (-)

Count	119	*Skewness*	0.25568
Mean	0.70638	*Skewness Standard Error*	0.21991
Mean LCL	0.68127	*Kurtosis*	2.62305
Mean UCL	0.73149	*Kurtosis Standard Error*	0.42897
Variance	0.01349	*Alternative Skewness (Fisher's)*	0.25896
Standard Deviation	0.11615	*Alternative Kurtosis (Fisher's)*	-0.34111
Mean Standard Error	0.01065	*Coefficient of Variation*	0.16443
Minimum	0.46701	*Mean Deviation*	0.09428
Maximum	0.99233	*Second Moment*	0.01338
Range	0.52532	*Third Moment*	0.0004
Sum	84.05938	*Fourth Moment*	0.00047
Sum Standard Error	1.26704	*Median*	0.71129
Total Sum Squares	60.96989	*Median Error*	0.00122
Adjusted Sum Squares	1.59191	*Percentile 25% (Q1)*	0.6291
Geometric Mean	0.69692	*Percentile 75% (Q2)*	0.77829
Harmonic Mean	0.68745	*IQR*	0.14919
Mode	#N/A	*MAD*	0.08077

Lemniscate ratio (-)

Count	119	*Skewness*	0.91696
Mean	2.17518	*Skewness Standard Error*	0.21991
Mean LCL	2.01406	*Kurtosis*	3.62533
Mean UCL	2.3363	*Kurtosis Standard Error*	0.42897
Variance	0.55543	*Alternative Skewness (Fisher's)*	0.92871
Standard Deviation	0.74527	*Alternative Kurtosis (Fisher's)*	0.70459
Mean Standard Error	0.06832	*Coefficient of Variation*	0.34263
Minimum	1.01552	*Mean Deviation*	0.59039
Maximum	4.58508	*Second Moment*	0.55076
Range	3.56957	*Third Moment*	0.3748
Sum	258.84674	*Fourth Moment*	1.09971
Sum Standard Error	8.12997	*Median*	1.97655
Total Sum Squares	628.57992	*Median Error*	0.00785
Adjusted Sum Squares	65.54095	*Percentile 25% (Q1)*	1.65891
Geometric Mean	2.05892	*Percentile 75% (Q2)*	2.55376
Harmonic Mean	1.95178	*IQR*	0.89485
Mode	#N/A	*MAD*	0.44391

Outlet slope (°)

Count	119	*Skewness*	1.08681
Mean	9.51176	*Skewness Standard Error*	0.21991
Mean LCL	8.30254	*Kurtosis*	5.1071
Mean UCL	10.72099	*Kurtosis Standard Error*	0.42897
Variance	31.28543	*Alternative Skewness (Fisher's)*	1.10074
Standard Deviation	5.59334	*Alternative Kurtosis (Fisher's)*	2.25055
Mean Standard Error	0.51274	*Coefficient of Variation*	0.58804
Minimum	0.53	*Mean Deviation*	4.38288
Maximum	33.6	*Second Moment*	31.02253
Range	33.07	*Third Moment*	187.7892
Sum	1,131.9	*Fourth Moment*	4,915.05925
Sum Standard Error	61.01612	*Median*	8.86
Total Sum Squares	14,458.0476	*Median Error*	0.05891
Adjusted Sum Squares	3,691.68113	*Percentile 25% (Q1)*	5.29
Geometric Mean	7.76508	*Percentile 75% (Q2)*	12.57
Harmonic Mean	5.45395	*IQR*	7.28
Mode	#N/A	*MAD*	3.57

200m slope (°)

Count	119	*Skewness*	1.02806
Mean	9.53353	*Skewness Standard Error*	0.21991
Mean LCL	8.34391	*Kurtosis*	4.63923
Mean UCL	10.72315	*Kurtosis Standard Error*	0.42897
Variance	30.27892	*Alternative Skewness (Fisher's)*	1.04123
Standard Deviation	5.50263	*Alternative Kurtosis (Fisher's)*	1.76241
Mean Standard Error	0.50443	*Coefficient of Variation*	0.57719
Minimum	0.51	*Mean Deviation*	4.18907
Maximum	31.62	*Second Moment*	30.02448
Range	31.11	*Third Moment*	169.13377
Sum	1,134.49	*Fourth Moment*	4,182.12068
Sum Standard Error	60.02659	*Median*	8.73
Total Sum Squares	14,388.6067	*Median Error*	0.05795
Adjusted Sum Squares	3,572.91292	*Percentile 25% (Q1)*	5.5175
Geometric Mean	7.82272	*Percentile 75% (Q2)*	12.175
Harmonic Mean	5.4845	*IQR*	6.6575
Mode	#N/A	*MAD*	3.33

Average slope (°)

Count	119	*Skewness*	0.83378
Mean	10.44933	*Skewness Standard Error*	0.21991
Mean LCL	9.34486	*Kurtosis*	4.48015
Mean UCL	11.5538	*Kurtosis Standard Error*	0.42897
Variance	26.09941	*Alternative Skewness (Fisher's)*	0.84446
Standard Deviation	5.10876	*Alternative Kurtosis (Fisher's)*	1.59644
Mean Standard Error	0.46832	*Coefficient of Variation*	0.48891
Minimum	0.64	*Mean Deviation*	3.90718
Maximum	30.21	*Second Moment*	25.88009
Range	29.57	*Third Moment*	109.77363
Sum	1,243.47	*Fourth Moment*	3,000.70972
Sum Standard Error	55.72998	*Median*	9.61
Total Sum Squares	16,073.1565	*Median Error*	0.05381
Adjusted Sum Squares	3,079.73095	*Percentile 25% (Q1)*	7.215
Geometric Mean	8.98086	*Percentile 75% (Q2)*	13.15
Harmonic Mean	6.61482	*IQR*	5.935
Mode	#N/A	*MAD*	3.12

1st-order catchments - Training set – Mollo - Reactive catchments

Max. elevation (m asl)			
Count	33	*Skewness*	0.25073
Mean	2,321.83212	*Skewness Standard Error*	0.39606
Mean LCL	2,191.53509	*Kurtosis*	1.79023
Mean UCL	2,452.12915	*Kurtosis Standard Error*	0.72512
Variance	93,437.18141	*Alternative Skewness (Fisher's)*	0.26283
Standard Deviation	305.67496	*Alternative Kurtosis (Fisher's)*	-1.20884
Mean Standard Error	53.21118	*Coefficient of Variation*	0.13165
Minimum	1,921.87	*Mean Deviation*	270.84279
Maximum	2,895.08	*Second Moment*	90,605.75167
Range	973.21	*Third Moment*	6,838,253.01244
Sum	76,620.46	*Fourth Moment*	1.46968E+10
Sum Standard Error	1,755.96896	*Median*	2,299.89
Total Sum Squares	180,889,834.9752	*Median Error*	11.6093
Adjusted Sum Squares	2,989,989.80515	*Percentile 25% (Q1)*	2,021.7775
Geometric Mean	2,302.5463	*Percentile 75% (Q2)*	2,584.76
Harmonic Mean	2,283.61624	*IQR*	562.9825
Mode	#N/A	*MAD*	285.94
Mean elevation (m asl)			
Count	33	*Skewness*	0.68087
Mean	1,897.93997	*Skewness Standard Error*	0.39606
Mean LCL	1,777.23995	*Kurtosis*	2.32634
Mean UCL	2,018.63999	*Kurtosis Standard Error*	0.72512
Variance	80,179.87664	*Alternative Skewness (Fisher's)*	0.71373
Standard Deviation	283.16051	*Alternative Kurtosis (Fisher's)*	-0.58165
Mean Standard Error	49.29192	*Coefficient of Variation*	0.14919
Minimum	1,574.201	*Mean Deviation*	236.93069
Maximum	2,541.106	*Second Moment*	77,750.18341
Range	966.905	*Third Moment*	14,761,047.80146
Sum	62,632.019	*Fourth Moment*	1.4063E+10
Sum Standard Error	1,626.63331	*Median*	1,819.962
Total Sum Squares	121,437,568.29548	*Median Error*	10.75421
Adjusted Sum Squares	2,565,756.05255	*Percentile 25% (Q1)*	1,679.92125
Geometric Mean	1,878.47782	*Percentile 75% (Q2)*	2,173.536
Harmonic Mean	1,860.10928	*IQR*	493.61475
Mode	#N/A	*MAD*	205.747
Min. elevation (m asl)			
Count	33	*Skewness*	1.20806
Mean	1,413.69424	*Skewness Standard Error*	0.39606
Mean LCL	1,286.85769	*Kurtosis*	3.82921
Mean UCL	1,540.5308	*Kurtosis Standard Error*	0.72512
Variance	88,540.01328	*Alternative Skewness (Fisher's)*	1.26637
Standard Deviation	297.55674	*Alternative Kurtosis (Fisher's)*	1.17653
Mean Standard Error	51.79798	*Coefficient of Variation*	0.21048
Minimum	1,042.26	*Mean Deviation*	233.44419
Maximum	2,253.47	*Second Moment*	85,856.98258
Range	1,211.21	*Third Moment*	30,391,517.64707
Sum	46,651.91	*Fourth Moment*	2.82267E+10
Sum Standard Error	1,709.33333	*Median*	1,319.22
Total Sum Squares	68,784,816.9901	*Median Error*	11.30097
Adjusted Sum Squares	2,833,280.42501	*Percentile 25% (Q1)*	1,211.27
Geometric Mean	1,386.79685	*Percentile 75% (Q2)*	1,587.33
Harmonic Mean	1,363.03812	*IQR*	376.06
Mode	1,211.27	*MAD*	137.

Melton ratio (-)

Count	33	*Skewness*	0.33003
Mean	0.59285	*Skewness Standard Error*	0.39606
Mean LCL	0.51013	*Kurtosis*	1.8699
Mean UCL	0.67557	*Kurtosis Standard Error*	0.72512
Variance	0.03766	*Alternative Skewness (Fisher's)*	0.34596
Standard Deviation	0.19407	*Alternative Kurtosis (Fisher's)*	-1.11564
Mean Standard Error	0.03378	*Coefficient of Variation*	0.32734
Minimum	0.31173	*Mean Deviation*	0.16826
Maximum	0.97064	*Second Moment*	0.03652
Range	0.6589	*Third Moment*	0.0023
Sum	19.56409	*Fourth Moment*	0.00249
Sum Standard Error	1.11482	*Median*	0.52566
Total Sum Squares	12.80377	*Median Error*	0.00737
Adjusted Sum Squares	1.20517	*Percentile 25% (Q1)*	0.4575
Geometric Mean	0.5622	*Percentile 75% (Q2)*	0.77323
Harmonic Mean	0.5328	*IQR*	0.31574
Mode	#N/A	*MAD*	0.15115

Mean slope (°)

Count	33	*Skewness*	0.63401
Mean	25.98674	*Skewness Standard Error*	0.39606
Mean LCL	24.45175	*Kurtosis*	2.93455
Mean UCL	27.52173	*Kurtosis Standard Error*	0.72512
Variance	12.96769	*Alternative Skewness (Fisher's)*	0.66461
Standard Deviation	3.60107	*Alternative Kurtosis (Fisher's)*	0.12988
Mean Standard Error	0.62687	*Coefficient of Variation*	0.13857
Minimum	20.697	*Mean Deviation*	2.73048
Maximum	34.58064	*Second Moment*	12.57473
Range	13.88364	*Third Moment*	28.27104
Sum	857.56247	*Fourth Moment*	464.02241
Sum Standard Error	20.68656	*Median*	25.5827
Total Sum Squares	22,700.22028	*Median Error*	0.13677
Adjusted Sum Squares	414.96604	*Percentile 25% (Q1)*	23.68362
Geometric Mean	25.75392	*Percentile 75% (Q2)*	28.70838
Harmonic Mean	25.52987	*IQR*	5.02477
Mode	#N/A	*MAD*	2.43261

Mean orientation (0-360)

Count	33	*Skewness*	0.21053
Mean	171.10494	*Skewness Standard Error*	0.39606
Mean LCL	150.07678	*Kurtosis*	2.00377
Mean UCL	192.13311	*Kurtosis Standard Error*	0.72512
Variance	2,433.62464	*Alternative Skewness (Fisher's)*	0.22069
Standard Deviation	49.33178	*Alternative Kurtosis (Fisher's)*	-0.95902
Mean Standard Error	8.58756	*Coefficient of Variation*	0.28831
Minimum	87.28545	*Mean Deviation*	42.16071
Maximum	265.7154	*Second Moment*	2,359.87844
Range	178.42995	*Third Moment*	24,135.38343
Sum	5,646.46316	*Fourth Moment*	11,159,075.17109
Sum Standard Error	283.38951	*Median*	162.0569
Total Sum Squares	1,044,013.75262	*Median Error*	1.87358
Adjusted Sum Squares	77,875.98846	*Percentile 25% (Q1)*	132.83128
Geometric Mean	164.06689	*Percentile 75% (Q2)*	215.13338
Harmonic Mean	157.03675	*IQR*	82.3021
Mode	#N/A	*MAD*	44.3875

Area (km2)

Count	33	*Skewness*	1.56434
Mean	3.01142	*Skewness Standard Error*	0.39606
Mean LCL	2.12708	*Kurtosis*	5.6876
Mean UCL	3.89576	*Kurtosis Standard Error*	0.72512
Variance	4.30414	*Alternative Skewness (Fisher's)*	1.63984
Standard Deviation	2.07464	*Alternative Kurtosis (Fisher's)*	3.35066
Mean Standard Error	0.36115	*Coefficient of Variation*	0.68893
Minimum	1.01745	*Mean Deviation*	1.59484
Maximum	10.26843	*Second Moment*	4.17372
Range	9.25098	*Third Moment*	13.33875
Sum	99.37678	*Fourth Moment*	99.07754
Sum Standard Error	11.91792	*Median*	2.1588
Total Sum Squares	436.99759	*Median Error*	0.07879
Adjusted Sum Squares	137.73264	*Percentile 25% (Q1)*	1.60073
Geometric Mean	2.47343	*Percentile 75% (Q2)*	4.06951
Harmonic Mean	2.08119	*IQR*	2.46879
Mode	#N/A	*MAD*	1.08478

Stream length (km)

Count	33	*Skewness*	1.14696
Mean	1.61269	*Skewness Standard Error*	0.39606
Mean LCL	1.03291	*Kurtosis*	4.42494
Mean UCL	2.19248	*Kurtosis Standard Error*	0.72512
Variance	1.85005	*Alternative Skewness (Fisher's)*	1.20231
Standard Deviation	1.36016	*Alternative Kurtosis (Fisher's)*	1.87348
Mean Standard Error	0.23677	*Coefficient of Variation*	0.84341
Minimum	0.09528	*Mean Deviation*	1.06259
Maximum	5.98267	*Second Moment*	1.79398
Range	5.88739	*Third Moment*	2.75598
Sum	53.21891	*Fourth Moment*	14.24114
Sum Standard Error	7.81355	*Median*	1.43635
Total Sum Squares	145.02733	*Median Error*	0.05166
Adjusted Sum Squares	59.20149	*Percentile 25% (Q1)*	0.50723
Geometric Mean	1.00283	*Percentile 75% (Q2)*	2.38777
Harmonic Mean	0.49715	*IQR*	1.88054
Mode	#N/A	*MAD*	0.97755

Perimeter (m)

Count	33	*Skewness*	0.93091
Mean	9,614.54545	*Skewness Standard Error*	0.39606
Mean LCL	8,196.66955	*Kurtosis*	3.69869
Mean UCL	11,032.42136	*Kurtosis Standard Error*	0.72512
Variance	11,064,381.81818	*Alternative Skewness (Fisher's)*	0.97583
Standard Deviation	3,326.31655	*Alternative Kurtosis (Fisher's)*	1.02385
Mean Standard Error	579.03739	*Coefficient of Variation*	0.34597
Minimum	5,480.	*Mean Deviation*	2,684.95868
Maximum	19,760.	*Second Moment*	10,729,097.52066
Range	14,280.	*Third Moment*	3.27152E+10
Sum	317,280.	*Fourth Moment*	4.2577E+14
Sum Standard Error	19,108.23383	*Median*	9,360.
Total Sum Squares	3,404,563,200.	*Median Error*	126.3309
Adjusted Sum Squares	354,060,218.18182	*Percentile 25% (Q1)*	6,920.
Geometric Mean	9,108.85319	*Percentile 75% (Q2)*	12,210.
Harmonic Mean	8,657.94269	*IQR*	5,290.
Mode	#N/A	*MAD*	2,480.

Form factor (-)

Count	33	*Skewness*	0.06355
Mean	0.42481	*Skewness Standard Error*	0.39606
Mean LCL	0.37484	*Kurtosis*	1.78807
Mean UCL	0.47478	*Kurtosis Standard Error*	0.72512
Variance	0.01374	*Alternative Skewness (Fisher's)*	0.06662
Standard Deviation	0.11723	*Alternative Kurtosis (Fisher's)*	-1.21138
Mean Standard Error	0.02041	*Coefficient of Variation*	0.27596
Minimum	0.2392	*Mean Deviation*	0.10173
Maximum	0.6337	*Second Moment*	0.01333
Range	0.3945	*Third Moment*	0.0001
Sum	14.01867	*Fourth Moment*	0.00032
Sum Standard Error	0.67344	*Median*	0.43382
Total Sum Squares	6.39503	*Median Error*	0.00445
Adjusted Sum Squares	0.43978	*Percentile 25% (Q1)*	0.31621
Geometric Mean	0.40853	*Percentile 75% (Q2)*	0.51062
Harmonic Mean	0.39214	*IQR*	0.19442
Mode	#N/A	*MAD*	0.10573

Basin Elongation (-)

Count	33	*Skewness*	-0.09491
Mean	0.72843	*Skewness Standard Error*	0.39606
Mean LCL	0.68454	*Kurtosis*	1.75758
Mean UCL	0.77231	*Kurtosis Standard Error*	0.72512
Variance	0.0106	*Alternative Skewness (Fisher's)*	-0.09949
Standard Deviation	0.10295	*Alternative Kurtosis (Fisher's)*	-1.24704
Mean Standard Error	0.01792	*Coefficient of Variation*	0.14133
Minimum	0.55187	*Mean Deviation*	0.08961
Maximum	0.89825	*Second Moment*	0.01028
Range	0.34638	*Third Moment*	-0.0001
Sum	24.03808	*Fourth Moment*	0.00019
Sum Standard Error	0.5914	*Median*	0.7432
Total Sum Squares	17.84913	*Median Error*	0.00391
Adjusted Sum Squares	0.33915	*Percentile 25% (Q1)*	0.6345
Geometric Mean	0.72122	*Percentile 75% (Q2)*	0.80631
Harmonic Mean	0.71392	*IQR*	0.17181
Mode	#N/A	*MAD*	0.09162

Lemniscate ratio (-)

Count	33	*Skewness*	0.56719
Mean	2.00284	*Skewness Standard Error*	0.39606
Mean LCL	1.7502	*Kurtosis*	2.10957
Mean UCL	2.25547	*Kurtosis Standard Error*	0.72512
Variance	0.35127	*Alternative Skewness (Fisher's)*	0.59456
Standard Deviation	0.59268	*Alternative Kurtosis (Fisher's)*	-0.83526
Mean Standard Error	0.10317	*Coefficient of Variation*	0.29592
Minimum	1.23938	*Mean Deviation*	0.51489
Maximum	3.28346	*Second Moment*	0.34062
Range	2.04408	*Third Moment*	0.11275
Sum	66.09367	*Fourth Moment*	0.24476
Sum Standard Error	3.40467	*Median*	1.81044
Total Sum Squares	143.61548	*Median Error*	0.02251
Adjusted Sum Squares	11.24053	*Percentile 25% (Q1)*	1.55545
Geometric Mean	1.92249	*Percentile 75% (Q2)*	2.51988
Harmonic Mean	1.84883	*IQR*	0.96444
Mode	#N/A	*MAD*	0.43198

Outlet slope (°)

Count	33	*Skewness*	1.45213
Mean	10.50576	*Skewness Standard Error*	0.39606
Mean LCL	7.49289	*Kurtosis*	5.15987
Mean UCL	13.51862	*Kurtosis Standard Error*	0.72512
Variance	49.95862	*Alternative Skewness (Fisher's)*	1.52222
Standard Deviation	7.06814	*Alternative Kurtosis (Fisher's)*	2.73327
Mean Standard Error	1.23041	*Coefficient of Variation*	0.67279
Minimum	2.5	*Mean Deviation*	4.95001
Maximum	33.6	*Second Moment*	48.44472
Range	31.1	*Third Moment*	489.63909
Sum	346.69	*Fourth Moment*	12,109.65487
Sum Standard Error	40.60338	*Median*	10.05
Total Sum Squares	5,240.9169	*Median Error*	0.26844
Adjusted Sum Squares	1,598.67581	*Percentile 25% (Q1)*	5.94
Geometric Mean	8.55504	*Percentile 75% (Q2)*	12.3
Harmonic Mean	6.91217	*IQR*	6.36
Mode	#N/A	*MAD*	3.66

200m slope (°)

Count	33	*Skewness*	1.52754
Mean	9.8297	*Skewness Standard Error*	0.39606
Mean LCL	6.99806	*Kurtosis*	5.43067
Mean UCL	12.66133	*Kurtosis Standard Error*	0.72512
Variance	44.12917	*Alternative Skewness (Fisher's)*	1.60126
Standard Deviation	6.64298	*Alternative Kurtosis (Fisher's)*	3.05007
Mean Standard Error	1.15639	*Coefficient of Variation*	0.67581
Minimum	2.39	*Mean Deviation*	4.73965
Maximum	31.62	*Second Moment*	42.79192
Range	29.23	*Third Moment*	427.5975
Sum	324.38	*Fourth Moment*	9,944.36256
Sum Standard Error	38.16101	*Median*	9.42
Total Sum Squares	4,600.6904	*Median Error*	0.2523
Adjusted Sum Squares	1,412.1333	*Percentile 25% (Q1)*	5.105
Geometric Mean	8.05475	*Percentile 75% (Q2)*	12.
Harmonic Mean	6.62608	*IQR*	6.895
Mode	3.29	*MAD*	4.3

Average slope (°)

Count	33	*Skewness*	0.88258
Mean	11.12333	*Skewness Standard Error*	0.39606
Mean LCL	8.75334	*Kurtosis*	3.21755
Mean UCL	13.49333	*Kurtosis Standard Error*	0.72512
Variance	30.91325	*Alternative Skewness (Fisher's)*	0.92518
Standard Deviation	5.55997	*Alternative Kurtosis (Fisher's)*	0.46096
Mean Standard Error	0.96787	*Coefficient of Variation*	0.49985
Minimum	2.86	*Mean Deviation*	4.23636
Maximum	26.21	*Second Moment*	29.97648
Range	23.35	*Third Moment*	144.85271
Sum	367.07	*Fourth Moment*	2,891.25749
Sum Standard Error	31.93959	*Median*	9.61
Total Sum Squares	5,072.2659	*Median Error*	0.21116
Adjusted Sum Squares	989.22393	*Percentile 25% (Q1)*	8.1775
Geometric Mean	9.8441	*Percentile 75% (Q2)*	14.56
Harmonic Mean	8.61181	*IQR*	6.3825
Mode	5.43	*MAD*	2.09

1st-order catchments - Training set – NWCat - all catchments.

Max. elevation (m asl)			
Count	446	*Skewness*	-0.55389
Mean	2,390.19563	*Skewness Standard Error*	0.11534
Mean LCL	2,344.96258	*Kurtosis*	2.52907
Mean UCL	2,435.42867	*Kurtosis Standard Error*	0.22914
Variance	167,402.99986	*Alternative Skewness (Fisher's)*	-0.55576
Standard Deviation	409.14912	*Alternative Kurtosis (Fisher's)*	-0.46268
Mean Standard Error	19.37377	*Coefficient of Variation*	0.17118
Minimum	1,242.57	*Mean Deviation*	343.39965
Maximum	3,027.67	*Second Moment*	167,027.65682
Range	1,785.1	*Third Moment*	-37,809,757.20552
Sum	1,066,027.25	*Fourth Moment*	7.05565E+10
Sum Standard Error	8,640.7024	*Median*	2,454.82
Total Sum Squares	2,622,508,007.0083	*Median Error*	1.14976
Adjusted Sum Squares	74,494,334.93977	*Percentile 25% (Q1)*	2,082.535
Geometric Mean	2,351.66738	*Percentile 75% (Q2)*	2,746.685
Harmonic Mean	2,309.11947	*IQR*	664.15
Mode	2,850.46	*MAD*	310.6
Mean elevation (m asl)			
Count	446	*Skewness*	-0.29759
Mean	1,941.97299	*Skewness Standard Error*	0.11534
Mean LCL	1,896.09187	*Kurtosis*	2.10817
Mean UCL	1,987.85411	*Kurtosis Standard Error*	0.22914
Variance	172,234.29022	*Alternative Skewness (Fisher's)*	-0.2986
Standard Deviation	415.01119	*Alternative Kurtosis (Fisher's)*	-0.88833
Mean Standard Error	19.65135	*Coefficient of Variation*	0.21371
Minimum	934.8588	*Mean Deviation*	353.28297
Maximum	2,671.48	*Second Moment*	171,848.11468
Range	1,736.6212	*Third Moment*	-21,199,983.57866
Sum	866,119.953	*Fourth Moment*	6.2258E+10
Sum Standard Error	8,764.50189	*Median*	1,961.291
Total Sum Squares	1,758,625,812.92627	*Median Error*	1.16623
Adjusted Sum Squares	76,644,259.14887	*Percentile 25% (Q1)*	1,626.09
Geometric Mean	1,893.77773	*Percentile 75% (Q2)*	2,293.0205
Harmonic Mean	1,841.6203	*IQR*	666.9305
Mode	#N/A	*MAD*	334.4535
Min. elevation (m asl)			
Count	446	*Skewness*	0.29466
Mean	1,449.30496	*Skewness Standard Error*	0.11534
Mean LCL	1,399.85198	*Kurtosis*	2.01146
Mean UCL	1,498.75793	*Kurtosis Standard Error*	0.22914
Variance	200,095.04461	*Alternative Skewness (Fisher's)*	0.29566
Standard Deviation	447.31985	*Alternative Kurtosis (Fisher's)*	-0.98614
Mean Standard Error	21.18121	*Coefficient of Variation*	0.30864
Minimum	667.96	*Mean Deviation*	380.65154
Maximum	2,426.05	*Second Moment*	199,646.40101
Range	1,758.09	*Third Moment*	26,285,512.98867
Sum	646,390.01	*Fourth Moment*	8.0174E+10
Sum Standard Error	9,446.81904	*Median*	1,394.425
Total Sum Squares	1,025,858,539.3065	*Median Error*	1.25702
Adjusted Sum Squares	89,042,294.84955	*Percentile 25% (Q1)*	1,085.205
Geometric Mean	1,379.77624	*Percentile 75% (Q2)*	1,823.235
Harmonic Mean	1,311.28664	*IQR*	738.03
Mode	934.81	*MAD*	338.94

Melton ratio (-)

Count	446	*Skewness*	0.57616
Mean	0.6683	*Skewness Standard Error*	0.11534
Mean LCL	0.64462	*Kurtosis*	3.09285
Mean UCL	0.69198	*Kurtosis Standard Error*	0.22914
Variance	0.04587	*Alternative Skewness (Fisher's)*	0.5781
Standard Deviation	0.21417	*Alternative Kurtosis (Fisher's)*	0.10747
Mean Standard Error	0.01014	*Coefficient of Variation*	0.32047
Minimum	0.17954	*Mean Deviation*	0.17224
Maximum	1.3812	*Second Moment*	0.04576
Range	1.20166	*Third Moment*	0.00564
Sum	298.0618	*Fourth Moment*	0.00648
Sum Standard Error	4.52293	*Median*	0.6491
Total Sum Squares	219.60574	*Median Error*	0.0006
Adjusted Sum Squares	20.41104	*Percentile 25% (Q1)*	0.49862
Geometric Mean	0.63442	*Percentile 75% (Q2)*	0.80066
Harmonic Mean	0.60039	*IQR*	0.30204
Mode	#N/A	*MAD*	0.15076

Mean slope (°)

Count	446	*Skewness*	-0.05107
Mean	27.69303	*Skewness Standard Error*	0.11534
Mean LCL	27.12941	*Kurtosis*	2.79687
Mean UCL	28.25664	*Kurtosis Standard Error*	0.22914
Variance	25.99071	*Alternative Skewness (Fisher's)*	-0.05125
Standard Deviation	5.09811	*Alternative Kurtosis (Fisher's)*	-0.19185
Mean Standard Error	0.2414	*Coefficient of Variation*	0.18409
Minimum	11.54949	*Mean Deviation*	4.12094
Maximum	41.77694	*Second Moment*	25.93243
Range	30.22745	*Third Moment*	-6.74484
Sum	12,351.09094	*Fourth Moment*	1,880.86836
Sum Standard Error	107.66548	*Median*	27.81966
Total Sum Squares	353,604.98509	*Median Error*	0.01433
Adjusted Sum Squares	11,565.86534	*Percentile 25% (Q1)*	23.97541
Geometric Mean	27.20064	*Percentile 75% (Q2)*	31.00414
Harmonic Mean	26.67594	*IQR*	7.02873
Mode	#N/A	*MAD*	3.6335

Mean orientation (0-360)

Count	446	*Skewness*	0.1758
Mean	172.85534	*Skewness Standard Error*	0.11534
Mean LCL	166.69619	*Kurtosis*	1.96458
Mean UCL	179.0145	*Kurtosis Standard Error*	0.22914
Variance	3,103.79704	*Alternative Skewness (Fisher's)*	0.1764
Standard Deviation	55.71173	*Alternative Kurtosis (Fisher's)*	-1.03354
Mean Standard Error	2.63803	*Coefficient of Variation*	0.3223
Minimum	67.38541	*Mean Deviation*	47.76291
Maximum	293.9064	*Second Moment*	3,096.83785
Range	226.52099	*Third Moment*	30,297.51541
Sum	77,093.48379	*Fourth Moment*	18,841,151.10246
Sum Standard Error	1,176.56002	*Median*	166.
Total Sum Squares	14,707,210.40624	*Median Error*	0.15656
Adjusted Sum Squares	1,381,189.6823	*Percentile 25% (Q1)*	126.4209
Geometric Mean	163.50568	*Percentile 75% (Q2)*	218.112
Harmonic Mean	153.98367	*IQR*	91.6911
Mode	#N/A	*MAD*	43.85115

Area (km2)

Count	446	*Skewness*	2.84551
Mean	2.32317	*Skewness Standard Error*	0.11534
Mean LCL	2.15149	*Kurtosis*	14.70776
Mean UCL	2.49485	*Kurtosis Standard Error*	0.22914
Variance	2.41144	*Alternative Skewness (Fisher's)*	2.85513
Standard Deviation	1.55288	*Alternative Kurtosis (Fisher's)*	11.85365
Mean Standard Error	0.07353	*Coefficient of Variation*	0.66843
Minimum	1.00243	*Mean Deviation*	1.04672
Maximum	13.05238	*Second Moment*	2.40604
Range	12.04995	*Third Moment*	10.61974
Sum	1,036.13338	*Fourth Moment*	85.1433
Sum Standard Error	32.79487	*Median*	1.83124
Total Sum Squares	3,480.20476	*Median Error*	0.00436
Adjusted Sum Squares	1,073.09182	*Percentile 25% (Q1)*	1.33698
Geometric Mean	2.00331	*Percentile 75% (Q2)*	2.73986
Harmonic Mean	1.79126	*IQR*	1.40289
Mode	#N/A	*MAD*	0.61468

Stream length (km)

Count	446	*Skewness*	1.76612
Mean	1.35014	*Skewness Standard Error*	0.11534
Mean LCL	1.22166	*Kurtosis*	7.11897
Mean UCL	1.47862	*Kurtosis Standard Error*	0.22914
Variance	1.3506	*Alternative Skewness (Fisher's)*	1.77209
Standard Deviation	1.16215	*Alternative Kurtosis (Fisher's)*	4.17909
Mean Standard Error	0.05503	*Coefficient of Variation*	0.86076
Minimum	0.005	*Mean Deviation*	0.8458
Maximum	7.21949	*Second Moment*	1.34757
Range	7.21449	*Third Moment*	2.76279
Sum	602.16236	*Fourth Moment*	12.92765
Sum Standard Error	24.54316	*Median*	1.08739
Total Sum Squares	1,414.01967	*Median Error*	0.00327
Adjusted Sum Squares	601.01629	*Percentile 25% (Q1)*	0.52851
Geometric Mean	0.87892	*Percentile 75% (Q2)*	1.75768
Harmonic Mean	0.32085	*IQR*	1.22917
Mode	0.087	*MAD*	0.61555

Perimeter (m)

Count	446	*Skewness*	1.72522
Mean	9,075.33632	*Skewness Standard Error*	0.11534
Mean LCL	8,775.71578	*Kurtosis*	7.41369
Mean UCL	9,374.95686	*Kurtosis Standard Error*	0.22914
Variance	7,345,049.66191	*Alternative Skewness (Fisher's)*	1.73105
Standard Deviation	2,710.17521	*Alternative Kurtosis (Fisher's)*	4.47715
Mean Standard Error	128.33052	*Coefficient of Variation*	0.29863
Minimum	5,120.	*Mean Deviation*	1,983.21141
Maximum	22,600.	*Second Moment*	7,328,580.9407
Range	17,480.	*Third Moment*	3.42275E+10
Sum	4,047,600.	*Fourth Moment*	3.98175E+14
Sum Standard Error	57,235.40992	*Median*	8,520.
Total Sum Squares	4.00019E+10	*Median Error*	7.61592
Adjusted Sum Squares	3,268,547,099.55157	*Percentile 25% (Q1)*	7,240.
Geometric Mean	8,741.97601	*Percentile 75% (Q2)*	10,320.
Harmonic Mean	8,458.80418	*IQR*	3,080.
Mode	#N/A	*MAD*	1,460.

Form factor (-)

Count	446	*Skewness*	0.34879
Mean	0.41197	*Skewness Standard Error*	0.11534
Mean LCL	0.39772	*Kurtosis*	2.64993
Mean UCL	0.42621	*Kurtosis Standard Error*	0.22914
Variance	0.0166	*Alternative Skewness (Fisher's)*	0.34997
Standard Deviation	0.12884	*Alternative Kurtosis (Fisher's)*	-0.34045
Mean Standard Error	0.0061	*Coefficient of Variation*	0.31275
Minimum	0.14224	*Mean Deviation*	0.1049
Maximum	0.76279	*Second Moment*	0.01656
Range	0.62054	*Third Moment*	0.00074
Sum	183.73678	*Fourth Moment*	0.00073
Sum Standard Error	2.72098	*Median*	0.40575
Total Sum Squares	83.08041	*Median Error*	0.00036
Adjusted Sum Squares	7.38712	*Percentile 25% (Q1)*	0.31488
Geometric Mean	0.39128	*Percentile 75% (Q2)*	0.50021
Harmonic Mean	0.36989	*IQR*	0.18533
Mode	#N/A	*MAD*	0.09242

Basin Elongation (-)

Count	446	*Skewness*	-0.01369
Mean	0.7152	*Skewness Standard Error*	0.11534
Mean LCL	0.70257	*Kurtosis*	2.52923
Mean UCL	0.72783	*Kurtosis Standard Error*	0.22914
Variance	0.01305	*Alternative Skewness (Fisher's)*	-0.01373
Standard Deviation	0.11426	*Alternative Kurtosis (Fisher's)*	-0.46251
Mean Standard Error	0.00541	*Coefficient of Variation*	0.15975
Minimum	0.42557	*Mean Deviation*	0.09329
Maximum	0.9855	*Second Moment*	0.01303
Range	0.55993	*Third Moment*	-0.00002
Sum	318.97766	*Fourth Moment*	0.00043
Sum Standard Error	2.41294	*Median*	0.71876
Total Sum Squares	233.94094	*Median Error*	0.00032
Adjusted Sum Squares	5.80922	*Percentile 25% (Q1)*	0.63318
Geometric Mean	0.70583	*Percentile 75% (Q2)*	0.79805
Harmonic Mean	0.69616	*IQR*	0.16487
Mode	#N/A	*MAD*	0.08154

Lemniscate ratio (-)

Count	446	*Skewness*	1.30806
Mean	2.12335	*Skewness Standard Error*	0.11534
Mean LCL	2.03947	*Kurtosis*	5.11932
Mean UCL	2.20723	*Kurtosis Standard Error*	0.22914
Variance	0.57565	*Alternative Skewness (Fisher's)*	1.31248
Standard Deviation	0.75871	*Alternative Kurtosis (Fisher's)*	2.15685
Mean Standard Error	0.03593	*Coefficient of Variation*	0.35732
Minimum	1.02964	*Mean Deviation*	0.58077
Maximum	5.52151	*Second Moment*	0.57436
Range	4.49187	*Third Moment*	0.56938
Sum	947.01346	*Fourth Moment*	1.68879
Sum Standard Error	16.02306	*Median*	1.93569
Total Sum Squares	2,267.00243	*Median Error*	0.00213
Adjusted Sum Squares	256.16275	*Percentile 25% (Q1)*	1.57613
Geometric Mean	2.00727	*Percentile 75% (Q2)*	2.5066
Harmonic Mean	1.90646	*IQR*	0.93048
Mode	#N/A	*MAD*	0.42298

Outlet slope (°)

Count	446	*Skewness*	0.62837
Mean	9.26547	*Skewness Standard Error*	0.11534
Mean LCL	8.4691	*Kurtosis*	3.04303
Mean UCL	10.06184	*Kurtosis Standard Error*	0.22914
Variance	51.88959	*Alternative Skewness (Fisher's)*	0.63049
Standard Deviation	7.20344	*Alternative Kurtosis (Fisher's)*	0.05709
Mean Standard Error	0.34109	*Coefficient of Variation*	0.77745
Minimum	0.E+0	*Mean Deviation*	5.92486
Maximum	34.47	*Second Moment*	51.77324
Range	34.47	*Third Moment*	234.08363
Sum	4,132.4	*Fourth Moment*	8,156.75237
Sum Standard Error	152.12743	*Median*	8.755
Total Sum Squares	61,379.4974	*Median Error*	0.02024
Adjusted Sum Squares	23,090.86565	*Percentile 25% (Q1)*	2.875
Geometric Mean	5.91627	*Percentile 75% (Q2)*	14.485
Harmonic Mean	3.39442	*IQR*	11.61
Mode	0.E+0	*MAD*	5.875

200m slope (°)

Count	446	*Skewness*	0.5541
Mean	9.8722	*Skewness Standard Error*	0.11534
Mean LCL	9.06906	*Kurtosis*	3.02546
Mean UCL	10.67533	*Kurtosis Standard Error*	0.22914
Variance	52.77539	*Alternative Skewness (Fisher's)*	0.55597
Standard Deviation	7.26467	*Alternative Kurtosis (Fisher's)*	0.03932
Mean Standard Error	0.34399	*Coefficient of Variation*	0.73587
Minimum	0.E+0	*Mean Deviation*	5.97324
Maximum	34.85	*Second Moment*	52.65706
Range	34.85	*Third Moment*	211.72603
Sum	4,403.	*Fourth Moment*	8,388.88156
Sum Standard Error	153.42042	*Median*	9.56
Total Sum Squares	66,952.3336	*Median Error*	0.02041
Adjusted Sum Squares	23,485.04885	*Percentile 25% (Q1)*	3.17
Geometric Mean	6.45391	*Percentile 75% (Q2)*	15.27
Harmonic Mean	3.36305	*IQR*	12.1
Mode	0.E+0	*MAD*	5.975

Average slope (°)

Count	446	*Skewness*	0.03676
Mean	11.96265	*Skewness Standard Error*	0.11534
Mean LCL	11.19091	*Kurtosis*	2.38242
Mean UCL	12.73438	*Kurtosis Standard Error*	0.22914
Variance	48.72931	*Alternative Skewness (Fisher's)*	0.03688
Standard Deviation	6.98064	*Alternative Kurtosis (Fisher's)*	-0.61099
Mean Standard Error	0.33054	*Coefficient of Variation*	0.58354
Minimum	0.E+0	*Mean Deviation*	5.71744
Maximum	32.04	*Second Moment*	48.62005
Range	32.04	*Third Moment*	12.46189
Sum	5,335.34	*Fourth Moment*	5,631.82486
Sum Standard Error	147.42209	*Median*	12.245
Total Sum Squares	85,509.3268	*Median Error*	0.01962
Adjusted Sum Squares	21,684.54448	*Percentile 25% (Q1)*	6.74
Geometric Mean	8.7517	*Percentile 75% (Q2)*	17.305
Harmonic Mean	4.56302	*IQR*	10.565
Mode	0.E+0	*MAD*	5.115

1st-order catchments - Training set – NWCat - reactive catchments.

Max. elevation (m asl)			
Count	25	*Skewness*	0.32163
Mean	2,604.918	*Skewness Standard Error*	0.44475
Mean LCL	2,489.35797	*Kurtosis*	1.99972
Mean UCL	2,720.47803	*Kurtosis Standard Error*	0.79214
Variance	53,753.11367	*Alternative Skewness (Fisher's)*	0.34253
Standard Deviation	231.84718	*Alternative Kurtosis (Fisher's)*	-0.94896
Mean Standard Error	46.36944	*Coefficient of Variation*	0.089
Minimum	2,252.	*Mean Deviation*	194.93792
Maximum	3,025.84	*Second Moment*	51,602.98912
Range	773.84	*Third Moment*	3,770,214.89475
Sum	65,122.95	*Fourth Moment*	5,324,996,439.6776
Sum Standard Error	1,159.23589	*Median*	2,566.7
Total Sum Squares	170,930,019.3961	*Median Error*	11.62309
Adjusted Sum Squares	1,290,074.728	*Percentile 25% (Q1)*	2,445.5475
Geometric Mean	2,595.14412	*Percentile 75% (Q2)*	2,776.085
Harmonic Mean	2,585.52098	*IQR*	330.5375
Mode	#N/A	*MAD*	186.79
Mean elevation (m asl)			
Count	25	*Skewness*	-0.06952
Mean	2,038.18556	*Skewness Standard Error*	0.44475
Mean LCL	1,896.92606	*Kurtosis*	1.95811
Mean UCL	2,179.44506	*Kurtosis Standard Error*	0.79214
Variance	80,319.99974	*Alternative Skewness (Fisher's)*	-0.07404
Standard Deviation	283.40783	*Alternative Kurtosis (Fisher's)*	-1.00028
Mean Standard Error	56.68157	*Coefficient of Variation*	0.13905
Minimum	1,546.505	*Mean Deviation*	243.78609
Maximum	2,547.027	*Second Moment*	77,107.19975
Range	1,000.522	*Third Moment*	-1,488,611.36571
Sum	50,954.639	*Fourth Moment*	1.1642E+10
Sum Standard Error	1,417.03916	*Median*	2,117.274
Total Sum Squares	105,782,689.41846	*Median Error*	14.20796
Adjusted Sum Squares	1,927,679.99364	*Percentile 25% (Q1)*	1,805.0495
Geometric Mean	2,018.88439	*Percentile 75% (Q2)*	2,247.231
Harmonic Mean	1,999.29382	*IQR*	442.1815
Mode	#N/A	*MAD*	251.432
Min. elevation (m asl)			
Count	25	*Skewness*	-0.0208
Mean	1,391.6576	*Skewness Standard Error*	0.44475
Mean LCL	1,272.21263	*Kurtosis*	1.99207
Mean UCL	1,511.10257	*Kurtosis Standard Error*	0.79214
Variance	57,428.05261	*Alternative Skewness (Fisher's)*	-0.02215
Standard Deviation	239.64151	*Alternative Kurtosis (Fisher's)*	-0.9584
Mean Standard Error	47.9283	*Coefficient of Variation*	0.1722
Minimum	1,015.04	*Mean Deviation*	200.2217
Maximum	1,854.51	*Second Moment*	55,130.93051
Range	839.47	*Third Moment*	-269,194.69378
Sum	34,791.44	*Fourth Moment*	6,054,722,873.12157
Sum Standard Error	1,198.20754	*Median*	1,434.88
Total Sum Squares	49,796,045.1536	*Median Error*	12.01384
Adjusted Sum Squares	1,378,273.26266	*Percentile 25% (Q1)*	1,240.545
Geometric Mean	1,371.3735	*Percentile 75% (Q2)*	1,617.94
Harmonic Mean	1,350.77641	*IQR*	377.395
Mode	1,434.88	*MAD*	184.51

Melton ratio (-)

Count	25	*Skewness*	0.86834
Mean	0.85702	*Skewness Standard Error*	0.44475
Mean LCL	0.74727	*Kurtosis*	3.10885
Mean UCL	0.96678	*Kurtosis Standard Error*	0.79214
Variance	0.04849	*Alternative Skewness (Fisher's)*	0.92478
Standard Deviation	0.2202	*Alternative Kurtosis (Fisher's)*	0.41882
Mean Standard Error	0.04404	*Coefficient of Variation*	0.25693
Minimum	0.52157	*Mean Deviation*	0.16651
Maximum	1.3812	*Second Moment*	0.04655
Range	0.85963	*Third Moment*	0.00872
Sum	21.42558	*Fourth Moment*	0.00674
Sum Standard Error	1.10098	*Median*	0.82408
Total Sum Squares	19.52588	*Median Error*	0.01104
Adjusted Sum Squares	1.16366	*Percentile 25% (Q1)*	0.70755
Geometric Mean	0.83201	*Percentile 75% (Q2)*	0.96174
Harmonic Mean	0.80888	*IQR*	0.25419
Mode	#N/A	*MAD*	0.11708

Mean slope (°)

Count	25	*Skewness*	0.25706
Mean	32.19546	*Skewness Standard Error*	0.44475
Mean LCL	30.30263	*Kurtosis*	2.46838
Mean UCL	34.08828	*Kurtosis Standard Error*	0.79214
Variance	14.42143	*Alternative Skewness (Fisher's)*	0.27377
Standard Deviation	3.79756	*Alternative Kurtosis (Fisher's)*	-0.37101
Mean Standard Error	0.75951	*Coefficient of Variation*	0.11795
Minimum	25.51472	*Mean Deviation*	3.05095
Maximum	39.8771	*Second Moment*	13.84457
Range	14.36238	*Third Moment*	13.24204
Sum	804.88642	*Fourth Moment*	473.11936
Sum Standard Error	18.98778	*Median*	31.6712
Total Sum Squares	26,259.80016	*Median Error*	0.19038
Adjusted Sum Squares	346.1142	*Percentile 25% (Q1)*	30.03421
Geometric Mean	31.98197	*Percentile 75% (Q2)*	34.76713
Harmonic Mean	31.77012	*IQR*	4.73291
Mode	#N/A	*MAD*	2.75058

Mean orientation (0-360)

Count	25	*Skewness*	-0.96117
Mean	209.2482	*Skewness Standard Error*	0.44475
Mean LCL	183.74364	*Kurtosis*	2.71531
Mean UCL	234.75277	*Kurtosis Standard Error*	0.79214
Variance	2,618.32871	*Alternative Skewness (Fisher's)*	-1.02365
Standard Deviation	51.16961	*Alternative Kurtosis (Fisher's)*	-0.06649
Mean Standard Error	10.23392	*Coefficient of Variation*	0.24454
Minimum	84.71014	*Mean Deviation*	41.25477
Maximum	265.7687	*Second Moment*	2,513.59556
Range	181.05856	*Third Moment*	-121,128.248
Sum	5,231.20504	*Fourth Moment*	17,155,782.81848
Sum Standard Error	255.84804	*Median*	221.6209
Total Sum Squares	1,157,460.13583	*Median Error*	2.56526
Adjusted Sum Squares	62,839.88901	*Percentile 25% (Q1)*	184.6522
Geometric Mean	201.67654	*Percentile 75% (Q2)*	246.6711
Harmonic Mean	192.22097	*IQR*	62.0189
Mode	#N/A	*MAD*	25.3557

Area (km2)

Count	25	*Skewness*	1.13081
Mean	2.32085	*Skewness Standard Error*	0.44475
Mean LCL	1.72726	*Kurtosis*	3.72065
Mean UCL	2.91444	*Kurtosis Standard Error*	0.79214
Variance	1.41829	*Alternative Skewness (Fisher's)*	1.20431
Standard Deviation	1.19092	*Alternative Kurtosis (Fisher's)*	1.17329
Mean Standard Error	0.23818	*Coefficient of Variation*	0.51314
Minimum	1.0369	*Mean Deviation*	0.9529
Maximum	5.72053	*Second Moment*	1.36156
Range	4.68363	*Third Moment*	1.79657
Sum	58.0213	*Fourth Moment*	6.89748
Sum Standard Error	5.9546	*Median*	2.00365
Total Sum Squares	168.69778	*Median Error*	0.0597
Adjusted Sum Squares	34.03893	*Percentile 25% (Q1)*	1.38095
Geometric Mean	2.07307	*Percentile 75% (Q2)*	3.05104
Harmonic Mean	1.87435	*IQR*	1.67009
Mode	#N/A	*MAD*	0.69515

Stream length (km)

Count	25	*Skewness*	0.58408
Mean	1.33107	*Skewness Standard Error*	0.44475
Mean LCL	0.78802	*Kurtosis*	2.38654
Mean UCL	1.87412	*Kurtosis Standard Error*	0.79214
Variance	1.18706	*Alternative Skewness (Fisher's)*	0.62205
Standard Deviation	1.08952	*Alternative Kurtosis (Fisher's)*	-0.47194
Mean Standard Error	0.2179	*Coefficient of Variation*	0.81853
Minimum	0.005	*Mean Deviation*	0.89154
Maximum	3.8224	*Second Moment*	1.13958
Range	3.8174	*Third Moment*	0.71055
Sum	33.27675	*Fourth Moment*	3.09927
Sum Standard Error	5.44762	*Median*	1.13419
Total Sum Squares	72.78321	*Median Error*	0.05462
Adjusted Sum Squares	28.48953	*Percentile 25% (Q1)*	0.43919
Geometric Mean	0.63303	*Percentile 75% (Q2)*	2.12991
Harmonic Mean	0.06793	*IQR*	1.69072
Mode	#N/A	*MAD*	0.9377

Perimeter (m)

Count	25	*Skewness*	0.36126
Mean	9,286.4	*Skewness Standard Error*	0.44475
Mean LCL	8,266.36784	*Kurtosis*	2.1591
Mean UCL	10,306.43216	*Kurtosis Standard Error*	0.79214
Variance	4,188,090.66667	*Alternative Skewness (Fisher's)*	0.38474
Standard Deviation	2,046.48251	*Alternative Kurtosis (Fisher's)*	-0.75242
Mean Standard Error	409.2965	*Coefficient of Variation*	0.22037
Minimum	6,280.	*Mean Deviation*	1,725.056
Maximum	13,480.	*Second Moment*	4,020,567.04
Range	7,200.	*Third Moment*	2,912,362,610.688
Sum	232,160.	*Fourth Moment*	3.49017E+13
Sum Standard Error	10,232.41255	*Median*	8,760.
Total Sum Squares	2,256,444,800.	*Median Error*	102.59542
Adjusted Sum Squares	100,514,176.	*Percentile 25% (Q1)*	7,780.
Geometric Mean	9,073.6703	*Percentile 75% (Q2)*	10,690.
Harmonic Mean	8,867.24369	*IQR*	2,910.
Mode	8,760.	*MAD*	1,640.

Form factor (-)

Count	25	*Skewness*	0.3981
Mean	0.40439	*Skewness Standard Error*	0.44475
Mean LCL	0.33586	*Kurtosis*	2.32209
Mean UCL	0.47293	*Kurtosis Standard Error*	0.79214
Variance	0.0189	*Alternative Skewness (Fisher's)*	0.42398
Standard Deviation	0.13749	*Alternative Kurtosis (Fisher's)*	-0.55142
Mean Standard Error	0.0275	*Coefficient of Variation*	0.34
Minimum	0.19798	*Mean Deviation*	0.11658
Maximum	0.71793	*Second Moment*	0.01815
Range	0.51996	*Third Moment*	0.00097
Sum	10.10986	*Fourth Moment*	0.00076
Sum Standard Error	0.68746	*Median*	0.36426
Total Sum Squares	4.54207	*Median Error*	0.00689
Adjusted Sum Squares	0.4537	*Percentile 25% (Q1)*	0.32124
Geometric Mean	0.38189	*Percentile 75% (Q2)*	0.53209
Harmonic Mean	0.35979	*IQR*	0.21084
Mode	#N/A	*MAD*	0.12122

Basin Elongation (-)

Count	25	*Skewness*	0.11379
Mean	0.70752	*Skewness Standard Error*	0.44475
Mean LCL	0.64669	*Kurtosis*	2.14853
Mean UCL	0.76836	*Kurtosis Standard Error*	0.79214
Variance	0.0149	*Alternative Skewness (Fisher's)*	0.12119
Standard Deviation	0.12205	*Alternative Kurtosis (Fisher's)*	-0.76544
Mean Standard Error	0.02441	*Coefficient of Variation*	0.1725
Minimum	0.50207	*Mean Deviation*	0.10226
Maximum	0.95609	*Second Moment*	0.0143
Range	0.45402	*Third Moment*	0.00019
Sum	17.68811	*Fourth Moment*	0.00044
Sum Standard Error	0.61025	*Median*	0.68102
Total Sum Squares	12.87228	*Median Error*	0.00612
Adjusted Sum Squares	0.35751	*Percentile 25% (Q1)*	0.63955
Geometric Mean	0.69731	*Percentile 75% (Q2)*	0.82302
Harmonic Mean	0.68703	*IQR*	0.18347
Mode	#N/A	*MAD*	0.1052

Lemniscate ratio (-)

Count	25	*Skewness*	0.77028
Mean	2.18292	*Skewness Standard Error*	0.44475
Mean LCL	1.79006	*Kurtosis*	2.75814
Mean UCL	2.57578	*Kurtosis Standard Error*	0.79214
Variance	0.62124	*Alternative Skewness (Fisher's)*	0.82035
Standard Deviation	0.78819	*Alternative Kurtosis (Fisher's)*	-0.01368
Mean Standard Error	0.15764	*Coefficient of Variation*	0.36107
Minimum	1.09397	*Mean Deviation*	0.59909
Maximum	3.96714	*Second Moment*	0.59639
Range	2.87318	*Third Moment*	0.35477
Sum	54.57301	*Fourth Moment*	0.98101
Sum Standard Error	3.94093	*Median*	2.15616
Total Sum Squares	134.03824	*Median Error*	0.03951
Adjusted Sum Squares	14.90971	*Percentile 25% (Q1)*	1.54859
Geometric Mean	2.05661	*Percentile 75% (Q2)*	2.49498
Harmonic Mean	1.94216	*IQR*	0.94639
Mode	#N/A	*MAD*	0.53839

Outlet slope (°)

Count	25	*Skewness*	0.10337
Mean	9.0252	*Skewness Standard Error*	0.44475
Mean LCL	6.09032	*Kurtosis*	2.37506
Mean UCL	11.96008	*Kurtosis Standard Error*	0.79214
Variance	34.67111	*Alternative Skewness (Fisher's)*	0.11009
Standard Deviation	5.88822	*Alternative Kurtosis (Fisher's)*	-0.48609
Mean Standard Error	1.17764	*Coefficient of Variation*	0.65242
Minimum	0.E+0	*Mean Deviation*	4.67539
Maximum	21.69	*Second Moment*	33.28426
Range	21.69	*Third Moment*	19.85013
Sum	225.63	*Fourth Moment*	2,631.19471
Sum Standard Error	29.44109	*Median*	10.02
Total Sum Squares	2,868.4625	*Median Error*	0.29519
Adjusted Sum Squares	832.10662	*Percentile 25% (Q1)*	4.5525
Geometric Mean	6.62996	*Percentile 75% (Q2)*	12.715
Harmonic Mean	6.88174	*IQR*	8.1625
Mode	0.E+0	*MAD*	3.3

200m slope (°)

Count	25	*Skewness*	1.49727
Mean	9.6996	*Skewness Standard Error*	0.44475
Mean LCL	6.03425	*Kurtosis*	6.58793
Mean UCL	13.36495	*Kurtosis Standard Error*	0.79214
Variance	54.07795	*Alternative Skewness (Fisher's)*	1.59459
Standard Deviation	7.35377	*Alternative Kurtosis (Fisher's)*	4.70923
Mean Standard Error	1.47075	*Coefficient of Variation*	0.75815
Minimum	0.E+0	*Mean Deviation*	5.04678
Maximum	34.85	*Second Moment*	51.91484
Range	34.85	*Third Moment*	560.06471
Sum	242.49	*Fourth Moment*	17,755.46538
Sum Standard Error	36.76886	*Median*	9.55
Total Sum Squares	3,649.9269	*Median Error*	0.36866
Adjusted Sum Squares	1,297.8709	*Percentile 25% (Q1)*	4.7625
Geometric Mean	7.08545	*Percentile 75% (Q2)*	12.39
Harmonic Mean	6.36203	*IQR*	7.6275
Mode	0.E+0	*MAD*	2.86

Average slope (°)

Count	25	*Skewness*	-0.10355
Mean	13.906	*Skewness Standard Error*	0.44475
Mean LCL	10.10638	*Kurtosis*	2.51815
Mean UCL	17.70562	*Kurtosis Standard Error*	0.79214
Variance	58.11233	*Alternative Skewness (Fisher's)*	-0.11028
Standard Deviation	7.62314	*Alternative Kurtosis (Fisher's)*	-0.30963
Mean Standard Error	1.52463	*Coefficient of Variation*	0.54819
Minimum	0.E+0	*Mean Deviation*	5.59616
Maximum	27.49	*Second Moment*	55.78784
Range	27.49	*Third Moment*	-43.14645
Sum	347.65	*Fourth Moment*	7,837.20136
Sum Standard Error	38.11572	*Median*	14.59
Total Sum Squares	6,229.1169	*Median Error*	0.38217
Adjusted Sum Squares	1,394.696	*Percentile 25% (Q1)*	11.11
Geometric Mean	10.62351	*Percentile 75% (Q2)*	17.9125
Harmonic Mean	7.53943	*IQR*	6.8025
Mode	#N/A	*MAD*	3.72

1st-order catchments - Training set – all zones – all catchments.

Max. elevation (m asl)			
Count	1022	*Skewness*	-0.17701
Mean	2,073.22994	*Skewness Standard Error*	0.07643
Mean LCL	2,034.86228	*Kurtosis*	2.10444
Mean UCL	2,111.59761	*Kurtosis Standard Error*	0.15242
Variance	277,119.86774	*Alternative Skewness (Fisher's)*	-0.17727
Standard Deviation	526.42176	*Alternative Kurtosis (Fisher's)*	-0.89406
Mean Standard Error	16.46677	*Coefficient of Variation*	0.25391
Minimum	816.	*Mean Deviation*	442.16116
Maximum	3,028.	*Second Moment*	276,848.71327
Range	2,212.	*Third Moment*	-25,784,579.75174
Sum	2,118,841.	*Fourth Moment*	1.61296E+11
Sum Standard Error	16,829.03755	*Median*	2,082.5
Total Sum Squares	4,675,783,987.	*Median Error*	0.64557
Adjusted Sum Squares	282,939,384.9638	*Percentile 25% (Q1)*	1,648.5
Geometric Mean	1,999.97934	*Percentile 75% (Q2)*	2,505.5
Harmonic Mean	1,920.03921	*IQR*	857.
Mode	#N/A	*MAD*	431.
Mean elevation (m asl)			
Count	1022	*Skewness*	0.13173
Mean	1,663.86791	*Skewness Standard Error*	0.07643
Mean LCL	1,629.02703	*Kurtosis*	2.095
Mean UCL	1,698.70878	*Kurtosis Standard Error*	0.15242
Variance	228,515.20389	*Alternative Skewness (Fisher's)*	0.13193
Standard Deviation	478.03264	*Alternative Kurtosis (Fisher's)*	-0.90355
Mean Standard Error	14.95313	*Coefficient of Variation*	0.2873
Minimum	637.	*Mean Deviation*	400.14062
Maximum	2,671.	*Second Moment*	228,291.6078
Range	2,034.	*Third Moment*	14,369,285.00442
Sum	1,700,473.	*Fourth Moment*	1.09185E+11
Sum Standard Error	15,282.09862	*Median*	1,634.5
Total Sum Squares	3,062,676,473.	*Median Error*	0.58623
Adjusted Sum Squares	233,314,023.16732	*Percentile 25% (Q1)*	1,285.5
Geometric Mean	1,591.98223	*Percentile 75% (Q2)*	2,042.5
Harmonic Mean	1,517.41848	*IQR*	757.
Mode	#N/A	*MAD*	374.
Min. elevation (m asl)			
Count	1022	*Skewness*	0.70694
Mean	1,249.03131	*Skewness Standard Error*	0.07643
Mean LCL	1,217.97017	*Kurtosis*	2.76967
Mean UCL	1,280.09245	*Kurtosis Standard Error*	0.15242
Variance	181,623.33888	*Alternative Skewness (Fisher's)*	0.70798
Standard Deviation	426.1729	*Alternative Kurtosis (Fisher's)*	-0.22556
Mean Standard Error	13.33093	*Coefficient of Variation*	0.3412
Minimum	474.	*Mean Deviation*	343.84828
Maximum	2,426.	*Second Moment*	181,445.62524
Range	1,952.	*Third Moment*	54,639,199.48723
Sum	1,276,510.	*Fourth Moment*	9.11846E+10
Sum Standard Error	13,624.20832	*Median*	1,157.
Total Sum Squares	1,779,838,388.	*Median Error*	0.52263
Adjusted Sum Squares	185,437,428.99804	*Percentile 25% (Q1)*	937.5
Geometric Mean	1,180.45002	*Percentile 75% (Q2)*	1,485.5
Harmonic Mean	1,116.19769	*IQR*	548.
Mode	629.	*MAD*	265.

Melton ratio (-)

Count	1022	*Skewness*	0.58288
Mean	0.58647	*Skewness Standard Error*	0.07643
Mean LCL	0.57055	*Kurtosis*	3.11368
Mean UCL	0.60238	*Kurtosis Standard Error*	0.15242
Variance	0.04769	*Alternative Skewness (Fisher's)*	0.58374
Standard Deviation	0.21838	*Alternative Kurtosis (Fisher's)*	0.12013
Mean Standard Error	0.00683	*Coefficient of Variation*	0.37236
Minimum	0.1	*Mean Deviation*	0.17462
Maximum	1.38	*Second Moment*	0.04764
Range	1.28	*Third Moment*	0.00606
Sum	599.37	*Fourth Moment*	0.00707
Sum Standard Error	6.98125	*Median*	0.56
Total Sum Squares	400.2013	*Median Error*	0.00027
Adjusted Sum Squares	48.69015	*Percentile 25% (Q1)*	0.43
Geometric Mean	0.54528	*Percentile 75% (Q2)*	0.72
Harmonic Mean	0.50201	*IQR*	0.29
Mode	0.48	*MAD*	0.15

Mean slope (°)

Count	1022	*Skewness*	0.10044
Mean	25.99119	*Skewness Standard Error*	0.07643
Mean LCL	25.60831	*Kurtosis*	2.97001
Mean UCL	26.37408	*Kurtosis Standard Error*	0.15242
Variance	27.59738	*Alternative Skewness (Fisher's)*	0.10058
Standard Deviation	5.25332	*Alternative Kurtosis (Fisher's)*	-0.02424
Mean Standard Error	0.16433	*Coefficient of Variation*	0.20212
Minimum	9.	*Mean Deviation*	4.17944
Maximum	42.	*Second Moment*	27.57037
Range	33.	*Third Moment*	14.53953
Sum	26,563.	*Fourth Moment*	2,257.58054
Sum Standard Error	167.94201	*Median*	26.
Total Sum Squares	718,581.	*Median Error*	0.00644
Adjusted Sum Squares	28,176.92074	*Percentile 25% (Q1)*	23.
Geometric Mean	25.43726	*Percentile 75% (Q2)*	30.
Harmonic Mean	24.84479	*IQR*	7.
Mode	24.	*MAD*	3.

Mean orientation (0-360)

Count	1022	*Skewness*	0.0667
Mean	175.75245	*Skewness Standard Error*	0.07643
Mean LCL	172.29655	*Kurtosis*	2.31545
Mean UCL	179.20834	*Kurtosis Standard Error*	0.15242
Variance	2,248.31574	*Alternative Skewness (Fisher's)*	0.0668
Standard Deviation	47.41641	*Alternative Kurtosis (Fisher's)*	-0.68202
Mean Standard Error	1.48321	*Coefficient of Variation*	0.26979
Minimum	67.	*Mean Deviation*	39.38706
Maximum	294.	*Second Moment*	2,246.11582
Range	227.	*Third Moment*	7,100.46029
Sum	179,619.	*Fourth Moment*	11,681,511.63066
Sum Standard Error	1,515.84257	*Median*	174.
Total Sum Squares	33,864,009.	*Median Error*	0.05815
Adjusted Sum Squares	2,295,530.36888	*Percentile 25% (Q1)*	140.5
Geometric Mean	168.96195	*Percentile 75% (Q2)*	211.
Harmonic Mean	161.75439	*IQR*	70.5
Mode	160.	*MAD*	36.

Area (km2)

Count	1022	*Skewness*	2.58975
Mean	2.29111	*Skewness Standard Error*	0.07643
Mean LCL	2.18542	*Kurtosis*	12.92055
Mean UCL	2.39681	*Kurtosis Standard Error*	0.15242
Variance	2.10287	*Alternative Skewness (Fisher's)*	2.59356
Standard Deviation	1.45013	*Alternative Kurtosis (Fisher's)*	9.97515
Mean Standard Error	0.04536	*Coefficient of Variation*	0.63294
Minimum	1.	*Mean Deviation*	1.00641
Maximum	13.05	*Second Moment*	2.10082
Range	12.05	*Third Moment*	7.88569
Sum	2,341.51885	*Fourth Moment*	57.02386
Sum Standard Error	46.35877	*Median*	1.83
Total Sum Squares	7,511.72051	*Median Error*	0.00178
Adjusted Sum Squares	2,147.03311	*Percentile 25% (Q1)*	1.33
Geometric Mean	1.99306	*Percentile 75% (Q2)*	2.73
Harmonic Mean	1.78934	*IQR*	1.4
Mode	#N/A	*MAD*	0.6

Stream length (km)

Count	1022	*Skewness*	2.16375
Mean	1.34596	*Skewness Standard Error*	0.07643
Mean LCL	1.26026	*Kurtosis*	10.8214
Mean UCL	1.43165	*Kurtosis Standard Error*	0.15242
Variance	1.38254	*Alternative Skewness (Fisher's)*	2.16693
Standard Deviation	1.17581	*Alternative Kurtosis (Fisher's)*	7.86569
Mean Standard Error	0.03678	*Coefficient of Variation*	0.87359
Minimum	0.005	*Mean Deviation*	0.84518
Maximum	9.55	*Second Moment*	1.38118
Range	9.545	*Third Moment*	3.51224
Sum	1,375.5677	*Fourth Moment*	20.64364
Sum Standard Error	37.58926	*Median*	1.06
Total Sum Squares	3,263.0244	*Median Error*	0.00144
Adjusted Sum Squares	1,411.56991	*Percentile 25% (Q1)*	0.53
Geometric Mean	0.89599	*Percentile 75% (Q2)*	1.825
Harmonic Mean	0.37027	*IQR*	1.295
Mode	0.49	*MAD*	0.60871

Perimeter (m)

Count	1022	*Skewness*	1.96216
Mean	9,072.5636	*Skewness Standard Error*	0.07643
Mean LCL	8,866.9605	*Kurtosis*	9.57474
Mean UCL	9,278.1667	*Kurtosis Standard Error*	0.15242
Variance	7,957,858.84757	*Alternative Skewness (Fisher's)*	1.96505
Standard Deviation	2,820.96771	*Alternative Kurtosis (Fisher's)*	6.61291
Mean Standard Error	88.24146	*Coefficient of Variation*	0.31093
Minimum	5,080.	*Mean Deviation*	2,049.93869
Maximum	27,880.	*Second Moment*	7,950,072.29292
Range	22,800.	*Third Moment*	4.39837E+10
Sum	9,272,160.	*Fourth Moment*	6.05159E+14
Sum Standard Error	90,182.76854	*Median*	8,440.
Total Sum Squares	9.22472E+10	*Median Error*	3.45945
Adjusted Sum Squares	8,124,973,883.36595	*Percentile 25% (Q1)*	7,160.
Geometric Mean	8,719.27177	*Percentile 75% (Q2)*	10,240.
Harmonic Mean	8,423.21296	*IQR*	3,080.
Mode	7,800.	*MAD*	1,480.

Form factor (-)

Count	1022	*Skewness*	0.36233
Mean	0.40337	*Skewness Standard Error*	0.07643
Mean LCL	0.39377	*Kurtosis*	2.53745
Mean UCL	0.41296	*Kurtosis Standard Error*	0.15242
Variance	0.01734	*Alternative Skewness (Fisher's)*	0.36286
Standard Deviation	0.13169	*Alternative Kurtosis (Fisher's)*	-0.45893
Mean Standard Error	0.00412	*Coefficient of Variation*	0.32649
Minimum	0.13	*Mean Deviation*	0.10848
Maximum	0.77	*Second Moment*	0.01733
Range	0.64	*Third Moment*	0.00083
Sum	412.24	*Fourth Moment*	0.00076
Sum Standard Error	4.21008	*Median*	0.39
Total Sum Squares	183.991	*Median Error*	0.00016
Adjusted Sum Squares	17.70742	*Percentile 25% (Q1)*	0.31
Geometric Mean	0.38133	*Percentile 75% (Q2)*	0.49
Harmonic Mean	0.35872	*IQR*	0.18
Mode	0.32	*MAD*	0.09

Basin Elongation (-)

Count	1022	*Skewness*	0.01154
Mean	0.70673	*Skewness Standard Error*	0.07643
Mean LCL	0.69814	*Kurtosis*	2.43321
Mean UCL	0.71533	*Kurtosis Standard Error*	0.15242
Variance	0.01391	*Alternative Skewness (Fisher's)*	0.01156
Standard Deviation	0.11793	*Alternative Kurtosis (Fisher's)*	-0.56368
Mean Standard Error	0.00369	*Coefficient of Variation*	0.16686
Minimum	0.4	*Mean Deviation*	0.09735
Maximum	0.99	*Second Moment*	0.01389
Range	0.59	*Third Moment*	0.00002
Sum	722.28	*Fourth Moment*	0.00047
Sum Standard Error	3.76996	*Median*	0.7
Total Sum Squares	524.657	*Median Error*	0.00014
Adjusted Sum Squares	14.19868	*Percentile 25% (Q1)*	0.62
Geometric Mean	0.69663	*Percentile 75% (Q2)*	0.79
Harmonic Mean	0.68625	*IQR*	0.17
Mode	0.72	*MAD*	0.09

Lemniscate ratio (-)

Count	1022	*Skewness*	1.27321
Mean	2.19041	*Skewness Standard Error*	0.07643
Mean LCL	2.13106	*Kurtosis*	4.92389
Mean UCL	2.24976	*Kurtosis Standard Error*	0.15242
Variance	0.66312	*Alternative Skewness (Fisher's)*	1.27509
Standard Deviation	0.81432	*Alternative Kurtosis (Fisher's)*	1.93923
Mean Standard Error	0.02547	*Coefficient of Variation*	0.37177
Minimum	1.02	*Mean Deviation*	0.62652
Maximum	6.14	*Second Moment*	0.66247
Range	5.12	*Third Moment*	0.68652
Sum	2,238.6	*Fourth Moment*	2.16095
Sum Standard Error	26.03286	*Median*	2.02
Total Sum Squares	5,580.5008	*Median Error*	0.001
Adjusted Sum Squares	677.04683	*Percentile 25% (Q1)*	1.59
Geometric Mean	2.06032	*Percentile 75% (Q2)*	2.575
Harmonic Mean	1.94752	*IQR*	0.985
Mode	1.55	*MAD*	0.47

Outlet slope (°)

Count	1022	*Skewness*	0.91894
Mean	8.70759	*Skewness Standard Error*	0.07643
Mean LCL	8.22561	*Kurtosis*	3.78345
Mean UCL	9.18957	*Kurtosis Standard Error*	0.15242
Variance	43.73137	*Alternative Skewness (Fisher's)*	0.92029
Standard Deviation	6.61297	*Alternative Kurtosis (Fisher's)*	0.79319
Mean Standard Error	0.20686	*Coefficient of Variation*	0.75945
Minimum	0.E+0	*Mean Deviation*	5.29213
Maximum	36.23	*Second Moment*	43.68858
Range	36.23	*Third Moment*	265.36185
Sum	8,899.16	*Fourth Moment*	7,221.44869
Sum Standard Error	211.40829	*Median*	7.65
Total Sum Squares	122,139.9958	*Median Error*	0.00811
Adjusted Sum Squares	44,649.73288	*Percentile 25% (Q1)*	3.395
Geometric Mean	6.027	*Percentile 75% (Q2)*	12.69
Harmonic Mean	3.83702	*IQR*	9.295
Mode	0.E+0	*MAD*	4.46

200m slope (°)

Count	1022	*Skewness*	0.91868
Mean	8.95705	*Skewness Standard Error*	0.07643
Mean LCL	8.47472	*Kurtosis*	3.82192
Mean UCL	9.43937	*Kurtosis Standard Error*	0.15242
Variance	43.79466	*Alternative Skewness (Fisher's)*	0.92003
Standard Deviation	6.61775	*Alternative Kurtosis (Fisher's)*	0.83185
Mean Standard Error	0.20701	*Coefficient of Variation*	0.73883
Minimum	0.E+0	*Mean Deviation*	5.30862
Maximum	34.85	*Second Moment*	43.7518
Range	34.85	*Third Moment*	265.86201
Sum	9,154.1	*Fourth Moment*	7,316.00612
Sum Standard Error	211.56119	*Median*	7.855
Total Sum Squares	126,708.0286	*Median Error*	0.00812
Adjusted Sum Squares	44,714.34288	*Percentile 25% (Q1)*	3.64
Geometric Mean	6.3223	*Percentile 75% (Q2)*	13.23
Harmonic Mean	3.9229	*IQR*	9.59
Mode	0.E+0	*MAD*	4.565

Average slope (°)

Count	1022	*Skewness*	0.49957
Mean	10.36714	*Skewness Standard Error*	0.07643
Mean LCL	9.90386	*Kurtosis*	2.86838
Mean UCL	10.83042	*Kurtosis Standard Error*	0.15242
Variance	40.40385	*Alternative Skewness (Fisher's)*	0.5003
Standard Deviation	6.3564	*Alternative Kurtosis (Fisher's)*	-0.12637
Mean Standard Error	0.19883	*Coefficient of Variation*	0.61313
Minimum	0.E+0	*Mean Deviation*	5.13672
Maximum	32.04	*Second Moment*	40.36431
Range	32.04	*Third Moment*	128.11292
Sum	10,595.22	*Fourth Moment*	4,673.39356
Sum Standard Error	203.20613	*Median*	10.105
Total Sum Squares	151,094.486	*Median Error*	0.0078
Adjusted Sum Squares	41,252.32666	*Percentile 25% (Q1)*	5.395
Geometric Mean	7.9138	*Percentile 75% (Q2)*	14.59
Harmonic Mean	5.07689	*IQR*	9.195
Mode	0.E+0	*MAD*	4.635

1st-order catchments - Training set – all zones – reactive catchments.

Max. elevation (m asl)			
Count	78	*Skewness*	-0.42597
Mean	2,345.65769	*Skewness Standard Error*	0.2687
Mean LCL	2,247.80299	*Kurtosis*	2.96411
Mean UCL	2,443.5124	*Kurtosis Standard Error*	0.51739
Variance	132,328.68803	*Alternative Skewness (Fisher's)*	-0.43437
Standard Deviation	363.7701	*Alternative Kurtosis (Fisher's)*	0.04275
Mean Standard Error	41.18885	*Coefficient of Variation*	0.15508
Minimum	1,376.27	*Mean Deviation*	291.65351
Maximum	3,025.84	*Second Moment*	130,632.16639
Range	1,649.57	*Third Moment*	-20,112,053.83418
Sum	182,961.3	*Fourth Moment*	5.05818E+10
Sum Standard Error	3,212.73056	*Median*	2,413.56
Total Sum Squares	439,353,889.7182	*Median Error*	5.84511
Adjusted Sum Squares	10,189,308.97858	*Percentile 25% (Q1)*	2,085.685
Geometric Mean	2,315.56817	*Percentile 75% (Q2)*	2,601.9
Harmonic Mean	2,282.77982	*IQR*	516.215
Mode	#N/A	*MAD*	215.17
Mean elevation (m asl)			
Count	78	*Skewness*	-0.05371
Mean	1,859.98459	*Skewness Standard Error*	0.2687
Mean LCL	1,769.33192	*Kurtosis*	2.73316
Mean UCL	1,950.63726	*Kurtosis Standard Error*	0.51739
Variance	113,566.89385	*Alternative Skewness (Fisher's)*	-0.05477
Standard Deviation	336.99688	*Alternative Kurtosis (Fisher's)*	-0.20371
Mean Standard Error	38.15738	*Coefficient of Variation*	0.18118
Minimum	1,067.994	*Mean Deviation*	270.50651
Maximum	2,547.027	*Second Moment*	112,110.90803
Range	1,479.033	*Third Moment*	-2,016,322.07483
Sum	145,078.798	*Fourth Moment*	3.43528E+10
Sum Standard Error	2,976.27581	*Median*	1,805.0625
Total Sum Squares	278,588,979.40507	*Median Error*	5.41491
Adjusted Sum Squares	8,744,650.82655	*Percentile 25% (Q1)*	1,639.595
Geometric Mean	1,828.36136	*Percentile 75% (Q2)*	2,154.705
Harmonic Mean	1,794.81267	*IQR*	515.11
Mode	#N/A	*MAD*	217.5055
Min. elevation (m asl)			
Count	78	*Skewness*	0.67586
Mean	1,346.66295	*Skewness Standard Error*	0.2687
Mean LCL	1,270.0629	*Kurtosis*	3.51289
Mean UCL	1,423.263	*Kurtosis Standard Error*	0.51739
Variance	81,086.51921	*Alternative Skewness (Fisher's)*	0.68919
Standard Deviation	284.75695	*Alternative Kurtosis (Fisher's)*	0.62841
Mean Standard Error	32.24238	*Coefficient of Variation*	0.21145
Minimum	802.62	*Mean Deviation*	225.43245
Maximum	2,253.47	*Second Moment*	80,046.94845
Range	1,450.85	*Third Moment*	15,306,543.10148
Sum	105,039.71	*Fourth Moment*	2.25089E+10
Sum Standard Error	2,514.90527	*Median*	1,304.115
Total Sum Squares	147,696,747.5805	*Median Error*	4.57551
Adjusted Sum Squares	6,243,661.97942	*Percentile 25% (Q1)*	1,142.28
Geometric Mean	1,318.15308	*Percentile 75% (Q2)*	1,542.43
Harmonic Mean	1,290.61258	*IQR*	400.15
Mode	1,434.88	*MAD*	186.225

Melton ratio (-)

Count	78	*Skewness*	0.6722
Mean	0.67016	*Skewness Standard Error*	0.2687
Mean LCL	0.60795	*Kurtosis*	3.5309
Mean UCL	0.73238	*Kurtosis Standard Error*	0.51739
Variance	0.05349	*Alternative Skewness (Fisher's)*	0.68545
Standard Deviation	0.23128	*Alternative Kurtosis (Fisher's)*	0.64762
Mean Standard Error	0.02619	*Coefficient of Variation*	0.34511
Minimum	0.25177	*Mean Deviation*	0.18321
Maximum	1.3812	*Second Moment*	0.05281
Range	1.12942	*Third Moment*	0.00816
Sum	52.27279	*Fourth Moment*	0.00985
Sum Standard Error	2.04264	*Median*	0.69364
Total Sum Squares	39.15022	*Median Error*	0.00372
Adjusted Sum Squares	4.11888	*Percentile 25% (Q1)*	0.48296
Geometric Mean	0.63148	*Percentile 75% (Q2)*	0.8067
Harmonic Mean	0.59317	*IQR*	0.32374
Mode	#N/A	*MAD*	0.16718

Mean slope (°)

Count	78	*Skewness*	0.4337
Mean	28.28002	*Skewness Standard Error*	0.2687
Mean LCL	27.03303	*Kurtosis*	2.61798
Mean UCL	29.52701	*Kurtosis Standard Error*	0.51739
Variance	21.48909	*Alternative Skewness (Fisher's)*	0.44225
Standard Deviation	4.63563	*Alternative Kurtosis (Fisher's)*	-0.32664
Mean Standard Error	0.52488	*Coefficient of Variation*	0.16392
Minimum	19.56865	*Mean Deviation*	3.79082
Maximum	39.8771	*Second Moment*	21.21358
Range	20.30845	*Third Moment*	42.37547
Sum	2,205.84151	*Fourth Moment*	1,178.13215
Sum Standard Error	40.94079	*Median*	27.61627
Total Sum Squares	64,035.90015	*Median Error*	0.07449
Adjusted Sum Squares	1,654.65955	*Percentile 25% (Q1)*	25.23295
Geometric Mean	27.91301	*Percentile 75% (Q2)*	31.55932
Harmonic Mean	27.55429	*IQR*	6.32638
Mode	#N/A	*MAD*	3.16035

Mean orientation (0-360)

Count	78	*Skewness*	-0.04274
Mean	183.42297	*Skewness Standard Error*	0.2687
Mean LCL	170.33577	*Kurtosis*	1.9116
Mean UCL	196.51017	*Kurtosis Standard Error*	0.51739
Variance	2,366.92221	*Alternative Skewness (Fisher's)*	-0.04358
Standard Deviation	48.65102	*Alternative Kurtosis (Fisher's)*	-1.08048
Mean Standard Error	5.50864	*Coefficient of Variation*	0.26524
Minimum	84.71014	*Mean Deviation*	42.54736
Maximum	265.7687	*Second Moment*	2,336.57705
Range	181.05856	*Third Moment*	-4,826.88783
Sum	14,306.9914	*Fourth Moment*	10,436,548.66488
Sum Standard Error	429.67422	*Median*	184.8217
Total Sum Squares	2,806,483.81672	*Median Error*	0.78173
Adjusted Sum Squares	182,253.01006	*Percentile 25% (Q1)*	146.56275
Geometric Mean	176.62945	*Percentile 75% (Q2)*	221.35345
Harmonic Mean	169.48294	*IQR*	74.7907
Mode	#N/A	*MAD*	37.29115

Area (km2)			
Count	78	*Skewness*	1.81088
Mean	2.68978	*Skewness Standard Error*	0.2687
Mean LCL	2.25536	*Kurtosis*	7.95198
Mean UCL	3.1242	*Kurtosis Standard Error*	0.51739
Variance	2.60802	*Alternative Skewness (Fisher's)*	1.84659
Standard Deviation	1.61494	*Alternative Kurtosis (Fisher's)*	5.36577
Mean Standard Error	0.18286	*Coefficient of Variation*	0.6004
Minimum	1.01225	*Mean Deviation*	1.22519
Maximum	10.26843	*Second Moment*	2.57458
Range	9.25618	*Third Moment*	7.48086
Sum	209.80283	*Fourth Moment*	52.70959
Sum Standard Error	14.26273	*Median*	2.15714
Total Sum Squares	765.14096	*Median Error*	0.02595
Adjusted Sum Squares	200.81755	*Percentile 25% (Q1)*	1.56715
Geometric Mean	2.31908	*Percentile 75% (Q2)*	3.51633
Harmonic Mean	2.03188	*IQR*	1.94918
Mode	#N/A	*MAD*	0.86696

Stream length (km)			
Count	78	*Skewness*	0.90416
Mean	1.53604	*Skewness Standard Error*	0.2687
Mean LCL	1.20052	*Kurtosis*	3.72245
Mean UCL	1.87156	*Kurtosis Standard Error*	0.51739
Variance	1.5557	*Alternative Skewness (Fisher's)*	0.92198
Standard Deviation	1.24728	*Alternative Kurtosis (Fisher's)*	0.85205
Mean Standard Error	0.14123	*Coefficient of Variation*	0.81201
Minimum	0.005	*Mean Deviation*	1.01611
Maximum	5.98267	*Second Moment*	1.53576
Range	5.97767	*Third Moment*	1.7208
Sum	119.8108	*Fourth Moment*	8.77962
Sum Standard Error	11.01567	*Median*	1.28758
Total Sum Squares	303.82298	*Median Error*	0.02004
Adjusted Sum Squares	119.78928	*Percentile 25% (Q1)*	0.43549
Geometric Mean	0.87662	*Percentile 75% (Q2)*	2.29628
Harmonic Mean	0.16378	*IQR*	1.86079
Mode	#N/A	*MAD*	0.87554

Perimeter (m)			
Count	78	*Skewness*	0.88988
Mean	9,578.46154	*Skewness Standard Error*	0.2687
Mean LCL	8,830.2593	*Kurtosis*	4.09185
Mean UCL	10,326.66378	*Kurtosis Standard Error*	0.51739
Variance	7,736,215.78422	*Alternative Skewness (Fisher's)*	0.90743
Standard Deviation	2,781.40536	*Alternative Kurtosis (Fisher's)*	1.24627
Mean Standard Error	314.93214	*Coefficient of Variation*	0.29038
Minimum	5,480.	*Mean Deviation*	2,196.84418
Maximum	19,760.	*Second Moment*	7,637,033.53057
Range	14,280.	*Third Moment*	1.87811E+10
Sum	747,120.	*Fourth Moment*	2.38654E+14
Sum Standard Error	24,564.70702	*Median*	9,480.
Total Sum Squares	7,751,948,800.	*Median Error*	44.69198
Adjusted Sum Squares	595,688,615.38462	*Percentile 25% (Q1)*	7,360.
Geometric Mean	9,208.43046	*Percentile 75% (Q2)*	11,380.
Harmonic Mean	8,864.68	*IQR*	4,020.
Mode	#N/A	*MAD*	2,040.

Form factor (-)

Count	78	*Skewness*	0.27827
Mean	0.41372	*Skewness Standard Error*	0.2687
Mean LCL	0.37862	*Kurtosis*	2.06701
Mean UCL	0.44882	*Kurtosis Standard Error*	0.51739
Variance	0.01703	*Alternative Skewness (Fisher's)*	0.28375
Standard Deviation	0.13048	*Alternative Kurtosis (Fisher's)*	-0.91463
Mean Standard Error	0.01477	*Coefficient of Variation*	0.31539
Minimum	0.18356	*Mean Deviation*	0.11394
Maximum	0.71793	*Second Moment*	0.01681
Range	0.53437	*Third Moment*	0.00061
Sum	32.27039	*Fourth Moment*	0.00058
Sum Standard Error	1.15239	*Median*	0.38199
Total Sum Squares	14.66197	*Median Error*	0.0021
Adjusted Sum Squares	1.31097	*Percentile 25% (Q1)*	0.31181
Geometric Mean	0.39308	*Percentile 75% (Q2)*	0.51139
Harmonic Mean	0.37259	*IQR*	0.19958
Mode	#N/A	*MAD*	0.10031

Basin Elongation (-)

Count	78	*Skewness*	0.04335
Mean	0.71672	*Skewness Standard Error*	0.2687
Mean LCL	0.68574	*Kurtosis*	1.99735
Mean UCL	0.74769	*Kurtosis Standard Error*	0.51739
Variance	0.01326	*Alternative Skewness (Fisher's)*	0.04421
Standard Deviation	0.11514	*Alternative Kurtosis (Fisher's)*	-0.98897
Mean Standard Error	0.01304	*Coefficient of Variation*	0.16065
Minimum	0.48345	*Mean Deviation*	0.10078
Maximum	0.95609	*Second Moment*	0.01309
Range	0.47264	*Third Moment*	0.00006
Sum	55.90383	*Fourth Moment*	0.00034
Sum Standard Error	1.01688	*Median*	0.69737
Total Sum Squares	41.08794	*Median Error*	0.00185
Adjusted Sum Squares	1.02078	*Percentile 25% (Q1)*	0.63009
Geometric Mean	0.70745	*Percentile 75% (Q2)*	0.80692
Harmonic Mean	0.69809	*IQR*	0.17684
Mode	#N/A	*MAD*	0.09291

Lemniscate ratio (-)

Count	78	*Skewness*	0.8002
Mean	2.10796	*Skewness Standard Error*	0.2687
Mean LCL	1.91632	*Kurtosis*	3.16409
Mean UCL	2.29961	*Kurtosis Standard Error*	0.51739
Variance	0.50756	*Alternative Skewness (Fisher's)*	0.81597
Standard Deviation	0.71243	*Alternative Kurtosis (Fisher's)*	0.25617
Mean Standard Error	0.08067	*Coefficient of Variation*	0.33797
Minimum	1.09397	*Mean Deviation*	0.58901
Maximum	4.27861	*Second Moment*	0.50105
Range	3.18464	*Third Moment*	0.28381
Sum	164.42113	*Fourth Moment*	0.79436
Sum Standard Error	6.29204	*Median*	2.0568
Total Sum Squares	385.67587	*Median Error*	0.01145
Adjusted Sum Squares	39.08217	*Percentile 25% (Q1)*	1.54273
Geometric Mean	1.99808	*Percentile 75% (Q2)*	2.55997
Harmonic Mean	1.89837	*IQR*	1.01724
Mode	#N/A	*MAD*	0.51407

Outlet slope (°)

Count	78	*Skewness*	1.15456
Mean	9.24128	*Skewness Standard Error*	0.2687
Mean LCL	7.57308	*Kurtosis*	5.218
Mean UCL	10.90948	*Kurtosis Standard Error*	0.51739
Variance	38.45805	*Alternative Skewness (Fisher's)*	1.17732
Standard Deviation	6.20146	*Alternative Kurtosis (Fisher's)*	2.44809
Mean Standard Error	0.70218	*Coefficient of Variation*	0.67106
Minimum	0.E+0	*Mean Deviation*	4.60849
Maximum	33.6	*Second Moment*	37.965
Range	33.6	*Third Moment*	270.07916
Sum	720.82	*Fourth Moment*	7,520.91481
Sum Standard Error	54.76977	*Median*	8.83
Total Sum Squares	9,622.5706	*Median Error*	0.09965
Adjusted Sum Squares	2,961.26967	*Percentile 25% (Q1)*	4.435
Geometric Mean	7.21125	*Percentile 75% (Q2)*	12.09
Harmonic Mean	6.58423	*IQR*	7.655
Mode	0.E+0	*MAD*	3.775

200m slope (°)

Count	78	*Skewness*	1.64174
Mean	9.01282	*Skewness Standard Error*	0.2687
Mean LCL	7.29849	*Kurtosis*	7.03486
Mean UCL	10.72715	*Kurtosis Standard Error*	0.51739
Variance	40.61449	*Alternative Skewness (Fisher's)*	1.67411
Standard Deviation	6.37295	*Alternative Kurtosis (Fisher's)*	4.38702
Mean Standard Error	0.72159	*Coefficient of Variation*	0.7071
Minimum	0.E+0	*Mean Deviation*	4.55809
Maximum	34.85	*Second Moment*	40.09379
Range	34.85	*Third Moment*	416.79257
Sum	703.	*Fourth Moment*	11,308.61862
Sum Standard Error	56.28437	*Median*	8.365
Total Sum Squares	9,463.3286	*Median Error*	0.1024
Adjusted Sum Squares	3,127.31578	*Percentile 25% (Q1)*	4.535
Geometric Mean	7.07253	*Percentile 75% (Q2)*	11.505
Harmonic Mean	6.2447	*IQR*	6.97
Mode	0.E+0	*MAD*	3.51

Average slope (°)

Count	78	*Skewness*	0.61026
Mean	11.40179	*Skewness Standard Error*	0.2687
Mean LCL	9.72049	*Kurtosis*	3.03836
Mean UCL	13.0831	*Kurtosis Standard Error*	0.51739
Variance	39.06451	*Alternative Skewness (Fisher's)*	0.62229
Standard Deviation	6.25016	*Alternative Kurtosis (Fisher's)*	0.12199
Mean Standard Error	0.70769	*Coefficient of Variation*	0.54817
Minimum	0.E+0	*Mean Deviation*	4.86592
Maximum	27.49	*Second Moment*	38.56368
Range	27.49	*Third Moment*	146.14352
Sum	889.34	*Fourth Moment*	4,518.5201
Sum Standard Error	55.19992	*Median*	10.655
Total Sum Squares	13,148.0394	*Median Error*	0.10043
Adjusted Sum Squares	3,007.96715	*Percentile 25% (Q1)*	7.155
Geometric Mean	9.48044	*Percentile 75% (Q2)*	14.955
Harmonic Mean	7.68133	*IQR*	7.8
Mode	#N/A	*MAD*	4.06

1st-order catchments - Test set – Andorra – all catchments.

Max. elevation (m asl)			
Count	113	*Skewness*	-1.08243
Mean	2,596.69027	*Skewness Standard Error*	0.22543
Mean LCL	2,540.61192	*Kurtosis*	3.48251
Mean UCL	2,652.76861	*Kurtosis Standard Error*	0.43915
Variance	63,797.92999	*Alternative Skewness (Fisher's)*	-1.09705
Standard Deviation	252.58252	*Alternative Kurtosis (Fisher's)*	0.5596
Mean Standard Error	23.76096	*Coefficient of Variation*	0.09727
Minimum	1,835.	*Mean Deviation*	199.47012
Maximum	2,913.	*Second Moment*	63,233.34654
Range	1,078.	*Third Moment*	-17,211,512.21465
Sum	293,426.	*Fourth Moment*	1.39247E+10
Sum Standard Error	2,684.98903	*Median*	2,673.
Total Sum Squares	769,081,806.	*Median Error*	2.80146
Adjusted Sum Squares	7,145,368.15929	*Percentile 25% (Q1)*	2,505.5
Geometric Mean	2,583.45617	*Percentile 75% (Q2)*	2,791.5
Harmonic Mean	2,569.06356	*IQR*	286.
Mode	#N/A	*MAD*	131.
Mean elevation (m asl)			
Count	113	*Skewness*	-0.77188
Mean	2,208.15929	*Skewness Standard Error*	0.22543
Mean LCL	2,139.86122	*Kurtosis*	2.45651
Mean UCL	2,276.45737	*Kurtosis Standard Error*	0.43915
Variance	94,630.93221	*Alternative Skewness (Fisher's)*	-0.78231
Standard Deviation	307.62141	*Alternative Kurtosis (Fisher's)*	-0.51329
Mean Standard Error	28.93859	*Coefficient of Variation*	0.13931
Minimum	1,468.608	*Mean Deviation*	257.93409
Maximum	2,608.527	*Second Moment*	93,793.49034
Range	1,139.919	*Third Moment*	-22,172,319.12769
Sum	249,522.	*Fourth Moment*	2.16105E+10
Sum Standard Error	3,270.06045	*Median*	2,298.112
Total Sum Squares	561,582,987.27533	*Median Error*	3.41191
Adjusted Sum Squares	10,598,664.40808	*Percentile 25% (Q1)*	2,006.2555
Geometric Mean	2,184.90932	*Percentile 75% (Q2)*	2,458.00075
Harmonic Mean	2,159.59115	*IQR*	451.74525
Mode	#N/A	*MAD*	188.877
Min. elevation (m asl)			
Count	113	*Skewness*	-0.3722
Mean	1,747.24779	*Skewness Standard Error*	0.22543
Mean LCL	1,658.5678	*Kurtosis*	2.08314
Mean UCL	1,835.92777	*Kurtosis Standard Error*	0.43915
Variance	159,539.18805	*Alternative Skewness (Fisher's)*	-0.37723
Standard Deviation	399.42357	*Alternative Kurtosis (Fisher's)*	-0.90372
Mean Standard Error	37.57461	*Coefficient of Variation*	0.2286
Minimum	905.	*Mean Deviation*	345.4803
Maximum	2,436.	*Second Moment*	158,127.33683
Range	1,531.	*Third Moment*	-23,403,822.17711
Sum	197,439.	*Fourth Moment*	5.20874E+10
Sum Standard Error	4,245.93079	*Median*	1,863.
Total Sum Squares	362,843,245.	*Median Error*	4.43012
Adjusted Sum Squares	17,868,389.06195	*Percentile 25% (Q1)*	1,440.
Geometric Mean	1,696.99469	*Percentile 75% (Q2)*	2,070.
Harmonic Mean	1,641.81859	*IQR*	630.
Mode	#N/A	*MAD*	309.

Melton ratio (-)

Count	113	*Skewness*	0.68039
Mean	0.59998	*Skewness Standard Error*	0.22543
Mean LCL	0.55829	*Kurtosis*	2.70959
Mean UCL	0.64168	*Kurtosis Standard Error*	0.43915
Variance	0.03527	*Alternative Skewness (Fisher's)*	0.68958
Standard Deviation	0.18781	*Alternative Kurtosis (Fisher's)*	-0.24865
Mean Standard Error	0.01767	*Coefficient of Variation*	0.31303
Minimum	0.31084	*Mean Deviation*	0.15605
Maximum	1.11209	*Second Moment*	0.03496
Range	0.80125	*Third Moment*	0.00445
Sum	67.79827	*Fourth Moment*	0.00331
Sum Standard Error	1.99646	*Median*	0.54684
Total Sum Squares	44.62851	*Median Error*	0.00208
Adjusted Sum Squares	3.95059	*Percentile 25% (Q1)*	0.46063
Geometric Mean	0.57254	*Percentile 75% (Q2)*	0.7299
Harmonic Mean	0.54706	*IQR*	0.26927
Mode	#N/A	*MAD*	0.12094

Mean slope (°)

Count	113	*Skewness*	0.09788
Mean	24.56578	*Skewness Standard Error*	0.22543
Mean LCL	23.56272	*Kurtosis*	3.38806
Mean UCL	25.56883	*Kurtosis Standard Error*	0.43915
Variance	20.41099	*Alternative Skewness (Fisher's)*	0.0992
Standard Deviation	4.51785	*Alternative Kurtosis (Fisher's)*	0.46084
Mean Standard Error	0.425	*Coefficient of Variation*	0.18391
Minimum	14.36723	*Mean Deviation*	3.42593
Maximum	36.59921	*Second Moment*	20.23036
Range	22.23198	*Third Moment*	8.90655
Sum	2,775.93291	*Fourth Moment*	1,386.62388
Sum Standard Error	48.02542	*Median*	24.75687
Total Sum Squares	70,478.9819	*Median Error*	0.05011
Adjusted Sum Squares	2,286.03039	*Percentile 25% (Q1)*	22.11968
Geometric Mean	24.13834	*Percentile 75% (Q2)*	26.82178
Harmonic Mean	23.68831	*IQR*	4.7021
Mode	#N/A	*MAD*	2.36141

Mean orientation (0-360)

Count	113	*Skewness*	-0.05577
Mean	184.28401	*Skewness Standard Error*	0.22543
Mean LCL	171.74084	*Kurtosis*	2.04685
Mean UCL	196.82718	*Kurtosis Standard Error*	0.43915
Variance	3,191.76474	*Alternative Skewness (Fisher's)*	-0.05652
Standard Deviation	56.49571	*Alternative Kurtosis (Fisher's)*	-0.94167
Mean Standard Error	5.31467	*Coefficient of Variation*	0.30657
Minimum	57.34697	*Mean Deviation*	47.94727
Maximum	285.676	*Second Moment*	3,163.51903
Range	228.32903	*Third Moment*	-9,923.01799
Sum	20,824.09341	*Fourth Moment*	20,484,566.94934
Sum Standard Error	600.55759	*Median*	181.8163
Total Sum Squares	4,195,025.14062	*Median Error*	0.62661
Adjusted Sum Squares	357,477.65081	*Percentile 25% (Q1)*	135.0559
Geometric Mean	174.76	*Percentile 75% (Q2)*	229.69108
Harmonic Mean	164.1642	*IQR*	94.63518
Mode	#N/A	*MAD*	47.1057

Area (km2)

Count	113	*Skewness*	2.03842
Mean	2.31491	*Skewness Standard Error*	0.22543
Mean LCL	1.99775	*Kurtosis*	8.73849
Mean UCL	2.63206	*Kurtosis Standard Error*	0.43915
Variance	2.04057	*Alternative Skewness (Fisher's)*	2.06595
Standard Deviation	1.42849	*Alternative Kurtosis (Fisher's)*	6.05577
Mean Standard Error	0.13438	*Coefficient of Variation*	0.61708
Minimum	1.0124	*Mean Deviation*	1.05898
Maximum	9.158	*Second Moment*	2.02251
Range	8.1456	*Third Moment*	5.86316
Sum	261.5844	*Fourth Moment*	35.74531
Sum Standard Error	15.18501	*Median*	1.8348
Total Sum Squares	834.08735	*Median Error*	0.01584
Adjusted Sum Squares	228.54401	*Percentile 25% (Q1)*	1.264
Geometric Mean	2.00255	*Percentile 75% (Q2)*	2.9424
Harmonic Mean	1.77956	*IQR*	1.6784
Mode	1.8208	*MAD*	0.7008

Stream length (km)

Count	113	*Skewness*	1.23624
Mean	1.16636	*Skewness Standard Error*	0.22543
Mean LCL	0.95307	*Kurtosis*	4.46259
Mean UCL	1.37965	*Kurtosis Standard Error*	0.43915
Variance	0.92291	*Alternative Skewness (Fisher's)*	1.25294
Standard Deviation	0.96068	*Alternative Kurtosis (Fisher's)*	1.58447
Mean Standard Error	0.09037	*Coefficient of Variation*	0.82366
Minimum	0.00707	*Mean Deviation*	0.74932
Maximum	4.34568	*Second Moment*	0.91474
Range	4.33861	*Third Moment*	1.08156
Sum	131.79892	*Fourth Moment*	3.73409
Sum Standard Error	10.21219	*Median*	0.91094
Total Sum Squares	257.09115	*Median Error*	0.01066
Adjusted Sum Squares	103.36587	*Percentile 25% (Q1)*	0.39981
Geometric Mean	0.73856	*Percentile 75% (Q2)*	1.7075
Harmonic Mean	0.22913	*IQR*	1.30769
Mode	#N/A	*MAD*	0.5703

Perimeter (m)

Count	113	*Skewness*	1.12969
Mean	8,727.43363	*Skewness Standard Error*	0.22543
Mean LCL	8,197.95914	*Kurtosis*	4.20068
Mean UCL	9,256.90811	*Kurtosis Standard Error*	0.43915
Variance	5,687,301.39064	*Alternative Skewness (Fisher's)*	1.14495
Standard Deviation	2,384.80636	*Alternative Kurtosis (Fisher's)*	1.31058
Mean Standard Error	224.34371	*Coefficient of Variation*	0.27325
Minimum	5,360.	*Mean Deviation*	1,883.95019
Maximum	17,440.	*Second Moment*	5,636,971.28984
Range	12,080.	*Third Moment*	1.51192E+10
Sum	986,200.	*Fourth Moment*	1.33478E+14
Sum Standard Error	25,350.83938	*Median*	8,240.
Total Sum Squares	9,243,972,800.	*Median Error*	26.45054
Adjusted Sum Squares	636,977,755.75221	*Percentile 25% (Q1)*	6,930.
Geometric Mean	8,441.39061	*Percentile 75% (Q2)*	9,990.
Harmonic Mean	8,188.07725	*IQR*	3,060.
Mode	#N/A	*MAD*	1,520.

Form factor (-)

Count	113	*Skewness*	0.17173
Mean	0.4472	*Skewness Standard Error*	0.22543
Mean LCL	0.41905	*Kurtosis*	2.33394
Mean UCL	0.47535	*Kurtosis Standard Error*	0.43915
Variance	0.01608	*Alternative Skewness (Fisher's)*	0.17405
Standard Deviation	0.12679	*Alternative Kurtosis (Fisher's)*	-0.64146
Mean Standard Error	0.01193	*Coefficient of Variation*	0.28353
Minimum	0.20701	*Mean Deviation*	0.10307
Maximum	0.72935	*Second Moment*	0.01593
Range	0.52235	*Third Moment*	0.00035
Sum	50.53344	*Fourth Moment*	0.00059
Sum Standard Error	1.34783	*Median*	0.44874
Total Sum Squares	24.39904	*Median Error*	0.00141
Adjusted Sum Squares	1.80056	*Percentile 25% (Q1)*	0.34931
Geometric Mean	0.4286	*Percentile 75% (Q2)*	0.52817
Harmonic Mean	0.40931	*IQR*	0.17886
Mode	#N/A	*MAD*	0.08286

Basin Elongation (-)

Count	113	*Skewness*	-0.11325
Mean	0.74679	*Skewness Standard Error*	0.22543
Mean LCL	0.72268	*Kurtosis*	2.32372
Mean UCL	0.77091	*Kurtosis Standard Error*	0.43915
Variance	0.01179	*Alternative Skewness (Fisher's)*	-0.11478
Standard Deviation	0.1086	*Alternative Kurtosis (Fisher's)*	-0.65215
Mean Standard Error	0.01022	*Coefficient of Variation*	0.14542
Minimum	0.51339	*Mean Deviation*	0.08864
Maximum	0.96366	*Second Moment*	0.01169
Range	0.45027	*Third Moment*	-0.00014
Sum	84.38769	*Fourth Moment*	0.00032
Sum Standard Error	1.15446	*Median*	0.75588
Total Sum Squares	64.34117	*Median Error*	0.0012
Adjusted Sum Squares	1.32097	*Percentile 25% (Q1)*	0.66689
Geometric Mean	0.73872	*Percentile 75% (Q2)*	0.82005
Harmonic Mean	0.73041	*IQR*	0.15317
Mode	#N/A	*MAD*	0.0714

Lemniscate ratio (-)

Count	113	*Skewness*	1.03516
Mean	1.91881	*Skewness Standard Error*	0.22543
Mean LCL	1.78258	*Kurtosis*	3.64214
Mean UCL	2.05505	*Kurtosis Standard Error*	0.43915
Variance	0.37654	*Alternative Skewness (Fisher's)*	1.04914
Standard Deviation	0.61363	*Alternative Kurtosis (Fisher's)*	0.72652
Mean Standard Error	0.05773	*Coefficient of Variation*	0.31979
Minimum	1.07684	*Mean Deviation*	0.48321
Maximum	3.79402	*Second Moment*	0.37321
Range	2.71718	*Third Moment*	0.23601
Sum	216.82605	*Fourth Moment*	0.50728
Sum Standard Error	6.52294	*Median*	1.75024
Total Sum Squares	458.2212	*Median Error*	0.00681
Adjusted Sum Squares	42.1722	*Percentile 25% (Q1)*	1.48855
Geometric Mean	1.83248	*Percentile 75% (Q2)*	2.30716
Harmonic Mean	1.75626	*IQR*	0.81861
Mode	#N/A	*MAD*	0.32275

Outlet slope (°)

Count	113	*Skewness*	0.25852
Mean	8.32637	*Skewness Standard Error*	0.22543
Mean LCL	7.14308	*Kurtosis*	2.06924
Mean UCL	9.50966	*Kurtosis Standard Error*	0.43915
Variance	28.40528	*Alternative Skewness (Fisher's)*	0.26201
Standard Deviation	5.32966	*Alternative Kurtosis (Fisher's)*	-0.91826
Mean Standard Error	0.50137	*Coefficient of Variation*	0.64009
Minimum	0.E+0	*Mean Deviation*	4.59314
Maximum	21.32	*Second Moment*	28.15391
Range	21.32	*Third Moment*	38.61898
Sum	940.88	*Fourth Moment*	1,640.16981
Sum Standard Error	56.65507	*Median*	7.25
Total Sum Squares	11,015.508	*Median Error*	0.05911
Adjusted Sum Squares	3,181.39141	*Percentile 25% (Q1)*	3.81
Geometric Mean	6.36351	*Percentile 75% (Q2)*	12.88
Harmonic Mean	5.70468	*IQR*	9.07
Mode	0.E+0	*MAD*	4.16

200m slope (°)

Count	113	*Skewness*	0.25209
Mean	10.00097	*Skewness Standard Error*	0.22543
Mean LCL	8.60202	*Kurtosis*	2.22213
Mean UCL	11.39992	*Kurtosis Standard Error*	0.43915
Variance	39.70276	*Alternative Skewness (Fisher's)*	0.25549
Standard Deviation	6.30101	*Alternative Kurtosis (Fisher's)*	-0.75838
Mean Standard Error	0.59275	*Coefficient of Variation*	0.63004
Minimum	0.E+0	*Mean Deviation*	5.30581
Maximum	26.09	*Second Moment*	39.35141
Range	26.09	*Third Moment*	62.22962
Sum	1,130.11	*Fourth Moment*	3,441.04105
Sum Standard Error	66.98068	*Median*	9.52
Total Sum Squares	15,748.9095	*Median Error*	0.06989
Adjusted Sum Squares	4,446.70939	*Percentile 25% (Q1)*	4.5475
Geometric Mean	7.4341	*Percentile 75% (Q2)*	15.25
Harmonic Mean	5.23509	*IQR*	10.7025
Mode	0.E+0	*MAD*	5.51

Average slope (°)

Count	113	*Skewness*	0.1038
Mean	10.86204	*Skewness Standard Error*	0.22543
Mean LCL	9.50203	*Kurtosis*	2.42824
Mean UCL	12.22204	*Kurtosis Standard Error*	0.43915
Variance	37.52289	*Alternative Skewness (Fisher's)*	0.10521
Standard Deviation	6.12559	*Alternative Kurtosis (Fisher's)*	-0.54285
Mean Standard Error	0.57625	*Coefficient of Variation*	0.56395
Minimum	0.E+0	*Mean Deviation*	4.99872
Maximum	26.37	*Second Moment*	37.19083
Range	26.37	*Third Moment*	23.54331
Sum	1,227.41	*Fourth Moment*	3,358.63751
Sum Standard Error	65.11594	*Median*	11.34
Total Sum Squares	17,534.7341	*Median Error*	0.06794
Adjusted Sum Squares	4,202.56323	*Percentile 25% (Q1)*	5.695
Geometric Mean	8.54156	*Percentile 75% (Q2)*	15.1375
Harmonic Mean	6.90319	*IQR*	9.4425
Mode	0.E+0	*MAD*	4.82

1st-order catchments - Test set – Andorra – reactive catchments.

Max. elevation (m asl)			
Count	41	*Skewness*	-0.97799
Mean	2,699.95122	*Skewness Standard Error*	0.36037
Mean LCL	2,629.87991	*Kurtosis*	2.82455
Mean UCL	2,770.02253	*Kurtosis Standard Error*	0.67105
Variance	34,281.94756	*Alternative Skewness (Fisher's)*	-1.01553
Standard Deviation	185.15385	*Alternative Kurtosis (Fisher's)*	-0.03694
Mean Standard Error	28.91617	*Coefficient of Variation*	0.06858
Minimum	2,290.	*Mean Deviation*	149.13742
Maximum	2,913.	*Second Moment*	33,445.8025
Range	623.	*Third Moment*	-5,982,017.63854
Sum	110,698.	*Fourth Moment*	3,159,608,078.02099
Sum Standard Error	1,185.56309	*Median*	2,769.
Total Sum Squares	300,250,478.	*Median Error*	5.6599
Adjusted Sum Squares	1,371,277.90244	*Percentile 25% (Q1)*	2,598.75
Geometric Mean	2,693.44728	*Percentile 75% (Q2)*	2,830.5
Harmonic Mean	2,686.62632	*IQR*	231.75
Mode	#N/A	*MAD*	100.
Mean elevation (m asl)			
Count	41	*Skewness*	-0.86596
Mean	2,275.87683	*Skewness Standard Error*	0.36037
Mean LCL	2,175.93167	*Kurtosis*	2.70167
Mean UCL	2,375.82199	*Kurtosis Standard Error*	0.67105
Variance	69,744.27262	*Alternative Skewness (Fisher's)*	-0.8992
Standard Deviation	264.09141	*Alternative Kurtosis (Fisher's)*	-0.17624
Mean Standard Error	41.24415	*Coefficient of Variation*	0.11604
Minimum	1,591.371	*Mean Deviation*	219.46152
Maximum	2,608.527	*Second Moment*	68,043.1928
Range	1,017.156	*Third Moment*	-15,370,026.16044
Sum	93,310.95	*Fourth Moment*	1.25084E+10
Sum Standard Error	1,691.01011	*Median*	2,375.724
Total Sum Squares	215,153,999.9268	*Median Error*	8.07291
Adjusted Sum Squares	2,789,770.90479	*Percentile 25% (Q1)*	2,072.635
Geometric Mean	2,259.67306	*Percentile 75% (Q2)*	2,474.268
Harmonic Mean	2,242.14717	*IQR*	401.633
Mode	#N/A	*MAD*	126.474
Min. elevation (m asl)			
Count	41	*Skewness*	-0.47915
Mean	1,775.07317	*Skewness Standard Error*	0.36037
Mean LCL	1,630.02244	*Kurtosis*	2.46062
Mean UCL	1,920.1239	*Kurtosis Standard Error*	0.67105
Variance	146,901.01951	*Alternative Skewness (Fisher's)*	-0.49754
Standard Deviation	383.27669	*Alternative Kurtosis (Fisher's)*	-0.4495
Mean Standard Error	59.85776	*Coefficient of Variation*	0.21592
Minimum	905.	*Mean Deviation*	324.50684
Maximum	2,436.	*Second Moment*	143,318.06782
Range	1,531.	*Third Moment*	-25,997,138.28357
Sum	72,778.	*Fourth Moment*	5.05413E+10
Sum Standard Error	2,454.16825	*Median*	1,902.
Total Sum Squares	135,062,316.	*Median Error*	11.71625
Adjusted Sum Squares	5,876,040.78049	*Percentile 25% (Q1)*	1,544.
Geometric Mean	1,729.46319	*Percentile 75% (Q2)*	2,070.
Harmonic Mean	1,677.91399	*IQR*	526.
Mode	#N/A	*MAD*	293.

Melton ratio (-)

Count	41	*Skewness*	0.62913
Mean	0.60256	*Skewness Standard Error*	0.36037
Mean LCL	0.53264	*Kurtosis*	2.53096
Mean UCL	0.67249	*Kurtosis Standard Error*	0.67105
Variance	0.03414	*Alternative Skewness (Fisher's)*	0.65328
Standard Deviation	0.18477	*Alternative Kurtosis (Fisher's)*	-0.36976
Mean Standard Error	0.02886	*Coefficient of Variation*	0.30664
Minimum	0.32603	*Mean Deviation*	0.14916
Maximum	1.04149	*Second Moment*	0.03331
Range	0.71546	*Third Moment*	0.00382
Sum	24.70504	*Fourth Moment*	0.00281
Sum Standard Error	1.18312	*Median*	0.55778
Total Sum Squares	16.25196	*Median Error*	0.00565
Adjusted Sum Squares	1.36563	*Percentile 25% (Q1)*	0.47677
Geometric Mean	0.57628	*Percentile 75% (Q2)*	0.72462
Harmonic Mean	0.55156	*IQR*	0.24785
Mode	#N/A	*MAD*	0.11

Mean slope (°)

Count	41	*Skewness*	0.77448
Mean	26.13389	*Skewness Standard Error*	0.36037
Mean LCL	24.64999	*Kurtosis*	4.31737
Mean UCL	27.61779	*Kurtosis Standard Error*	0.67105
Variance	15.37422	*Alternative Skewness (Fisher's)*	0.8042
Standard Deviation	3.921	*Alternative Kurtosis (Fisher's)*	1.65531
Mean Standard Error	0.61236	*Coefficient of Variation*	0.15003
Minimum	17.16924	*Mean Deviation*	2.73481
Maximum	36.59921	*Second Moment*	14.99924
Range	19.42997	*Third Moment*	44.98966
Sum	1,071.48937	*Fourth Moment*	971.30894
Sum Standard Error	25.10664	*Median*	26.04049
Total Sum Squares	28,617.15109	*Median Error*	0.11986
Adjusted Sum Squares	614.9689	*Percentile 25% (Q1)*	24.05176
Geometric Mean	25.85805	*Percentile 75% (Q2)*	27.4769
Harmonic Mean	25.58866	*IQR*	3.42514
Mode	#N/A	*MAD*	1.94903

Mean orientation (0-360)

Count	41	*Skewness*	0.03454
Mean	176.60493	*Skewness Standard Error*	0.36037
Mean LCL	157.57704	*Kurtosis*	2.41309
Mean UCL	195.63281	*Kurtosis Standard Error*	0.67105
Variance	2,527.9359	*Alternative Skewness (Fisher's)*	0.03586
Standard Deviation	50.27858	*Alternative Kurtosis (Fisher's)*	-0.50338
Mean Standard Error	7.8522	*Coefficient of Variation*	0.2847
Minimum	65.01188	*Mean Deviation*	41.79539
Maximum	285.2942	*Second Moment*	2,466.27893
Range	220.28232	*Third Moment*	4,230.2831
Sum	7,240.80202	*Fourth Moment*	14,677,694.3158
Sum Standard Error	321.94001	*Median*	169.2833
Total Sum Squares	1,379,878.75048	*Median Error*	1.53695
Adjusted Sum Squares	101,117.43602	*Percentile 25% (Q1)*	132.93393
Geometric Mean	168.99239	*Percentile 75% (Q2)*	218.3509
Harmonic Mean	160.51453	*IQR*	85.41698
Mode	#N/A	*MAD*	40.5252

Area (km2)

Count	41	*Skewness*	1.16961
Mean	2.76519	*Skewness Standard Error*	0.36037
Mean LCL	2.1438	*Kurtosis*	4.36806
Mean UCL	3.38658	*Kurtosis Standard Error*	0.67105
Variance	2.69597	*Alternative Skewness (Fisher's)*	1.21451
Standard Deviation	1.64194	*Alternative Kurtosis (Fisher's)*	1.71278
Mean Standard Error	0.25643	*Coefficient of Variation*	0.59379
Minimum	1.0124	*Mean Deviation*	1.2948
Maximum	8.3056	*Second Moment*	2.63021
Range	7.2932	*Third Moment*	4.98918
Sum	113.3728	*Fourth Moment*	30.21835
Sum Standard Error	10.51355	*Median*	2.536
Total Sum Squares	421.33611	*Median Error*	0.05019
Adjusted Sum Squares	107.83875	*Percentile 25% (Q1)*	1.4372
Geometric Mean	2.35264	*Percentile 75% (Q2)*	3.8135
Harmonic Mean	2.01964	*IQR*	2.3763
Mode	#N/A	*MAD*	1.1252

Stream length (km)

Count	41	*Skewness*	0.96855
Mean	1.37964	*Skewness Standard Error*	0.36037
Mean LCL	0.94888	*Kurtosis*	3.10056
Mean UCL	1.81041	*Kurtosis Standard Error*	0.67105
Variance	1.29558	*Alternative Skewness (Fisher's)*	1.00572
Standard Deviation	1.13824	*Alternative Kurtosis (Fisher's)*	0.27594
Mean Standard Error	0.17776	*Coefficient of Variation*	0.82502
Minimum	0.02164	*Mean Deviation*	0.91713
Maximum	4.34568	*Second Moment*	1.26398
Range	4.32404	*Third Moment*	1.37636
Sum	56.5653	*Fourth Moment*	4.95363
Sum Standard Error	7.28827	*Median*	0.94798
Total Sum Squares	129.86319	*Median Error*	0.03479
Adjusted Sum Squares	51.82335	*Percentile 25% (Q1)*	0.53599
Geometric Mean	0.88684	*Percentile 75% (Q2)*	2.16216
Harmonic Mean	0.36396	*IQR*	1.62617
Mode	#N/A	*MAD*	0.6166

Perimeter (m)

Count	41	*Skewness*	0.61679
Mean	9,353.17073	*Skewness Standard Error*	0.36037
Mean LCL	8,294.95279	*Kurtosis*	2.33886
Mean UCL	10,411.38868	*Kurtosis Standard Error*	0.67105
Variance	7,818,712.19512	*Alternative Skewness (Fisher's)*	0.64047
Standard Deviation	2,796.19602	*Alternative Kurtosis (Fisher's)*	-0.58753
Mean Standard Error	436.69245	*Coefficient of Variation*	0.29896
Minimum	5,360.	*Mean Deviation*	2,337.70375
Maximum	15,920.	*Second Moment*	7,628,011.89768
Range	10,560.	*Third Moment*	1.29944E+10
Sum	383,480.	*Fourth Moment*	1.3609E+14
Sum Standard Error	17,904.39052	*Median*	8,720.
Total Sum Squares	3,899,502,400.	*Median Error*	85.4759
Adjusted Sum Squares	312,748,487.80488	*Percentile 25% (Q1)*	7,190.
Geometric Mean	8,968.92609	*Percentile 75% (Q2)*	11,690.
Harmonic Mean	8,615.58731	*IQR*	4,500.
Mode	#N/A	*MAD*	1,960.

Form factor (-)

Count	41	*Skewness*	0.08254
Mean	0.4708	*Skewness Standard Error*	0.36037
Mean LCL	0.42062	*Kurtosis*	2.24481
Mean UCL	0.52099	*Kurtosis Standard Error*	0.67105
Variance	0.01759	*Alternative Skewness (Fisher's)*	0.08571
Standard Deviation	0.13261	*Alternative Kurtosis (Fisher's)*	-0.69414
Mean Standard Error	0.02071	*Coefficient of Variation*	0.28167
Minimum	0.21648	*Mean Deviation*	0.10753
Maximum	0.72935	*Second Moment*	0.01716
Range	0.51287	*Third Moment*	0.00019
Sum	19.30287	*Fourth Moment*	0.00066
Sum Standard Error	0.84913	*Median*	0.47611
Total Sum Squares	9.79126	*Median Error*	0.00405
Adjusted Sum Squares	0.70343	*Percentile 25% (Q1)*	0.38954
Geometric Mean	0.4515	*Percentile 75% (Q2)*	0.57504
Harmonic Mean	0.43122	*IQR*	0.1855
Mode	#N/A	*MAD*	0.08716

Basin Elongation (-)

Count	41	*Skewness*	-0.19058
Mean	0.76639	*Skewness Standard Error*	0.36037
Mean LCL	0.72427	*Kurtosis*	2.30182
Mean UCL	0.80852	*Kurtosis Standard Error*	0.67105
Variance	0.01239	*Alternative Skewness (Fisher's)*	-0.1979
Standard Deviation	0.11131	*Alternative Kurtosis (Fisher's)*	-0.62952
Mean Standard Error	0.01738	*Coefficient of Variation*	0.14524
Minimum	0.52501	*Mean Deviation*	0.09039
Maximum	0.96366	*Second Moment*	0.01209
Range	0.43865	*Third Moment*	-0.00025
Sum	31.42204	*Fourth Moment*	0.00034
Sum Standard Error	0.71274	*Median*	0.77859
Total Sum Squares	24.57718	*Median Error*	0.0034
Adjusted Sum Squares	0.49561	*Percentile 25% (Q1)*	0.70426
Geometric Mean	0.7582	*Percentile 75% (Q2)*	0.8556
Harmonic Mean	0.74971	*IQR*	0.15134
Mode	#N/A	*MAD*	0.07487

Lemniscate ratio (-)

Count	41	*Skewness*	1.09161
Mean	1.82134	*Skewness Standard Error*	0.36037
Mean LCL	1.59804	*Kurtosis*	3.76353
Mean UCL	2.04463	*Kurtosis Standard Error*	0.67105
Variance	0.34813	*Alternative Skewness (Fisher's)*	1.13351
Standard Deviation	0.59002	*Alternative Kurtosis (Fisher's)*	1.02748
Mean Standard Error	0.09215	*Coefficient of Variation*	0.32395
Minimum	1.07684	*Mean Deviation*	0.4566
Maximum	3.62799	*Second Moment*	0.33963
Range	2.55115	*Third Moment*	0.21607
Sum	74.67482	*Fourth Moment*	0.43413
Sum Standard Error	3.77798	*Median*	1.64962
Total Sum Squares	149.93304	*Median Error*	0.01804
Adjusted Sum Squares	13.92501	*Percentile 25% (Q1)*	1.43379
Geometric Mean	1.73953	*Percentile 75% (Q2)*	2.03121
Harmonic Mean	1.66821	*IQR*	0.59742
Mode	#N/A	*MAD*	0.32403

Outlet slope (°)

Count	41	*Skewness*	-0.10151
Mean	8.74293	*Skewness Standard Error*	0.36037
Mean LCL	6.83881	*Kurtosis*	2.14824
Mean UCL	10.64705	*Kurtosis Standard Error*	0.67105
Variance	25.31479	*Alternative Skewness (Fisher's)*	-0.10541
Standard Deviation	5.03138	*Alternative Kurtosis (Fisher's)*	-0.80361
Mean Standard Error	0.78577	*Coefficient of Variation*	0.57548
Minimum	0.E+0	*Mean Deviation*	4.18989
Maximum	18.51	*Second Moment*	24.69736
Range	18.51	*Third Moment*	-12.45938
Sum	358.46	*Fourth Moment*	1,310.34114
Sum Standard Error	32.21656	*Median*	9.03
Total Sum Squares	4,146.5812	*Median Error*	0.1538
Adjusted Sum Squares	1,012.59165	*Percentile 25% (Q1)*	5.25
Geometric Mean	6.94168	*Percentile 75% (Q2)*	13.2025
Harmonic Mean	7.99466	*IQR*	7.9525
Mode	0.E+0	*MAD*	3.92

200m slope (°)

Count	41	*Skewness*	-0.18031
Mean	10.47463	*Skewness Standard Error*	0.36037
Mean LCL	8.15544	*Kurtosis*	1.86126
Mean UCL	12.79383	*Kurtosis Standard Error*	0.67105
Variance	37.55417	*Alternative Skewness (Fisher's)*	-0.18723
Standard Deviation	6.12815	*Alternative Kurtosis (Fisher's)*	-1.12893
Mean Standard Error	0.95706	*Coefficient of Variation*	0.58505
Minimum	0.E+0	*Mean Deviation*	5.25233
Maximum	19.87	*Second Moment*	36.63821
Range	19.87	*Third Moment*	-39.987
Sum	429.46	*Fourth Moment*	2,498.48057
Sum Standard Error	39.23928	*Median*	11.67
Total Sum Squares	6,000.603	*Median Error*	0.18733
Adjusted Sum Squares	1,502.16662	*Percentile 25% (Q1)*	5.8925
Geometric Mean	7.91656	*Percentile 75% (Q2)*	15.7075
Harmonic Mean	6.5664	*IQR*	9.815
Mode	0.E+0	*MAD*	4.86

Average slope (°)

Count	41	*Skewness*	0.06834
Mean	11.9739	*Skewness Standard Error*	0.36037
Mean LCL	9.42569	*Kurtosis*	2.6658
Mean UCL	14.52211	*Kurtosis Standard Error*	0.67105
Variance	45.33731	*Alternative Skewness (Fisher's)*	0.07096
Standard Deviation	6.7333	*Alternative Kurtosis (Fisher's)*	-0.21691
Mean Standard Error	1.05156	*Coefficient of Variation*	0.56233
Minimum	0.E+0	*Mean Deviation*	5.16527
Maximum	26.37	*Second Moment*	44.23153
Range	26.37	*Third Moment*	20.10295
Sum	490.93	*Fourth Moment*	5,215.44717
Sum Standard Error	43.11415	*Median*	12.
Total Sum Squares	7,691.8405	*Median Error*	0.20583
Adjusted Sum Squares	1,813.49258	*Percentile 25% (Q1)*	8.67
Geometric Mean	9.27729	*Percentile 75% (Q2)*	17.1
Harmonic Mean	8.6384	*IQR*	8.43
Mode	0.E+0	*MAD*	5.1

2nd-order catchments - Training set – Berga - all catchments.

Max. elevation (m asl)			
Count	113	*Skewness*	-0.20781
Mean	1,914.31212	*Skewness Standard Error*	0.22543
Mean LCL	1,810.69723	*Kurtosis*	1.94878
Mean UCL	2,017.92702	*Kurtosis Standard Error*	0.43915
Variance	217,801.3497	*Alternative Skewness (Fisher's)*	-0.21062
Standard Deviation	466.69192	*Alternative Kurtosis (Fisher's)*	-1.04422
Mean Standard Error	43.90268	*Coefficient of Variation*	0.24379
Minimum	905.06	*Mean Deviation*	408.97361
Maximum	2,648.32	*Second Moment*	215,873.90412
Range	1,743.26	*Third Moment*	-20,843,457.42725
Sum	216,317.27	*Fourth Moment*	9.08162E+10
Sum Standard Error	4,961.00318	*Median*	1,937.2
Total Sum Squares	438,492,523.7347	*Median Error*	5.17621
Adjusted Sum Squares	24,393,751.16609	*Percentile 25% (Q1)*	1,527.3975
Geometric Mean	1,852.87627	*Percentile 75% (Q2)*	2,318.3225
Harmonic Mean	1,786.57208	*IQR*	790.925
Mode	#N/A	*MAD*	394.78
Mean elevation (m asl)			
Count	113	*Skewness*	-0.0872
Mean	1,331.48722	*Skewness Standard Error*	0.22543
Mean LCL	1,257.14874	*Kurtosis*	2.07686
Mean UCL	1,405.82569	*Kurtosis Standard Error*	0.43915
Variance	112,109.77462	*Alternative Skewness (Fisher's)*	-0.08838
Standard Deviation	334.82798	*Alternative Kurtosis (Fisher's)*	-0.91029
Mean Standard Error	31.49797	*Coefficient of Variation*	0.25147
Minimum	672.7447	*Mean Deviation*	282.89069
Maximum	1,994.68	*Second Moment*	111,117.65272
Range	1,321.9353	*Third Moment*	-3,229,900.29149
Sum	150,458.0554	*Fourth Moment*	2.56433E+10
Sum Standard Error	3,559.27022	*Median*	1,321.345
Total Sum Squares	212,889,272.05616	*Median Error*	3.71367
Adjusted Sum Squares	12,556,294.75749	*Percentile 25% (Q1)*	1,096.51925
Geometric Mean	1,286.7173	*Percentile 75% (Q2)*	1,618.5045
Harmonic Mean	1,239.24167	*IQR*	521.98525
Mode	#N/A	*MAD*	253.458
Min. elevation (m asl)			
Count	113	*Skewness*	0.14544
Mean	863.35673	*Skewness Standard Error*	0.22543
Mean LCL	813.30057	*Kurtosis*	2.50777
Mean UCL	913.41288	*Kurtosis Standard Error*	0.43915
Variance	50,831.2902	*Alternative Skewness (Fisher's)*	0.1474
Standard Deviation	225.45796	*Alternative Kurtosis (Fisher's)*	-0.45969
Mean Standard Error	21.2093	*Coefficient of Variation*	0.26114
Minimum	412.45	*Mean Deviation*	183.0623
Maximum	1,471.82	*Second Moment*	50,381.45577
Range	1,059.37	*Third Moment*	1,644,699.7017
Sum	97,559.31	*Fourth Moment*	6,365,453,919.07507
Sum Standard Error	2,396.65095	*Median*	874.54
Total Sum Squares	89,921,590.9421	*Median Error*	2.50062
Adjusted Sum Squares	5,693,104.50249	*Percentile 25% (Q1)*	678.89
Geometric Mean	832.8831	*Percentile 75% (Q2)*	1,015.24
Harmonic Mean	801.13537	*IQR*	336.35
Mode	#N/A	*MAD*	180.14

Melton ratio (-)

Count	113	*Skewness*	0.69251
Mean	0.3497	*Skewness Standard Error*	0.22543
Mean LCL	0.31886	*Kurtosis*	3.42171
Mean UCL	0.38054	*Kurtosis Standard Error*	0.43915
Variance	0.01929	*Alternative Skewness (Fisher's)*	0.70186
Standard Deviation	0.1389	*Alternative Kurtosis (Fisher's)*	0.49602
Mean Standard Error	0.01307	*Coefficient of Variation*	0.3972
Minimum	0.09045	*Mean Deviation*	0.10792
Maximum	0.8289	*Second Moment*	0.01912
Range	0.73846	*Third Moment*	0.00183
Sum	39.5162	*Fourth Moment*	0.00125
Sum Standard Error	1.47655	*Median*	0.33043
Total Sum Squares	15.97974	*Median Error*	0.00154
Adjusted Sum Squares	2.16089	*Percentile 25% (Q1)*	0.2524
Geometric Mean	0.32231	*Percentile 75% (Q2)*	0.4353
Harmonic Mean	0.29394	*IQR*	0.18291
Mode	#N/A	*MAD*	0.08545

Mean slope (°)

Count	113	*Skewness*	0.00075
Mean	24.32732	*Skewness Standard Error*	0.22543
Mean LCL	23.18817	*Kurtosis*	3.18081
Mean UCL	25.46648	*Kurtosis Standard Error*	0.43915
Variance	26.32584	*Alternative Skewness (Fisher's)*	0.00076
Standard Deviation	5.13087	*Alternative Kurtosis (Fisher's)*	0.24411
Mean Standard Error	0.48267	*Coefficient of Variation*	0.21091
Minimum	12.58024	*Mean Deviation*	3.89392
Maximum	38.87977	*Second Moment*	26.09287
Range	26.29953	*Third Moment*	0.10026
Sum	2,748.98762	*Fourth Moment*	2,165.6177
Sum Standard Error	54.54191	*Median*	24.66379
Total Sum Squares	69,824.00693	*Median Error*	0.05691
Adjusted Sum Squares	2,948.49423	*Percentile 25% (Q1)*	21.32721
Geometric Mean	23.75613	*Percentile 75% (Q2)*	27.51173
Harmonic Mean	23.13788	*IQR*	6.18452
Mode	#N/A	*MAD*	3.21289

Mean orientation (0-360)

Count	113	*Skewness*	-0.03633
Mean	177.86658	*Skewness Standard Error*	0.22543
Mean LCL	171.77248	*Kurtosis*	2.35776
Mean UCL	183.96068	*Kurtosis Standard Error*	0.43915
Variance	753.41604	*Alternative Skewness (Fisher's)*	-0.03682
Standard Deviation	27.44843	*Alternative Kurtosis (Fisher's)*	-0.61655
Mean Standard Error	2.58213	*Coefficient of Variation*	0.15432
Minimum	123.5042	*Mean Deviation*	22.50226
Maximum	236.1284	*Second Moment*	746.74865
Range	112.6242	*Third Moment*	-741.40844
Sum	20,098.9235	*Fourth Moment*	1,314,766.69164
Sum Standard Error	291.78076	*Median*	180.7283
Total Sum Squares	3,659,309.37453	*Median Error*	0.30444
Adjusted Sum Squares	84,382.59702	*Percentile 25% (Q1)*	158.68285
Geometric Mean	175.71177	*Percentile 75% (Q2)*	196.04168
Harmonic Mean	173.50474	*IQR*	37.35883
Mode	#N/A	*MAD*	18.6655

Area (km2)

Count	113	*Skewness*	1.91661
Mean	11.31884	*Skewness Standard Error*	0.22543
Mean LCL	9.55058	*Kurtosis*	7.48309
Mean UCL	13.08709	*Kurtosis Standard Error*	0.43915
Variance	63.43192	*Alternative Skewness (Fisher's)*	1.94249
Standard Deviation	7.96442	*Alternative Kurtosis (Fisher's)*	4.743
Mean Standard Error	0.74923	*Coefficient of Variation*	0.70364
Minimum	2.20213	*Mean Deviation*	5.85354
Maximum	45.16895	*Second Moment*	62.87058
Range	42.96683	*Third Moment*	955.4448
Sum	1,279.0284	*Fourth Moment*	29,578.46407
Sum Standard Error	84.6629	*Median*	8.63708
Total Sum Squares	21,581.48693	*Median Error*	0.08834
Adjusted Sum Squares	7,104.375	*Percentile 25% (Q1)*	6.16014
Geometric Mean	9.28761	*Percentile 75% (Q2)*	14.36675
Harmonic Mean	7.76283	*IQR*	8.20661
Mode	#N/A	*MAD*	3.63205

Stream length (km)

Count	113	*Skewness*	1.25324
Mean	21.23628	*Skewness Standard Error*	0.22543
Mean LCL	19.31323	*Kurtosis*	4.91518
Mean UCL	23.15934	*Kurtosis Standard Error*	0.43915
Variance	75.02393	*Alternative Skewness (Fisher's)*	1.27016
Standard Deviation	8.66164	*Alternative Kurtosis (Fisher's)*	2.05774
Mean Standard Error	0.81482	*Coefficient of Variation*	0.40787
Minimum	9.1	*Mean Deviation*	6.76301
Maximum	54.86	*Second Moment*	74.36
Range	45.76	*Third Moment*	803.60518
Sum	2,399.7	*Fourth Moment*	27,178.06414
Sum Standard Error	92.07445	*Median*	18.82
Total Sum Squares	59,363.389	*Median Error*	0.09607
Adjusted Sum Squares	8,402.68024	*Percentile 25% (Q1)*	15.25
Geometric Mean	19.72477	*Percentile 75% (Q2)*	26.295
Harmonic Mean	18.40738	*IQR*	11.045
Mode	#N/A	*MAD*	4.75

Perimeter (m)

Count	113	*Skewness*	1.22995
Mean	20,921.76991	*Skewness Standard Error*	0.22543
Mean LCL	19,039.40941	*Kurtosis*	4.78161
Mean UCL	22,804.13041	*Kurtosis Standard Error*	0.43915
Variance	71,882,268.26802	*Alternative Skewness (Fisher's)*	1.24656
Standard Deviation	8,478.34113	*Alternative Kurtosis (Fisher's)*	1.91807
Mean Standard Error	797.57524	*Coefficient of Variation*	0.40524
Minimum	9,120.	*Mean Deviation*	6,649.27246
Maximum	53,560.	*Second Moment*	71,246,142.00016
Range	44,440.	*Third Moment*	7.39658E+11
Sum	2,364,160.	*Fourth Moment*	2.42715E+16
Sum Standard Error	90,126.00243	*Median*	18,440.
Total Sum Squares	5.75132E+10	*Median Error*	94.03562
Adjusted Sum Squares	8,050,814,046.0177	*Percentile 25% (Q1)*	14,960.
Geometric Mean	19,448.72076	*Percentile 75% (Q2)*	26,010.
Harmonic Mean	18,166.00301	*IQR*	11,050.
Mode	18,720.	*MAD*	4,600.

Form factor (-)

Count	113	*Skewness*	-0.07328
Mean	0.0245	*Skewness Standard Error*	0.22543
Mean LCL	0.0233	*Kurtosis*	2.63882
Mean UCL	0.02569	*Kurtosis Standard Error*	0.43915
Variance	0.00003	*Alternative Skewness (Fisher's)*	-0.07427
Standard Deviation	0.00538	*Alternative Kurtosis (Fisher's)*	-0.32265
Mean Standard Error	0.00051	*Coefficient of Variation*	0.21963
Minimum	0.01162	*Mean Deviation*	0.00438
Maximum	0.03989	*Second Moment*	0.00003
Range	0.02826	*Third Moment*	0.
Sum	2.76799	*Fourth Moment*	0.
Sum Standard Error	0.05719	*Median*	0.02532
Total Sum Squares	0.07104	*Median Error*	0.00006
Adjusted Sum Squares	0.00324	*Percentile 25% (Q1)*	0.02015
Geometric Mean	0.02387	*Percentile 75% (Q2)*	0.028
Harmonic Mean	0.02321	*IQR*	0.00785
Mode	#N/A	*MAD*	0.00407

Basin Elongation (-)

Count	113	*Skewness*	-0.07932
Mean	1.42941	*Skewness Standard Error*	0.22543
Mean LCL	1.37753	*Kurtosis*	2.26912
Mean UCL	1.48129	*Kurtosis Standard Error*	0.43915
Variance	0.0546	*Alternative Skewness (Fisher's)*	-0.08039
Standard Deviation	0.23367	*Alternative Kurtosis (Fisher's)*	-0.70924
Mean Standard Error	0.02198	*Coefficient of Variation*	0.16348
Minimum	0.87712	*Mean Deviation*	0.194
Maximum	1.89669	*Second Moment*	0.05412
Range	1.01957	*Third Moment*	-0.001
Sum	161.5232	*Fourth Moment*	0.00665
Sum Standard Error	2.48399	*Median*	1.45193
Total Sum Squares	236.9983	*Median Error*	0.00259
Adjusted Sum Squares	6.1156	*Percentile 25% (Q1)*	1.25548
Geometric Mean	1.40983	*Percentile 75% (Q2)*	1.61077
Harmonic Mean	1.3896	*IQR*	0.3553
Mode	#N/A	*MAD*	0.17015

Lemniscate ratio (-)

Count	113	*Skewness*	0.80435
Mean	0.71963	*Skewness Standard Error*	0.22543
Mean LCL	0.69161	*Kurtosis*	3.43466
Mean UCL	0.74765	*Kurtosis Standard Error*	0.43915
Variance	0.01593	*Alternative Skewness (Fisher's)*	0.81521
Standard Deviation	0.1262	*Alternative Kurtosis (Fisher's)*	0.50956
Mean Standard Error	0.01187	*Coefficient of Variation*	0.17536
Minimum	0.52723	*Mean Deviation*	0.10345
Maximum	1.14009	*Second Moment*	0.01578
Range	0.61286	*Third Moment*	0.0016
Sum	81.31836	*Fourth Moment*	0.00086
Sum Standard Error	1.3415	*Median*	0.68874
Total Sum Squares	60.30295	*Median Error*	0.0014
Adjusted Sum Squares	1.7837	*Percentile 25% (Q1)*	0.62579
Geometric Mean	0.70931	*Percentile 75% (Q2)*	0.80119
Harmonic Mean	0.69959	*IQR*	0.1754
Mode	#N/A	*MAD*	0.08308

Outlet slope (°)

Count	113	*Skewness*	1.11393
Mean	8.07965	*Skewness Standard Error*	0.22543
Mean LCL	6.66461	*Kurtosis*	3.28683
Mean UCL	9.49469	*Kurtosis Standard Error*	0.43915
Variance	40.6213	*Alternative Skewness (Fisher's)*	1.12897
Standard Deviation	6.37348	*Alternative Kurtosis (Fisher's)*	0.35497
Mean Standard Error	0.59957	*Coefficient of Variation*	0.78883
Minimum	0.E+0	*Mean Deviation*	5.09334
Maximum	25.75	*Second Moment*	40.26182
Range	25.75	*Third Moment*	284.57513
Sum	913.	*Fourth Moment*	5,327.98936
Sum Standard Error	67.75106	*Median*	5.55
Total Sum Squares	11,926.302	*Median Error*	0.07069
Adjusted Sum Squares	4,549.58519	*Percentile 25% (Q1)*	3.385
Geometric Mean	5.81538	*Percentile 75% (Q2)*	11.86
Harmonic Mean	3.82391	*IQR*	8.475
Mode	#N/A	*MAD*	2.79

200m slope (°)

Count	113	*Skewness*	1.37814
Mean	7.63876	*Skewness Standard Error*	0.22543
Mean LCL	6.26569	*Kurtosis*	4.48368
Mean UCL	9.01183	*Kurtosis Standard Error*	0.43915
Variance	38.24736	*Alternative Skewness (Fisher's)*	1.39675
Standard Deviation	6.18444	*Alternative Kurtosis (Fisher's)*	1.60652
Mean Standard Error	0.58178	*Coefficient of Variation*	0.80961
Minimum	0.E+0	*Mean Deviation*	4.78296
Maximum	29.33	*Second Moment*	37.90888
Range	29.33	*Third Moment*	321.66575
Sum	863.18	*Fourth Moment*	6,443.41809
Sum Standard Error	65.74155	*Median*	5.72
Total Sum Squares	10,877.3296	*Median Error*	0.06859
Adjusted Sum Squares	4,283.70383	*Percentile 25% (Q1)*	3.375
Geometric Mean	5.53175	*Percentile 75% (Q2)*	10.96
Harmonic Mean	3.8442	*IQR*	7.585
Mode	4.29	*MAD*	2.97

Average slope (°)

Count	113	*Skewness*	1.18472
Mean	8.25637	*Skewness Standard Error*	0.22543
Mean LCL	6.97755	*Kurtosis*	4.21762
Mean UCL	9.53519	*Kurtosis Standard Error*	0.43915
Variance	33.17686	*Alternative Skewness (Fisher's)*	1.20072
Standard Deviation	5.75994	*Alternative Kurtosis (Fisher's)*	1.3283
Mean Standard Error	0.54185	*Coefficient of Variation*	0.69764
Minimum	0.E+0	*Mean Deviation*	4.47633
Maximum	28.1	*Second Moment*	32.88326
Range	28.1	*Third Moment*	223.39762
Sum	932.97	*Fourth Moment*	4,560.54625
Sum Standard Error	61.22895	*Median*	6.76
Total Sum Squares	11,418.7551	*Median Error*	0.06389
Adjusted Sum Squares	3,715.80801	*Percentile 25% (Q1)*	3.955
Geometric Mean	6.3679	*Percentile 75% (Q2)*	11.0575
Harmonic Mean	4.56993	*IQR*	7.1025
Mode	#N/A	*MAD*	3.33

2nd-order catchments - Training set – Berga – reactive catchments.

Max. elevation (m asl)			
Count	12	*Skewness*	-0.81191
Mean	2,251.29083	*Skewness Standard Error*	0.58177
Mean LCL	2,000.24326	*Kurtosis*	3.09755
Mean UCL	2,502.3384	*Kurtosis Standard Error*	0.91655
Variance	102,369.1459	*Alternative Skewness (Fisher's)*	-0.93281
Standard Deviation	319.95179	*Alternative Kurtosis (Fisher's)*	0.88833
Mean Standard Error	92.36213	*Coefficient of Variation*	0.14212
Minimum	1,542.42	*Mean Deviation*	231.71569
Maximum	2,648.06	*Second Moment*	93,838.38374
Range	1,105.64	*Third Moment*	-23,338,813.67164
Sum	27,015.49	*Fourth Moment*	2.72759E+10
Sum Standard Error	1,108.3455	*Median*	2,306.345
Total Sum Squares	61,945,785.5999	*Median Error*	33.41667
Adjusted Sum Squares	1,126,060.60489	*Percentile 25% (Q1)*	2,211.82
Geometric Mean	2,228.28258	*Percentile 75% (Q2)*	2,577.71
Harmonic Mean	2,202.85349	*IQR*	365.89
Mode	#N/A	*MAD*	182.945
Mean elevation (m asl)			
Count	12	*Skewness*	-0.43837
Mean	1,534.54617	*Skewness Standard Error*	0.58177
Mean LCL	1,345.30376	*Kurtosis*	2.22795
Mean UCL	1,723.78857	*Kurtosis Standard Error*	0.91655
Variance	58,169.31647	*Alternative Skewness (Fisher's)*	-0.50365
Standard Deviation	241.18316	*Alternative Kurtosis (Fisher's)*	-0.49337
Mean Standard Error	69.62358	*Coefficient of Variation*	0.15717
Minimum	1,126.897	*Mean Deviation*	186.0465
Maximum	1,852.938	*Second Moment*	53,321.87343
Range	726.041	*Third Moment*	-5,397,620.96288
Sum	18,414.554	*Fourth Moment*	6,334,546,016.34045
Sum Standard Error	835.48297	*Median*	1,535.709
Total Sum Squares	28,897,845.73277	*Median Error*	25.18986
Adjusted Sum Squares	639,862.48119	*Percentile 25% (Q1)*	1,446.321
Geometric Mean	1,516.01225	*Percentile 75% (Q2)*	1,760.753
Harmonic Mean	1,496.34831	*IQR*	314.432
Mode	#N/A	*MAD*	146.5605
Min. elevation (m asl)			
Count	12	*Skewness*	-0.35193
Mean	910.63417	*Skewness Standard Error*	0.58177
Mean LCL	748.63971	*Kurtosis*	2.12816
Mean UCL	1,072.62862	*Kurtosis Standard Error*	0.91655
Variance	42,624.30852	*Alternative Skewness (Fisher's)*	-0.40434
Standard Deviation	206.45655	*Alternative Kurtosis (Fisher's)*	-0.65192
Mean Standard Error	59.59887	*Coefficient of Variation*	0.22672
Minimum	531.61	*Mean Deviation*	159.7275
Maximum	1,181.01	*Second Moment*	39,072.28281
Range	649.4	*Third Moment*	-2,718,053.95496
Sum	10,927.61	*Fourth Moment*	3,248,946,208.91837
Sum Standard Error	715.18648	*Median*	921.42
Total Sum Squares	10,419,922.4197	*Median Error*	21.56291
Adjusted Sum Squares	468,867.39369	*Percentile 25% (Q1)*	802.62
Geometric Mean	887.03102	*Percentile 75% (Q2)*	1,106.69
Harmonic Mean	861.31593	*IQR*	304.07
Mode	#N/A	*MAD*	179.94

Melton ratio (-)

Count	12	*Skewness*	-0.24965
Mean	0.39943	*Skewness Standard Error*	0.58177
Mean LCL	0.32009	*Kurtosis*	2.75402
Mean UCL	0.47877	*Kurtosis Standard Error*	0.91655
Variance	0.01023	*Alternative Skewness (Fisher's)*	-0.28683
Standard Deviation	0.10112	*Alternative Kurtosis (Fisher's)*	0.3425
Mean Standard Error	0.02919	*Coefficient of Variation*	0.25316
Minimum	0.22536	*Mean Deviation*	0.06989
Maximum	0.56417	*Second Moment*	0.00937
Range	0.33881	*Third Moment*	-0.00023
Sum	4.79316	*Fourth Moment*	0.00024
Sum Standard Error	0.35029	*Median*	0.39819
Total Sum Squares	2.02701	*Median Error*	0.01056
Adjusted Sum Squares	0.11248	*Percentile 25% (Q1)*	0.37722
Geometric Mean	0.38627	*Percentile 75% (Q2)*	0.4467
Harmonic Mean	0.37153	*IQR*	0.06948
Mode	#N/A	*MAD*	0.0359

Mean slope (°)

Count	12	*Skewness*	-0.22041
Mean	25.99311	*Skewness Standard Error*	0.58177
Mean LCL	23.20057	*Kurtosis*	2.25136
Mean UCL	28.78565	*Kurtosis Standard Error*	0.91655
Variance	12.66649	*Alternative Skewness (Fisher's)*	-0.25323
Standard Deviation	3.559	*Alternative Kurtosis (Fisher's)*	-0.45617
Mean Standard Error	1.0274	*Coefficient of Variation*	0.13692
Minimum	19.48814	*Mean Deviation*	2.89267
Maximum	31.55156	*Second Moment*	11.61095
Range	12.06342	*Third Moment*	-8.72038
Sum	311.91732	*Fourth Moment*	303.51577
Sum Standard Error	12.32874	*Median*	26.13598
Total Sum Squares	8,247.03263	*Median Error*	0.37171
Adjusted Sum Squares	139.33142	*Percentile 25% (Q1)*	24.51546
Geometric Mean	25.76178	*Percentile 75% (Q2)*	28.30666
Harmonic Mean	25.52271	*IQR*	3.7912
Mode	#N/A	*MAD*	2.08022

Mean orientation (0-360)

Count	12	*Skewness*	0.56897
Mean	172.86821	*Skewness Standard Error*	0.58177
Mean LCL	148.77772	*Kurtosis*	2.46217
Mean UCL	196.95869	*Kurtosis Standard Error*	0.91655
Variance	942.64488	*Alternative Skewness (Fisher's)*	0.65369
Standard Deviation	30.70252	*Alternative Kurtosis (Fisher's)*	-0.12122
Mean Standard Error	8.86305	*Coefficient of Variation*	0.17761
Minimum	133.5015	*Mean Deviation*	24.91674
Maximum	236.1284	*Second Moment*	864.09114
Range	102.6269	*Third Moment*	14,451.95643
Sum	2,074.4185	*Fourth Moment*	1,838,389.27957
Sum Standard Error	106.35666	*Median*	167.35825
Total Sum Squares	368,970.10308	*Median Error*	3.20666
Adjusted Sum Squares	10,369.09365	*Percentile 25% (Q1)*	148.7379
Geometric Mean	170.46968	*Percentile 75% (Q2)*	194.757
Harmonic Mean	168.18233	*IQR*	46.0191
Mode	#N/A	*MAD*	23.68975

Area (km2)

Count	12	*Skewness*	1.99068
Mean	13.89007	*Skewness Standard Error*	0.58177
Mean LCL	5.12353	*Kurtosis*	6.21611
Mean UCL	22.65661	*Kurtosis Standard Error*	0.91655
Variance	124.82847	*Alternative Skewness (Fisher's)*	2.28712
Standard Deviation	11.17267	*Alternative Kurtosis (Fisher's)*	5.84338
Mean Standard Error	3.22527	*Coefficient of Variation*	0.80436
Minimum	5.18843	*Mean Deviation*	7.73827
Maximum	45.16895	*Second Moment*	114.4261
Range	39.98053	*Third Moment*	2,436.62884
Sum	166.68088	*Fourth Moment*	81,389.65207
Sum Standard Error	38.70325	*Median*	8.87094
Total Sum Squares	3,688.32268	*Median Error*	1.16691
Adjusted Sum Squares	1,373.11318	*Percentile 25% (Q1)*	7.91925
Geometric Mean	11.31063	*Percentile 75% (Q2)*	19.31985
Harmonic Mean	9.76805	*IQR*	11.4006
Mode	#N/A	*MAD*	2.68935

Stream length (km)

Count	12	*Skewness*	1.53178
Mean	24.12667	*Skewness Standard Error*	0.58177
Mean LCL	15.55379	*Kurtosis*	4.61948
Mean UCL	32.69954	*Kurtosis Standard Error*	0.91655
Variance	119.37408	*Alternative Skewness (Fisher's)*	1.75988
Standard Deviation	10.92584	*Alternative Kurtosis (Fisher's)*	3.30651
Mean Standard Error	3.15402	*Coefficient of Variation*	0.45285
Minimum	14.15	*Mean Deviation*	8.31722
Maximum	52.3	*Second Moment*	109.42624
Range	38.15	*Third Moment*	1,753.39111
Sum	289.52	*Fourth Moment*	55,314.14801
Sum Standard Error	37.84824	*Median*	19.365
Total Sum Squares	8,298.2674	*Median Error*	1.14113
Adjusted Sum Squares	1,313.11487	*Percentile 25% (Q1)*	17.42
Geometric Mean	22.38138	*Percentile 75% (Q2)*	30.46
Harmonic Mean	21.06885	*IQR*	13.04
Mode	#N/A	*MAD*	3.18

Perimeter (m)

Count	12	*Skewness*	1.5057
Mean	23,706.66667	*Skewness Standard Error*	0.58177
Mean LCL	15,377.94117	*Kurtosis*	4.53268
Mean UCL	32,035.39217	*Kurtosis Standard Error*	0.91655
Variance	112,671,515.15152	*Alternative Skewness (Fisher's)*	1.72991
Standard Deviation	10,614.68394	*Alternative Kurtosis (Fisher's)*	3.16859
Mean Standard Error	3,064.19532	*Coefficient of Variation*	0.44775
Minimum	13,840.	*Mean Deviation*	8,095.55556
Maximum	50,920.	*Second Moment*	103,282,222.22222
Range	37,080.	*Third Moment*	1.58043E+12
Sum	284,480.	*Fourth Moment*	4.83511E+16
Sum Standard Error	36,770.34378	*Median*	19,080.
Total Sum Squares	7,983,459,200.	*Median Error*	1,108.62779
Adjusted Sum Squares	1,239,386,666.66667	*Percentile 25% (Q1)*	17,080.
Geometric Mean	22,018.37679	*Percentile 75% (Q2)*	29,920.
Harmonic Mean	20,739.58434	*IQR*	12,840.
Mode	#N/A	*MAD*	3,080.

Form factor (-)

Count	12	*Skewness*	-0.33867
Mean	0.02305	*Skewness Standard Error*	0.58177
Mean LCL	0.01936	*Kurtosis*	1.67949
Mean UCL	0.02674	*Kurtosis Standard Error*	0.91655
Variance	0.00002	*Alternative Skewness (Fisher's)*	-0.3891
Standard Deviation	0.00471	*Alternative Kurtosis (Fisher's)*	-1.3648
Mean Standard Error	0.00136	*Coefficient of Variation*	0.20424
Minimum	0.01651	*Mean Deviation*	0.004
Maximum	0.02995	*Second Moment*	0.00002
Range	0.01344	*Third Moment*	0.
Sum	0.27661	*Fourth Moment*	0.
Sum Standard Error	0.01631	*Median*	0.02515
Total Sum Squares	0.00662	*Median Error*	0.00049
Adjusted Sum Squares	0.00024	*Percentile 25% (Q1)*	0.0177
Geometric Mean	0.02258	*Percentile 75% (Q2)*	0.02591
Harmonic Mean	0.02209	*IQR*	0.00821
Mode	#N/A	*MAD*	0.00212

Basin Elongation (-)

Count	12	*Skewness*	0.09225
Mean	1.38418	*Skewness Standard Error*	0.58177
Mean LCL	1.27844	*Kurtosis*	2.28236
Mean UCL	1.48992	*Kurtosis Standard Error*	0.91655
Variance	0.01816	*Alternative Skewness (Fisher's)*	0.10599
Standard Deviation	0.13476	*Alternative Kurtosis (Fisher's)*	-0.40691
Mean Standard Error	0.0389	*Coefficient of Variation*	0.09736
Minimum	1.15093	*Mean Deviation*	0.11264
Maximum	1.62757	*Second Moment*	0.01665
Range	0.47664	*Third Moment*	0.0002
Sum	16.61014	*Fourth Moment*	0.00063
Sum Standard Error	0.46684	*Median*	1.37229
Total Sum Squares	23.19116	*Median Error*	0.01408
Adjusted Sum Squares	0.19977	*Percentile 25% (Q1)*	1.3076
Geometric Mean	1.37815	*Percentile 75% (Q2)*	1.48823
Harmonic Mean	1.37212	*IQR*	0.18063
Mode	#N/A	*MAD*	0.08279

Lemniscate ratio (-)

Count	12	*Skewness*	0.27338
Mean	0.7288	*Skewness Standard Error*	0.58177
Mean LCL	0.67266	*Kurtosis*	2.42443
Mean UCL	0.78494	*Kurtosis Standard Error*	0.91655
Variance	0.00512	*Alternative Skewness (Fisher's)*	0.31409
Standard Deviation	0.07155	*Alternative Kurtosis (Fisher's)*	-0.18118
Mean Standard Error	0.02065	*Coefficient of Variation*	0.09817
Minimum	0.61441	*Mean Deviation*	0.05943
Maximum	0.86886	*Second Moment*	0.00469
Range	0.25445	*Third Moment*	0.00009
Sum	8.74559	*Fourth Moment*	0.00005
Sum Standard Error	0.24784	*Median*	0.72992
Total Sum Squares	6.43009	*Median Error*	0.00747
Adjusted Sum Squares	0.05631	*Percentile 25% (Q1)*	0.68391
Geometric Mean	0.72561	*Percentile 75% (Q2)*	0.77125
Harmonic Mean	0.72245	*IQR*	0.08734
Mode	#N/A	*MAD*	0.04367

Outlet slope (°)

Count	12	*Skewness*	0.85241
Mean	8.19667	*Skewness Standard Error*	0.58177
Mean LCL	3.37357	*Kurtosis*	3.01944
Mean UCL	13.01977	*Kurtosis Standard Error*	0.91655
Variance	37.78415	*Alternative Skewness (Fisher's)*	0.97934
Standard Deviation	6.14688	*Alternative Kurtosis (Fisher's)*	0.76423
Mean Standard Error	1.77445	*Coefficient of Variation*	0.74992
Minimum	0.31	*Mean Deviation*	4.46611
Maximum	21.67	*Second Moment*	34.63547
Range	21.36	*Third Moment*	173.75199
Sum	98.36	*Fourth Moment*	3,622.17197
Sum Standard Error	21.29342	*Median*	7.195
Total Sum Squares	1,221.8498	*Median Error*	0.642
Adjusted Sum Squares	415.62567	*Percentile 25% (Q1)*	5.22
Geometric Mean	5.53983	*Percentile 75% (Q2)*	13.58
Harmonic Mean	2.30948	*IQR*	8.36
Mode	#N/A	*MAD*	3.095

200m slope (°)

Count	12	*Skewness*	0.53421
Mean	7.05917	*Skewness Standard Error*	0.58177
Mean LCL	3.23875	*Kurtosis*	2.18709
Mean UCL	10.87959	*Kurtosis Standard Error*	0.91655
Variance	23.70714	*Alternative Skewness (Fisher's)*	0.61376
Standard Deviation	4.869	*Alternative Kurtosis (Fisher's)*	-0.55829
Mean Standard Error	1.40556	*Coefficient of Variation*	0.68974
Minimum	0.54	*Mean Deviation*	3.85236
Maximum	15.82	*Second Moment*	21.73154
Range	15.28	*Third Moment*	54.11882
Sum	84.71	*Fourth Moment*	1,032.87471
Sum Standard Error	16.8667	*Median*	6.245
Total Sum Squares	858.7605	*Median Error*	0.50853
Adjusted Sum Squares	260.77849	*Percentile 25% (Q1)*	3.36
Geometric Mean	5.18264	*Percentile 75% (Q2)*	11.55
Harmonic Mean	3.02809	*IQR*	8.19
Mode	#N/A	*MAD*	3.19

Average slope (°)

Count	12	*Skewness*	1.32102
Mean	7.94417	*Skewness Standard Error*	0.58177
Mean LCL	3.17934	*Kurtosis*	4.55267
Mean UCL	12.709	*Kurtosis Standard Error*	0.91655
Variance	36.87668	*Alternative Skewness (Fisher's)*	1.51773
Standard Deviation	6.07262	*Alternative Kurtosis (Fisher's)*	3.20036
Mean Standard Error	1.75301	*Coefficient of Variation*	0.76441
Minimum	0.63	*Mean Deviation*	4.23986
Maximum	23.38	*Second Moment*	33.80362
Range	22.75	*Third Moment*	259.62916
Sum	95.33	*Fourth Moment*	5,202.2691
Sum Standard Error	21.03616	*Median*	6.665
Total Sum Squares	1,162.9609	*Median Error*	0.63424
Adjusted Sum Squares	405.64349	*Percentile 25% (Q1)*	4.56
Geometric Mean	5.78344	*Percentile 75% (Q2)*	10.34
Harmonic Mean	3.42777	*IQR*	5.78
Mode	#N/A	*MAD*	3.345

2nd-order catchments - Training set – Mollo - all catchments.

Max. elevation (m asl)			
Count	27	*Skewness*	-0.02103
Mean	2,129.40741	*Skewness Standard Error*	0.43095
Mean LCL	1,861.61016	*Kurtosis*	1.78369
Mean UCL	2,397.20465	*Kurtosis Standard Error*	0.77402
Variance	315,175.63533	*Alternative Skewness (Fisher's)*	-0.02228
Standard Deviation	561.40505	*Alternative Kurtosis (Fisher's)*	-1.21579
Mean Standard Error	108.04245	*Coefficient of Variation*	0.26364
Minimum	1,176.	*Mean Deviation*	471.41564
Maximum	2,910.	*Second Moment*	303,502.46365
Range	1,734.	*Third Moment*	-3,515,561.33801
Sum	57,494.	*Fourth Moment*	1.64302E+11
Sum Standard Error	2,917.14623	*Median*	2,053.
Total Sum Squares	130,622,716.	*Median Error*	26.05988
Adjusted Sum Squares	8,194,566.51852	*Percentile 25% (Q1)*	1,647.75
Geometric Mean	2,054.33152	*Percentile 75% (Q2)*	2,724.
Harmonic Mean	1,976.91373	*IQR*	1,076.25
Mode	#N/A	*MAD*	453.
Mean elevation (m asl)			
Count	27	*Skewness*	0.20656
Mean	1,613.44444	*Skewness Standard Error*	0.43095
Mean LCL	1,378.73812	*Kurtosis*	2.30661
Mean UCL	1,848.15077	*Kurtosis Standard Error*	0.77402
Variance	242,097.33333	*Alternative Skewness (Fisher's)*	0.21892
Standard Deviation	492.03387	*Alternative Kurtosis (Fisher's)*	-0.58132
Mean Standard Error	94.69196	*Coefficient of Variation*	0.30496
Minimum	733.	*Mean Deviation*	389.74486
Maximum	2,475.	*Second Moment*	233,130.76543
Range	1,742.	*Third Moment*	23,251,594.66941
Sum	43,563.	*Fourth Moment*	1.25364E+11
Sum Standard Error	2,556.68301	*Median*	1,524.
Total Sum Squares	76,581,011.	*Median Error*	22.83974
Adjusted Sum Squares	6,294,530.66667	*Percentile 25% (Q1)*	1,340.5
Geometric Mean	1,537.73757	*Percentile 75% (Q2)*	1,998.75
Harmonic Mean	1,458.53375	*IQR*	658.25
Mode	#N/A	*MAD*	324.
Min. elevation (m asl)			
Count	27	*Skewness*	0.68732
Mean	1,112.22222	*Skewness Standard Error*	0.43095
Mean LCL	903.87545	*Kurtosis*	3.19307
Mean UCL	1,320.569	*Kurtosis Standard Error*	0.77402
Variance	190,771.71795	*Alternative Skewness (Fisher's)*	0.72843
Standard Deviation	436.77422	*Alternative Kurtosis (Fisher's)*	0.49426
Mean Standard Error	84.05724	*Coefficient of Variation*	0.3927
Minimum	337.	*Mean Deviation*	297.7037
Maximum	1,989.	*Second Moment*	183,706.09877
Range	1,652.	*Third Moment*	54,118,615.03429
Sum	30,030.	*Fourth Moment*	1.0776E+11
Sum Standard Error	2,269.54541	*Median*	1,060.
Total Sum Squares	38,360,098.	*Median Error*	20.27464
Adjusted Sum Squares	4,960,064.66667	*Percentile 25% (Q1)*	963.25
Geometric Mean	1,028.39996	*Percentile 75% (Q2)*	1,212.
Harmonic Mean	937.98929	*IQR*	248.75
Mode	#N/A	*MAD*	102.

Melton ratio (-)

Count	27	*Skewness*	0.1748
Mean	0.31111	*Skewness Standard Error*	0.43095
Mean LCL	0.26889	*Kurtosis*	2.35959
Mean UCL	0.35333	*Kurtosis Standard Error*	0.77402
Variance	0.00783	*Alternative Skewness (Fisher's)*	0.18526
Standard Deviation	0.08851	*Alternative Kurtosis (Fisher's)*	-0.51703
Mean Standard Error	0.01703	*Coefficient of Variation*	0.28448
Minimum	0.14	*Mean Deviation*	0.07144
Maximum	0.49	*Second Moment*	0.00754
Range	0.35	*Third Moment*	0.00011
Sum	8.4	*Fourth Moment*	0.00013
Sum Standard Error	0.45989	*Median*	0.32
Total Sum Squares	2.817	*Median Error*	0.00411
Adjusted Sum Squares	0.20367	*Percentile 25% (Q1)*	0.24
Geometric Mean	0.29843	*Percentile 75% (Q2)*	0.38
Harmonic Mean	0.28517	*IQR*	0.14
Mode	0.24	*MAD*	0.07

Mean slope (°)

Count	27	*Skewness*	-0.18376
Mean	24.55556	*Skewness Standard Error*	0.43095
Mean LCL	22.99951	*Kurtosis*	2.3322
Mean UCL	26.1116	*Kurtosis Standard Error*	0.77402
Variance	10.64103	*Alternative Skewness (Fisher's)*	-0.19475
Standard Deviation	3.26206	*Alternative Kurtosis (Fisher's)*	-0.55027
Mean Standard Error	0.62778	*Coefficient of Variation*	0.13284
Minimum	18.	*Mean Deviation*	2.60905
Maximum	30.	*Second Moment*	10.24691
Range	12.	*Third Moment*	-6.02743
Sum	663.	*Fourth Moment*	244.87883
Sum Standard Error	16.95015	*Median*	25.
Total Sum Squares	16,557.	*Median Error*	0.15142
Adjusted Sum Squares	276.66667	*Percentile 25% (Q1)*	22.75
Geometric Mean	24.34006	*Percentile 75% (Q2)*	27.
Harmonic Mean	24.11784	*IQR*	4.25
Mode	#N/A	*MAD*	2.

Mean orientation (0-360)

Count	27	*Skewness*	0.40388
Mean	168.2963	*Skewness Standard Error*	0.43095
Mean LCL	153.78623	*Kurtosis*	2.20929
Mean UCL	182.80637	*Kurtosis Standard Error*	0.77402
Variance	925.29345	*Alternative Skewness (Fisher's)*	0.42804
Standard Deviation	30.41864	*Alternative Kurtosis (Fisher's)*	-0.69939
Mean Standard Error	5.85407	*Coefficient of Variation*	0.18074
Minimum	119.	*Mean Deviation*	25.71468
Maximum	237.	*Second Moment*	891.02332
Range	118.	*Third Moment*	10,742.02733
Sum	4,544.	*Fourth Moment*	1,754,008.68835
Sum Standard Error	158.05987	*Median*	168.
Total Sum Squares	788,796.	*Median Error*	1.412
Adjusted Sum Squares	24,057.62963	*Percentile 25% (Q1)*	141.
Geometric Mean	165.71204	*Percentile 75% (Q2)*	194.75
Harmonic Mean	163.20917	*IQR*	53.75
Mode	141.	*MAD*	27.

Area (km2)

Count	27	*Skewness*	2.05143
Mean	12.69222	*Skewness Standard Error*	0.43095
Mean LCL	7.95838	*Kurtosis*	7.12748
Mean UCL	17.42606	*Kurtosis Standard Error*	0.77402
Variance	98.48452	*Alternative Skewness (Fisher's)*	2.17413
Standard Deviation	9.92394	*Alternative Kurtosis (Fisher's)*	5.26801
Mean Standard Error	1.90986	*Coefficient of Variation*	0.78189
Minimum	3.75	*Mean Deviation*	6.84091
Maximum	46.78	*Second Moment*	94.83694
Range	43.03	*Third Moment*	1,894.62716
Sum	342.69	*Fourth Moment*	64,104.88742
Sum Standard Error	51.56629	*Median*	9.85
Total Sum Squares	6,910.0951	*Median Error*	0.46066
Adjusted Sum Squares	2,560.59747	*Percentile 25% (Q1)*	6.83
Geometric Mean	10.22564	*Percentile 75% (Q2)*	18.245
Harmonic Mean	8.59132	*IQR*	11.415
Mode	#N/A	*MAD*	3.69

Stream length (km)

Count	27	*Skewness*	2.07697
Mean	20.71259	*Skewness Standard Error*	0.43095
Mean LCL	16.15455	*Kurtosis*	7.87552
Mean UCL	25.27063	*Kurtosis Standard Error*	0.77402
Variance	91.30548	*Alternative Skewness (Fisher's)*	2.2012
Standard Deviation	9.55539	*Alternative Kurtosis (Fisher's)*	6.17563
Mean Standard Error	1.83894	*Coefficient of Variation*	0.46133
Minimum	11.36	*Mean Deviation*	6.67141
Maximum	55.67	*Second Moment*	87.9238
Range	44.31	*Third Moment*	1,712.3435
Sum	559.24	*Fourth Moment*	60,882.42935
Sum Standard Error	49.65126	*Median*	18.1
Total Sum Squares	13,957.2528	*Median Error*	0.44355
Adjusted Sum Squares	2,373.94252	*Percentile 25% (Q1)*	15.39
Geometric Mean	19.17999	*Percentile 75% (Q2)*	24.51
Harmonic Mean	18.03469	*IQR*	9.12
Mode	#N/A	*MAD*	4.22

Perimeter (m)

Count	27	*Skewness*	2.07044
Mean	20,451.85185	*Skewness Standard Error*	0.43095
Mean LCL	15,955.04337	*Kurtosis*	7.85657
Mean UCL	24,948.66033	*Kurtosis Standard Error*	0.77402
Variance	88,868,777.20798	*Alternative Skewness (Fisher's)*	2.19428
Standard Deviation	9,427.02377	*Alternative Kurtosis (Fisher's)*	6.15264
Mean Standard Error	1,814.23157	*Coefficient of Variation*	0.46094
Minimum	11,240.	*Mean Deviation*	6,574.92455
Maximum	54,920.	*Second Moment*	85,577,341.01509
Range	43,680.	*Third Moment*	1.63909E+12
Sum	552,200.	*Fourth Moment*	5.75374E+16
Sum Standard Error	48,984.25241	*Median*	17,840.
Total Sum Squares	1.36041E+10	*Median Error*	437.59341
Adjusted Sum Squares	2,310,588,207.40741	*Percentile 25% (Q1)*	15,010.
Geometric Mean	18,938.08213	*Percentile 75% (Q2)*	24,310.
Harmonic Mean	17,804.15798	*IQR*	9,300.
Mode	17,840.	*MAD*	4,160.

Form factor (-)

Count	27	*Skewness*	-2.58734
Mean	0.02815	*Skewness Standard Error*	0.43095
Mean LCL	0.02584	*Kurtosis*	8.92594
Mean UCL	0.03045	*Kurtosis Standard Error*	0.77402
Variance	0.00002	*Alternative Skewness (Fisher's)*	-2.74209
Standard Deviation	0.00483	*Alternative Kurtosis (Fisher's)*	7.45014
Mean Standard Error	0.00093	*Coefficient of Variation*	0.17171
Minimum	0.01	*Mean Deviation*	0.00316
Maximum	0.03	*Second Moment*	0.00002
Range	0.02	*Third Moment*	0.
Sum	0.76	*Fourth Moment*	0.
Sum Standard Error	0.02512	*Median*	0.03
Total Sum Squares	0.022	*Median Error*	0.00022
Adjusted Sum Squares	0.00061	*Percentile 25% (Q1)*	0.03
Geometric Mean	0.02753	*Percentile 75% (Q2)*	0.03
Harmonic Mean	0.02656	*IQR*	0.E+0
Mode	0.03	*MAD*	0.E+0

Basin Elongation (-)

Count	27	*Skewness*	-0.8248
Mean	1.51111	*Skewness Standard Error*	0.43095
Mean LCL	1.43227	*Kurtosis*	5.92517
Mean UCL	1.58995	*Kurtosis Standard Error*	0.77402
Variance	0.02732	*Alternative Skewness (Fisher's)*	-0.87413
Standard Deviation	0.16528	*Alternative Kurtosis (Fisher's)*	3.80921
Mean Standard Error	0.03181	*Coefficient of Variation*	0.10938
Minimum	0.97	*Mean Deviation*	0.11218
Maximum	1.85	*Second Moment*	0.02631
Range	0.88	*Third Moment*	-0.00352
Sum	40.8	*Fourth Moment*	0.0041
Sum Standard Error	0.85883	*Median*	1.52
Total Sum Squares	62.3636	*Median Error*	0.00767
Adjusted Sum Squares	0.71027	*Percentile 25% (Q1)*	1.43
Geometric Mean	1.50154	*Percentile 75% (Q2)*	1.6225
Harmonic Mean	1.49078	*IQR*	0.1925
Mode	#N/A	*MAD*	0.09

Lemniscate ratio (-)

Count	27	*Skewness*	2.35983
Mean	0.67074	*Skewness Standard Error*	0.43095
Mean LCL	0.62841	*Kurtosis*	11.15106
Mean UCL	0.71308	*Kurtosis Standard Error*	0.77402
Variance	0.00788	*Alternative Skewness (Fisher's)*	2.50098
Standard Deviation	0.08875	*Alternative Kurtosis (Fisher's)*	10.14995
Mean Standard Error	0.01708	*Coefficient of Variation*	0.13231
Minimum	0.54	*Mean Deviation*	0.05501
Maximum	1.03	*Second Moment*	0.00758
Range	0.49	*Third Moment*	0.00156
Sum	18.11	*Fourth Moment*	0.00064
Sum Standard Error	0.46115	*Median*	0.66
Total Sum Squares	12.3519	*Median Error*	0.00412
Adjusted Sum Squares	0.20479	*Percentile 25% (Q1)*	0.6275
Geometric Mean	0.66588	*Percentile 75% (Q2)*	0.7025
Harmonic Mean	0.6616	*IQR*	0.075
Mode	0.66	*MAD*	0.04

Outlet slope (°)

Count	27	*Skewness*	0.18166
Mean	9.41296	*Skewness Standard Error*	0.43095
Mean LCL	6.94203	*Kurtosis*	1.7139
Mean UCL	11.8839	*Kurtosis Standard Error*	0.77402
Variance	26.83259	*Alternative Skewness (Fisher's)*	0.19253
Standard Deviation	5.18002	*Alternative Kurtosis (Fisher's)*	-1.30047
Mean Standard Error	0.9969	*Coefficient of Variation*	0.55031
Minimum	2.18	*Mean Deviation*	4.59026
Maximum	19.48	*Second Moment*	25.83879
Range	17.3	*Third Moment*	23.86025
Sum	254.15	*Fourth Moment*	1,144.27372
Sum Standard Error	26.91617	*Median*	9.61
Total Sum Squares	3,089.9519	*Median Error*	0.24045
Adjusted Sum Squares	697.64736	*Percentile 25% (Q1)*	4.53
Geometric Mean	7.86894	*Percentile 75% (Q2)*	14.0725
Harmonic Mean	6.39986	*IQR*	9.5425
Mode	#N/A	*MAD*	4.7

200m slope (°)

Count	27	*Skewness*	0.13925
Mean	8.95148	*Skewness Standard Error*	0.43095
Mean LCL	6.63077	*Kurtosis*	1.64061
Mean UCL	11.2722	*Kurtosis Standard Error*	0.77402
Variance	23.66921	*Alternative Skewness (Fisher's)*	0.14758
Standard Deviation	4.8651	*Alternative Kurtosis (Fisher's)*	-1.3894
Mean Standard Error	0.93629	*Coefficient of Variation*	0.5435
Minimum	2.14	*Mean Deviation*	4.32598
Maximum	17.37	*Second Moment*	22.79257
Range	15.23	*Third Moment*	15.15252
Sum	241.69	*Fourth Moment*	852.29626
Sum Standard Error	25.27981	*Median*	8.73
Total Sum Squares	2,778.8829	*Median Error*	0.22583
Adjusted Sum Squares	615.39934	*Percentile 25% (Q1)*	4.855
Geometric Mean	7.49465	*Percentile 75% (Q2)*	13.75
Harmonic Mean	6.07503	*IQR*	8.895
Mode	13.84	*MAD*	4.07

Average slope (°)

Count	27	*Skewness*	0.44883
Mean	9.67185	*Skewness Standard Error*	0.43095
Mean LCL	7.33195	*Kurtosis*	2.58906
Mean UCL	12.01176	*Kurtosis Standard Error*	0.77402
Variance	24.06232	*Alternative Skewness (Fisher's)*	0.47568
Standard Deviation	4.90534	*Alternative Kurtosis (Fisher's)*	-0.2386
Mean Standard Error	0.94403	*Coefficient of Variation*	0.50718
Minimum	2.23	*Mean Deviation*	4.00724
Maximum	20.61	*Second Moment*	23.17112
Range	18.38	*Third Moment*	50.06183
Sum	261.14	*Fourth Moment*	1,390.07049
Sum Standard Error	25.48887	*Median*	8.99
Total Sum Squares	3,151.3276	*Median Error*	0.2277
Adjusted Sum Squares	625.62021	*Percentile 25% (Q1)*	6.2025
Geometric Mean	8.34853	*Percentile 75% (Q2)*	12.8875
Harmonic Mean	6.94073	*IQR*	6.685
Mode	#N/A	*MAD*	3.54

2nd-order catchments - Training set – Mollo – reactive catchments.

Max. elevation (m asl)			
Count	13	*Skewness*	-0.23061
Mean	2,465.61538	*Skewness Standard Error*	0.56695
Mean LCL	2,190.34469	*Kurtosis*	1.52047
Mean UCL	2,740.88608	*Kurtosis Standard Error*	0.9097
Variance	137,047.25641	*Alternative Skewness (Fisher's)*	-0.26185
Standard Deviation	370.19894	*Alternative Kurtosis (Fisher's)*	-1.60511
Mean Standard Error	102.67471	*Coefficient of Variation*	0.15014
Minimum	1,941.	*Mean Deviation*	317.85799
Maximum	2,910.	*Second Moment*	126,505.15976
Range	969.	*Third Moment*	-10,376,185.75876
Sum	32,053.	*Fourth Moment*	2.43329E+10
Sum Standard Error	1,334.77127	*Median*	2,521.
Total Sum Squares	80,674,937.	*Median Error*	35.69043
Adjusted Sum Squares	1,644,567.07692	*Percentile 25% (Q1)*	2,167.25
Geometric Mean	2,439.09868	*Percentile 75% (Q2)*	2,860.5
Harmonic Mean	2,411.99888	*IQR*	693.25
Mode	#N/A	*MAD*	352.
Mean elevation (m asl)			
Count	13	*Skewness*	0.50154
Mean	1,856.53846	*Skewness Standard Error*	0.56695
Mean LCL	1,608.26277	*Kurtosis*	2.05614
Mean UCL	2,104.81416	*Kurtosis Standard Error*	0.9097
Variance	111,485.60256	*Alternative Skewness (Fisher's)*	0.56948
Standard Deviation	333.8946	*Alternative Kurtosis (Fisher's)*	-0.78698
Mean Standard Error	92.6057	*Coefficient of Variation*	0.17985
Minimum	1,483.	*Mean Deviation*	272.73373
Maximum	2,432.	*Second Moment*	102,909.78698
Range	949.	*Third Moment*	16,557,324.26491
Sum	24,135.	*Fourth Moment*	2.17754E+10
Sum Standard Error	1,203.87409	*Median*	1,848.
Total Sum Squares	46,145,383.	*Median Error*	32.19037
Adjusted Sum Squares	1,337,827.23077	*Percentile 25% (Q1)*	1,539.
Geometric Mean	1,829.8628	*Percentile 75% (Q2)*	2,098.5
Harmonic Mean	1,804.45877	*IQR*	559.5
Mode	#N/A	*MAD*	283.
Min. elevation (m asl)			
Count	13	*Skewness*	1.42935
Mean	1,249.07692	*Skewness Standard Error*	0.56695
Mean LCL	986.92331	*Kurtosis*	3.64793
Mean UCL	1,511.23054	*Kurtosis Standard Error*	0.9097
Variance	124,297.41026	*Alternative Skewness (Fisher's)*	1.62296
Standard Deviation	352.55838	*Alternative Kurtosis (Fisher's)*	1.64412
Mean Standard Error	97.7821	*Coefficient of Variation*	0.28226
Minimum	907.	*Mean Deviation*	262.4142
Maximum	1,989.	*Second Moment*	114,736.07101
Range	1,082.	*Third Moment*	55,550,533.4447
Sum	16,238.	*Fourth Moment*	4.80227E+10
Sum Standard Error	1,271.16731	*Median*	1,098.
Total Sum Squares	21,774,080.	*Median Error*	33.98972
Adjusted Sum Squares	1,491,568.92308	*Percentile 25% (Q1)*	1,066.25
Geometric Mean	1,211.2675	*Percentile 75% (Q2)*	1,362.
Harmonic Mean	1,180.65522	*IQR*	295.75
Mode	#N/A	*MAD*	77.

Melton ratio (-)

Count	13	*Skewness*	0.11273
Mean	0.33692	*Skewness Standard Error*	0.56695
Mean LCL	0.2797	*Kurtosis*	2.17713
Mean UCL	0.39415	*Kurtosis Standard Error*	0.9097
Variance	0.00592	*Alternative Skewness (Fisher's)*	0.128
Standard Deviation	0.07696	*Alternative Kurtosis (Fisher's)*	-0.60221
Mean Standard Error	0.02135	*Coefficient of Variation*	0.22842
Minimum	0.21	*Mean Deviation*	0.0587
Maximum	0.47	*Second Moment*	0.00547
Range	0.26	*Third Moment*	0.00005
Sum	4.38	*Fourth Moment*	0.00007
Sum Standard Error	0.27749	*Median*	0.34
Total Sum Squares	1.5468	*Median Error*	0.00742
Adjusted Sum Squares	0.07108	*Percentile 25% (Q1)*	0.2875
Geometric Mean	0.3286	*Percentile 75% (Q2)*	0.4175
Harmonic Mean	0.32012	*IQR*	0.13
Mode	#N/A	*MAD*	0.06

Mean slope (°)

Count	13	*Skewness*	0.23504
Mean	25.30769	*Skewness Standard Error*	0.56695
Mean LCL	23.21807	*Kurtosis*	2.28125
Mean UCL	27.39731	*Kurtosis Standard Error*	0.9097
Variance	7.89744	*Alternative Skewness (Fisher's)*	0.26688
Standard Deviation	2.81024	*Alternative Kurtosis (Fisher's)*	-0.44318
Mean Standard Error	0.77942	*Coefficient of Variation*	0.11104
Minimum	21.	*Mean Deviation*	2.17751
Maximum	30.	*Second Moment*	7.28994
Range	9.	*Third Moment*	4.62631
Sum	329.	*Fourth Moment*	121.23301
Sum Standard Error	10.13246	*Median*	25.
Total Sum Squares	8,421.	*Median Error*	0.27093
Adjusted Sum Squares	94.76923	*Percentile 25% (Q1)*	24.
Geometric Mean	25.16466	*Percentile 75% (Q2)*	27.
Harmonic Mean	25.02284	*IQR*	3.
Mode	#N/A	*MAD*	2.

Mean orientation (0-360)

Count	13	*Skewness*	0.97346
Mean	164.76923	*Skewness Standard Error*	0.56695
Mean LCL	141.35123	*Kurtosis*	2.94128
Mean UCL	188.18723	*Kurtosis Standard Error*	0.9097
Variance	991.85897	*Alternative Skewness (Fisher's)*	1.10532
Standard Deviation	31.49379	*Alternative Kurtosis (Fisher's)*	0.56487
Mean Standard Error	8.73481	*Coefficient of Variation*	0.19114
Minimum	132.	*Mean Deviation*	26.48521
Maximum	237.	*Second Moment*	915.56213
Range	105.	*Third Moment*	26,968.09376
Sum	2,142.	*Fourth Moment*	2,465,543.15262
Sum Standard Error	113.55248	*Median*	149.
Total Sum Squares	364,838.	*Median Error*	3.03628
Adjusted Sum Squares	11,902.30769	*Percentile 25% (Q1)*	142.25
Geometric Mean	162.23341	*Percentile 75% (Q2)*	192.5
Harmonic Mean	159.93947	*IQR*	50.25
Mode	141.	*MAD*	12.

Area (km2)

Count	13	*Skewness*	1.49517
Mean	14.44385	*Skewness Standard Error*	0.56695
Mean LCL	8.26583	*Kurtosis*	5.02405
Mean UCL	20.62187	*Kurtosis Standard Error*	0.9097
Variance	69.03179	*Alternative Skewness (Fisher's)*	1.6977
Standard Deviation	8.30854	*Alternative Kurtosis (Fisher's)*	3.74582
Mean Standard Error	2.30437	*Coefficient of Variation*	0.57523
Minimum	5.62	*Mean Deviation*	6.18781
Maximum	36.82	*Second Moment*	63.72165
Range	31.2	*Third Moment*	760.53843
Sum	187.77	*Fourth Moment*	20,399.89781
Sum Standard Error	29.95686	*Median*	12.13
Total Sum Squares	3,540.5025	*Median Error*	0.80102
Adjusted Sum Squares	828.38151	*Percentile 25% (Q1)*	9.95
Geometric Mean	12.68761	*Percentile 75% (Q2)*	18.875
Harmonic Mean	11.29139	*IQR*	8.925
Mode	#N/A	*MAD*	5.01

Stream length (km)

Count	13	*Skewness*	0.5028
Mean	21.1	*Skewness Standard Error*	0.56695
Mean LCL	16.74852	*Kurtosis*	2.55908
Mean UCL	25.45148	*Kurtosis Standard Error*	0.9097
Variance	34.24718	*Alternative Skewness (Fisher's)*	0.5709
Standard Deviation	5.85211	*Alternative Kurtosis (Fisher's)*	-0.01886
Mean Standard Error	1.62308	*Coefficient of Variation*	0.27735
Minimum	12.81	*Mean Deviation*	4.78462
Maximum	33.47	*Second Moment*	31.61278
Range	20.66	*Third Moment*	89.36899
Sum	274.3	*Fourth Moment*	2,557.4622
Sum Standard Error	21.10008	*Median*	19.78
Total Sum Squares	6,198.6962	*Median Error*	0.56419
Adjusted Sum Squares	410.9662	*Percentile 25% (Q1)*	17.9425
Geometric Mean	20.37192	*Percentile 75% (Q2)*	25.7625
Harmonic Mean	19.67254	*IQR*	7.82
Mode	#N/A	*MAD*	4.84

Perimeter (m)

Count	13	*Skewness*	0.48564
Mean	20,876.92308	*Skewness Standard Error*	0.56695
Mean LCL	16,590.96331	*Kurtosis*	2.51804
Mean UCL	25,162.88285	*Kurtosis Standard Error*	0.9097
Variance	33,223,589.74359	*Alternative Skewness (Fisher's)*	0.55142
Standard Deviation	5,763.99078	*Alternative Kurtosis (Fisher's)*	-0.08153
Mean Standard Error	1,598.64341	*Coefficient of Variation*	0.27609
Minimum	12,680.	*Mean Deviation*	4,704.3787
Maximum	32,960.	*Second Moment*	30,667,928.99408
Range	20,280.	*Third Moment*	8.24784E+10
Sum	271,400.	*Fourth Moment*	2.36828E+15
Sum Standard Error	20,782.36432	*Median*	19,680.
Total Sum Squares	6,064,680,000.	*Median Error*	555.69932
Adjusted Sum Squares	398,683,076.92308	*Percentile 25% (Q1)*	17,840.
Geometric Mean	20,161.41252	*Percentile 75% (Q2)*	25,450.
Harmonic Mean	19,472.7642	*IQR*	7,610.
Mode	17,840.	*MAD*	4,880.

Form factor (-)

Count	13	*Skewness*	#N/A
Mean	0.03	*Skewness Standard Error*	0.56695
Mean LCL	#N/A	*Kurtosis*	#N/A
Mean UCL	#N/A	*Kurtosis Standard Error*	0.9097
Variance	-1.41172E-22	*Alternative Skewness (Fisher's)*	#N/A
Standard Deviation	#N/A	*Alternative Kurtosis (Fisher's)*	#N/A
Mean Standard Error	#N/A	*Coefficient of Variation*	#N/A
Minimum	0.03	*Mean Deviation*	0.E+0
Maximum	0.03	*Second Moment*	0.E+0
Range	0.E+0	*Third Moment*	0.E+0
Sum	0.39	*Fourth Moment*	0.E+0
Sum Standard Error	#N/A	*Median*	0.03
Total Sum Squares	0.0117	*Median Error*	#N/A
Adjusted Sum Squares	0.E+0	*Percentile 25% (Q1)*	0.03
Geometric Mean	0.03	*Percentile 75% (Q2)*	0.03
Harmonic Mean	0.03	*IQR*	0.E+0
Mode	0.03	*MAD*	0.E+0

Basin Elongation (-)

Count	13	*Skewness*	1.06537
Mean	1.54154	*Skewness Standard Error*	0.56695
Mean LCL	1.45836	*Kurtosis*	3.6104
Mean UCL	1.62472	*Kurtosis Standard Error*	0.9097
Variance	0.01251	*Alternative Skewness (Fisher's)*	1.20967
Standard Deviation	0.11187	*Alternative Kurtosis (Fisher's)*	1.58679
Mean Standard Error	0.03103	*Coefficient of Variation*	0.07257
Minimum	1.41	*Mean Deviation*	0.08059
Maximum	1.81	*Second Moment*	0.01155
Range	0.4	*Third Moment*	0.00132
Sum	20.04	*Fourth Moment*	0.00048
Sum Standard Error	0.40334	*Median*	1.53
Total Sum Squares	31.0426	*Median Error*	0.01078
Adjusted Sum Squares	0.15017	*Percentile 25% (Q1)*	1.4775
Geometric Mean	1.53795	*Percentile 75% (Q2)*	1.615
Harmonic Mean	1.53452	*IQR*	0.1375
Mode	#N/A	*MAD*	0.06

Lemniscate ratio (-)

Count	13	*Skewness*	-0.81723
Mean	0.65231	*Skewness Standard Error*	0.56695
Mean LCL	0.61889	*Kurtosis*	3.15267
Mean UCL	0.68572	*Kurtosis Standard Error*	0.9097
Variance	0.00202	*Alternative Skewness (Fisher's)*	-0.92792
Standard Deviation	0.04494	*Alternative Kurtosis (Fisher's)*	0.88772
Mean Standard Error	0.01246	*Coefficient of Variation*	0.06889
Minimum	0.55	*Mean Deviation*	0.0329
Maximum	0.71	*Second Moment*	0.00186
Range	0.16	*Third Moment*	-0.00007
Sum	8.48	*Fourth Moment*	0.00001
Sum Standard Error	0.16202	*Median*	0.66
Total Sum Squares	5.5558	*Median Error*	0.00433
Adjusted Sum Squares	0.02423	*Percentile 25% (Q1)*	0.6425
Geometric Mean	0.65082	*Percentile 75% (Q2)*	0.695
Harmonic Mean	0.64927	*IQR*	0.0525
Mode	#N/A	*MAD*	0.02

Outlet slope (°)

Count	13	*Skewness*	-0.44891
Mean	10.67462	*Skewness Standard Error*	0.56695
Mean LCL	6.74403	*Kurtosis*	1.66547
Mean UCL	14.6052	*Kurtosis Standard Error*	0.9097
Variance	27.94244	*Alternative Skewness (Fisher's)*	-0.50971
Standard Deviation	5.28606	*Alternative Kurtosis (Fisher's)*	-1.38365
Mean Standard Error	1.46609	*Coefficient of Variation*	0.4952
Minimum	2.72	*Mean Deviation*	4.51278
Maximum	17.75	*Second Moment*	25.79302
Range	15.03	*Third Moment*	-58.80454
Sum	138.77	*Fourth Moment*	1,108.00332
Sum Standard Error	19.05916	*Median*	12.12
Total Sum Squares	1,816.6257	*Median Error*	0.50962
Adjusted Sum Squares	335.30932	*Percentile 25% (Q1)*	5.8075
Geometric Mean	9.00469	*Percentile 75% (Q2)*	14.675
Harmonic Mean	7.14938	*IQR*	8.8675
Mode	#N/A	*MAD*	2.66

200m slope (°)

Count	13	*Skewness*	-0.35251
Mean	10.16692	*Skewness Standard Error*	0.56695
Mean LCL	6.25069	*Kurtosis*	1.48149
Mean UCL	14.08316	*Kurtosis Standard Error*	0.9097
Variance	27.73879	*Alternative Skewness (Fisher's)*	-0.40026
Standard Deviation	5.26676	*Alternative Kurtosis (Fisher's)*	-1.66463
Mean Standard Error	1.46074	*Coefficient of Variation*	0.51803
Minimum	2.58	*Mean Deviation*	4.69763
Maximum	16.83	*Second Moment*	25.60504
Range	14.25	*Third Moment*	-45.67308
Sum	132.17	*Fourth Moment*	971.29433
Sum Standard Error	18.98958	*Median*	11.87
Total Sum Squares	1,676.6277	*Median Error*	0.50776
Adjusted Sum Squares	332.86548	*Percentile 25% (Q1)*	5.3475
Geometric Mean	8.48617	*Percentile 75% (Q2)*	13.9675
Harmonic Mean	6.70018	*IQR*	8.62
Mode	13.84	*MAD*	4.07

Average slope (°)

Count	13	*Skewness*	0.06896
Mean	11.34538	*Skewness Standard Error*	0.56695
Mean LCL	7.15348	*Kurtosis*	2.08607
Mean UCL	15.53729	*Kurtosis Standard Error*	0.9097
Variance	31.78136	*Alternative Skewness (Fisher's)*	0.07831
Standard Deviation	5.6375	*Alternative Kurtosis (Fisher's)*	-0.74127
Mean Standard Error	1.56356	*Coefficient of Variation*	0.4969
Minimum	2.99	*Mean Deviation*	4.44651
Maximum	20.61	*Second Moment*	29.33664
Range	17.62	*Third Moment*	10.95826
Sum	147.49	*Fourth Moment*	1,795.35298
Sum Standard Error	20.32628	*Median*	11.87
Total Sum Squares	2,054.7071	*Median Error*	0.5435
Adjusted Sum Squares	381.37632	*Percentile 25% (Q1)*	8.33
Geometric Mean	9.75757	*Percentile 75% (Q2)*	15.85
Harmonic Mean	7.97225	*IQR*	7.52
Mode	#N/A	*MAD*	3.55

2nd-order catchments - Training set – NWCat - all catchments.

Max. elevation (m asl)			
Count	86	*Skewness*	-1.02636
Mean	2,615.06093	*Skewness Standard Error*	0.25664
Mean LCL	2,534.62438	*Kurtosis*	3.5733
Mean UCL	2,695.49748	*Kurtosis Standard Error*	0.49591
Variance	98,976.96404	*Alternative Skewness (Fisher's)*	-1.04467
Standard Deviation	314.60605	*Alternative Kurtosis (Fisher's)*	0.68123
Mean Standard Error	33.92484	*Coefficient of Variation*	0.12031
Minimum	1,622.44	*Mean Deviation*	248.17627
Maximum	3,026.53	*Second Moment*	97,826.06911
Range	1,404.09	*Third Moment*	-31,403,612.25155
Sum	224,895.24	*Fourth Moment*	3.41963E+10
Sum Standard Error	2,917.53644	*Median*	2,676.965
Total Sum Squares	596,527,797.4624	*Median Error*	4.58489
Adjusted Sum Squares	8,413,041.94313	*Percentile 25% (Q1)*	2,464.62
Geometric Mean	2,594.29001	*Percentile 75% (Q2)*	2,881.565
Harmonic Mean	2,571.13768	*IQR*	416.945
Mode	#N/A	*MAD*	204.6
Mean elevation (m asl)			
Count	86	*Skewness*	-0.47506
Mean	1,985.66116	*Skewness Standard Error*	0.25664
Mean LCL	1,896.14546	*Kurtosis*	2.29056
Mean UCL	2,075.17686	*Kurtosis Standard Error*	0.49591
Variance	122,581.71204	*Alternative Skewness (Fisher's)*	-0.48354
Standard Deviation	350.11671	*Alternative Kurtosis (Fisher's)*	-0.67933
Mean Standard Error	37.75406	*Coefficient of Variation*	0.17632
Minimum	1,234.274	*Mean Deviation*	292.10654
Maximum	2,504.504	*Second Moment*	121,156.3433
Range	1,270.23	*Third Moment*	-20,034,191.15588
Sum	170,766.86	*Fourth Moment*	3.36228E+10
Sum Standard Error	3,246.84882	*Median*	2,050.0395
Total Sum Squares	349,504,567.31726	*Median Error*	5.1024
Adjusted Sum Squares	10,419,445.52355	*Percentile 25% (Q1)*	1,740.757
Geometric Mean	1,952.41076	*Percentile 75% (Q2)*	2,237.3395
Harmonic Mean	1,916.36098	*IQR*	496.5825
Mode	#N/A	*MAD*	235.574
Min. elevation (m asl)			
Count	86	*Skewness*	0.22232
Mean	1,318.11465	*Skewness Standard Error*	0.25664
Mean LCL	1,217.19581	*Kurtosis*	2.25162
Mean UCL	1,419.03349	*Kurtosis Standard Error*	0.49591
Variance	155,801.54994	*Alternative Skewness (Fisher's)*	0.22629
Standard Deviation	394.71705	*Alternative Kurtosis (Fisher's)*	-0.72064
Mean Standard Error	42.56343	*Coefficient of Variation*	0.29946
Minimum	594.81	*Mean Deviation*	324.52186
Maximum	2,129.98	*Second Moment*	153,989.90401
Range	1,535.17	*Third Moment*	13,434,452.65982
Sum	113,357.86	*Fourth Moment*	5.33923E+10
Sum Standard Error	3,660.45534	*Median*	1,334.77
Total Sum Squares	162,661,787.835	*Median Error*	5.75238
Adjusted Sum Squares	13,243,131.74454	*Percentile 25% (Q1)*	952.905
Geometric Mean	1,257.73245	*Percentile 75% (Q2)*	1,606.11
Harmonic Mean	1,196.23246	*IQR*	653.205
Mode	#N/A	*MAD*	294.46

Melton ratio (-)

Count	86	*Skewness*	0.43328
Mean	0.4395	*Skewness Standard Error*	0.25664
Mean LCL	0.40458	*Kurtosis*	2.82031
Mean UCL	0.47443	*Kurtosis Standard Error*	0.49591
Variance	0.01866	*Alternative Skewness (Fisher's)*	0.44101
Standard Deviation	0.13661	*Alternative Kurtosis (Fisher's)*	-0.11744
Mean Standard Error	0.01473	*Coefficient of Variation*	0.31082
Minimum	0.1758	*Mean Deviation*	0.11251
Maximum	0.81795	*Second Moment*	0.01844
Range	0.64215	*Third Moment*	0.00109
Sum	37.79723	*Fourth Moment*	0.00096
Sum Standard Error	1.26684	*Median*	0.4174
Total Sum Squares	18.19821	*Median Error*	0.00199
Adjusted Sum Squares	1.58623	*Percentile 25% (Q1)*	0.34165
Geometric Mean	0.41829	*Percentile 75% (Q2)*	0.5436
Harmonic Mean	0.39671	*IQR*	0.20195
Mode	#N/A	*MAD*	0.1037

Mean slope (°)

Count	86	*Skewness*	-0.07801
Mean	27.32624	*Skewness Standard Error*	0.25664
Mean LCL	26.35444	*Kurtosis*	2.6571
Mean UCL	28.29803	*Kurtosis Standard Error*	0.49591
Variance	14.44698	*Alternative Skewness (Fisher's)*	-0.0794
Standard Deviation	3.80092	*Alternative Kurtosis (Fisher's)*	-0.29055
Mean Standard Error	0.40986	*Coefficient of Variation*	0.13909
Minimum	18.67522	*Mean Deviation*	3.02811
Maximum	35.55633	*Second Moment*	14.27899
Range	16.88111	*Third Moment*	-4.20914
Sum	2,350.05659	*Fourth Moment*	541.75519
Sum Standard Error	35.24826	*Median*	27.32839
Total Sum Squares	65,446.20215	*Median Error*	0.05539
Adjusted Sum Squares	1,227.99313	*Percentile 25% (Q1)*	24.70447
Geometric Mean	27.05722	*Percentile 75% (Q2)*	30.00053
Harmonic Mean	26.77941	*IQR*	5.29606
Mode	#N/A	*MAD*	2.67214

Mean orientation (0-360)

Count	86	*Skewness*	0.0969
Mean	178.15789	*Skewness Standard Error*	0.25664
Mean LCL	168.81986	*Kurtosis*	2.31783
Mean UCL	187.49592	*Kurtosis Standard Error*	0.49591
Variance	1,333.94518	*Alternative Skewness (Fisher's)*	0.09863
Standard Deviation	36.52321	*Alternative Kurtosis (Fisher's)*	-0.6504
Mean Standard Error	3.9384	*Coefficient of Variation*	0.205
Minimum	100.8693	*Mean Deviation*	30.43553
Maximum	259.4286	*Second Moment*	1,318.43419
Range	158.5593	*Third Moment*	4,638.87735
Sum	15,321.5784	*Fourth Moment*	4,029,018.53685
Sum Standard Error	338.70236	*Median*	177.8223
Total Sum Squares	2,843,045.39462	*Median Error*	0.53227
Adjusted Sum Squares	113,385.34035	*Percentile 25% (Q1)*	149.0041
Geometric Mean	174.36104	*Percentile 75% (Q2)*	204.47315
Harmonic Mean	170.47657	*IQR*	55.46905
Mode	#N/A	*MAD*	27.44965

Area (km2)

Count	86	*Skewness*	1.73627
Mean	11.07424	*Skewness Standard Error*	0.25664
Mean LCL	9.02761	*Kurtosis*	6.34234
Mean UCL	13.12087	*Kurtosis Standard Error*	0.49591
Variance	64.07764	*Alternative Skewness (Fisher's)*	1.76724
Standard Deviation	8.00485	*Alternative Kurtosis (Fisher's)*	3.61828
Mean Standard Error	0.86319	*Coefficient of Variation*	0.72284
Minimum	2.82725	*Mean Deviation*	5.97519
Maximum	45.52798	*Second Moment*	63.33255
Range	42.70073	*Third Moment*	875.09952
Sum	952.38488	*Fourth Moment*	25,439.21388
Sum Standard Error	74.23394	*Median*	8.41266
Total Sum Squares	15,993.54093	*Median Error*	0.11666
Adjusted Sum Squares	5,446.59965	*Percentile 25% (Q1)*	5.53879
Geometric Mean	8.98181	*Percentile 75% (Q2)*	13.63599
Harmonic Mean	7.51165	*IQR*	8.0972
Mode	#N/A	*MAD*	3.29598

Stream length (km)

Count	86	*Skewness*	1.24443
Mean	20.04453	*Skewness Standard Error*	0.25664
Mean LCL	18.0267	*Kurtosis*	4.13591
Mean UCL	22.06237	*Kurtosis Standard Error*	0.49591
Variance	62.28725	*Alternative Skewness (Fisher's)*	1.26663
Standard Deviation	7.89223	*Alternative Kurtosis (Fisher's)*	1.27798
Mean Standard Error	0.85104	*Coefficient of Variation*	0.39373
Minimum	9.44	*Mean Deviation*	6.1336
Maximum	43.61	*Second Moment*	61.56298
Range	34.17	*Third Moment*	601.10627
Sum	1,723.83	*Fourth Moment*	15,675.10238
Sum Standard Error	73.18951	*Median*	17.45
Total Sum Squares	39,847.7871	*Median Error*	0.11502
Adjusted Sum Squares	5,294.41653	*Percentile 25% (Q1)*	14.27
Geometric Mean	18.74898	*Percentile 75% (Q2)*	24.105
Harmonic Mean	17.66209	*IQR*	9.835
Mode	#N/A	*MAD*	3.975

Perimeter (m)

Count	86	*Skewness*	1.25192
Mean	19,783.72093	*Skewness Standard Error*	0.25664
Mean LCL	17,793.08616	*Kurtosis*	4.14867
Mean UCL	21,774.3557	*Kurtosis Standard Error*	0.49591
Variance	60,619,233.05062	*Alternative Skewness (Fisher's)*	1.27426
Standard Deviation	7,785.83541	*Alternative Kurtosis (Fisher's)*	1.29151
Mean Standard Error	839.56822	*Coefficient of Variation*	0.39355
Minimum	9,360.	*Mean Deviation*	6,053.97512
Maximum	43,120.	*Second Moment*	59,914,358.2477
Range	33,760.	*Third Moment*	5.80596E+11
Sum	1,701,400.	*Fourth Moment*	1.48926E+16
Sum Standard Error	72,202.86727	*Median*	17,120.
Total Sum Squares	3.88127E+10	*Median Error*	113.46625
Adjusted Sum Squares	5,152,634,809.30233	*Percentile 25% (Q1)*	14,080.
Geometric Mean	18,508.97278	*Percentile 75% (Q2)*	23,740.
Harmonic Mean	17,442.29506	*IQR*	9,660.
Mode	#N/A	*MAD*	3,760.

Form factor (-)

Count	86	*Skewness*	-0.39272
Mean	0.02593	*Skewness Standard Error*	0.25664
Mean LCL	0.02483	*Kurtosis*	2.62321
Mean UCL	0.02703	*Kurtosis Standard Error*	0.49591
Variance	0.00002	*Alternative Skewness (Fisher's)*	-0.39973
Standard Deviation	0.0043	*Alternative Kurtosis (Fisher's)*	-0.3265
Mean Standard Error	0.00046	*Coefficient of Variation*	0.16594
Minimum	0.01555	*Mean Deviation*	0.00345
Maximum	0.03353	*Second Moment*	0.00002
Range	0.01798	*Third Moment*	0.
Sum	2.23012	*Fourth Moment*	0.
Sum Standard Error	0.0399	*Median*	0.02639
Total Sum Squares	0.0594	*Median Error*	0.00006
Adjusted Sum Squares	0.00157	*Percentile 25% (Q1)*	0.02295
Geometric Mean	0.02555	*Percentile 75% (Q2)*	0.02917
Harmonic Mean	0.02514	*IQR*	0.00623
Mode	#N/A	*MAD*	0.00287

Basin Elongation (-)

Count	86	*Skewness*	-0.52885
Mean	1.51617	*Skewness Standard Error*	0.25664
Mean LCL	1.46125	*Kurtosis*	2.86505
Mean UCL	1.57109	*Kurtosis Standard Error*	0.49591
Variance	0.04615	*Alternative Skewness (Fisher's)*	-0.53829
Standard Deviation	0.21482	*Alternative Kurtosis (Fisher's)*	-0.06999
Mean Standard Error	0.02316	*Coefficient of Variation*	0.14168
Minimum	0.90695	*Mean Deviation*	0.17471
Maximum	1.93508	*Second Moment*	0.04561
Range	1.02813	*Third Moment*	-0.00515
Sum	130.39066	*Fourth Moment*	0.00596
Sum Standard Error	1.99212	*Median*	1.52742
Total Sum Squares	201.61684	*Median Error*	0.00313
Adjusted Sum Squares	3.92238	*Percentile 25% (Q1)*	1.39057
Geometric Mean	1.49994	*Percentile 75% (Q2)*	1.68185
Harmonic Mean	1.48234	*IQR*	0.29128
Mode	#N/A	*MAD*	0.143

Lemniscate ratio (-)

Count	86	*Skewness*	1.39177
Mean	0.67461	*Skewness Standard Error*	0.25664
Mean LCL	0.64653	*Kurtosis*	5.34967
Mean UCL	0.70268	*Kurtosis Standard Error*	0.49591
Variance	0.01206	*Alternative Skewness (Fisher's)*	1.4166
Standard Deviation	0.10981	*Alternative Kurtosis (Fisher's)*	2.56537
Mean Standard Error	0.01184	*Coefficient of Variation*	0.16278
Minimum	0.51677	*Mean Deviation*	0.08295
Maximum	1.1026	*Second Moment*	0.01192
Range	0.58582	*Third Moment*	0.00181
Sum	58.01632	*Fourth Moment*	0.00076
Sum Standard Error	1.01834	*Median*	0.6547
Total Sum Squares	40.16325	*Median Error*	0.0016
Adjusted Sum Squares	1.02496	*Percentile 25% (Q1)*	0.5968
Geometric Mean	0.66669	*Percentile 75% (Q2)*	0.72171
Harmonic Mean	0.65956	*IQR*	0.12492
Mode	#N/A	*MAD*	0.06202

Outlet slope (°)

Count	86	*Skewness*	0.85303
Mean	8.20163	*Skewness Standard Error*	0.25664
Mean LCL	6.57946	*Kurtosis*	4.36287
Mean UCL	9.82379	*Kurtosis Standard Error*	0.49591
Variance	40.2547	*Alternative Skewness (Fisher's)*	0.86824
Standard Deviation	6.34466	*Alternative Kurtosis (Fisher's)*	1.51871
Mean Standard Error	0.68416	*Coefficient of Variation*	0.77359
Minimum	0.E+0	*Mean Deviation*	5.01608
Maximum	33.55	*Second Moment*	39.78662
Range	33.55	*Third Moment*	214.07607
Sum	705.34	*Fourth Moment*	6,906.32194
Sum Standard Error	58.83795	*Median*	8.085
Total Sum Squares	9,206.5854	*Median Error*	0.09246
Adjusted Sum Squares	3,421.64917	*Percentile 25% (Q1)*	3.045
Geometric Mean	5.27121	*Percentile 75% (Q2)*	12.345
Harmonic Mean	2.52826	*IQR*	9.3
Mode	0.E+0	*MAD*	4.78

200m slope (°)

Count	86	*Skewness*	1.11615
Mean	8.41	*Skewness Standard Error*	0.25664
Mean LCL	6.81514	*Kurtosis*	5.24775
Mean UCL	10.00486	*Kurtosis Standard Error*	0.49591
Variance	38.91123	*Alternative Skewness (Fisher's)*	1.13606
Standard Deviation	6.23789	*Alternative Kurtosis (Fisher's)*	2.45727
Mean Standard Error	0.67265	*Coefficient of Variation*	0.74172
Minimum	0.E+0	*Mean Deviation*	4.65186
Maximum	34.13	*Second Moment*	38.45878
Range	34.13	*Third Moment*	266.20542
Sum	723.26	*Fourth Moment*	7,761.82698
Sum Standard Error	57.84778	*Median*	7.95
Total Sum Squares	9,390.0714	*Median Error*	0.09091
Adjusted Sum Squares	3,307.4548	*Percentile 25% (Q1)*	3.67
Geometric Mean	5.84314	*Percentile 75% (Q2)*	11.695
Harmonic Mean	2.94877	*IQR*	8.025
Mode	0.E+0	*MAD*	4.21

Average slope (°)

Count	86	*Skewness*	0.33972
Mean	10.17837	*Skewness Standard Error*	0.25664
Mean LCL	8.6409	*Kurtosis*	2.59613
Mean UCL	11.71585	*Kurtosis Standard Error*	0.49591
Variance	36.16131	*Alternative Skewness (Fisher's)*	0.34578
Standard Deviation	6.01343	*Alternative Kurtosis (Fisher's)*	-0.35522
Mean Standard Error	0.64844	*Coefficient of Variation*	0.5908
Minimum	0.E+0	*Mean Deviation*	4.8538
Maximum	26.9	*Second Moment*	35.74083
Range	26.9	*Third Moment*	72.58809
Sum	875.34	*Fourth Moment*	3,316.31308
Sum Standard Error	55.76623	*Median*	9.54
Total Sum Squares	11,983.2474	*Median Error*	0.08764
Adjusted Sum Squares	3,073.71117	*Percentile 25% (Q1)*	5.675
Geometric Mean	7.81257	*Percentile 75% (Q2)*	14.5
Harmonic Mean	3.86627	*IQR*	8.825
Mode	0.E+0	*MAD*	4.625

2nd-order catchments - Training set – NWCat – reactive catchments.

Max. elevation (m asl)			
Count	27	*Skewness*	-0.32061
Mean	2,807.84333	*Skewness Standard Error*	0.43095
Mean LCL	2,729.31951	*Kurtosis*	1.72352
Mean UCL	2,886.36715	*Kurtosis Standard Error*	0.77402
Variance	27,098.37544	*Alternative Skewness (Fisher's)*	-0.33978
Standard Deviation	164.61584	*Alternative Kurtosis (Fisher's)*	-1.2888
Mean Standard Error	31.68033	*Coefficient of Variation*	0.05863
Minimum	2,522.58	*Mean Deviation*	146.63284
Maximum	3,026.53	*Second Moment*	26,094.7319
Range	503.95	*Third Moment*	-1,351,457.6187
Sum	75,811.77	*Fourth Moment*	1,173,603,669.6422
Sum Standard Error	855.36901	*Median*	2,885.
Total Sum Squares	213,572,130.7441	*Median Error*	7.64131
Adjusted Sum Squares	704,557.7614	*Percentile 25% (Q1)*	2,672.6825
Geometric Mean	2,803.12961	*Percentile 75% (Q2)*	2,954.4
Harmonic Mean	2,798.35481	*IQR*	281.7175
Mode	#N/A	*MAD*	126.68
Mean elevation (m asl)			
Count	27	*Skewness*	-0.66941
Mean	2,197.14267	*Skewness Standard Error*	0.43095
Mean LCL	2,080.61837	*Kurtosis*	2.53609
Mean UCL	2,313.66696	*Kurtosis Standard Error*	0.77402
Variance	59,672.38668	*Alternative Skewness (Fisher's)*	-0.70945
Standard Deviation	244.27932	*Alternative Kurtosis (Fisher's)*	-0.30288
Mean Standard Error	47.01158	*Coefficient of Variation*	0.11118
Minimum	1,661.463	*Mean Deviation*	195.1644
Maximum	2,504.504	*Second Moment*	57,462.29829
Range	843.041	*Third Moment*	-9,220,761.86523
Sum	59,322.852	*Fourth Moment*	8,373,939,837.51428
Sum Standard Error	1,269.31259	*Median*	2,230.584
Total Sum Squares	131,892,251.29133	*Median Error*	11.33921
Adjusted Sum Squares	1,551,482.05378	*Percentile 25% (Q1)*	2,028.1665
Geometric Mean	2,183.24302	*Percentile 75% (Q2)*	2,424.311
Harmonic Mean	2,168.49367	*IQR*	396.1445
Mode	#N/A	*MAD*	201.608
Min. elevation (m asl)			
Count	27	*Skewness*	-0.02726
Mean	1,526.33889	*Skewness Standard Error*	0.43095
Mean LCL	1,359.47163	*Kurtosis*	2.10714
Mean UCL	1,693.20615	*Kurtosis Standard Error*	0.77402
Variance	122,372.18196	*Alternative Skewness (Fisher's)*	-0.02889
Standard Deviation	349.81736	*Alternative Kurtosis (Fisher's)*	-0.82333
Mean Standard Error	67.32238	*Coefficient of Variation*	0.22919
Minimum	930.74	*Mean Deviation*	280.04123
Maximum	2,127.02	*Second Moment*	117,839.87892
Range	1,196.28	*Third Moment*	-1,102,558.99588
Sum	41,211.15	*Fourth Moment*	2.92603E+10
Sum Standard Error	1,817.7043	*Median*	1,567.33
Total Sum Squares	66,083,857.6317	*Median Error*	16.23819
Adjusted Sum Squares	3,181,676.73087	*Percentile 25% (Q1)*	1,334.02
Geometric Mean	1,485.85971	*Percentile 75% (Q2)*	1,784.9375
Harmonic Mean	1,443.86569	*IQR*	450.9175
Mode	#N/A	*MAD*	210.85

Melton ratio (-)

Count	27	*Skewness*	0.89738
Mean	0.42054	*Skewness Standard Error*	0.43095
Mean LCL	0.35518	*Kurtosis*	3.8869
Mean UCL	0.4859	*Kurtosis Standard Error*	0.77402
Variance	0.01877	*Alternative Skewness (Fisher's)*	0.95105
Standard Deviation	0.13702	*Alternative Kurtosis (Fisher's)*	1.33611
Mean Standard Error	0.02637	*Coefficient of Variation*	0.32581
Minimum	0.19203	*Mean Deviation*	0.10323
Maximum	0.81795	*Second Moment*	0.01808
Range	0.62592	*Third Moment*	0.00218
Sum	11.35466	*Fourth Moment*	0.00127
Sum Standard Error	0.71196	*Median*	0.40324
Total Sum Squares	5.26324	*Median Error*	0.00636
Adjusted Sum Squares	0.48812	*Percentile 25% (Q1)*	0.32134
Geometric Mean	0.40048	*Percentile 75% (Q2)*	0.52443
Harmonic Mean	0.38139	*IQR*	0.20309
Mode	#N/A	*MAD*	0.09322

Mean slope (°)

Count	27	*Skewness*	0.32645
Mean	28.70702	*Skewness Standard Error*	0.43095
Mean LCL	27.31325	*Kurtosis*	2.5091
Mean UCL	30.1008	*Kurtosis Standard Error*	0.77402
Variance	8.53739	*Alternative Skewness (Fisher's)*	0.34597
Standard Deviation	2.92188	*Alternative Kurtosis (Fisher's)*	-0.33563
Mean Standard Error	0.56232	*Coefficient of Variation*	0.10178
Minimum	23.75854	*Mean Deviation*	2.29663
Maximum	34.53099	*Second Moment*	8.22119
Range	10.77245	*Third Moment*	7.6951
Sum	775.08964	*Fourth Moment*	169.5847
Sum Standard Error	15.18254	*Median*	29.12537
Total Sum Squares	22,472.48873	*Median Error*	0.13563
Adjusted Sum Squares	221.97206	*Percentile 25% (Q1)*	26.56073
Geometric Mean	28.56557	*Percentile 75% (Q2)*	30.2811
Harmonic Mean	28.4259	*IQR*	3.72037
Mode	#N/A	*MAD*	1.75275

Mean orientation (0-360)

Count	27	*Skewness*	-0.10176
Mean	176.88465	*Skewness Standard Error*	0.43095
Mean LCL	163.82813	*Kurtosis*	2.12874
Mean UCL	189.94117	*Kurtosis Standard Error*	0.77402
Variance	749.19589	*Alternative Skewness (Fisher's)*	-0.10785
Standard Deviation	27.37144	*Alternative Kurtosis (Fisher's)*	-0.79713
Mean Standard Error	5.26764	*Coefficient of Variation*	0.15474
Minimum	120.2844	*Mean Deviation*	22.57067
Maximum	221.6604	*Second Moment*	721.44789
Range	101.376	*Third Moment*	-1,971.96271
Sum	4,775.8855	*Fourth Moment*	1,107,981.39867
Sum Standard Error	142.22619	*Median*	176.1888
Total Sum Squares	864,259.91939	*Median Error*	1.27056
Adjusted Sum Squares	19,479.09312	*Percentile 25% (Q1)*	156.40265
Geometric Mean	174.78178	*Percentile 75% (Q2)*	201.1606
Harmonic Mean	172.61951	*IQR*	44.75795
Mode	#N/A	*MAD*	21.6751

Area (km2)

Count	27	*Skewness*	1.35011
Mean	11.24047	*Skewness Standard Error*	0.43095
Mean LCL	7.91173	*Kurtosis*	4.31292
Mean UCL	14.56922	*Kurtosis Standard Error*	0.77402
Variance	48.69688	*Alternative Skewness (Fisher's)*	1.43087
Standard Deviation	6.97831	*Alternative Kurtosis (Fisher's)*	1.85301
Mean Standard Error	1.34298	*Coefficient of Variation*	0.62082
Minimum	2.8613	*Mean Deviation*	5.274
Maximum	31.1847	*Second Moment*	46.89329
Range	28.3234	*Third Moment*	433.54756
Sum	303.4928	*Fourth Moment*	9,484.0201
Sum Standard Error	36.26039	*Median*	8.43625
Total Sum Squares	4,677.52176	*Median Error*	0.32393
Adjusted Sum Squares	1,266.11881	*Percentile 25% (Q1)*	6.32896
Geometric Mean	9.54093	*Percentile 75% (Q2)*	15.34363
Harmonic Mean	8.17397	*IQR*	9.01467
Mode	#N/A	*MAD*	3.26268

Stream length (km)

Count	27	*Skewness*	1.03635
Mean	20.28519	*Skewness Standard Error*	0.43095
Mean LCL	17.14088	*Kurtosis*	3.42225
Mean UCL	23.42949	*Kurtosis Standard Error*	0.77402
Variance	43.45006	*Alternative Skewness (Fisher's)*	1.09833
Standard Deviation	6.59167	*Alternative Kurtosis (Fisher's)*	0.77233
Mean Standard Error	1.26857	*Coefficient of Variation*	0.32495
Minimum	11.1	*Mean Deviation*	5.08392
Maximum	37.09	*Second Moment*	41.8408
Range	25.99	*Third Moment*	280.48193
Sum	547.7	*Fourth Moment*	5,991.1719
Sum Standard Error	34.2513	*Median*	18.47
Total Sum Squares	12,239.8976	*Median Error*	0.30598
Adjusted Sum Squares	1,129.70167	*Percentile 25% (Q1)*	16.105
Geometric Mean	19.3734	*Percentile 75% (Q2)*	23.445
Harmonic Mean	18.57137	*IQR*	7.34
Mode	#N/A	*MAD*	3.93

Perimeter (m)

Count	27	*Skewness*	1.05892
Mean	19,988.14815	*Skewness Standard Error*	0.43095
Mean LCL	16,868.26373	*Kurtosis*	3.45079
Mean UCL	23,108.03257	*Kurtosis Standard Error*	0.77402
Variance	42,777,700.2849	*Alternative Skewness (Fisher's)*	1.12226
Standard Deviation	6,540.46637	*Alternative Kurtosis (Fisher's)*	0.80695
Mean Standard Error	1,258.71334	*Coefficient of Variation*	0.32722
Minimum	11,040.	*Mean Deviation*	5,046.6941
Maximum	36,760.	*Second Moment*	41,193,341.01509
Range	25,720.	*Third Moment*	2.79965E+11
Sum	539,680.	*Fourth Moment*	5.85561E+15
Sum Standard Error	33,985.26015	*Median*	18,400.
Total Sum Squares	1.18994E+10	*Median Error*	303.60218
Adjusted Sum Squares	1,112,220,207.40741	*Percentile 25% (Q1)*	15,770.
Geometric Mean	19,082.3546	*Percentile 75% (Q2)*	23,200.
Harmonic Mean	18,291.20056	*IQR*	7,430.
Mode	#N/A	*MAD*	3,720.

Form factor (-)

Count	27	*Skewness*	-0.62852
Mean	0.02567	*Skewness Standard Error*	0.43095
Mean LCL	0.024	*Kurtosis*	3.47467
Mean UCL	0.02734	*Kurtosis Standard Error*	0.77402
Variance	0.00001	*Alternative Skewness (Fisher's)*	-0.66611
Standard Deviation	0.0035	*Alternative Kurtosis (Fisher's)*	0.83593
Mean Standard Error	0.00067	*Coefficient of Variation*	0.13643
Minimum	0.01606	*Mean Deviation*	0.00265
Maximum	0.03221	*Second Moment*	0.00001
Range	0.01614	*Third Moment*	0.
Sum	0.69312	*Fourth Moment*	0.
Sum Standard Error	0.0182	*Median*	0.02627
Total Sum Squares	0.01811	*Median Error*	0.00016
Adjusted Sum Squares	0.00032	*Percentile 25% (Q1)*	0.02366
Geometric Mean	0.02542	*Percentile 75% (Q2)*	0.02846
Harmonic Mean	0.02514	*IQR*	0.0048
Mode	#N/A	*MAD*	0.00247

Basin Elongation (-)

Count	27	*Skewness*	-0.82874
Mean	1.54438	*Skewness Standard Error*	0.43095
Mean LCL	1.43198	*Kurtosis*	3.26848
Mean UCL	1.65678	*Kurtosis Standard Error*	0.77402
Variance	0.05553	*Alternative Skewness (Fisher's)*	-0.8783
Standard Deviation	0.23564	*Alternative Kurtosis (Fisher's)*	0.58575
Mean Standard Error	0.04535	*Coefficient of Variation*	0.15258
Minimum	0.90695	*Mean Deviation*	0.19136
Maximum	1.8462	*Second Moment*	0.05347
Range	0.93926	*Third Moment*	-0.01025
Sum	41.6982	*Fourth Moment*	0.00934
Sum Standard Error	1.22441	*Median*	1.6217
Total Sum Squares	65.84144	*Median Error*	0.01094
Adjusted Sum Squares	1.44366	*Percentile 25% (Q1)*	1.39318
Geometric Mean	1.52489	*Percentile 75% (Q2)*	1.73298
Harmonic Mean	1.50278	*IQR*	0.3398
Mode	#N/A	*MAD*	0.15949

Lemniscate ratio (-)

Count	27	*Skewness*	1.81534
Mean	0.66543	*Skewness Standard Error*	0.43095
Mean LCL	0.60564	*Kurtosis*	6.73226
Mean UCL	0.72523	*Kurtosis Standard Error*	0.77402
Variance	0.01571	*Alternative Skewness (Fisher's)*	1.92392
Standard Deviation	0.12534	*Alternative Kurtosis (Fisher's)*	4.78848
Mean Standard Error	0.02412	*Coefficient of Variation*	0.18836
Minimum	0.54165	*Mean Deviation*	0.09193
Maximum	1.1026	*Second Moment*	0.01513
Range	0.56095	*Third Moment*	0.00338
Sum	17.96674	*Fourth Moment*	0.00154
Sum Standard Error	0.65131	*Median*	0.61664
Total Sum Squares	12.36418	*Median Error*	0.00582
Adjusted Sum Squares	0.40849	*Percentile 25% (Q1)*	0.58776
Geometric Mean	0.65578	*Percentile 75% (Q2)*	0.72645
Harmonic Mean	0.64751	*IQR*	0.13869
Mode	#N/A	*MAD*	0.06446

Outlet slope (°)

Count	27	*Skewness*	1.96479
Mean	6.34	*Skewness Standard Error*	0.43095
Mean LCL	2.84887	*Kurtosis*	8.06706
Mean UCL	9.83113	*Kurtosis Standard Error*	0.77402
Variance	53.56382	*Alternative Skewness (Fisher's)*	2.0823
Standard Deviation	7.31873	*Alternative Kurtosis (Fisher's)*	6.40803
Mean Standard Error	1.40849	*Coefficient of Variation*	1.15437
Minimum	0.E+0	*Mean Deviation*	5.26074
Maximum	33.55	*Second Moment*	51.57997
Range	33.55	*Third Moment*	727.84146
Sum	171.18	*Fourth Moment*	21,462.36223
Sum Standard Error	38.02924	*Median*	4.95
Total Sum Squares	2,477.9404	*Median Error*	0.33973
Adjusted Sum Squares	1,392.6592	*Percentile 25% (Q1)*	0.33
Geometric Mean	3.1744	*Percentile 75% (Q2)*	9.58
Harmonic Mean	1.37242	*IQR*	9.25
Mode	0.E+0	*MAD*	4.63

200m slope (°)

Count	27	*Skewness*	2.016
Mean	6.8963	*Skewness Standard Error*	0.43095
Mean LCL	3.45654	*Kurtosis*	8.56551
Mean UCL	10.33605	*Kurtosis Standard Error*	0.77402
Variance	51.99905	*Alternative Skewness (Fisher's)*	2.13658
Standard Deviation	7.21104	*Alternative Kurtosis (Fisher's)*	7.01282
Mean Standard Error	1.38776	*Coefficient of Variation*	1.04564
Minimum	0.E+0	*Mean Deviation*	4.95959
Maximum	34.13	*Second Moment*	50.07316
Range	34.13	*Third Moment*	714.32832
Sum	186.2	*Fourth Moment*	21,476.49402
Sum Standard Error	37.46965	*Median*	6.63
Total Sum Squares	2,636.0658	*Median Error*	0.33473
Adjusted Sum Squares	1,351.97543	*Percentile 25% (Q1)*	1.22
Geometric Mean	4.04972	*Percentile 75% (Q2)*	9.43
Harmonic Mean	1.85247	*IQR*	8.21
Mode	0.E+0	*MAD*	3.54

Average slope (°)

Count	27	*Skewness*	0.69583
Mean	9.06259	*Skewness Standard Error*	0.43095
Mean LCL	5.58676	*Kurtosis*	2.8527
Mean UCL	12.53843	*Kurtosis Standard Error*	0.77402
Variance	53.09567	*Alternative Skewness (Fisher's)*	0.73745
Standard Deviation	7.28668	*Alternative Kurtosis (Fisher's)*	0.08127
Mean Standard Error	1.40232	*Coefficient of Variation*	0.80404
Minimum	0.E+0	*Mean Deviation*	5.84307
Maximum	26.9	*Second Moment*	51.12917
Range	26.9	*Third Moment*	254.39403
Sum	244.69	*Fourth Moment*	7,457.50139
Sum Standard Error	37.86269	*Median*	8.12
Total Sum Squares	3,598.0133	*Median Error*	0.33824
Adjusted Sum Squares	1,380.48752	*Percentile 25% (Q1)*	3.7425
Geometric Mean	5.63118	*Percentile 75% (Q2)*	14.3425
Harmonic Mean	1.93107	*IQR*	10.6
Mode	0.E+0	*MAD*	4.82

2nd-order catchments - Training set – all zones – all catchments.

Max. elevation m asl)			
Count	226	*Skewness*	-0.43198
Mean	2,206.66597	*Skewness Standard Error*	0.16115
Mean LCL	2,122.78985	*Kurtosis*	2.15293
Mean UCL	2,290.5421	*Kurtosis Standard Error*	0.31808
Variance	289,619.33707	*Alternative Skewness (Fisher's)*	-0.43488
Standard Deviation	538.16293	*Alternative Kurtosis (Fisher's)*	-0.83909
Mean Standard Error	35.79807	*Coefficient of Variation*	0.24388
Minimum	905.06	*Mean Deviation*	456.11713
Maximum	3,026.53	*Second Moment*	288,337.83558
Range	2,121.47	*Third Moment*	-66,883,746.77621
Sum	498,706.51	*Fourth Moment*	1.78992E+11
Sum Standard Error	8,090.3628	*Median*	2,291.67
Total Sum Squares	1,165,643,037.1971	*Median Error*	2.98446
Adjusted Sum Squares	65,164,350.84144	*Percentile 25% (Q1)*	1,763.565
Geometric Mean	2,132.18324	*Percentile 75% (Q2)*	2,648.19
Harmonic Mean	2,047.92697	*IQR*	884.625
Mode	#N/A	*MAD*	405.19
Mean elevation (m asl)			
Count	226	*Skewness*	0.05737
Mean	1,614.10582	*Skewness Standard Error*	0.16115
Mean LCL	1,540.51069	*Kurtosis*	2.15796
Mean UCL	1,687.70096	*Kurtosis Standard Error*	0.31808
Variance	222,971.34636	*Alternative Skewness (Fisher's)*	0.05776
Standard Deviation	472.19842	*Alternative Kurtosis (Fisher's)*	-0.83395
Mean Standard Error	31.41017	*Coefficient of Variation*	0.29254
Minimum	672.7447	*Mean Deviation*	390.35066
Maximum	2,504.504	*Second Moment*	221,984.74748
Range	1,831.7593	*Third Moment*	6,000,700.43907
Sum	364,787.9154	*Fourth Moment*	1.06338E+11
Sum Standard Error	7,098.69877	*Median*	1,600.7205
Total Sum Squares	638,974,850.37342	*Median Error*	2.61864
Adjusted Sum Squares	50,168,552.93148	*Percentile 25% (Q1)*	1,254.881
Geometric Mean	1,540.42141	*Percentile 75% (Q2)*	1,994.7945
Harmonic Mean	1,462.08987	*IQR*	739.9135
Mode	#N/A	*MAD*	348.645
Min. elevation (m asl)			
Count	226	*Skewness*	0.79196
Mean	1,066.13792	*Skewness Standard Error*	0.16115
Mean LCL	1,005.49792	*Kurtosis*	3.22491
Mean UCL	1,126.77792	*Kurtosis Standard Error*	0.31808
Variance	151,380.27572	*Alternative Skewness (Fisher's)*	0.79726
Standard Deviation	389.07618	*Alternative Kurtosis (Fisher's)*	0.25699
Mean Standard Error	25.88096	*Coefficient of Variation*	0.36494
Minimum	337.	*Mean Deviation*	304.07384
Maximum	2,129.98	*Second Moment*	150,710.4515
Range	1,792.98	*Third Moment*	46,336,104.62027
Sum	240,947.17	*Fourth Moment*	7.32494E+10
Sum Standard Error	5,849.09756	*Median*	979.325
Total Sum Squares	290,943,476.7771	*Median Error*	2.15768
Adjusted Sum Squares	34,060,562.03812	*Percentile 25% (Q1)*	799.645
Geometric Mean	999.17471	*Percentile 75% (Q2)*	1,300.39
Harmonic Mean	934.93831	*IQR*	500.745
Mode	#N/A	*MAD*	222.885

Melton ratio (-)

Count	226	*Skewness*	0.57585
Mean	0.37926	*Skewness Standard Error*	0.16115
Mean LCL	0.35725	*Kurtosis*	3.12122
Mean UCL	0.40127	*Kurtosis Standard Error*	0.31808
Variance	0.01994	*Alternative Skewness (Fisher's)*	0.57971
Standard Deviation	0.14122	*Alternative Kurtosis (Fisher's)*	0.15097
Mean Standard Error	0.00939	*Coefficient of Variation*	0.37235
Minimum	0.09045	*Mean Deviation*	0.11225
Maximum	0.8289	*Second Moment*	0.01985
Range	0.73846	*Third Moment*	0.00161
Sum	85.71343	*Fourth Moment*	0.00123
Sum Standard Error	2.12296	*Median*	0.35872
Total Sum Squares	36.99495	*Median Error*	0.00078
Adjusted Sum Squares	4.48702	*Percentile 25% (Q1)*	0.28441
Geometric Mean	0.35266	*Percentile 75% (Q2)*	0.46372
Harmonic Mean	0.32476	*IQR*	0.1793
Mode	0.24	*MAD*	0.08835

Mean slope (°)

Count	226	*Skewness*	-0.19872
Mean	25.49577	*Skewness Standard Error*	0.16115
Mean LCL	24.767	*Kurtosis*	3.24354
Mean UCL	26.22454	*Kurtosis Standard Error*	0.31808
Variance	21.86422	*Alternative Skewness (Fisher's)*	-0.20005
Standard Deviation	4.67592	*Alternative Kurtosis (Fisher's)*	0.27604
Mean Standard Error	0.31104	*Coefficient of Variation*	0.1834
Minimum	12.58024	*Mean Deviation*	3.59896
Maximum	38.87977	*Second Moment*	21.76748
Range	26.29953	*Third Moment*	-20.18182
Sum	5,762.04421	*Fourth Moment*	1,536.86249
Sum Standard Error	70.29448	*Median*	25.66773
Total Sum Squares	151,827.20908	*Median Error*	0.02593
Adjusted Sum Squares	4,919.45033	*Percentile 25% (Q1)*	22.99205
Geometric Mean	25.03447	*Percentile 75% (Q2)*	28.45001
Harmonic Mean	24.52605	*IQR*	5.45796
Mode	#N/A	*MAD*	2.73804

Mean orientation (0-360)

Count	226	*Skewness*	0.09698
Mean	176.83408	*Skewness Standard Error*	0.16115
Mean LCL	171.91572	*Kurtosis*	2.46091
Mean UCL	181.75244	*Kurtosis Standard Error*	0.31808
Variance	995.84389	*Alternative Skewness (Fisher's)*	0.09763
Standard Deviation	31.55699	*Alternative Kurtosis (Fisher's)*	-0.52419
Mean Standard Error	2.09914	*Coefficient of Variation*	0.17846
Minimum	100.8693	*Mean Deviation*	26.04223
Maximum	259.4286	*Second Moment*	991.4375
Range	158.5593	*Third Moment*	3,027.43303
Sum	39,964.5019	*Fourth Moment*	2,418,945.4399
Sum Standard Error	474.40565	*Median*	176.7612
Total Sum Squares	7,291,150.76916	*Median Error*	0.175
Adjusted Sum Squares	224,064.87484	*Percentile 25% (Q1)*	152.3235
Geometric Mean	173.97443	*Percentile 75% (Q2)*	198.092
Harmonic Mean	171.05932	*IQR*	45.7685
Mode	141.	*MAD*	23.2705

Area (km2)

Count	226	*Skewness*	1.91374
Mean	11.38984	*Skewness Standard Error*	0.16115
Mean LCL	10.11023	*Kurtosis*	7.30144
Mean UCL	12.66944	*Kurtosis Standard Error*	0.31808
Variance	67.40669	*Alternative Skewness (Fisher's)*	1.92655
Standard Deviation	8.21016	*Alternative Kurtosis (Fisher's)*	4.42517
Mean Standard Error	0.54613	*Coefficient of Variation*	0.72083
Minimum	2.20213	*Mean Deviation*	6.02589
Maximum	46.78	*Second Moment*	67.10843
Range	44.57788	*Third Moment*	1,052.08086
Sum	2,574.10328	*Fourth Moment*	32,882.3215
Sum Standard Error	123.42573	*Median*	8.57416
Total Sum Squares	44,485.12296	*Median Error*	0.04553
Adjusted Sum Squares	15,166.50495	*Percentile 25% (Q1)*	5.82578
Geometric Mean	9.27605	*Percentile 75% (Q2)*	14.18444
Harmonic Mean	7.7535	*IQR*	8.35866
Mode	#N/A	*MAD*	3.50259

Stream length (km)

Count	226	*Skewness*	1.3999
Mean	20.72022	*Skewness Standard Error*	0.16115
Mean LCL	19.40017	*Kurtosis*	5.32422
Mean UCL	22.04027	*Kurtosis Standard Error*	0.31808
Variance	71.7351	*Alternative Skewness (Fisher's)*	1.40927
Standard Deviation	8.46966	*Alternative Kurtosis (Fisher's)*	2.4035
Mean Standard Error	0.56339	*Coefficient of Variation*	0.40876
Minimum	9.1	*Mean Deviation*	6.5308
Maximum	55.67	*Second Moment*	71.41769
Range	46.57	*Third Moment*	844.89949
Sum	4,682.77	*Fourth Moment*	27,156.11344
Sum Standard Error	127.32688	*Median*	18.16
Total Sum Squares	113,168.4289	*Median Error*	0.04697
Adjusted Sum Squares	16,140.39849	*Percentile 25% (Q1)*	14.77
Geometric Mean	19.28298	*Percentile 75% (Q2)*	24.92
Harmonic Mean	18.07256	*IQR*	10.15
Mode	#N/A	*MAD*	4.255

Perimeter (m)

Count	226	*Skewness*	1.38934
Mean	20,432.56637	*Skewness Standard Error*	0.16115
Mean LCL	19,135.74739	*Kurtosis*	5.25196
Mean UCL	21,729.38535	*Kurtosis Standard Error*	0.31808
Variance	69,232,428.05113	*Alternative Skewness (Fisher's)*	1.39864
Standard Deviation	8,320.60263	*Alternative Kurtosis (Fisher's)*	2.32961
Mean Standard Error	553.47825	*Coefficient of Variation*	0.40722
Minimum	9,120.	*Mean Deviation*	6,430.85598
Maximum	54,920.	*Second Moment*	68,926,089.87391
Range	45,800.	*Third Moment*	7.95031E+11
Sum	4,617,760.	*Fourth Moment*	2.4951E+16
Sum Standard Error	125,086.08532	*Median*	17,980.
Total Sum Squares	1.0993E+11	*Median Error*	46.14305
Adjusted Sum Squares	1.55773E+10	*Percentile 25% (Q1)*	14,680.
Geometric Mean	19,025.05124	*Percentile 75% (Q2)*	24,740.
Harmonic Mean	17,840.99598	*IQR*	10,060.
Mode	#N/A	*MAD*	4,160.

Form factor (-)

Count	226	*Skewness*	-0.46674
Mean	0.02548	*Skewness Standard Error*	0.16115
Mean LCL	0.02469	*Kurtosis*	2.82192
Mean UCL	0.02627	*Kurtosis Standard Error*	0.31808
Variance	0.00003	*Alternative Skewness (Fisher's)*	-0.46986
Standard Deviation	0.00505	*Alternative Kurtosis (Fisher's)*	-0.15506
Mean Standard Error	0.00034	*Coefficient of Variation*	0.19828
Minimum	0.01	*Mean Deviation*	0.0041
Maximum	0.03989	*Second Moment*	0.00003
Range	0.02989	*Third Moment*	0.
Sum	5.75811	*Fourth Moment*	0.
Sum Standard Error	0.07595	*Median*	0.02641
Total Sum Squares	0.15245	*Median Error*	0.00003
Adjusted Sum Squares	0.00574	*Percentile 25% (Q1)*	0.022
Geometric Mean	0.02492	*Percentile 75% (Q2)*	0.02994
Harmonic Mean	0.02428	*IQR*	0.00794
Mode	0.03	*MAD*	0.00359

Basin Elongation (-)

Count	226	*Skewness*	-0.33663
Mean	1.47219	*Skewness Standard Error*	0.16115
Mean LCL	1.43747	*Kurtosis*	2.57702
Mean UCL	1.5069	*Kurtosis Standard Error*	0.31808
Variance	0.04961	*Alternative Skewness (Fisher's)*	-0.33889
Standard Deviation	0.22273	*Alternative Kurtosis (Fisher's)*	-0.40546
Mean Standard Error	0.01482	*Coefficient of Variation*	0.15129
Minimum	0.87712	*Mean Deviation*	0.18005
Maximum	1.93508	*Second Moment*	0.04939
Range	1.05796	*Third Moment*	-0.0037
Sum	332.71386	*Fourth Moment*	0.00629
Sum Standard Error	3.34842	*Median*	1.49528
Total Sum Squares	500.97874	*Median Error*	0.00124
Adjusted Sum Squares	11.16231	*Percentile 25% (Q1)*	1.30989
Geometric Mean	1.45437	*Percentile 75% (Q2)*	1.6383
Harmonic Mean	1.43541	*IQR*	0.32841
Mode	#N/A	*MAD*	0.15322

Lemniscate ratio (-)

Count	226	*Skewness*	1.13114
Mean	0.69666	*Skewness Standard Error*	0.16115
Mean LCL	0.67827	*Kurtosis*	4.31394
Mean UCL	0.71505	*Kurtosis Standard Error*	0.31808
Variance	0.01392	*Alternative Skewness (Fisher's)*	1.13872
Standard Deviation	0.118	*Alternative Kurtosis (Fisher's)*	1.37051
Mean Standard Error	0.00785	*Coefficient of Variation*	0.16938
Minimum	0.51677	*Mean Deviation*	0.09137
Maximum	1.14009	*Second Moment*	0.01386
Range	0.62332	*Third Moment*	0.00185
Sum	157.44468	*Fourth Moment*	0.00083
Sum Standard Error	1.77397	*Median*	0.6697
Total Sum Squares	112.8181	*Median Error*	0.00065
Adjusted Sum Squares	3.13303	*Percentile 25% (Q1)*	0.61
Geometric Mean	0.68757	*Percentile 75% (Q2)*	0.76396
Harmonic Mean	0.67924	*IQR*	0.15396
Mode	0.66	*MAD*	0.06963

Outlet slope (°)

Count	226	*Skewness*	0.92385
Mean	8.28535	*Skewness Standard Error*	0.16115
Mean LCL	7.31572	*Kurtosis*	3.58743
Mean UCL	9.25499	*Kurtosis Standard Error*	0.31808
Variance	38.70487	*Alternative Skewness (Fisher's)*	0.93003
Standard Deviation	6.22132	*Alternative Kurtosis (Fisher's)*	0.62766
Mean Standard Error	0.41384	*Coefficient of Variation*	0.75088
Minimum	0.E+0	*Mean Deviation*	5.05006
Maximum	33.55	*Second Moment*	38.53361
Range	33.55	*Third Moment*	220.98387
Sum	1,872.49	*Fourth Moment*	5,326.75797
Sum Standard Error	93.52701	*Median*	6.64
Total Sum Squares	24,222.8393	*Median Error*	0.0345
Adjusted Sum Squares	8,708.59682	*Percentile 25% (Q1)*	3.455
Geometric Mean	5.80808	*Percentile 75% (Q2)*	12.47
Harmonic Mean	3.33406	*IQR*	9.015
Mode	0.E+0	*MAD*	3.86

200m slope (°)

Count	226	*Skewness*	1.17485
Mean	8.08907	*Skewness Standard Error*	0.16115
Mean LCL	7.14483	*Kurtosis*	4.61928
Mean UCL	9.03331	*Kurtosis Standard Error*	0.31808
Variance	36.70405	*Alternative Skewness (Fisher's)*	1.18271
Standard Deviation	6.05839	*Alternative Kurtosis (Fisher's)*	1.68271
Mean Standard Error	0.403	*Coefficient of Variation*	0.74896
Minimum	0.E+0	*Mean Deviation*	4.75158
Maximum	34.13	*Second Moment*	36.54164
Range	34.13	*Third Moment*	259.51519
Sum	1,828.13	*Fourth Moment*	6,168.08107
Sum Standard Error	91.07752	*Median*	6.725
Total Sum Squares	23,046.2839	*Median Error*	0.0336
Adjusted Sum Squares	8,258.4109	*Percentile 25% (Q1)*	3.43
Geometric Mean	5.85692	*Percentile 75% (Q2)*	11.51
Harmonic Mean	3.58707	*IQR*	8.08
Mode	0.E+0	*MAD*	3.67

Average slope (°)

Count	226	*Skewness*	0.75274
Mean	9.15686	*Skewness Standard Error*	0.16115
Mean LCL	8.25082	*Kurtosis*	3.18162
Mean UCL	10.06289	*Kurtosis Standard Error*	0.31808
Variance	33.79409	*Alternative Skewness (Fisher's)*	0.75778
Standard Deviation	5.81327	*Alternative Kurtosis (Fisher's)*	0.21273
Mean Standard Error	0.38669	*Coefficient of Variation*	0.63485
Minimum	0.E+0	*Mean Deviation*	4.67016
Maximum	28.1	*Second Moment*	33.64456
Range	28.1	*Third Moment*	146.89824
Sum	2,069.45	*Fourth Moment*	3,601.45687
Sum Standard Error	87.39258	*Median*	8.185
Total Sum Squares	26,553.3301	*Median Error*	0.03224
Adjusted Sum Squares	7,603.66947	*Percentile 25% (Q1)*	4.535
Geometric Mean	7.10948	*Percentile 75% (Q2)*	12.605
Harmonic Mean	4.44352	*IQR*	8.07
Mode	0.E+0	*MAD*	4.17

2nd-order catchments - Training set – all zones – reactive catchments.

Max. elevation (m asl)			
Count	52	*Skewness*	-0.92032
Mean	2,593.85115	*Skewness Standard Error*	0.324
Mean LCL	2,476.48084	*Kurtosis*	3.20334
Mean UCL	2,711.22147	*Kurtosis Standard Error*	0.61235
Variance	124,186.9669	*Alternative Skewness (Fisher's)*	-0.94789
Standard Deviation	352.40171	*Alternative Kurtosis (Fisher's)*	0.34923
Mean Standard Error	48.86932	*Coefficient of Variation*	0.13586
Minimum	1,542.42	*Mean Deviation*	278.46478
Maximum	3,026.53	*Second Moment*	121,798.756
Range	1,484.11	*Third Moment*	-39,120,405.62255
Sum	134,880.26	*Fourth Moment*	4.75213E+10
Sum Standard Error	2,541.20489	*Median*	2,656.995
Total Sum Squares	356,192,853.344	*Median Error*	8.49365
Adjusted Sum Squares	6,333,535.31193	*Percentile 25% (Q1)*	2,386.54
Geometric Mean	2,567.66455	*Percentile 75% (Q2)*	2,892.97
Harmonic Mean	2,538.35271	*IQR*	506.43
Mode	#N/A	*MAD*	236.33
Mean elevation (m asl)			
Count	52	*Skewness*	-0.28354
Mean	1,959.08473	*Skewness Standard Error*	0.324
Mean LCL	1,832.57067	*Kurtosis*	2.06618
Mean UCL	2,085.5988	*Kurtosis Standard Error*	0.61235
Variance	144,290.293	*Alternative Skewness (Fisher's)*	-0.29203
Standard Deviation	379.85562	*Alternative Kurtosis (Fisher's)*	-0.90535
Mean Standard Error	52.6765	*Coefficient of Variation*	0.19389
Minimum	1,126.897	*Mean Deviation*	322.41197
Maximum	2,504.504	*Second Moment*	141,515.47967
Range	1,377.607	*Third Moment*	-15,094,500.35417
Sum	101,872.406	*Fourth Moment*	4.13786E+10
Sum Standard Error	2,739.17784	*Median*	1,996.4545
Total Sum Squares	206,935,480.0241	*Median Error*	9.15535
Adjusted Sum Squares	7,358,804.94278	*Percentile 25% (Q1)*	1,663.22
Geometric Mean	1,920.33719	*Percentile 75% (Q2)*	2,288.145
Harmonic Mean	1,878.95627	*IQR*	624.925
Mode	#N/A	*MAD*	324.437
Min. elevation (m asl)			
Count	52	*Skewness*	0.37917
Mean	1,314.93769	*Skewness Standard Error*	0.324
Mean LCL	1,180.03775	*Kurtosis*	2.24135
Mean UCL	1,449.83764	*Kurtosis Standard Error*	0.61235
Variance	164,052.5696	*Alternative Skewness (Fisher's)*	0.39053
Standard Deviation	405.03404	*Alternative Kurtosis (Fisher's)*	-0.7121
Mean Standard Error	56.16811	*Coefficient of Variation*	0.30803
Minimum	531.61	*Mean Deviation*	340.0779
Maximum	2,127.02	*Second Moment*	160,897.71249
Range	1,595.41	*Third Moment*	24,471,462.13778
Sum	68,376.76	*Fourth Moment*	5.80242E+10
Sum Standard Error	2,920.74196	*Median*	1,187.745
Total Sum Squares	98,277,860.0514	*Median Error*	9.76221
Adjusted Sum Squares	8,366,681.04952	*Percentile 25% (Q1)*	1,040.31
Geometric Mean	1,253.40685	*Percentile 75% (Q2)*	1,606.12
Harmonic Mean	1,191.49077	*IQR*	565.81
Mode	#N/A	*MAD*	256.415

Melton ratio (-)

Count	52	*Skewness*	0.93812
Mean	0.39477	*Skewness Standard Error*	0.324
Mean LCL	0.35483	*Kurtosis*	4.59048
Mean UCL	0.4347	*Kurtosis Standard Error*	0.61235
Variance	0.01438	*Alternative Skewness (Fisher's)*	0.96622
Standard Deviation	0.11992	*Alternative Kurtosis (Fisher's)*	1.87962
Mean Standard Error	0.01663	*Coefficient of Variation*	0.30376
Minimum	0.19203	*Mean Deviation*	0.08935
Maximum	0.81795	*Second Moment*	0.0141
Range	0.62592	*Third Moment*	0.00157
Sum	20.52783	*Fourth Moment*	0.00091
Sum Standard Error	0.86472	*Median*	0.38557
Total Sum Squares	8.83706	*Median Error*	0.00289
Adjusted Sum Squares	0.73337	*Percentile 25% (Q1)*	0.31002
Geometric Mean	0.37799	*Percentile 75% (Q2)*	0.4467
Harmonic Mean	0.36186	*IQR*	0.13668
Mode	#N/A	*MAD*	0.06573

Mean slope (°)

Count	52	*Skewness*	0.02761
Mean	27.2309	*Skewness Standard Error*	0.324
Mean LCL	26.10639	*Kurtosis*	2.72303
Mean UCL	28.35541	*Kurtosis Standard Error*	0.61235
Variance	11.39947	*Alternative Skewness (Fisher's)*	0.02844
Standard Deviation	3.37631	*Alternative Kurtosis (Fisher's)*	-0.18068
Mean Standard Error	0.46821	*Coefficient of Variation*	0.12399
Minimum	19.48814	*Mean Deviation*	2.7001
Maximum	34.53099	*Second Moment*	11.18025
Range	15.04285	*Third Moment*	1.03217
Sum	1,416.00696	*Fourth Moment*	340.37307
Sum Standard Error	24.34692	*Median*	27.15191
Total Sum Squares	39,140.52136	*Median Error*	0.08138
Adjusted Sum Squares	581.37308	*Percentile 25% (Q1)*	25.
Geometric Mean	27.02253	*Percentile 75% (Q2)*	29.62624
Harmonic Mean	26.81058	*IQR*	4.62624
Mode	#N/A	*MAD*	2.24018

Mean orientation (0-360)

Count	52	*Skewness*	0.32571
Mean	172.92892	*Skewness Standard Error*	0.324
Mean LCL	163.25363	*Kurtosis*	2.19949
Mean UCL	182.60422	*Kurtosis Standard Error*	0.61235
Variance	843.89364	*Alternative Skewness (Fisher's)*	0.33547
Standard Deviation	29.04985	*Alternative Kurtosis (Fisher's)*	-0.75828
Mean Standard Error	4.02849	*Coefficient of Variation*	0.16799
Minimum	120.2844	*Mean Deviation*	24.73609
Maximum	237.	*Second Moment*	827.66492
Range	116.7156	*Third Moment*	7,755.57666
Sum	8,992.304	*Fourth Moment*	1,506,712.5649
Sum Standard Error	209.48143	*Median*	171.81885
Total Sum Squares	1,598,068.02247	*Median Error*	0.70017
Adjusted Sum Squares	43,038.57577	*Percentile 25% (Q1)*	148.
Geometric Mean	170.57036	*Percentile 75% (Q2)*	194.757
Harmonic Mean	168.26015	*IQR*	46.757
Mode	141.	*MAD*	23.4499

Area (km2)

Count	52	*Skewness*	1.85163
Mean	12.65276	*Skewness Standard Error*	0.324
Mean LCL	9.8617	*Kurtosis*	6.85638
Mean UCL	15.44383	*Kurtosis Standard Error*	0.61235
Variance	70.22631	*Alternative Skewness (Fisher's)*	1.90709
Standard Deviation	8.38011	*Alternative Kurtosis (Fisher's)*	4.3795
Mean Standard Error	1.16211	*Coefficient of Variation*	0.66231
Minimum	2.8613	*Mean Deviation*	6.09917
Maximum	45.16895	*Second Moment*	68.8758
Range	42.30765	*Third Moment*	1,058.41006
Sum	657.94368	*Fourth Moment*	32,525.79644
Sum Standard Error	60.42986	*Median*	9.96161
Total Sum Squares	11,906.34694	*Median Error*	0.20198
Adjusted Sum Squares	3,581.54157	*Percentile 25% (Q1)*	7.12
Geometric Mean	10.65592	*Percentile 75% (Q2)*	16.90833
Harmonic Mean	9.15012	*IQR*	9.78833
Mode	#N/A	*MAD*	3.40554

Stream length (km)

Count	52	*Skewness*	1.6329
Mean	21.37538	*Skewness Standard Error*	0.324
Mean LCL	18.83046	*Kurtosis*	6.59562
Mean UCL	23.92031	*Kurtosis Standard Error*	0.61235
Variance	58.38615	*Alternative Skewness (Fisher's)*	1.68181
Standard Deviation	7.64108	*Alternative Kurtosis (Fisher's)*	4.09182
Mean Standard Error	1.05963	*Coefficient of Variation*	0.35747
Minimum	11.1	*Mean Deviation*	5.68334
Maximum	52.3	*Second Moment*	57.26334
Range	41.2	*Third Moment*	707.57854
Sum	1,111.52	*Fourth Moment*	21,627.6327
Sum Standard Error	55.10063	*Median*	19.17
Total Sum Squares	26,736.8612	*Median Error*	0.18417
Adjusted Sum Squares	2,977.69369	*Percentile 25% (Q1)*	16.59
Geometric Mean	20.28277	*Percentile 75% (Q2)*	25.37
Harmonic Mean	19.3724	*IQR*	8.78
Mode	#N/A	*MAD*	4.195

Perimeter (m)

Count	52	*Skewness*	1.58676
Mean	21,068.46154	*Skewness Standard Error*	0.324
Mean LCL	18,571.80922	*Kurtosis*	6.30627
Mean UCL	23,565.11385	*Kurtosis Standard Error*	0.61235
Variance	56,192,146.60633	*Alternative Skewness (Fisher's)*	1.63429
Standard Deviation	7,496.14211	*Alternative Kurtosis (Fisher's)*	3.77259
Mean Standard Error	1,039.52788	*Coefficient of Variation*	0.3558
Minimum	11,040.	*Mean Deviation*	5,598.5503
Maximum	50,920.	*Second Moment*	55,111,528.40237
Range	39,880.	*Third Moment*	6.49196E+11
Sum	1,095,560.	*Fourth Moment*	1.91539E+16
Sum Standard Error	54,055.44953	*Median*	18,960.
Total Sum Squares	2.59476E+10	*Median Error*	180.67348
Adjusted Sum Squares	2,865,799,476.92308	*Percentile 25% (Q1)*	16,120.
Geometric Mean	19,996.19155	*Percentile 75% (Q2)*	25,120.
Harmonic Mean	19,101.33778	*IQR*	9,000.
Mode	#N/A	*MAD*	4,180.

Form factor (-)

Count	52	*Skewness*	-0.94443
Mean	0.02615	*Skewness Standard Error*	0.324
Mean LCL	0.02477	*Kurtosis*	3.09584
Mean UCL	0.02753	*Kurtosis Standard Error*	0.61235
Variance	0.00002	*Alternative Skewness (Fisher's)*	-0.97272
Standard Deviation	0.00415	*Alternative Kurtosis (Fisher's)*	0.23064
Mean Standard Error	0.00058	*Coefficient of Variation*	0.15858
Minimum	0.01606	*Mean Deviation*	0.00325
Maximum	0.03221	*Second Moment*	0.00002
Range	0.01614	*Third Moment*	0.
Sum	1.35972	*Fourth Moment*	0.
Sum Standard Error	0.0299	*Median*	0.02648
Total Sum Squares	0.03643	*Median Error*	0.0001
Adjusted Sum Squares	0.00088	*Percentile 25% (Q1)*	0.02493
Geometric Mean	0.02578	*Percentile 75% (Q2)*	0.03
Harmonic Mean	0.02536	*IQR*	0.00507
Mode	0.03	*MAD*	0.00337

Basin Elongation (-)

Count	52	*Skewness*	-0.42877
Mean	1.5067	*Skewness Standard Error*	0.324
Mean LCL	1.44029	*Kurtosis*	3.28587
Mean UCL	1.57311	*Kurtosis Standard Error*	0.61235
Variance	0.03976	*Alternative Skewness (Fisher's)*	-0.44161
Standard Deviation	0.1994	*Alternative Kurtosis (Fisher's)*	0.44029
Mean Standard Error	0.02765	*Coefficient of Variation*	0.13234
Minimum	0.90695	*Mean Deviation*	0.15682
Maximum	1.8462	*Second Moment*	0.039
Range	0.93926	*Third Moment*	-0.0033
Sum	78.34834	*Fourth Moment*	0.005
Sum Standard Error	1.43792	*Median*	1.505
Total Sum Squares	120.0752	*Median Error*	0.00481
Adjusted Sum Squares	2.02786	*Percentile 25% (Q1)*	1.39601
Geometric Mean	1.49288	*Percentile 75% (Q2)*	1.64131
Harmonic Mean	1.47794	*IQR*	0.2453
Mode	#N/A	*MAD*	0.12497

Lemniscate ratio (-)

Count	52	*Skewness*	1.59445
Mean	0.67678	*Skewness Standard Error*	0.324
Mean LCL	0.64273	*Kurtosis*	7.32167
Mean UCL	0.71082	*Kurtosis Standard Error*	0.61235
Variance	0.01045	*Alternative Skewness (Fisher's)*	1.6422
Standard Deviation	0.10221	*Alternative Kurtosis (Fisher's)*	4.89285
Mean Standard Error	0.01417	*Coefficient of Variation*	0.15102
Minimum	0.54165	*Mean Deviation*	0.07362
Maximum	1.1026	*Second Moment*	0.01025
Range	0.56095	*Third Moment*	0.00165
Sum	35.19233	*Fourth Moment*	0.00077
Sum Standard Error	0.73703	*Median*	0.665
Total Sum Squares	24.35008	*Median Error*	0.00246
Adjusted Sum Squares	0.53276	*Percentile 25% (Q1)*	0.61
Geometric Mean	0.67	*Percentile 75% (Q2)*	0.72218
Harmonic Mean	0.66385	*IQR*	0.11218
Mode	#N/A	*MAD*	0.05537

Outlet slope (°)

Count	52	*Skewness*	1.17686
Mean	7.85212	*Skewness Standard Error*	0.324
Mean LCL	5.61045	*Kurtosis*	5.34976
Mean UCL	10.09378	*Kurtosis Standard Error*	0.61235
Variance	45.30037	*Alternative Skewness (Fisher's)*	1.21211
Standard Deviation	6.73055	*Alternative Kurtosis (Fisher's)*	2.71731
Mean Standard Error	0.93336	*Coefficient of Variation*	0.85716
Minimum	0.E+0	*Mean Deviation*	5.2245
Maximum	33.55	*Second Moment*	44.42921
Range	33.55	*Third Moment*	348.51915
Sum	408.31	*Fourth Moment*	10,560.18815
Sum Standard Error	48.53472	*Median*	7.385
Total Sum Squares	5,516.4159	*Median Error*	0.16222
Adjusted Sum Squares	2,310.31867	*Percentile 25% (Q1)*	2.72
Geometric Mean	4.68459	*Percentile 75% (Q2)*	12.12
Harmonic Mean	1.94847	*IQR*	9.4
Mode	0.E+0	*MAD*	4.7

200m slope (°)

Count	52	*Skewness*	1.39426
Mean	7.75154	*Skewness Standard Error*	0.324
Mean LCL	5.6415	*Kurtosis*	6.82774
Mean UCL	9.86158	*Kurtosis Standard Error*	0.61235
Variance	40.13655	*Alternative Skewness (Fisher's)*	1.43602
Standard Deviation	6.33534	*Alternative Kurtosis (Fisher's)*	4.34792
Mean Standard Error	0.87855	*Coefficient of Variation*	0.8173
Minimum	0.E+0	*Mean Deviation*	4.85391
Maximum	34.13	*Second Moment*	39.36469
Range	34.13	*Third Moment*	344.35357
Sum	403.08	*Fourth Moment*	10,580.12787
Sum Standard Error	45.68479	*Median*	6.725
Total Sum Squares	5,171.454	*Median Error*	0.1527
Adjusted Sum Squares	2,046.96388	*Percentile 25% (Q1)*	3.24
Geometric Mean	5.15784	*Percentile 75% (Q2)*	11.87
Harmonic Mean	2.53928	*IQR*	8.63
Mode	0.E+0	*MAD*	4.085

Average slope (°)

Count	52	*Skewness*	0.63772
Mean	9.37519	*Skewness Standard Error*	0.324
Mean LCL	7.16535	*Kurtosis*	2.8548
Mean UCL	11.58503	*Kurtosis Standard Error*	0.61235
Variance	44.02316	*Alternative Skewness (Fisher's)*	0.65682
Standard Deviation	6.635	*Alternative Kurtosis (Fisher's)*	-0.0353
Mean Standard Error	0.92011	*Coefficient of Variation*	0.70772
Minimum	0.E+0	*Mean Deviation*	5.35233
Maximum	26.9	*Second Moment*	43.17656
Range	26.9	*Third Moment*	180.92595
Sum	487.51	*Fourth Moment*	5,321.96142
Sum Standard Error	47.84563	*Median*	8.295
Total Sum Squares	6,815.6813	*Median Error*	0.15992
Adjusted Sum Squares	2,245.1813	*Percentile 25% (Q1)*	4.56
Geometric Mean	6.50068	*Percentile 75% (Q2)*	13.42
Harmonic Mean	2.72061	*IQR*	8.86
Mode	0.E+0	*MAD*	4.745

2nd-order catchments - Test set – Andorra – all catchments.

Max. elevation (m asl)			
Count	25	*Skewness*	-1.86258
Mean	2,712.8	*Skewness Standard Error*	0.44475
Mean LCL	2,602.63264	*Kurtosis*	6.5595
Mean UCL	2,822.96736	*Kurtosis Standard Error*	0.79214
Variance	48,853.33333	*Alternative Skewness (Fisher's)*	-1.98364
Standard Deviation	221.0279	*Alternative Kurtosis (Fisher's)*	4.67417
Mean Standard Error	44.20558	*Coefficient of Variation*	0.08148
Minimum	1,958.	*Mean Deviation*	158.24
Maximum	2,913.	*Second Moment*	46,899.2
Range	955.	*Third Moment*	-18,917,500.752
Sum	67,820.	*Fourth Moment*	1.44279E+10
Sum Standard Error	1,105.13951	*Median*	2,793.
Total Sum Squares	185,154,576.	*Median Error*	11.0807
Adjusted Sum Squares	1,172,480.	*Percentile 25% (Q1)*	2,670.
Geometric Mean	2,703.08731	*Percentile 75% (Q2)*	2,866.75
Harmonic Mean	2,692.12008	*IQR*	196.75
Mode	#N/A	*MAD*	94.
Mean elevation (m asl)			
Count	25	*Skewness*	-1.06263
Mean	2,152.84968	*Skewness Standard Error*	0.44475
Mean LCL	2,017.83179	*Kurtosis*	2.87411
Mean UCL	2,287.86757	*Kurtosis Standard Error*	0.79214
Variance	73,378.85865	*Alternative Skewness (Fisher's)*	-1.1317
Standard Deviation	270.88532	*Alternative Kurtosis (Fisher's)*	0.12934
Mean Standard Error	54.17706	*Coefficient of Variation*	0.12583
Minimum	1,498.302	*Mean Deviation*	221.88774
Maximum	2,469.089	*Second Moment*	70,443.7043
Range	970.787	*Third Moment*	-19,867,681.67934
Sum	53,821.242	*Fourth Moment*	1.42622E+10
Sum Standard Error	1,354.42662	*Median*	2,263.891
Total Sum Squares	117,630,136.2245	*Median Error*	13.58018
Adjusted Sum Squares	1,761,092.6076	*Percentile 25% (Q1)*	1,965.81475
Geometric Mean	2,134.68964	*Percentile 75% (Q2)*	2,344.865
Harmonic Mean	2,114.623	*IQR*	379.05025
Mode	#N/A	*MAD*	87.201
Min. elevation (m asl)			
Count	25	*Skewness*	-0.46621
Mean	1,454.92	*Skewness Standard Error*	0.44475
Mean LCL	1,296.43989	*Kurtosis*	2.06939
Mean UCL	1,613.40011	*Kurtosis Standard Error*	0.79214
Variance	101,096.91	*Alternative Skewness (Fisher's)*	-0.49651
Standard Deviation	317.9574	*Alternative Kurtosis (Fisher's)*	-0.86305
Mean Standard Error	63.59148	*Coefficient of Variation*	0.21854
Minimum	874.	*Mean Deviation*	261.2768
Maximum	1,843.	*Second Moment*	97,053.0336
Range	969.	*Third Moment*	-14,095,974.55142
Sum	36,373.	*Fourth Moment*	1.94921E+10
Sum Standard Error	1,589.78701	*Median*	1,429.
Total Sum Squares	55,346,131.	*Median Error*	15.94002
Adjusted Sum Squares	2,426,325.84	*Percentile 25% (Q1)*	1,282.25
Geometric Mean	1,417.7927	*Percentile 75% (Q2)*	1,775.25
Harmonic Mean	1,377.0976	*IQR*	493.
Mode	#N/A	*MAD*	267.

Melton ratio (-)

Count	25	*Skewness*	0.71842
Mean	0.41412	*Skewness Standard Error*	0.44475
Mean LCL	0.35638	*Kurtosis*	3.83779
Mean UCL	0.47187	*Kurtosis Standard Error*	0.79214
Variance	0.01342	*Alternative Skewness (Fisher's)*	0.76511
Standard Deviation	0.11585	*Alternative Kurtosis (Fisher's)*	1.31775
Mean Standard Error	0.02317	*Coefficient of Variation*	0.27976
Minimum	0.18363	*Mean Deviation*	0.08682
Maximum	0.70404	*Second Moment*	0.01289
Range	0.52041	*Third Moment*	0.00105
Sum	10.3531	*Fourth Moment*	0.00064
Sum Standard Error	0.57927	*Median*	0.40913
Total Sum Squares	4.60959	*Median Error*	0.00581
Adjusted Sum Squares	0.32213	*Percentile 25% (Q1)*	0.33509
Geometric Mean	0.39888	*Percentile 75% (Q2)*	0.46922
Harmonic Mean	0.38324	*IQR*	0.13413
Mode	#N/A	*MAD*	0.0631

Mean slope (°)

Count	25	*Skewness*	0.98558
Mean	25.66112	*Skewness Standard Error*	0.44475
Mean LCL	23.98933	*Kurtosis*	5.28885
Mean UCL	27.33291	*Kurtosis Standard Error*	0.79214
Variance	11.24998	*Alternative Skewness (Fisher's)*	1.04964
Standard Deviation	3.3541	*Alternative Kurtosis (Fisher's)*	3.1072
Mean Standard Error	0.67082	*Coefficient of Variation*	0.13071
Minimum	18.84461	*Mean Deviation*	2.34433
Maximum	36.03762	*Second Moment*	10.79998
Range	17.19301	*Third Moment*	34.9805
Sum	641.52812	*Fourth Moment*	616.88944
Sum Standard Error	16.7705	*Median*	25.50643
Total Sum Squares	16,732.33269	*Median Error*	0.16815
Adjusted Sum Squares	269.99954	*Percentile 25% (Q1)*	23.63386
Geometric Mean	25.46142	*Percentile 75% (Q2)*	27.39165
Harmonic Mean	25.26927	*IQR*	3.75779
Mode	#N/A	*MAD*	1.94762

Mean orientation (0-360)

Count	25	*Skewness*	0.6095
Mean	178.96904	*Skewness Standard Error*	0.44475
Mean LCL	159.33431	*Kurtosis*	2.75819
Mean UCL	198.60376	*Kurtosis Standard Error*	0.79214
Variance	1,551.80748	*Alternative Skewness (Fisher's)*	0.64911
Standard Deviation	39.39299	*Alternative Kurtosis (Fisher's)*	-0.01361
Mean Standard Error	7.8786	*Coefficient of Variation*	0.22011
Minimum	121.47	*Mean Deviation*	31.6823
Maximum	275.9583	*Second Moment*	1,489.73518
Range	154.4883	*Third Moment*	35,045.66258
Sum	4,474.2259	*Fourth Moment*	6,121,290.3212
Sum Standard Error	196.96494	*Median*	175.4317
Total Sum Squares	837,991.2756	*Median Error*	1.97487
Adjusted Sum Squares	37,243.37943	*Percentile 25% (Q1)*	147.75438
Geometric Mean	174.99205	*Percentile 75% (Q2)*	209.6719
Harmonic Mean	171.21301	*IQR*	61.91753
Mode	#N/A	*MAD*	29.8992

Area (km2)

Count	25	*Skewness*	1.67538
Mean	11.68362	*Skewness Standard Error*	0.44475
Mean LCL	7.60534	*Kurtosis*	5.69863
Mean UCL	15.76189	*Kurtosis Standard Error*	0.79214
Variance	66.94852	*Alternative Skewness (Fisher's)*	1.78427
Standard Deviation	8.18221	*Alternative Kurtosis (Fisher's)*	3.61254
Mean Standard Error	1.63644	*Coefficient of Variation*	0.70031
Minimum	3.6308	*Mean Deviation*	5.77797
Maximum	38.	*Second Moment*	64.27058
Range	34.3692	*Third Moment*	863.24114
Sum	292.0904	*Fourth Moment*	23,539.38315
Sum Standard Error	40.91104	*Median*	9.428
Total Sum Squares	5,019.43662	*Median Error*	0.4102
Adjusted Sum Squares	1,606.76455	*Percentile 25% (Q1)*	5.5932
Geometric Mean	9.61117	*Percentile 75% (Q2)*	15.1228
Harmonic Mean	8.07656	*IQR*	9.5296
Mode	#N/A	*MAD*	3.9228

Stream length (km)

Count	25	*Skewness*	1.1228
Mean	18.9828	*Skewness Standard Error*	0.44475
Mean LCL	15.74381	*Kurtosis*	3.78956
Mean UCL	22.22179	*Kurtosis Standard Error*	0.79214
Variance	42.22875	*Alternative Skewness (Fisher's)*	1.19577
Standard Deviation	6.49837	*Alternative Kurtosis (Fisher's)*	1.25827
Mean Standard Error	1.29967	*Coefficient of Variation*	0.34233
Minimum	11.75	*Mean Deviation*	5.08518
Maximum	36.27	*Second Moment*	40.5396
Range	24.52	*Third Moment*	289.81479
Sum	474.57	*Fourth Moment*	6,227.98179
Sum Standard Error	32.49183	*Median*	17.08
Total Sum Squares	10,022.1575	*Median Error*	0.32578
Adjusted Sum Squares	1,013.4901	*Percentile 25% (Q1)*	14.1275
Geometric Mean	18.05416	*Percentile 75% (Q2)*	23.4375
Harmonic Mean	17.2532	*IQR*	9.31
Mode	#N/A	*MAD*	4.07

Perimeter (m)

Count	25	*Skewness*	1.13919
Mean	18,833.6	*Skewness Standard Error*	0.44475
Mean LCL	15,613.00642	*Kurtosis*	3.85484
Mean UCL	22,054.19358	*Kurtosis Standard Error*	0.79214
Variance	41,750,357.33333	*Alternative Skewness (Fisher's)*	1.21324
Standard Deviation	6,461.45164	*Alternative Kurtosis (Fisher's)*	1.33878
Mean Standard Error	1,292.29033	*Coefficient of Variation*	0.34308
Minimum	11,640.	*Mean Deviation*	5,038.208
Maximum	36,080.	*Second Moment*	40,080,343.04
Range	24,440.	*Third Moment*	2.89064E+11
Sum	470,840.	*Fourth Moment*	6.19255E+15
Sum Standard Error	32,307.25821	*Median*	16,960.
Total Sum Squares	9,869,620,800.	*Median Error*	323.92915
Adjusted Sum Squares	1,002,008,576.	*Percentile 25% (Q1)*	14,060.
Geometric Mean	17,909.96909	*Percentile 75% (Q2)*	23,180.
Harmonic Mean	17,113.62088	*IQR*	9,120.
Mode	#N/A	*MAD*	4,040.

Form factor (-)

Count	25	*Skewness*	-0.28283
Mean	0.02967	*Skewness Standard Error*	0.44475
Mean LCL	0.02802	*Kurtosis*	2.75283
Mean UCL	0.03131	*Kurtosis Standard Error*	0.79214
Variance	0.00001	*Alternative Skewness (Fisher's)*	-0.30121
Standard Deviation	0.0033	*Alternative Kurtosis (Fisher's)*	-0.02023
Mean Standard Error	0.00066	*Coefficient of Variation*	0.11126
Minimum	0.02191	*Mean Deviation*	0.00257
Maximum	0.03518	*Second Moment*	0.00001
Range	0.01327	*Third Moment*	0.
Sum	0.74172	*Fourth Moment*	0.
Sum Standard Error	0.01651	*Median*	0.03009
Total Sum Squares	0.02227	*Median Error*	0.00017
Adjusted Sum Squares	0.00026	*Percentile 25% (Q1)*	0.02799
Geometric Mean	0.02949	*Percentile 75% (Q2)*	0.03163
Harmonic Mean	0.0293	*IQR*	0.00364
Mode	#N/A	*MAD*	0.00203

Basin Elongation (-)

Count	25	*Skewness*	-0.44161
Mean	1.62576	*Skewness Standard Error*	0.44475
Mean LCL	1.55215	*Kurtosis*	2.21361
Mean UCL	1.69936	*Kurtosis Standard Error*	0.79214
Variance	0.02181	*Alternative Skewness (Fisher's)*	-0.47031
Standard Deviation	0.14767	*Alternative Kurtosis (Fisher's)*	-0.68519
Mean Standard Error	0.02953	*Coefficient of Variation*	0.09083
Minimum	1.30765	*Mean Deviation*	0.11902
Maximum	1.83123	*Second Moment*	0.02093
Range	0.52358	*Third Moment*	-0.00134
Sum	40.64393	*Fourth Moment*	0.00097
Sum Standard Error	0.73834	*Median*	1.64354
Total Sum Squares	66.60052	*Median Error*	0.0074
Adjusted Sum Squares	0.52334	*Percentile 25% (Q1)*	1.51442
Geometric Mean	1.6191	*Percentile 75% (Q2)*	1.75891
Harmonic Mean	1.61224	*IQR*	0.24449
Mode	#N/A	*MAD*	0.1203

Lemniscate ratio (-)

Count	25	*Skewness*	0.73564
Mean	0.62026	*Skewness Standard Error*	0.44475
Mean LCL	0.59064	*Kurtosis*	2.68071
Mean UCL	0.64988	*Kurtosis Standard Error*	0.79214
Variance	0.00353	*Alternative Skewness (Fisher's)*	0.78346
Standard Deviation	0.05943	*Alternative Kurtosis (Fisher's)*	-0.10916
Mean Standard Error	0.01189	*Coefficient of Variation*	0.09581
Minimum	0.54608	*Mean Deviation*	0.0476
Maximum	0.76473	*Second Moment*	0.00339
Range	0.21865	*Third Moment*	0.00015
Sum	15.50642	*Fourth Moment*	0.00003
Sum Standard Error	0.29715	*Median*	0.60844
Total Sum Squares	9.70273	*Median Error*	0.00298
Adjusted Sum Squares	0.08477	*Percentile 25% (Q1)*	0.57449
Geometric Mean	0.61763	*Percentile 75% (Q2)*	0.67562
Harmonic Mean	0.6151	*IQR*	0.10113
Mode	#N/A	*MAD*	0.04735

Outlet slope (°)

Count	25	*Skewness*	0.1662
Mean	10.3716	*Skewness Standard Error*	0.44475
Mean LCL	8.01825	*Kurtosis*	2.53924
Mean UCL	12.72495	*Kurtosis Standard Error*	0.79214
Variance	22.29267	*Alternative Skewness (Fisher's)*	0.17701
Standard Deviation	4.72151	*Alternative Kurtosis (Fisher's)*	-0.28363
Mean Standard Error	0.9443	*Coefficient of Variation*	0.45523
Minimum	2.41	*Mean Deviation*	3.83674
Maximum	21.32	*Second Moment*	21.40097
Range	18.91	*Third Moment*	16.45472
Sum	259.29	*Fourth Moment*	1,162.97469
Sum Standard Error	23.60756	*Median*	10.82
Total Sum Squares	3,224.2763	*Median Error*	0.2367
Adjusted Sum Squares	535.02414	*Percentile 25% (Q1)*	6.845
Geometric Mean	9.14294	*Percentile 75% (Q2)*	13.3875
Harmonic Mean	7.72388	*IQR*	6.5425
Mode	#N/A	*MAD*	3.42

200m slope (°)

Count	25	*Skewness*	0.11003
Mean	11.9036	*Skewness Standard Error*	0.44475
Mean LCL	8.91773	*Kurtosis*	2.60413
Mean UCL	14.88947	*Kurtosis Standard Error*	0.79214
Variance	35.88646	*Alternative Skewness (Fisher's)*	0.11718
Standard Deviation	5.99053	*Alternative Kurtosis (Fisher's)*	-0.2036
Mean Standard Error	1.19811	*Coefficient of Variation*	0.50325
Minimum	1.48	*Mean Deviation*	4.79328
Maximum	26.09	*Second Moment*	34.451
Range	24.61	*Third Moment*	22.24896
Sum	297.59	*Fourth Moment*	3,090.77121
Sum Standard Error	29.95265	*Median*	13.3
Total Sum Squares	4,403.6673	*Median Error*	0.30032
Adjusted Sum Squares	861.27498	*Percentile 25% (Q1)*	6.04
Geometric Mean	10.02058	*Percentile 75% (Q2)*	16.24
Harmonic Mean	7.63979	*IQR*	10.2
Mode	#N/A	*MAD*	3.45

Average slope (°)

Count	25	*Skewness*	0.40777
Mean	11.6652	*Skewness Standard Error*	0.44475
Mean LCL	8.84862	*Kurtosis*	3.10838
Mean UCL	14.48178	*Kurtosis Standard Error*	0.79214
Variance	31.93256	*Alternative Skewness (Fisher's)*	0.43427
Standard Deviation	5.65089	*Alternative Kurtosis (Fisher's)*	0.41824
Mean Standard Error	1.13018	*Coefficient of Variation*	0.48442
Minimum	2.14	*Mean Deviation*	4.43818
Maximum	26.37	*Second Moment*	30.65526
Range	24.23	*Third Moment*	69.21041
Sum	291.63	*Fourth Moment*	2,921.08492
Sum Standard Error	28.25445	*Median*	12.31
Total Sum Squares	4,168.3037	*Median Error*	0.28329
Adjusted Sum Squares	766.38142	*Percentile 25% (Q1)*	7.6075
Geometric Mean	10.1406	*Percentile 75% (Q2)*	14.7175
Harmonic Mean	8.367	*IQR*	7.11
Mode	#N/A	*MAD*	4.29

2nd-order catchments - Test set – Andorra – reactive catchments.

Max. elevation (m asl)			
Count	18	*Skewness*	-0.81654
Mean	2,717.22222	*Skewness Standard Error*	0.50561
Mean LCL	2,613.98319	*Kurtosis*	2.52186
Mean UCL	2,820.46125	*Kurtosis Standard Error*	0.86184
Variance	29,115.94771	*Alternative Skewness (Fisher's)*	-0.89273
Standard Deviation	170.63396	*Alternative Kurtosis (Fisher's)*	-0.2185
Mean Standard Error	40.21881	*Coefficient of Variation*	0.0628
Minimum	2,376.	*Mean Deviation*	138.75309
Maximum	2,913.	*Second Moment*	27,498.39506
Range	537.	*Third Moment*	-3,723,395.71879
Sum	48,910.	*Fourth Moment*	1,906,930,871.1861
Sum Standard Error	723.93857	*Median*	2,781.
Total Sum Squares	133,394,310.	*Median Error*	11.881
Adjusted Sum Squares	494,971.11111	*Percentile 25% (Q1)*	2,649.5
Geometric Mean	2,711.97335	*Percentile 75% (Q2)*	2,859.
Harmonic Mean	2,706.53444	*IQR*	209.5
Mode	2,804.	*MAD*	107.
Mean elevation (m asl)			
Count	18	*Skewness*	-0.71031
Mean	2,125.67322	*Skewness Standard Error*	0.50561
Mean LCL	1,973.55315	*Kurtosis*	2.07058
Mean UCL	2,277.7933	*Kurtosis Standard Error*	0.86184
Variance	63,214.42266	*Alternative Skewness (Fisher's)*	-0.77658
Standard Deviation	251.42479	*Alternative Kurtosis (Fisher's)*	-0.82585
Mean Standard Error	59.26139	*Coefficient of Variation*	0.11828
Minimum	1,596.482	*Mean Deviation*	217.33226
Maximum	2,398.368	*Second Moment*	59,702.51029
Range	801.886	*Third Moment*	-10,361,786.87526
Sum	38,262.118	*Fourth Moment*	7,380,340,114.76793
Sum Standard Error	1,066.70502	*Median*	2,222.2285
Total Sum Squares	82,407,404.84328	*Median Error*	17.50635
Adjusted Sum Squares	1,074,645.18518	*Percentile 25% (Q1)*	1,875.6785
Geometric Mean	2,110.69363	*Percentile 75% (Q2)*	2,337.007
Harmonic Mean	2,094.80676	*IQR*	461.3285
Mode	#N/A	*MAD*	135.7775
Min. elevation (m asl)			
Count	18	*Skewness*	-0.17206
Mean	1,416.33333	*Skewness Standard Error*	0.50561
Mean LCL	1,226.74945	*Kurtosis*	1.95705
Mean UCL	1,605.91721	*Kurtosis Standard Error*	0.86184
Variance	98,185.17647	*Alternative Skewness (Fisher's)*	-0.18811
Standard Deviation	313.34514	*Alternative Kurtosis (Fisher's)*	-0.97864
Mean Standard Error	73.85616	*Coefficient of Variation*	0.22124
Minimum	890.	*Mean Deviation*	248.25926
Maximum	1,843.	*Second Moment*	92,730.44444
Range	953.	*Third Moment*	-4,858,573.14815
Sum	25,494.	*Fourth Moment*	1.68286E+10
Sum Standard Error	1,329.41084	*Median*	1,412.
Total Sum Squares	37,777,150.	*Median Error*	21.81777
Adjusted Sum Squares	1,669,148.	*Percentile 25% (Q1)*	1,262.
Geometric Mean	1,381.49931	*Percentile 75% (Q2)*	1,753.
Harmonic Mean	1,344.91408	*IQR*	491.
Mode	#N/A	*MAD*	263.5

Melton ratio (-)

Count	18	*Skewness*	0.70494
Mean	0.4109	*Skewness Standard Error*	0.50561
Mean LCL	0.32886	*Kurtosis*	2.9947
Mean UCL	0.49294	*Kurtosis Standard Error*	0.86184
Variance	0.01839	*Alternative Skewness (Fisher's)*	0.77071
Standard Deviation	0.1356	*Alternative Kurtosis (Fisher's)*	0.41787
Mean Standard Error	0.03196	*Coefficient of Variation*	0.33
Minimum	0.18363	*Mean Deviation*	0.10871
Maximum	0.70404	*Second Moment*	0.01736
Range	0.52041	*Third Moment*	0.00161
Sum	7.39621	*Fourth Moment*	0.0009
Sum Standard Error	0.57529	*Median*	0.36211
Total Sum Squares	3.35167	*Median Error*	0.00944
Adjusted Sum Squares	0.31257	*Percentile 25% (Q1)*	0.32252
Geometric Mean	0.39063	*Percentile 75% (Q2)*	0.4957
Harmonic Mean	0.37081	*IQR*	0.17317
Mode	#N/A	*MAD*	0.08642

Mean slope (°)

Count	18	*Skewness*	0.94944
Mean	25.85491	*Skewness Standard Error*	0.50561
Mean LCL	23.59984	*Kurtosis*	4.63879
Mean UCL	28.10998	*Kurtosis Standard Error*	0.86184
Variance	13.892	*Alternative Skewness (Fisher's)*	1.03802
Standard Deviation	3.7272	*Alternative Kurtosis (Fisher's)*	2.63054
Mean Standard Error	0.87851	*Coefficient of Variation*	0.14416
Minimum	18.84461	*Mean Deviation*	2.62041
Maximum	36.03762	*Second Moment*	13.12022
Range	17.19301	*Third Moment*	45.12089
Sum	465.38837	*Fourth Moment*	798.523
Sum Standard Error	15.81316	*Median*	25.52365
Total Sum Squares	12,268.73815	*Median Error*	0.25952
Adjusted Sum Squares	236.16399	*Percentile 25% (Q1)*	23.70891
Geometric Mean	25.61484	*Percentile 75% (Q2)*	27.29466
Harmonic Mean	25.38474	*IQR*	3.58576
Mode	#N/A	*MAD*	1.81475

Mean orientation (0-360)

Count	18	*Skewness*	0.74259
Mean	179.34141	*Skewness Standard Error*	0.50561
Mean LCL	153.37792	*Kurtosis*	2.54137
Mean UCL	205.30489	*Kurtosis Standard Error*	0.86184
Variance	1,841.48877	*Alternative Skewness (Fisher's)*	0.81188
Standard Deviation	42.91257	*Alternative Kurtosis (Fisher's)*	-0.19224
Mean Standard Error	10.11459	*Coefficient of Variation*	0.23928
Minimum	127.0314	*Mean Deviation*	34.82034
Maximum	275.9583	*Second Moment*	1,739.18383
Range	148.9269	*Third Moment*	53,860.35909
Sum	3,228.1453	*Fourth Moment*	7,687,030.22803
Sum Standard Error	182.06262	*Median*	172.18845
Total Sum Squares	610,245.42445	*Median Error*	2.98794
Adjusted Sum Squares	31,305.30901	*Percentile 25% (Q1)*	146.3813
Geometric Mean	174.84	*Percentile 75% (Q2)*	214.1013
Harmonic Mean	170.71975	*IQR*	67.72
Mode	#N/A	*MAD*	27.86995

Area (km2)

Count	18	*Skewness*	1.28939
Mean	13.20844	*Skewness Standard Error*	0.50561
Mean LCL	7.70134	*Kurtosis*	4.21216
Mean UCL	18.71555	*Kurtosis Standard Error*	0.86184
Variance	82.84961	*Alternative Skewness (Fisher's)*	1.40969
Standard Deviation	9.10218	*Alternative Kurtosis (Fisher's)*	2.05637
Mean Standard Error	2.1454	*Coefficient of Variation*	0.68912
Minimum	3.6308	*Mean Deviation*	6.76637
Maximum	38.	*Second Moment*	78.24685
Range	34.3692	*Third Moment*	892.44955
Sum	237.752	*Fourth Moment*	25,789.25573
Sum Standard Error	38.61726	*Median*	10.7614
Total Sum Squares	4,548.77743	*Median Error*	0.63377
Adjusted Sum Squares	1,408.44335	*Percentile 25% (Q1)*	7.2258
Geometric Mean	10.70071	*Percentile 75% (Q2)*	17.3656
Harmonic Mean	8.69235	*IQR*	10.1398
Mode	#N/A	*MAD*	4.8422

Stream length (km)

Count	18	*Skewness*	0.79436
Mean	20.195	*Skewness Standard Error*	0.50561
Mean LCL	15.88158	*Kurtosis*	2.90995
Mean UCL	24.50842	*Kurtosis Standard Error*	0.86184
Variance	50.82606	*Alternative Skewness (Fisher's)*	0.86848
Standard Deviation	7.12924	*Alternative Kurtosis (Fisher's)*	0.30381
Mean Standard Error	1.68038	*Coefficient of Variation*	0.35302
Minimum	11.75	*Mean Deviation*	5.78
Maximum	36.27	*Second Moment*	48.00239
Range	24.52	*Third Moment*	264.18794
Sum	363.51	*Fourth Moment*	6,705.19492
Sum Standard Error	30.2468	*Median*	18.065
Total Sum Squares	8,205.1275	*Median Error*	0.4964
Adjusted Sum Squares	864.04305	*Percentile 25% (Q1)*	15.165
Geometric Mean	19.10017	*Percentile 75% (Q2)*	24.385
Harmonic Mean	18.11228	*IQR*	9.22
Mode	#N/A	*MAD*	5.35

Perimeter (m)

Count	18	*Skewness*	0.81137
Mean	20,015.55556	*Skewness Standard Error*	0.50561
Mean LCL	15,717.70238	*Kurtosis*	2.95601
Mean UCL	24,313.40873	*Kurtosis Standard Error*	0.86184
Variance	50,459,884.96732	*Alternative Skewness (Fisher's)*	0.88707
Standard Deviation	7,103.51216	*Alternative Kurtosis (Fisher's)*	0.36579
Mean Standard Error	1,674.31387	*Coefficient of Variation*	0.3549
Minimum	11,640.	*Mean Deviation*	5,732.83951
Maximum	36,080.	*Second Moment*	47,656,558.02469
Range	24,440.	*Third Moment*	2.66933E+11
Sum	360,280.	*Fourth Moment*	6.71353E+15
Sum Standard Error	30,137.6497	*Median*	17,840.
Total Sum Squares	8,069,022,400.	*Median Error*	494.60735
Adjusted Sum Squares	857,818,044.44444	*Percentile 25% (Q1)*	15,140.
Geometric Mean	18,921.46997	*Percentile 75% (Q2)*	24,060.
Harmonic Mean	17,935.27776	*IQR*	8,920.
Mode	#N/A	*MAD*	5,320.

Form factor (-)

Count	18	*Skewness*	-0.24274
Mean	0.02954	*Skewness Standard Error*	0.50561
Mean LCL	0.02741	*Kurtosis*	2.78489
Mean UCL	0.03166	*Kurtosis Standard Error*	0.86184
Variance	0.00001	*Alternative Skewness (Fisher's)*	-0.26539
Standard Deviation	0.00351	*Alternative Kurtosis (Fisher's)*	0.1355
Mean Standard Error	0.00083	*Coefficient of Variation*	0.11878
Minimum	0.02191	*Mean Deviation*	0.00268
Maximum	0.03518	*Second Moment*	0.00001
Range	0.01327	*Third Moment*	0.
Sum	0.53164	*Fourth Moment*	0.
Sum Standard Error	0.01488	*Median*	0.02976
Total Sum Squares	0.01591	*Median Error*	0.00024
Adjusted Sum Squares	0.00021	*Percentile 25% (Q1)*	0.02801
Geometric Mean	0.02933	*Percentile 75% (Q2)*	0.0315
Harmonic Mean	0.02912	*IQR*	0.00349
Mode	#N/A	*MAD*	0.00176

Basin Elongation (-)

Count	18	*Skewness*	-0.25364
Mean	1.61018	*Skewness Standard Error*	0.50561
Mean LCL	1.51986	*Kurtosis*	2.11864
Mean UCL	1.70049	*Kurtosis Standard Error*	0.86184
Variance	0.02228	*Alternative Skewness (Fisher's)*	-0.2773
Standard Deviation	0.14927	*Alternative Kurtosis (Fisher's)*	-0.76117
Mean Standard Error	0.03518	*Coefficient of Variation*	0.09271
Minimum	1.30765	*Mean Deviation*	0.12303
Maximum	1.83123	*Second Moment*	0.02104
Range	0.52358	*Third Moment*	-0.00077
Sum	28.98315	*Fourth Moment*	0.00094
Sum Standard Error	0.63331	*Median*	1.62956
Total Sum Squares	47.04674	*Median Error*	0.01039
Adjusted Sum Squares	0.3788	*Percentile 25% (Q1)*	1.49053
Geometric Mean	1.60349	*Percentile 75% (Q2)*	1.74712
Harmonic Mean	1.59668	*IQR*	0.25659
Mode	#N/A	*MAD*	0.12645

Lemniscate ratio (-)

Count	18	*Skewness*	0.56775
Mean	0.6263	*Skewness Standard Error*	0.50561
Mean LCL	0.58984	*Kurtosis*	2.56945
Mean UCL	0.66276	*Kurtosis Standard Error*	0.86184
Variance	0.00363	*Alternative Skewness (Fisher's)*	0.62073
Standard Deviation	0.06026	*Alternative Kurtosis (Fisher's)*	-0.15445
Mean Standard Error	0.0142	*Coefficient of Variation*	0.09622
Minimum	0.54608	*Mean Deviation*	0.04973
Maximum	0.76473	*Second Moment*	0.00343
Range	0.21865	*Third Moment*	0.00011
Sum	11.27343	*Fourth Moment*	0.00003
Sum Standard Error	0.25567	*Median*	0.61371
Total Sum Squares	7.1223	*Median Error*	0.0042
Adjusted Sum Squares	0.06174	*Percentile 25% (Q1)*	0.58611
Geometric Mean	0.62364	*Percentile 75% (Q2)*	0.68202
Harmonic Mean	0.62105	*IQR*	0.09591
Mode	#N/A	*MAD*	0.04745

Outlet slope (°)

Count	18	*Skewness*	0.26966
Mean	10.22833	*Skewness Standard Error*	0.50561
Mean LCL	7.04143	*Kurtosis*	2.30741
Mean UCL	13.41524	*Kurtosis Standard Error*	0.86184
Variance	27.74474	*Alternative Skewness (Fisher's)*	0.29482
Standard Deviation	5.26733	*Alternative Kurtosis (Fisher's)*	-0.50712
Mean Standard Error	1.24152	*Coefficient of Variation*	0.51497
Minimum	2.41	*Mean Deviation*	4.26389
Maximum	21.32	*Second Moment*	26.20337
Range	18.91	*Third Moment*	36.17044
Sum	184.11	*Fourth Moment*	1,584.30305
Sum Standard Error	22.34738	*Median*	10.435
Total Sum Squares	2,354.7991	*Median Error*	0.36676
Adjusted Sum Squares	471.66065	*Percentile 25% (Q1)*	6.585
Geometric Mean	8.74398	*Percentile 75% (Q2)*	14.54
Harmonic Mean	7.15486	*IQR*	7.955
Mode	#N/A	*MAD*	3.85

200m slope (°)

Count	18	*Skewness*	0.1474
Mean	11.99	*Skewness Standard Error*	0.50561
Mean LCL	8.00776	*Kurtosis*	2.4027
Mean UCL	15.97224	*Kurtosis Standard Error*	0.86184
Variance	43.32094	*Alternative Skewness (Fisher's)*	0.16115
Standard Deviation	6.58186	*Alternative Kurtosis (Fisher's)*	-0.37886
Mean Standard Error	1.55136	*Coefficient of Variation*	0.54895
Minimum	1.48	*Mean Deviation*	5.30333
Maximum	26.09	*Second Moment*	40.91422
Range	24.61	*Third Moment*	38.5743
Sum	215.82	*Fourth Moment*	4,022.05934
Sum Standard Error	27.92449	*Median*	13.085
Total Sum Squares	3,324.1378	*Median Error*	0.45829
Adjusted Sum Squares	736.456	*Percentile 25% (Q1)*	6.05
Geometric Mean	9.75605	*Percentile 75% (Q2)*	16.66
Harmonic Mean	7.06421	*IQR*	10.61
Mode	#N/A	*MAD*	4.2

Average slope (°)

Count	18	*Skewness*	0.2485
Mean	12.21556	*Skewness Standard Error*	0.50561
Mean LCL	8.53655	*Kurtosis*	3.01291
Mean UCL	15.89456	*Kurtosis Standard Error*	0.86184
Variance	36.97472	*Alternative Skewness (Fisher's)*	0.27168
Standard Deviation	6.08068	*Alternative Kurtosis (Fisher's)*	0.44237
Mean Standard Error	1.43323	*Coefficient of Variation*	0.49778
Minimum	2.14	*Mean Deviation*	4.54827
Maximum	26.37	*Second Moment*	34.92057
Range	24.23	*Third Moment*	51.27932
Sum	219.88	*Fourth Moment*	3,674.07709
Sum Standard Error	25.79816	*Median*	12.82
Total Sum Squares	3,314.5266	*Median Error*	0.42339
Adjusted Sum Squares	628.57024	*Percentile 25% (Q1)*	9.35
Geometric Mean	10.40819	*Percentile 75% (Q2)*	15.905
Harmonic Mean	8.2029	*IQR*	6.555
Mode	#N/A	*MAD*	3.47

Appendix 5: Dendrochronological field data

Table of cored trees.

Ring visibility: 1=bad; 2=more or less; 3= good.

Center (pith) visibility and selected trees: N=no; Y=yes

Tree Ref.	Ring visibility	Center visibility	Rings counted	Notes	Selected trees	Depositional unit (cf map)
Sc 01	3	N	28		Y	7
Sc 02	3	Y	33		Y	7
Sc 03	2	N	45		Y	7
Sc 04	3	Y	26		Y	7
Sc 05	2	N	23	center almost hit	Y	7
Sc 06	3	N	31	wedge SW 1	Y	7
Sc 07	2	N	47	wedge SW 2	Y	7
Sc 08	3	N	32	sample B	Y	7
Sc 08	1	N		sample A	N	
Sc 09	3	N	40		Y	7
Sc 10	3	N	38		Y	7
Sc 11	3	N	42		Y	7
Sc 12	3	N	47		Y	6
Sc 14	3	N	35		Y	6
Sc 15	3	N	55		Y	7
Sc 16	3	N	40		Y	7
Sc 17	3	N	37		Y	6
Sc 18	2	N	30		Y	7
Sc 19	2	N	42		Y	7
Sc 20	3	N	42		Y	6
Sc 21	2	N	50		Y	6
Sc 22	2	N	62	rotten before center	Y	6
Sc 23	2	N	46		Y	7
Sc 24	2	Y	65		Y	6
Sc 25	3	N	39		Y	6
Sc 26	1	N	38		N	
Sc 27	1	N		jammed; no bark		
Sc 28	3	N	28		Y	7
Sc 29	2	N	36	Rotten center	Y	7
Sc 30	2	N	40		Y	7
Sc 31	3	N	29	wedge SW 7	Y	7
Sc 32	1	N			N	
Sc 33	2	N	42		Y	7
Sc 34	2	N	30	wedge SW 8	Y	7
Sc 35	2	N				
Sc 36	2	N	37	wedge SW 9	Y	7
Sc 37	1	N		wedge SW 10		
Sc 38	1	N	35			
Sc 39	3	N	38		Y	7
Sc 40	3	N	47		Y	7

Sc 41	3	N	42	very near center	Y	5
Sc 42	3	N	50	center almost hit	Y	5
Sc 43	3	N	38		Y	5
Sc 44	3	N	31	no bark at both	Y	5
Sc 45	3	N	13		Y	4
Sc 46	3	N	25		Y	6
Sc 47	3	Y	29		Y	6
Sc 48	3	N	26		Y	6
Sc 49	3	Y	23		Y	6
Sc 50	2	N	30		Y	6
Sc 51	3	N	24		Y	6
Sc 52	3	Y	34		Y	6
Sc 53	3	Y	35		Y	6
Sc 54	1	N		20 rings visible		
Sc 55	2	N	26		Y	6
Sc 56	2	N	30		Y	5
Sc 57	2	N	25		Y	5
Sc 58	2	N	20		Y	5
Sc 59	2	N		jammed		
Sc 60	1	N				
Sc 61	2	N	28		Y	6
Sc 62	2	Y	29		Y	6
Sc 63	1	N		jammed		
Sc 64	1	N		jammed		
Sc 65	2	N	23		Y	6
Sc 66	2	N	30		Y	6
Sc 67	2	N	26		Y	6
Sc 68	1	N	21	central rings missing		
Sc 69	3	N	23		Y	6
Sc 70	1	N		jammed		
Sc 71	2	N	31		Y	6
Sc 72	2	N	21	jammed	Y	6

Table of wedges (scars)

Wounds' ref.	Rings' visibility	Contact's Presence	First overtopping ring's visibility	rings overtopping
SW 01	3	N		
SW 02	3	Y	N	13
SW 03	3	N		
SW 04	3	Y	N	14
SW 05	3	Y	N	10
SW 06	3	Y	Y	14
SW 07	3	Y	Y	14
SW 08	3	N		
SW 09	3	Y	Y	11
SW 10	3	Y	??	16
SW 11	3	Y	??	17

Map of cored trees, trees with branch whorls counted and wounded trees at Rebaixader

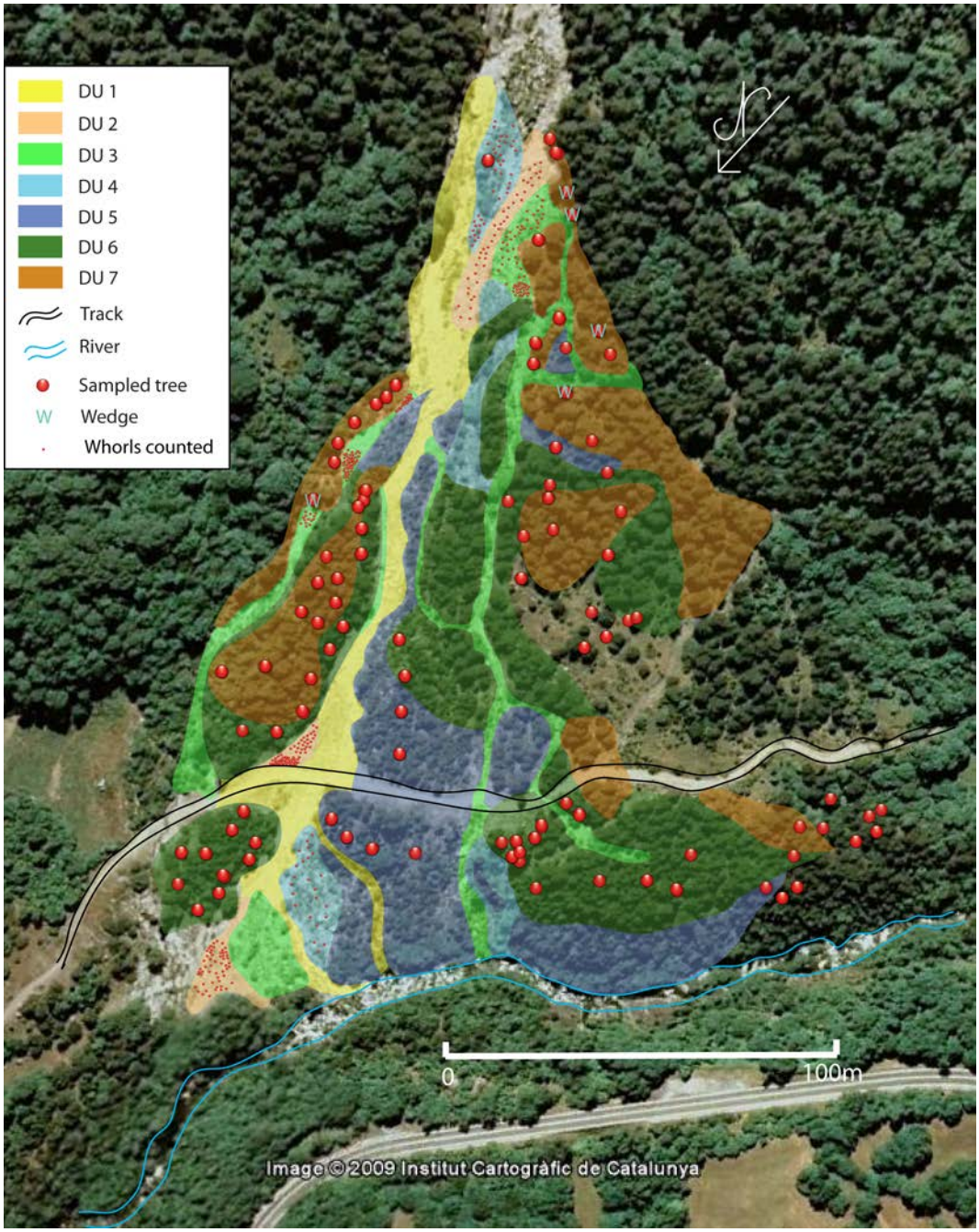

G.G. Chevalier – April 2013.